Functional properties of proteins encoded by the K15 gene of the Kaposi´s sarcoma-associated herpesvirus (KSHV)

Vom Fachbereich Chemie der Universität Hannover

zur Erlangung des Grades

Doktorin der Naturwissenschaften

Dr. rer. nat.

genehmigte Dissertation

von

Diplombiologin Melanie M. Brinkmann

geboren am 6. Januar 1974 in Neustadt am Rbg.

2004

Referent:	Prof. Dr. W. Müller
Co-Referent:	Prof. Dr. T. F. Schulz
Tag der Promotion:	18. Juni 2004

Zusammenfassung

Das K15 Gen des Kaposi Sarkom-assoziierten Herpesvirus (KSHV) besteht aus acht alternativ gespleissten Exons und kann potentiell für Transmembranproteine mit einer variablen Anzahl von Membrandomänen und einem cytoplasmatischen C-Terminus kodieren. Die C-terminale Domäne weist Bindungsmotive für Proteine mit SH2- und SH3-Domänen, und für Tumor Nekrose Faktor Rezeptor-assoziierte Faktoren (TRAFs) auf. Diese Eigenschaften erinnern an Transmembranproteine weiterer Vertreter der γ-Herpesviren wie Epstein-Barr Virus, Herpesvirus saimiri, Herpesvirus ateles und Rhesus Rhadinovirus. Diese γ-Herpesviren kodieren für Membranproteine, die intrazelluläre Signalkaskaden aktivieren können. In dieser Arbeit wurden die vom offenen Leserahmen K15 kodierten Proteine hinsichtlich ihrer zellulären Lokalisation und Signaleigenschaften charakterisiert. Desweiteren wurde die in vivo Expression von K15 Proteinen in einer Reihe von KSHV-infizierten Zell-Linien untersucht.

Es wurde gezeigt, dass ein 45 kDa K15 Protein von einem cDNA Konstrukt mit allen acht Exons exprimiert wird, das potentiell aus bis zu zwölf Transmembrandomänen besteht. Dieses Protein ist membranassoziiert und lokalisiert zum Teil in Membran-Mikrodomänen, sogenannten Lipid Rafts. Unter Verwendung von dominant negativen Mutanten und chemischen Inhibitoren wurde gezeigt, dass das 45 kDa K15 Protein den AP-1 Transkriptionsfaktor über den klassischen „Mitogen-activated protein kinase“ (MAPK) Signalweg (Ras-Raf-MEK-Erk) aktiviert. Zusätzlich wird die Aktivität der MAP kinase JNK1 und des Transkriptionsfaktors NF-κB von K15 induziert. Die Mitglieder der Src Familie der Protein Tyrosin Kinasen Src, Lck, Yes, Hck und Fyn interagieren mit der cytoplasmatischen Domäne des K15 Proteins und phosphorylieren das Y^{481} des potentiellen SH2-Bindemotives Y^{481}EEV. Ein K15 Expressionskonstrukt mit der Punktmutation Y^{481} zu F^{481} vermag weder die Transkriptionsfaktoren AP-1 und NF-κB, noch die MAP Kinasen Erk2 und JNK1 zu aktivieren, was auf eine wichtige Rolle der Phosphorylierung von K15 bei der Signaltransduktion hindeutet. Frühere Experimente zeigten, dass K15 mit TRAFs interagiert (Glenn et al., 1999). Eine dominant negative TRAF-2 Mutante inhibiert die K15 Signaltransduktion, was auf eine Rolle von TRAF-2 bei der Signalweiterleitung von K15 hindeutet. Ferner aktiviert das 45 kDa K15 Protein den Promotor des RTA Proteins von KSHV, und diese Aktivierung erfolgt über den Ras/MAPK Signalweg. K15 Spleissvarianten, die Proteine mit einer geringeren Anzahl an Transmembrandomänen exprimieren, waren nicht in der Lage, die von dem 45 kDa K15 Protein induzierten Signalwege zu aktivieren. Dies weist auf eine wichtige Rolle der Transmembrandomänen des K15 Proteins bei der Signaltransduktion hin. In KSHV-infizierten B Zellen wurde mit einem Antikörper gegen die cytoplasmatische Domäne von K15 ein 23 kDa Protein detektiert. Dieses Protein war jedoch nicht mit zellulären Membranen assoziiert. In de novo KSHV-infizierten 293-T Zellen konnte erstmals die Expression von K15 Transkripten mittels RT-PCR nachgewiesen werden.

Summary

The K15 gene of Kaposi's sarcoma-associated herpesvirus/human herpesvirus 8 (KSHV/HHV-8), encoded at the right end of the genome, consists of eight alternatively spliced exons and is predicted to encode membrane proteins with a variable number of transmembrane regions and a common C-terminal cytoplasmic domain with putative binding sites for SH2- and SH3- binding domains, as well as for TRAFs. These features are reminiscent of the viral terminal membrane proteins of other γ-herpesviruses Epstein-Barr virus, Herpesvirus saimiri, Herpesvirus ateles and Rhesus Rhadinovirus. Their terminal membrane proteins can activate a number of intracellular signaling pathways. The aim of this work was to functionally characterise the proteins derived from the KSHV K15 ORF concerning their localisation in transiently transfected cells, their ability to initiate intracellular signaling and to analyse K15 protein expression in vivo in KSHV infected cell lines.

A 45 kDa K15 protein derived from all eight K15 exons and containing up to 12 predicted transmembrane domains in addition to the cytoplasmic domain was shown to be associated with cellular membranes and to localise to lipid rafts. As shown with dominant negative mutants and chemical inhibitors, this K15 protein activated the AP-1 transcription factor via the classical Mitogen-activated Protein Kinase (MAPK) pathway Ras-Raf-MEK-Erk2 and the MAPK JNK1. Furthermore, the eight exon K15 protein activated the transcription factor NF-κB. Members of the Src family of non-receptor protein tyrosine kinases (PTK) Src, Lck, Yes, Hck and Fyn were shown to bind to the cytoplasmic C-terminal domain of K15 and to phosphorylate the tyrosine residue in the putative SH2-binding motif Y^{481}EEV. A K15 construct carrying the point mutation Y^{481} to F^{481} was unable to activate the transcription factors AP-1 and NF-κB, pointing to a role of tyrosine phosphorylation by PTKs in K15 signaling. Earlier experiments showed that TRAFs-1, -2 and -3 bind to the cytoplasmic domain of K15. A dominant negative TRAF-2 mutant inhibited the K15-mediated activation of the Ras/MAPK pathway, suggesting an involvement of TRAF-2 in the inititation of these signaling routes. Furthermore, the eight exon K15 protein was shown to activate the promoter of the KSHV gene ORF50/Rta, and this involved the Ras/MAPK pathway and TRAF-2. In addition to the eight exon K15 isoform, several splice variants are derived from the K15 ORF that are predicted to encode proteins with fewer transmembrane domains. These K15 splice variants, although containing the intact cytoplasmic domain like the 45 kDa K15 protein, activated the MAPK and NF-κB pathways only weakly. Therefore, the transmembrane region of K15 seems to be important for efficient signaling.

In B-cells naturally infected with KSHV, a 23 kDa protein was detected with K15 antiserum. However, unlike an experimentally generated K15 variant of this size, this protein was not associated with cellular membranes. K15 transcripts were also identified by RT-PCR in de novo KSHV-infected HEK 293-T cells one day post infection.

Keywords/Schlagworte

English:

Kaposi´s sarcoma-associated herpesvirus (KSHV)
K15
Signaling

Deutsch:

Kaposi Sarkom-assoziiertes Herpesvirus (KSHV)
K15
Signaltransduktion

List of contents

List of abbrevations

aa	amino acids
AIDS	acquired immunodeficiency disease syndrome
Amp	Ampicillin
Amp^r	Ampicillin-resistance
AP-1	activator protein 1
APS	Ammoniumpersulfate
ATCC	American Type Culture Collection
ATP	adenosine-triphosphate
BCBL	body cavity-based lymphoma
BCIP	5-bromo-4-chloro-3-indolylphosphate
bp	basepairs
BSA	bovine serum albumine
Cam	Chloramphenicol
Cam^r	Chloramphenicol-resistance
CBP	CREB-binding protein
CDK	cyclin-dependent kinase
cDNA	complementary DNA
Ci	Curie
CMV	Cytomegalie virus
CREB	CRE (cyclic AMP response element)-binding protein
Crk	chicken tumour virus regulator of kinase
Csk	C-terminal Src kinase
CTAR	C-terminal NF-κB activating region
DABCO	1,4-Diazabicyclo[2.2.2]octane
DED	death effector domain
DMEM	Dulbecco´s modified Eagle medium
DMF	Dimetylformamide
DMSO	Dimethylsulfoxide
DNA	deoxyribonucleic acid
DTT	Dithiothreitol
dNTP	deoxyribonucleoside triphosphate
EBV	Epstein-Barr Virus
ECL	enhanced chemiluminescence
E. coli	*Escherichia coli*
EDTA	Ethylenediaminetetraacetate
EGFR	epidermal growth factor receptor
ELISA	enzyme linked immunosorbent assay
Erk	extracellular signal regulated kinase
FADD	Fas-associated death domain
FAK	focal adhesion kinase
FCS	foetal calf serum
FLICE	FADD-like IL-1β-converting enzyme
FLIP	FLICE inhibitory protein
FKHR	Forkhead transcription factor
GFP	green fluorescent protein
GPCR	G protein-coupled receptor
GST	Glutathione S transferase
HA	Hemagglutinin
HAT	Hypoxanthine-aminopterin-thymidine

Hepes	N-2-Hydroxyethylpiperazin-N-2-ethansulfonic acid
HHV	human herpesvirus
HOS	homologue of slimb
HRP	Horse raddish peroxidase
HSV	Herpes simplex virus
HVA	Herpesvirus ateles
HVS	Herpesvirus saimiri
ICAM	intercellular adhesion molecule
IE	immediate early
Ig	Immunoglobulin
IKK	IκB kinase
IL	Interleukin
IPTG	Isopropylthio-β-D-galactoside
ITAM	immune receptor tyrosine-based activation motif
JAK	Janus kinase
JNK	c-jun N-terminal kinase
Kan	Kanamycin
Kan^r	Kanamycin-resistance
kb	kilobases
KCP	complement control protein
kDa	kilo Dalton
KS	Kaposi´s sarcoma
KSHV	Kaposi´s sarcoma-associated herpesvirus
LCL	lymphoblastoid cell lines
LFA	lymphocyte function-associated antigen
LMP1	latent membrane protein 1
LMP2A/B	latent membrane protein 2A/B
LPS	lipopolysaccharide
MAPK	mitogen-activated protein kinase
MCD	Multicentric Castleman´s disease
MCS	multiple cloning site
MEM	Modified Eagles´ medium
MOPS	3-(N-Morpholino)propansulfonic acid
mRNA	messenger RNA
NCBI	National Centre of Biotechnology Information
NEAA	non-essential amino acids
NEMO	NF-κB essential modulator
NFAT	nuclear factor of activated T lymphocytes
NF-κB	nuclear factor κB
NK	natural killer
NLS	nuclear localisation signal
OD	optical density
ORF	open reading frame
PAGE	Polyacrylamide gelelectrophoresis
PAN	polyadenylated nuclear
PBS	Phosphate buffered saline
PCR	polymerase chain reaction
PEL	primary effusion lymphoma
PFA	paraformaldehyde
PI3K	phospatidylinositol 3-kinase
PKA	protein kinase A (cAMP dependent)

PKC	protein kinase C (calcium dependent)
PMSF	Phenylmethylsulfonyl fluoride
PTK	non-receptor protein tyrosine kinase
RACE	rapid amplification of cDNA ends
RB	retinoblastoma protein
RIP	receptor interacting protein
RFP	red fluorescent protein
RNA	ribonucleic acid
rpm	rounds per minute
RPMI	Roswell Park Memorial Institute
RRV	Rhesus rhadinovirus
RSV	Rous Sarcoma virus
RT	room temperature
RTA	regulator of transcriptional activation
SCID	severe combined immunodeficiency
SDS	sodium dodecyl sulfate
SH	Src homology
SH-B	Src homology (SH) binding
STAT	signal transducer and activator of transcription
Stp	saimiri-transforming protein
SV40	Simian Virus 40
TAE	Tris-acetic acid EDTA buffer
TCA	Trichloroacetic acid
TES	transformation effector site
TGF	transforming growth factor
Tio	two-in-one protein
Tip	tyrosine kinase interacting protein
TMP	terminal membrane protein
TNF-α	tumour necrosis factor α
TNFR	Tumour necrosis factor receptor
TPA	Phorbol 12-myristate 13-acetate
TRADD	TNFR-associated death domain
TRAF	TNFR associated factor
TRE	TPA response element
Tris	Tris(hydromethyl)aminomethan
VEGF	vascular endothelial growth factor
VZV	Varizella zoster virus
Xgal	5-Bromo-4-chloro-3-indolyl-β-D-galactoside

Internationally used physical and biochemical abbrevations are not listed.

1 Introduction

1.1 The Family *Herpesviridae*

Herpesviruses are highly disseminated in nature and most animal species have yielded at least one but frequently several herpesviruses. Members of the *Herpesviridae* share a common virion morphology and several significant biological properties. A typical herpes virion consists of a core containing a double-stranded linear viral DNA, an icosahedral capsid (100-110 nm in diameter) containing 162 capsomers, the tegument which is surrounding the capsid, and an envelope in which viral glycoproteins are embedded (reviewed in Roizman & Pellett 2002).

Biological properties:
1. All herpesviruses encode a large array of enzymes involved in nucleic acid metabolism, DNA synthesis and processing of proteins.
2. The synthesis of viral DNA and capsid assembly occurs in the nucleus.
3. Production of infectious progeny virus is invariably accompanied by the destruction of the infected cell (lytic viral life cycle).
4. Herpesviruses are able to establish a latent infection in their natural hosts. In latently infected cells, viral genomes take the form of closed circular molecules (termed episomes), and only a small subset of viral genes are expressed (latent viral life cycle). Latent genomes retain the capacity to replicate upon reactivation.

Thus far, eight herpesviruses have been isolated from humans (human herpesvirus 1-8 [HHV-1 to -8]), and they have been categorized into three subfamilies according to their pathogenicity, host cells, replication characteristics and nucleotide sequence:

• α-herpesvirinae have a wide host cell range, multiply efficiently, rapidly spread in culture, efficiently destroy the cells they infect productively and are capable of establishing latent infections primarily but not exclusively in sensory ganglia (*Simplexvirus* Herpes simplex virus I and II [HSV-I, HSV-II], and *Varicellovirus* Varizella zoster virus [VZV or HHV-3]).
• β-herpesvirinae show a more restricted host range and grow slowly in cell culture. Infected cells become enlarged and carrier cultures are readily established. The virus latently infects secretory glands, lymphoreticular cells, kidneys and other tissues (*Cytomegalovirus* Cytomegalovirus [CMV or HHV-5], *Roseolovirus* HHV-6 and HHV-7).
• γ-herpesvirinae replicate in lymphoid cells in vitro and in vivo, being either specific for T- or B-lymphocytes. Latent virus is frequently demonstrated in lymphoid tissue. This subfamily contains two genera: *Lymphocryptovirus* (Epstein-Barr virus [EBV or HHV-4]) and *Rhadinovirus* (Kaposi´s sarcoma-associated herpesvirus [KSHV or HHV-8]). EBV and

KSHV both also infect epithelial cells, and KSHV can be detected in myeloid cells (monocytes, macrophages), keratinocytes and endothelial cells in vivo.

Herpesvirions vary in size from 120 to nearly 300 nm, and the viral DNA is variable concerning length (120-250 kb), base composition (31-75% total GC content) and copy number of terminal and internal reiterated sequences. Most herpesvirus genes contain a promoter/regulatory sequence spanning 50-200 bp upstream of a TATA box, a transcription initiation site 20-25 bp downstream of the TATA box, a 5´ nontranslated leader sequence of 30-300 bp, a single open rading frame (ORF), 10-30 bp of 3´ nontranslated sequence and a canonical polyadenylation signal. However, exceptions for this genetic architecture exist: genes without a TATA box (Chou & Roizman, 1986) and initiation from a second in-frame methionine (Markovitz et al., 1999) have been described. In addition, ORFs can be expressed that are situated entirely antisense to each other (Lagunoff & Roizman, 1994), gene overlaps are common, and each herpesvirus encodes a handful of spliced genes and can encode noncoding RNAs (reviewed in Roizman & Pellett 2002).

Between 70 (smallest genome) and over 200 (largest genome) gene products are encoded by Herpesviruses. Herpesvirus proteins frequently have multiple functions. In addition to viral proteins being involved in viral replication, establishment/maintenance of latency or reactivation from latency, an armamentarium of viral proteins is expressed to fend off the host cell defenses to infection (e.g. inhibition of apoptosis, blocking the activation of the interferon pathway).

Herpesviruses encode at least one gene of obvious host origin. In some cases, the host-acquired genes retain a function similar to their cellular counterparts, in other cases they have altered functions. KSHV for example encodes several “captured” cellular genes such as the viral G-protein coupled receptor (vGPCR), which is constitutively active and capable of transforming cells, or viral cyclin (vcyc) which is homologous to cellular D-type cyclin (see 1.2).

1.2 The Kaposi´s sarcoma-associated herpesvirus (KSHV)

The eighth human herpesvirus, Kaposi´s sarcoma-associated herpesvirus (KSHV or HHV-8), is the most recently discovered human DNA tumour virus. KSHV was originally isolated from Kaposi´s sarcoma (KS) tissues by representional difference analysis in 1994 by Chang et al. Today, the available epidemiological and molecular evidence strongly suggests that KSHV is the cause of three human neoplastic disorders, namely Kaposi´s sarcoma (Moore & Chang 1995, reviewed in Schulz 2000), a very rare form of B-cell lymphoma called body cavity-based lymphoma (BCBL) or primary effusion lymphoma (PEL) (Cesarman et al., 1995) and the plasma cell variant of multicentric Castleman´s disease (MCD) (Soulier et al., 1995).

The KSHV genome consists of a long unique coding region of 140 kb (GC content ~54%), which is flanked by 801 bp terminal tandem repeats rich in GC (85%), the so called terminal

repeats (total length varying between 20-30 kb, see figure 1) (Neipel et al., 1997, Russo et al., 1996). More than 90 putative KSHV open reading frames are described in the literature today. As for other members of the genus *rhadinovirus*, many KSHV genes have been described which show homologies to cellular genes implicated in signal transduction, cell cycle control and apoptosis.

Role of KSHV in neoplastic disease

Kaposi´s sarcoma

Kaposi´s sarcoma exclusively develops in KSHV-infected individuals. However, classic KS is a rare tumour in immunocompetent KSHV-infected individuals, while KS is much more common in immunosuppressed patients, e.g. HIV-infected patients (AIDS-KS) or transplant recipients.

In Africa, endemic KS (i.e. the clinically severe form of KS in HIV negative individuals) is mainly found in East and Central Africa, in spite of a high KSHV prevalence in most sub-Saharan Africa (reviewed in Dedicoat & Newton, 2003), which suggests the existence of other co-factors that promote KS development in KSHV positive individuals (reviewed in Schulz 2000).

The natural reservoir for KSHV are endothelial cell-derived spindle cells which are the neoplastic components of the KS tumour (Boshoff et al., 1995, Rainbow et al., 1997, reviewed in Schulz 2001). In these cells, four latent viral genes are expressed: ORF73/Lana-1, ORF K12/kaposin, ORF K13/vFLIP, ORF72/vcyclin (see figure 1 and below). The major population of spindle cells harbours viral episomes, however, in some spindle cells KSHV is not strictly latent but undergoes lytic replication (Staskus et al., 1997, Katano et al., 2000, Parravicini et al., 2000). Whereas other human DNA tumour viruses are thought to use viral proteins expressed during latency to induce proliferation and tumourigenesis, it seems that KSHV lytic genes, which experimentally appear to have the potential to promote tumourigenesis, contribute to the development of KS (see below).

Primary effusion lymphoma

Primary effusion lymphoma is a rare lymphoma in AIDS patients, and the presence of KSHV is considered an essential criterion for the diagnosis of PEL. In PEL cells, the latent genes Lana-1, vFLIP, vcyclin and kaposin are expressed (Rainbow et al., 1997, Parravicini et al., 2000, Katano et al., 2000, see figure 1). Lytic gene expression has been detected in a small subset of cells: the viral interleukin 6 homologue (vIL-6) was detected in 2-5% of tumour cells, whereas viral lytic proteins (see below) K8/kbZIP, the viral membrane glycoprotein K8.1, the three viral interferon regulatory factors (vIRF) K9, K10, K11, a viral processivity

factor ORF59/PF-8 and the minor capsid protein ORF65 were detected in less than 1% of PEL cells (Parravicini et al., 2000, Katano et al., 2000).

Multicentric Castleman´s diesease

Compared to PEL and KS tissue, KSHV appears to adopt a less restrictive pattern of gene expression in MCD, jugded by the detection of a number of lytic genes in a significant number of cells (Parravicini et al., 2000, Katano et al., 2000). This would suggest that MCD could represent the active viral lytic replication in lymphoid tissue.

Epidemiology of KSHV

Currently available seroepidemiology data indicate that KSHV is relatively rare in most northern, western and central European countries, the USA and Asian countries, with less than 5% of blood donors having antibodies. KSHV infection is more frequently found in the general population in Italy with prevalence rates of 30% in Sicily and south Italy (Calabro et al., 1998), Greece, Israel and Spain, but by far the highest frequency is found in most African countries, particularly in sub-Saharan Africa. Antibodies to KSHV are detected in 50-60% of adults and adolescents in most parts of sub-Saharan Africa investigated so far and 20-40% in South Africa. However, endemic KS, the HIV-negative variant of classic KS, appears to be more common in East Africa than in other parts of Africa, which implies the role of certain, yet unidentified co-factors associated with endemic KS (reviewed in Schulz 2001).

In western countries, KSHV seroprevalence rates range between 20-40% among homosexual men, but are significantly lower (below 5-10%) in HIV-infected intravenous drug users, women and patients with hemophilia. KS develops in 50% of KSHV and HIV infected homosexual men (Renwick et al., 1998, Jacobsen et al., 2000). In contrast, KSHV infection in immunocompotent individuals in Europe is rarely associated with disease, whereas occasionally observed in immunosuppressed patients (e.g. transplant patients). Despite a KSHV seroprevalence of 30% in Sicily, only very few individuals develop classic KS (population based incidence 3/100.000, Calabro et al., 1998).

Evolution

Based on sequence information and phylogenetic comparisons, KSHV has been placed with the γ_2-subfamily of herpesviruses, the *rhadinoviruses*. Following the discovery of KSHV, closely related *rhadinoviruses* have been identified in many non-human primates. Today, three branches of *rhadinovirus* are described based on phylogenetic analysis of the viral DNA polymerase genes, namely rhadinovirus 1 subgroup (RV-1) including KSHV and closely related viruses being found in Old World primate species (chimpanzee PanRHV1, gorilla GoRHV1, mandrill MnRHV1, African green monkey ChRV1 and macaque RFHVMm,

RFHVMn), a second group called RV-2 comprising slightly more distantly related γ_2-herpesviruses (chimpanzee PanRHV2, mandrill MnRHV2, African green monkey ChRV2, macaque RRV) and a third branch of the New World primate γ_2-herpesviruses Herpesvirus saimiri (HVS) and Herpesvirus ateles (HVA) (reviewed in Greensill & Schulz, 2000).

The study of genomic variation of KSHV isolates has revealed the existence of particular KSHV variants in certain geographic regions, suggesting that KSHV has co-evolved with human populations. This is best illustrated by the pattern of variability found in the K1 gene at the left side of the KSHV genome (see figures 1 and 2), and today K1 variants are grouped into four or five major clades designated A-E (see 1.3.5). In addition, two highly diverged alternative allelic forms of the ORF K15 region, located at the right end of the KSHV genome, have been identified. They are referred to as predominant K15 (K15-P) and minor K15 (K15-M). K15-P and K15-M only share 33% identity at the amino acid level (see 1.3.6 and figures 1-3 and 5, Poole et al., 1999). It seems probable that the 33% identity between K15-P and K15-M represents a level of evolutionary divergence that is consistent with an origin for one of them by recombination with a related virus from another great ape, another Old World primate species, or even a more distant host species.

Transmission

KSHV can be efficiently transmitted in childhood (Mayama et al., 1998, Gessain et al., 1999, Andreoni et al., 1999, Plancoulaine et al., 2000, Bourboulia et al., 1998), and given the excretion of KSHV in saliva, it is conceivable, but not yet proven, that KSHV can be transmitted by saliva from mother to child or sibling to sibling (Andreoni et al., 2002). Recent findings demonstrate an association between high viral DNA copy number in maternal saliva and transmission to her child (Dedicoat et al., 2004). While in endemic countries or populations the majority of infections appears to occur before puberty, transmission during adulthood accounts for most infections in non-endemic countries. Several studies indicate sexual contact being an important route of infection, especially among homosexual men. Parenteral transmission is discussed controversely, but among transplant patients, KSHV transmission through transplanted organs has been clearly documented (Regamey et al., 1998, Luppi et al., 2000). However, most cases of transplant KS appear to be due to reactivation of a pre-existing KSHV infection (reviewed in Luppi et al., 2002).

Virus culture

Several groups succeeded in establishing persistently infected PEL cell lines, which are infected with KSHV only or co-infected with EBV. In some PEL cell lines, only latent genes are expressed (e.g. BCP-1, BCBL-1), but in others KSHV will spontaneously switch into the lytic cycle (Jsc-1, ISI). The lytic viral replication cycle can also be artificially induced by the addition of the phorbol esters 12-*O*-tetradecanoylphorbol-13-acetate (TPA) or *n*-butyrate

(Miller et al., 1997a, Renne et al., 1996). A major drawback is the little in vitro infectivity of KSHV obtained from lytically induced PEL cell lines and the lack of an animal model. However, investigators succeeded in infecting the epithelial cell line 293 (Foreman et al., 1997, Renne et al., 1998), primary endothelial cell cultures (Cannon et al., 2000, Ciufo et al., 2001), endothelial cell lines immortalised by either human papillomavirus E6/E7 proteins (Moses et al., 1999) or telomerase (TIME cells; Lagunoff et al., 2002), human and murine fibroblasts, HeLa and the endothelial SLK cell line (Bechtel et al., 2003). Intriguingly, successful infection of human lymphoblastoid cells has not been achieved by some (Bechtel et al., 2003), whereas others have reported successful infection of primary B-cells which were simultaneously exposed to EBV and KSHV (Kliche et al., 1998). Infectious KSHV can be produced from 293 and TIME cells being provided in *trans* with a plasmid coding for the viral lytic transactivator RTA (regulator of transcriptional activation, see below; Bechtel et al., 2003).

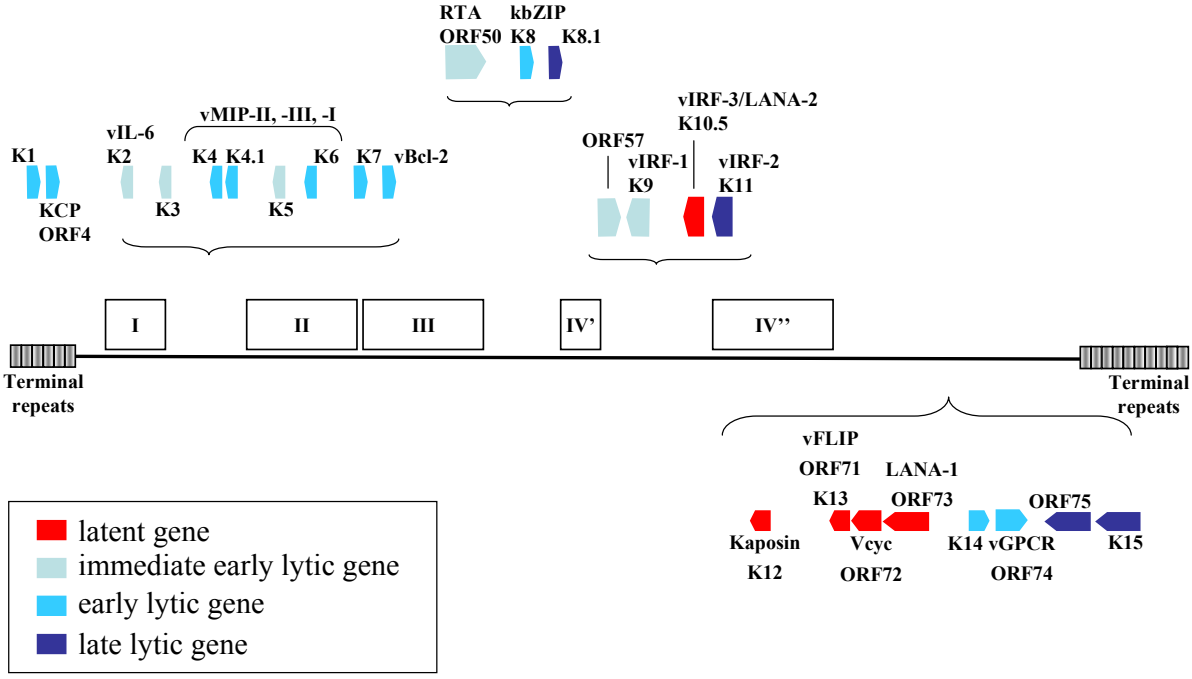

Figure 1: Schematic presentation of the KSHV genome. The long unique region, which codes for more than 90 open reading frames, encompasses 140 kb and is flanked by terminal repeat regions which consist of several 803 bp repeat subunits. The total length of the TR region of KSHV comprises 20-30 kbp. Boxes I – IV" indicate conserved genes within the group of herpesviruses. ORFs are colour-coded to distinguish between genes expressed during the latent or lytic viral life cycle. ORFs unique for KSHV are designated with the prefix "K" (K1-K15).

Pathogenesis

KSHV has the capacity to interfere with the control of cellular proliferation and to fend off the immune response. The next section will focus on the biochemical and cell biological features of individual KSHV proteins involved in cell entry, latent and lytic replication,

regulation of the cell cycle and apoptosis, angiogenesis, B-cell proliferation, and manipulation of the host immune system. Several KSHV proteins, as for example LANA-1 and vIRFs, play multiple roles in the manipulation of cellular functions.

Cell entry

KSHV shows a wide tropism in vitro (Vieira et al., 2001, Renne et al., 1998, Cerimele et al., 2001, Flore et al., 1998, Lagunoff et al., 2002, Moses et al., 1999), which may be due to its interaction with the ubiquitous host cell surface molecule heparan sulfate via viral glycoproteins gB and gK8.1 (Akula et al., 2001a, b, Birkmann et al., 2001, Wang et al., 2001). In addition, KSHV gB contains an RGD (arg-gly-asp) motif which binds specifically to $\alpha_3\beta_1$ integrin, which is also broadly expressed and has been detected on all cells susceptible to infection with KSHV (Akula et al., 2002, Wang et al., 2003a). Upon infection, the integrin-mediated activation of focal adhesion kinase (FAK) is induced, implicating a role for integrin not solely as a receptor for KSHV but also in the induction of signaling pathways inducing morphological changes and cytoskeletal rearrangements allowing entry of the virus (Naranatt et al., 2003). FAK phosphorylation appears to be induced by gB (Akula et al., 2002, Naranatt et al., 2003). In early stages of cell entry, cellular phosphatidylinositol 3-kinase (PI3K) seems to play a role, and cellular kinases protein kinase C-ζ (PKC-ζ) and Erk (extracellular signal regulated kinase) are involved in later stages of entry (Naranatt et al., 2003). Two reports described KSHV entry into epithelial 293-T cells (Inoue et al., 2003) and fibroblasts (Akula et al., 2003) to occur via endocytosis. However, in 293-T cells endocytosis of KSHV seems to be neither clathrin nor caveolae-dependent, whereas KSHV uses clathrin-mediated endocytosis for its entry into fibroblasts. The modulation of host cell gene expression after KSHV entry is diverse, with obvious differences in endothelial versus B-cells (Naranatt et al., 2004).

Latent replication

Latency is defined by the presence of episomal, extrachromosomal viral DNA in the cell nucleus with a restricted pattern of gene expression and absence of virion production (Judde et al., 2000). Five viral genes have been described to be expressed during KSHV latency, (colour coded in red in figure 1): the latency-associated nuclear antigen 1 (Lana-1/ORF73), the viral homologue of a D-type cyclin viral cyclin (vcyc/ORF72), a homologue of the FLICE (Fas-associated death domain-like IL-1-converting enzyme) apoptosis complex viral FLIP (viral FLICE inhibitory protein vFLIP/ORF71, K13), a group of membrane-associated proteins called kaposin A, B and C (K12) and an interferon regulatory factor (IRF) homologue designated Lana-2 (vIRF3/K10.5) (Jenner et al., 2001, Rivas et al., 2001). Among the proteins encoded by these five genes, only Lana-1 has been detected in all KSHV-infected cells (Rainbow et al., 1997, Katano et al., 2000). LANA-2 protein has only been detected in

infected B-cells in vivo and in vitro, suggesting a tissue-specific latency pattern for B-cells (Rivas et al., 2001).

Lana-1 is required for the persistence of the viral episome. It tethers viral episomes to host chromatin by binding to two motifs of 16 nucleotides within the terminal repeat subunits via its C-terminal region and to heterochromatin via its N-terminus (Garber et al., 2002, Ballestas et al., 1999, Viejo-Borbolla et al., 2003). In addition, LANA-1 has a role in the replication of latent episomes (Garber et al., 2002, reviewed in Viejo-Borbolla & Schulz 2003), and binds to p53 and retinoblastoma protein, thereby inhibiting activation of p53-dependent promoters and inducing activation of E2F-dependent genes (Friborg et al., 1999, Radkov et al., 2000). Furthermore, LANA-1 acts as a transcriptional activator and repressor (Garber et al., 2001, 2002, Renne et al., 2001, Hyun et al., 2001, Radkov et al., 2000, Groves et al., 2001, An et al., 2002, Krithivas et al., 2000, Schwam et al., 2000, Jeong et al., 2001, reviewed in Viejo-Borbolla & Schulz 2003) and interacts with RING3 (Platt et al., 1999) and other members of the BET family of cellular proteins. Two members of the BET family are known to be involved in cell cycle regulation. In addition, LANA-1 promotes S-phase entry probably by its interaction with the kinase GSK-3β (Fujimoro et al., 2003). Lana-1 has been shown to induce expression of cellular IL-6, which is a growth factor for KSHV-associated disease (Asou et al., 1998, Screpanti et al., 1996), in an AP-1 (activator protein 1) dependent fashion via interaction with the transcription factor c-jun, a member of the AP-1 family (An et al., 2002, 2004).

Lytic viral replication

During the lytic viral life cycle, viral particles are produced and released, resulting in the death of the host cell. Several observations suggest that a few viral proteins expressed during the lytic cycle (called immediate early, early and late lytic proteins according to the time point they are expressed after reactivation, see figure 1) have autocrine or paracrine effects and thereby might play a role in KSHV-related malignancies (reviewed in Schulz 2001 and Viejo-Borbolla & Schulz 2003). In EBV, two proteins synergistically mediate activation of the lytic cycle, termed EBV-RTA and ZTA. However, reactivation in KSHV is solely dependent on ORF50/RTA, which functions as a transcriptional activator of the early and late genes of KSHV. Ectopic expression of RTA triggers the lytic cycle (Sun et al., 1998) and dominant-negative ORF50 mutants were shown to inhibit reactivation in the KSHV positive PEL cell line BCBL-1 (Lukac et al., 1998, 1999). RTA can avtivate its own promoter, lytic viral genes and cellular genes through binding to specific DNA sequences and by interacting with cellular transcription factors (Deng et al., 2000, Chang et al., 2002, Gwack et al., 2002, Liang et al., 2002, Byun et al., 2002, Wang et al., 2003b, c). RTA also seems to be involved in promoting cell proliferation by suppressing p53-mediated apoptosis and by interacting with the transcription factor signal transducer and activator of transcription 3 (STAT3) (Gwack et al., 2003). The KSHV ZTA homologue termed kbZIP (ORF K8) cannot reactivate KSHV from

latency on its own, but has been shown to be a coregulator of RTA (Izumiya et al., 2003), to upregulate both CCAAT/enhancer-binding protein-α (C/EBPα) and $p21^{CIP-1}$ expression (Wu et al., 2003, Wang et al., 2003b, c) and repress p53 transcriptional activity (Park et al., 2000).

Cell cycle manipulation

Like its cellular homologue, viral cyclin (vcyc) mediates phosphorylation and thereby inactivation of the retinoblastoma protein (Rb) through association with the cyclin dependent kinase 6 (CDK6) (Swanton et al., 1997, Ellis et al., 1999). Vcyc might play a role in carcinogenesis, since it can promote the progression of resting cells into the S phase (Swanton et al., 1997, Ellis et al., 1999, Lundquist et al., 2003). This might occur by its inactivation of STAT 3, preventing growth-suppressive effects (Lundquist et al., 2003) or its activation of the cyclin A promoter, a regulator of S phase entry (Duro et al., 1999). Besides vcyc, Lana-1 is able to promote entry into S-phase (Fujimoro et al., 2003).

Angiogenesis and B-cell proliferation: vIL-6, vGPCR and vMIP I, II, III

The KSHV counterpart of the human cytokine IL-6, vIL-6, is able to support growth of IL-6-dependent B-cells in vitro (Moore et al., 1996) and mediates STAT and mitogen-activated protein kinase (MAPK) signaling pathways (Molden et al., 1997, Osborne et al., 1999). vIL-6 has been reported to support PEL growth in culture, to promote growth of transformed cells in mice, and vIL-6-induced VEGF is essential for tumour growth and dissemination in PEL inoculated mice (Aoki et al., 1999a, b, Jones et al., 1999). In all KSHV-associated disorders, high levels of vascular endothelial growth factor (VEGF) and its receptor kinase insert domain containing receptor (KDR) which induces angiogenesis have been detected (reviewed in Hayward, 2003).

The early lytic viral G protein-coupled receptor (vGPCR) is homologous to the human chemokine Interleukin 8 (IL-8) receptor, with the difference of being ligand-independent and thereby constitutively active (Cesarman et al., 1996, Arvanitakis et al., 1997). Depending on the cell type, vGPCR signals constitutively via multiple G protein subtypes. In endothelial cells for example, vGPCR signals via G protein subtype Gi and leads to increased cell survival (Montaner et al., 2001, Couty et al., 2001). In certain models, vGPCR activates the transcriptional potential of NF-κB and AP-1, signals via MAPKs, activates PI3K-Akt and induces secretion of VEGF (Arvanitakis et al., 1997, Bais et al., 1998, Burger et al., 1999, Couty et al., 2001, Schwarz & Murphy 2001, Montaner et al., 2001, Pati et al., 2001, Sodhi et al., 2000, Smit et al., 2002). In PEL cells, expression of vGPCR from an inducible plasmid led to induction of MAPKs Erk1/2 and p38, an increase of transcription of reporter genes under control of AP-1, NF-κB, CREB, NFAT and viral ORFs 50 and 57, and production of VEGF and vIL-6 (Cannon et al., 2003). An elegant study by Cannon & Cesarman (2004)

showed that AP-1 and CREB activation by vGPCR is mediated cooperatively by a Gq-Erk1/2 and a Gi-PI3K/Akt-Src (Lyn) axis in PEL cells.

vGPCR was shown to transform murine fibroblasts (NIH 3T3 cells) and can cause vascular KS-like lesions in vGPCR-transgenic mice (Yang et al., 2000a). Induction of proinflammatory cytokines and growth factors such as IL-2, IL-8, TNF-α, enhanced production of VEGF in the presence of vGPCR and the fact that only a few cells (e.g. 10% of KS cells) express vGPCR suggest that the angiogenic and tumourigenic activity of vGPCR is mediated by paracrine effects on surrounding cells (Shepard et al., 2001, reviewed in Schulz 2001).

The three chemokine homologues vMIP-I, -II, and –III, members of the macrophage inflammatory protein (MIP) family, are encoded by ORFs K6, K4 and K4.1 (figure 1), respectively, and seem to play a role in promoting leukocyte chemotaxis, eosinophil migration, angiogenesis (vMIP-I induced VEGF expression in PEL cell lines), inhibition of apoptosis and evasion of the immune response (Boshoff et al., 1997, Nicholas et al., 1997, Liu et al., 2001, reviewed in Schulz, 2001).

Inhibition of apoptosis

Inhibition of apoptosis is a hallmark of tumour cells. One cellular defense mechanism against viral infection is the induction of apoptosis, and viruses have successfully evolved strategies to interfere with apoptotic pathways, allowing them to prolong the life of virus-infected cells and consequently the time for replication and virus spread. Two apoptotic pathways exist in mammalian cells: the extrinsic pathway in which death receptors such as TNFR1 (tumour necrosis factor receptor) or Fas recruit intracellular adaptor molecules such as FADD (Fas-associated death domain), TRADD (TNFR-associated death domain) or RIP (receptor interacting protein) via death domain interactions, which then subsequently associate with and activate the upstream caspases (8 or 10) through death effector domain (DED) interactions leading to activation of the downstream caspases, and the intrinsic pathway in which mitochondria release caspase-activating enzymes (reviewed in Teodoro & Branton 1997). The observation that inhibition of NF-κB in PEL cell lines leads to apoptosis (Keller et al., 2000) and that a number of KSHV proteins can induce the NF-κB pathway which is known to have an antiapoptotic effect, suggests that some KSHV proteins could contribute to the protection against apoptosis. KSHV proteins vFLIP, K7/survivin, vBcl-2, vIRF-1, -2 and -3 have been shown to inhibit apoptosis, thereby possibly contributing to tumourigenesis.

vFLIP/ORF K13 [viral FLICE (FADD-like IL-1-converting enzyme)-inhibitory protein] contains two DEDs as cellular cFLIP proteins. cFLIPs are antiapoptotic proteins that prevent the association of the upstream caspases 8 and 10 with the adaptor molecules through DED-DED interactions (Irmler et al., 1997). vFLIP has been shown to block Fas-induced apoptosis and it has been postulated to act as a tumour progression factor by interfering with apoptotic

signals induced by virus-specific T killer cells (Thome et al., 1997, Djerbi et al., 1999, Belanger et al., 2001). vFLIP can modulate the NF-κB pathway, which may also play an antiapoptotic role, and physically interacts with signaling proteins such as TRAF-2, RIP and IκB kinase (IKK) (Chaudhary et al., 1999, Liu et al., 2002). Furthermore, vFLIP has been reported to induce cellular IL-6 expression via NF-κB and AP-1 pathways (An et al. 2003). vFLIP is transcribed from a polycistronic transcript together with vcyc and LANA-1 (Talbot et al., 1999), and translation of vFLIP is regulated by an internal ribosome entry site (IRES) (Low et al., 2001, Bieleski & Talbot 2001).

K7/survivin is a glycoprotein related to human survivin (a member of the inhibitor-of-apoptosis family) and seems to be an adaptor molecule bringing together Bcl-2 and effector caspases, allowing inhibition of the latter by Bcl-2 (Wang et al., 2002). The viral homologue of human Bcl-2, vBcl-2, may inhibit apoptosis, but biochemical studies showed that the mechanisms of action of the two proteins differ (Cheng et al., 1997, Sarid et al., 1997, reviewed in Schulz 2001).

The initial immune response against viral infection is regulated by interferon regulatory factors (IRFs) which are a family of interferon-responsive transcription factors that regulate by binding to interferon-stimulated response elements in the promoters of interferon-responsive genes. Hence, IRFs regulate expression of genes involved in e.g. pathogen response and cell proliferation. KSHV vIRF-1 (K9) and vIRF-2 (K11) inhibit interferon signaling and subsequently prevent induction of apoptosis (Gao et al., 1997, Kirchhoff et al., 2002). vIRF-1 and vIRF-3 (LANA-2, K10.5) were shown to inhibit the activation of p53-dependent promoters (Seo et al., 2001, Rivas et al., 2001).

Transforming and signaling KSHV proteins: kaposin, vIRF-1, vGPCR, K1 and K15

ORF K12/kaposin gives rise to three proteins named kaposin A, B and C (Sadler et al., 1999). Kaposin A, a type II membrane protein, can transform rodent fibroblasts to tumourigenicity and induces lymphocyte aggregation and adhesion (Kliche et al., 2001, Muralidhar et al., 1998). Kaposin A protein expression has been shown in PEL cells (Muralidhar et al., 2000, Kliche et al., 2001). vIRF-1 can transform NIH 3T3 cells (Gao et al., 1997) and the vGPCR causes tumours in transgenic mice and excerts a number of signaling activities e.g. activation of MAPK and NF-κB pathways (see above). Signaling activities of terminal membrane proteins K1 and K15 are described below in detail. Lana-1 has been found to transform rodent cells when co-transfected with constitutively active H-Ras (Radkov et al., 2000).

Mechanisms of immune evasion

Many viruses manage to fend off the host cell immune system. Especially herpesviruses that can establish long term infections are experts in outwitting the immune response. One escape mechanism realised by herpesviruses and also adenoviruses is to downregulate the number of major histocompatibility class (MHC) I proteins on the surface of the infected cells, hence antigens will not be presented efficiently and the cytotoxic T lymphocytes recognise the infected cell less efficiently. In addition, herpesviruses express a very limited number of proteins during latency to minimize the immune response. KSHV expresses two type III transmembrane proteins, K3 and K5, that have been shown to downregulate MHC class I molecules (with different specificities concerning HLA allotypes) by enhancing their endocytosis and degradation rate (Coscoy & Ganem, 2000, Means et al., 2002, Ishido et al., 2000a, Sanchez et al., 2002, Lorenzo et al., 2002). The K5 protein also downregulates ICAM-1 (intracellular adhesion molecule) and B7-2, molecules that promote cell-cell contact to ensure efficient killing, and this results in the inhibition of NK-cell mediated cytotoxicity (Ishido et al., 2000b, Coscoy & Ganem 2001). K5 seems to act like a membrane bound E3 ubiquitin ligase, and influences trafficking of host cell membrane proteins by ubiquitination (Coscoy & Ganem 2001). Both K3 and K5 transcripts are expressed immediately after viral reactivation (Haque et al., 2000, Rimessi et al., 2001) and both proteins localise to the endoplasmatic reticulum (Coscoy & Ganem, 2000). To adress the issue how KSHV suppresses the immune response during latency, Tomescu et al. (2003) analysed the expression of endothelial cell surface proteins after infection with KSHV and found MHC class I, ICAM-1 and PE-CAM (CD31) to be downregulated.

KSHV vIRF-1 and -2 (see above) can inhibit interferon signal transduction by direct binding to cellular IRFs, the CREB binding protein and other transcription factors (Burysek et al., 1999, Li et al., 2000, Lin et al., 2001, Seo et al., 2000). vMIP-I and –II can bind to chemokine receptors and act as chemoattractants for monocytes and Th2 cells, but not for Th1, NK or dendritic cells (Kledal et al., 1997, Boshoff et al., 1997, Endres et al., 1999, Dairaghi et al., 1999, Sozzani et al., 1998, Weber et al., 2001). Finally, three transcripts generated by alternative splicing are derived from KSHV ORF4 (KCP) that shows homology to cellular complement control proteins. All three protein isoforms are able to inhibit the complement component of the innate immune system, pointing to a role in evading complement attack during viral replication or persistence (Spiller et al., 2003).

1.3 Signaling activity of terminal membrane proteins of γ-*herpesviridae*: common strategies and differences

The analysis of the genomes of the human γ_1-herpesvirus/lymphocryptovirus Epstein-Barr virus (EBV; Baer et al., 1984) and the human γ_2-herpesvirus/rhadinovirus Kaposis´s sarcoma-associated herpesvirus (KSHV; Russo et al., 1996), as well as the genomes of monkey rhadinoviruses Rhesus rhadinovirus (RRV; Alexander et al., 2000, Searles et al., 1999), Herpesvirus saimiri (HVS; Albrecht et al., 1992) and Herpesvirus ateles (HVA; Albrecht et al., 2000) revealed that they all code for terminal membrane proteins (TMPs) adjacent to the terminal repeat region of the herpesvirus genomes. In the genome orientation preferred in the γ_2-herpesvirus field, EBV codes for the latent membrane protein 1 (LMP1), KSHV for K1, RRV for R1, HVS for saimiri-transforming proteins (Stp) A, B or C and tyrosine kinase-interacting protein (Tip), and HVA for the two-in-one protein Tio at the far left side of the long unique region (figure 2). At the opposite side of the long unique region, the tumour viruses KSHV, EBV and RRV additionally code for multiply spliced genes: ORF K15, latent membrane proteins 2A/2B (LMP2A/B) and a hitherto unannotated predicted gene between ORF75 and the terminal repeats, R15, respectively (figure 2). All of these viral terminal membrane proteins have a cytoplasmic domain with motifs allowing interaction with cellular effector molecules, and are capable of initiating cellular signaling cascades involved in normal B-cell or T-cell signaling or cellular growth control (figures 3, 4 and 6).

The TMPs of the γ–herpesviruses have been reported to directly interact with a variety of cellular signaling molecules such as non-receptor protein tyrosine kinases (PTK), tumour-necrosis factor receptor-associated factors (TRAFs), Ras or Janus kinase (JAK), thereby initiating further downstream signaling cascades as for example the MAPK or PI3K/Akt pathway. Several transcription factors were found to be activated by the viral TMPs, such as NFAT, Oct-2, AP-1, NF-κB or STAT. An overview of the signaling activities of the different viral TMPs presented here are summarised in table 1 and figure 6. The transforming potential of LMP1, K1, R1, Stp and Tip has been clearly demonstrated in a variety of experimental settings (table 1). However, the specific contributions of many signaling cascades to the oncogenic properties remain to be elucidated. LMP2A, K1 and Tip have been shown to exert dominant negative effects on cellular B or T lymphocyte signaling via the B-cell and T cell antigen receptors.

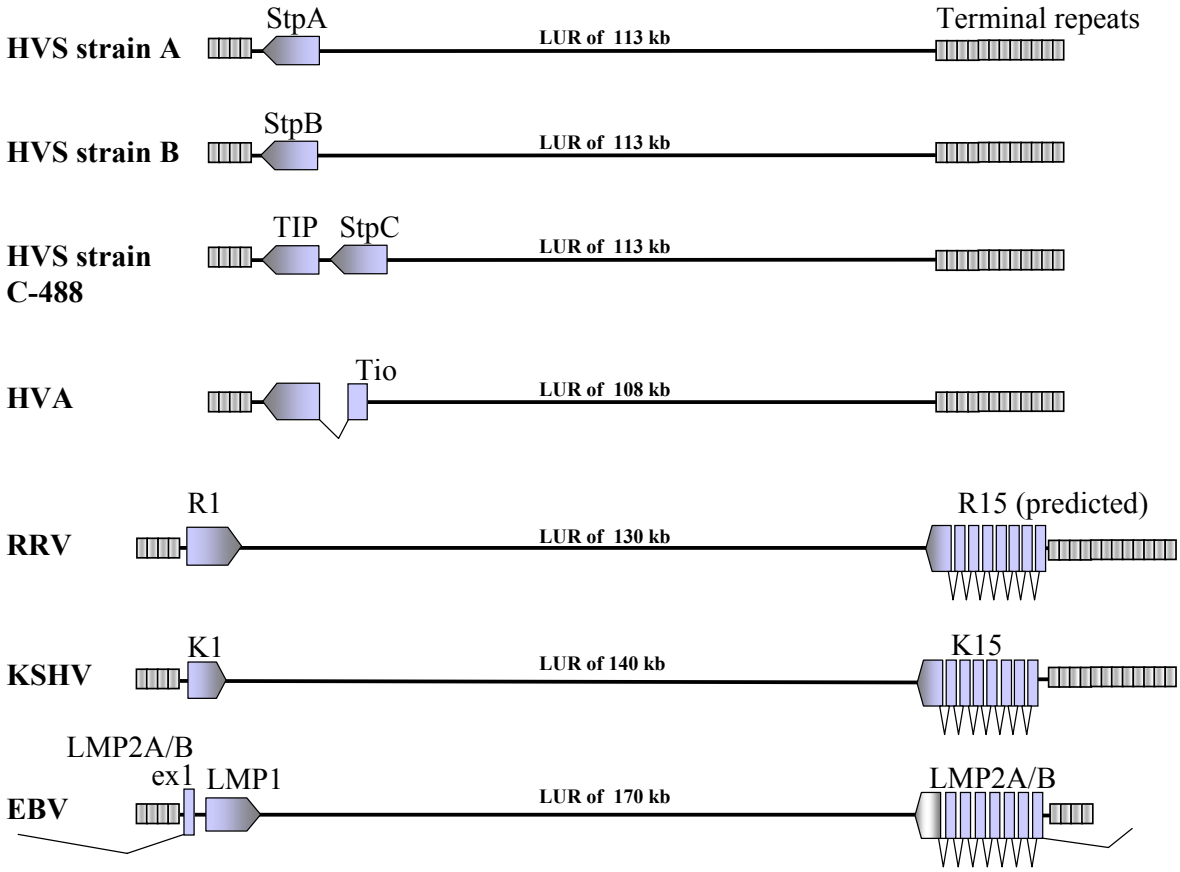

Figure 2: Genomic localisation of viral terminal membrane proteins of HVS, HVA, RRV, KSHV and EBV. At the "left" end of their genomes, monkey γ-herpesviruses HVS, HVA and RRV and human γ-herpesviruses KSHV and EBV code for membrane proteins with signaling activities and transforming potential. ORFs equivalent to R15, K15 or LMP2A/LMP2B, located at the "right" end of the viral genomes of RRV, KSHV and EBV, respectively, have not been identified so far in the genomes of HVA or HVS. The length of the terminal repeats flanking the long unique region (LUR) varies between the different herpesviruses (not to scale).

1.3.1 Epstein-Barr virus (EBV) and latent membrane proteins LMP1 and LMP2A

EBV, the only human member of the genus γ_1-herpesvirus/lymphocryptovirus, is associated with infectious mononucleosis and a variety of malignant diseases including African endemic Burkitt´s lymphoma (BL), Hodgkin´s disease, and lymphoproliferative disorders in immunodeficient individuals (reviewed in Rickinson & Kieff 2001). EBV is also associated with two epithelial malignancies: nasopharyngeal carcinoma (endemic in China) and oral hairy leukoplakia in AIDS patients (reviewed in Rickinson & Kieff 2001). In vitro, EBV can infect and efficiently transform and immortalize primary human B lymphocytes leading to the outgrowth of transformed and immortalized lymphoblastoid cell lines (LCLs) displaying elevated levels of several cellular activation antigens and adhesion molecules (reviewed in Rickinson & Kieff 2001). In LCLs, viral gene expression is restricted to a small subset of latent genes that encode six Epstein-Barr nuclear antigens (EBNA1, 2, 3A, 3B, 3C, and LP), three integral membrane proteins (LMP1, LMP2A, LMP2B), and two small nuclear RNAs

(reviewed in Farrell 1995). Five of these, namely EBNA1, 2, 3A, 3C, and LMP1, have been shown to be essential for the process of B-cell immortalization (reviewed in Izumi 2001).

1.3.1.1 LMP1

LMP1 has oncogenic properties

The latent membrane protein 1 (LMP1) is expressed in several EBV-associated malignancies, and this led to the suggestion that this protein contributes to tumourigenesis. The role of LMP1 as an oncoprotein has been clearly demonstrated in a variety of cell systems: LMP1 has transforming effects in rodent fibroblast cell lines, and Rat-1 cells expressing LMP1 are tumourigenic in nude mice (Baichwal & Sugden, 1988, Moorthy & Thorley-Lawson, 1993a, Wang et al., 1985, 1988b). In Rat-1 cells, LMP1 can induce loss of contact inhibition (Moorthy & Thorley-Lawson, 1993a, Wang et al., 1985). LMP1 alters the growth of EBV-negative Burkitt lymphoma lymphoblasts and of primary B lymphopcytes and induces many of the changes usually associated with EBV infection of primary B lymphocytes (Birkenbach et al., 1989, Peng & Lundgren, 1993, 1992, Peng-Pilon et al., 1995, Rowe et al., 1994, Wang et al., 1988a, 1990). LMP1 increases plasma membrane expression of adhesion molecules, induces higher levels of the lymphocyte function-associated antigen (LFA-1) mRNA and functionally activates adhesion (Wang et al., 1988a, b).

LMP1 expression can alter cell growth and gene expression in hematopoietic stem cells and epithelial cells (Dawson et al., 1990, Fahraeus et al., 1990, Fairbairn et al., 1993, Hu et al., 1993). Targeted expression of LMP1 in the skin or B-cell compartment of transgenic mice leads to the induction of epithelial hyperproliferation and lymphomagenesis, respectively (Kulwichit et al., 1998, Wilson et al., 1990). In monolayer cultures, LMP1 alters keratinocyte morphology and cytokeratin expression (Fahraeus et al., 1990), and cell differentiation is inhibited by LMP1 in raft cultures of immortalized human epithelial cell lines (Dawson et al., 1990). It has also recently been shown that LMP1 is critical for rendering LCLs tumourigenic in SCID mice (Dirmeier et al., 2003).

LMP1 is composed of six transmembrane domains and a cytoplasmic C-terminus with two distinct signaling regions termed CTAR-1/TES-1 and CTAR-2/TES-2

LMP1 contains a 24 aa arginine- and proline-rich hydrophilic N-terminus, followed by six transmembrane domains separated by five 8-10 aa long turns, and a 200 aa C-terminus rich in acidic residues (figure 3). LMP1, which has an apparent mass of 63 kDa, can be cleaved near the beginning of the C-terminal cytoplasmic domain (L^{242}), resulting in a soluble C-terminal domain of 25 kDa (Moorthy & Thorley-Lawson, 1990, 1993b). In addition, in the late lytic viral life cycle a lytic LMP1 protein is expressed that consists of transmembrane domains 5

and 6 and the C-terminal domain (Hudson et al., 1985), which does not have transforming capabilities (Baichwal & Sugden, 1989, Liebowitz et al., 1992).

Two regions in the C-terminal cytoplasmic domain of LMP1 have been defined to be critical for the contribution of LMP1 to the conversion of primary B lymphocytes to LCLs, and were therefore termed transformation effector sites (TES) 1 (aa 187-231) and 2 (aa 352-386) (Kaye et al., 1993, 1995, 1999, Izumi et al., 1997, 1999, Izumi & Kieff, 1997). Nearly the same regions were identified to be essential for the ability of LMP1 to activate the transcription factor NF-κB (Hammerskjold & Simurda, 1992, Laherty et al., 1992), and were therefore termed CTAR-1 (aa 194-232) and CTAR-2 (aa 351-386) for C-terminal NF-κB activating region (figure 3; Huen et al., 1995, Mitchell & Sugden, 1995, Floettmann & Rowe, 1997). NF-κB plays a key role in most of LMP1-stimulated gene expression (Devergne et al., 1998, He et al., 2000, Mehl et al., 2001, Zhang et al., 2001), and activation of the NF-κB pathway is linked to LMP1-induced immortalization of human primary B lymphocytes (Devergne et al., 1996, Izumi & Kieff, 1997, Cahir McFarland et al., 1999) and tumourigenic transformation of cultured rodent cells (He et al., 2000, Xin et al., 2001).

LMP1 induces the canonical and non-canonical NF-κB pathways

The mammalian NF-κB transcription factor is composed of dimers of p50 (precursor = p105), p52 (precursor = p100), p65/RelA, RelB and cRel that are complexed to inhibitor proteins called IκB. This leads to the retention of NF-κB in the cytoplasm in an inactive state. Two NF-κB pathways are described in the literature: the canonical (figure 35; reviewed in Ghosh & Karin 2002) and the very recently identified non-canonical/alternative pathway (figure 35; reviewed in Pomerantz & Baltimore 2002). The canonical pathway is triggered by inflammatory stimuli such as TNF-α, IL-1, double-stranded RNA and LPS. Upon stimulation, the IκB kinase (IKK) complex, consisting of the two catalytic subunits IKKα and IKKβ and the regulatory subunit IKKγ/NEMO, is activated and specifically phosphorylates the IκB proteins. Phosphorylation of IκB proteins leads to their ubiquitination and subsequent degradation by the proteasome, resulting in the release of NF-κB dimers (predominantly p50/RelA) and their translocation to the nucleus, where they act as transcription factors. This pathway depends on the IKK subunits IKKβ and IKKγ.

Only three cellular receptors have so far been described to signal via the non-canonical NF-κB pathway: CD40, B-cell activating factor receptor and lymphotoxin β-receptor (reviewed in Pomerantz & Baltimore 2002). This pathway involves the proteasome-mediated processing of the p52 precursor p100 to produce p52 and requires the MAP3K NIK and IKKα but is independent of IKKγ. Processing of p100 to p52 leads to the nuclear translocation of p52/RelB dimers. It is firmly established that LMP1 activates the canonical NF-κB pathway (see below). Very recently, three independent reports described the non-canonical NF-κB pathway to be targeted by LMP1 in fibroblast cell lines (Saito et al., 2003), in epithelial and

B-cells (Atkinson et al., 2003) and tumour tissue biopsies (Eliopoulos et al., 2003a). Thereby, LMP1 seems to activate the non-canonical pathway via CTAR-1 to induce processing of p100 to p52, resulting in the nuclear localisation of p52/RelB dimers, whereas it triggers the canonical pathway via CTAR-2 to induce p100 production (Saito et al., 2003, Atkinson et al., 2003).

LMP1 mimics cellular activated tumour necrosis factor receptors – interaction with TRAFs

Concerning the interaction of LMP1 with cellular effector proteins and downstream signaling effects, LMP1 mimics aspects of constitutively active tumour necrosis factor receptors (TNFR) such as CD40 or TNFR-1 (Brodeur et al., 1997, Devergne et al., 1996, 1998, Eliopoulos et al., 1999a,b, 1996, 1997, 1998, Floettmann et al., 1998, Franken et al., 1996, Hatzivassiliou et al., 1998, Kaye et al., 1996, Kilger et al., 1998, Miller et al., 1997b, Puls et al., 1999, Sandberg et al., 1997, Sylla et al., 1998, Uchida et al., 1999, Gires et al., 1997). Both LMP1 and activated CD40 receptor initiate overlapping signaling pathways that regulate major cell fate decisions including proliferation, differentiation, and apoptosis (reviewed in Baker & Reddy 1996). In LMP1 expressing transgenic mice for example, LMP1 can mimic CD40 signals to induce extrafollicular B-cell differentiation and blocks germinal center formation (Uchida et al., 1999).

LMP1 and CD40 share a PxQxT motif (figure 3; Devergne et al., 1996, Franken et al., 1996, Eliopoulos et al., 1997) that has been shown to be a binding site for TNFR-associated factors (TRAFs) (Ye et al., 1999, 2000). The PxQxT motif P^{204}QQAT of LMP1 is located to its CTAR-1 region (see figure 3). TRAFs are crucial downstream effector molecules of CD40 and other members of the TNFR family (Cheng et al., 1995, Hu et al., 1994, Rothe et al., 1994, Takeuchi et al., 1996). Whereas CD40 recruits TRAF molecules upon binding of CD40 ligand and receptor aggregation, LMP1 constitutively binds TRAFs through its CTAR-1 region. The binding affinity of the P^{204}xQxT motif of LMP1 is higher for TRAF-1 and -3 than for TRAF-2 and -5 (Mosialos et al., 1995, Brodeur et al., 1997, Devergne et al., 1996, 1998, Sandberg et al., 1997). TRAF-3 is discussed to act as a negative modulator by displacing TRAF-1 and TRAF-2 from CTAR-1 (Devergne et al., 1996, Kaye et al., 1996, Miller et al., 1997b).

LMP1 activates NF-κB via its CTAR-1 and CTAR-2 regions by directly interacting with TRAFs and TRADD

LMP1 is a potent activator of the transcription factor NF-κB. However, mutations in CTAR-1 that disrupt association with TRAF-2, -3 and -5 have little effect on NF-κB activation (Sandberg et al., 1997, Brodeur et al., 1997, Kieser et al., 1997, Devergne et al., 1998, Huen et al., 1995, Mitchell & Sugden, 1995). Via its CTAR-2 region, LMP1 directly associates with two proteins involved in apoptosis, TNFR-associated death domain (TRADD) and receptor

interacting protein (RIP) (Izumi & Kieff, 1997; see 1.2 and figure 3). However, unlike TNFR-1, LMP1 does not contain a death domain, nor does it induce cell death. In contrast, LMP1 signals via TRADD and RIP to TRAFs, which are known to mediate non-death signals from TRADD and RIP (Izumi & Kieff, 1997, Izumi et al., 1999a). A direct interaction of TRAFs and the CTAR-2 region of LMP1 has not been shown, but experiments with dominant negative TRAF-2 suggest that LMP1 and TRAF-2 might interact indirectly via this region (Kaye et al., 1996). A dominant negative mutant of TRAF-2 blocks NF-κB activation from CTAR-1 and CTAR-2, as do dominant negative mutants of the NF-κB-inducing kinase (NIK) or of IκB kinases (IKK) α and β (Kaye et al., 1996, Sylla et al., 1998). However, NIK may not be essential for NF-κB activation by LMP1 (Luftig et al., 2001).

An LMP1 CTAR-2 double mutant ($Y^{384}I$, $Y^{385}I$) that fails to interact with TRADD is defective in NF-κB activation and in B lymphocyte transformation (Izumi & Kieff, 1997), whereas RIP is not required for NF-κB activation (Izumi et al., 1999a). Although CTAR-1 is a weak NF-κB activator, it is sufficient for initial transformation, whereas CTAR-2, being the major NF-κB activating region, is insufficient for transformation in the absence of CTAR-1 (Izumi et al., 1997).

LMP1 has been reported to interact with HOS (homologue of slimb), a receptor for the $SCF^{\beta\text{-TrCP/HOS}}$ ubiquitin protein ligase (E3) that is involved in targeting the NF-κB inhibitory protein IκB for degradation thereby allowing NF-κB dependent transcription (Tang et al., 2003 and references therein). Based on the observation that mutations in the potential HOS binding site of LMP1 that abrogate HOS binding result in a more tumourigenic LMP1 variant, Tang et al. (2003) suggest that the extent of LMP1-induced NF-κB signaling could be restricted by its interaction with HOS.

In epithelial cells, LMP1 may enhance proliferative signals and protect cells from apoptosis by inducing the expression of the epidermal growth factor receptor (EGFR) and the antiapoptotic protein A20 (Miller et al., 1995a, Fries et al., 1996). TRAF binding to the P^{204}xQxT motif of LMP1 was shown to be nonessential in upregulating expression of CD40, Fas, adhesion molecules ICAM-1 and LFA-3, but critical in upregulating TRAF-1 and the EGFR (Devergne et al., 1998, Miller et al., 1998). However, Mehl et al. (2001) found NF-κB to be critical for ICAM-1 upregulation by LMP1.

LMP1 signals via MAPK pathways

Since LMP1 is able to transform Balb 3T3 cells without inducing NF-κB (Baichwal & Sugden, 1988, Martin et al., 1993, Mitchell & Sugden 1995), its transforming potential seems not to depend on NF-κB alone. Both AP-1 (activator protein 1) and NF-κB family members are proto-oncogenes, whose aberrant activation contributes to tumour formation (reviewed in Baeuerle & Baltimore 1996 and Karin et al., 1997). LMP1 has been shown to activate the transcription factor AP-1 via mitogen-activated protein kinases (MAPKs) c-jun N-terminal

kinase 1 (JNK1) and p38 in B-cells and epithelial cells (figure 6; Eliopoulos & Young 1998, Eliopoulos et al., 1999a, b, Kieser et al., 1997). In 293 epithelial cells, activation of JNK was dependent on aa 379-384 overlapping the CTAR-2 domain and TRADD binding domain, but not on CTAR-1 (Eliopoulos & Young 1998, Kieser et al., 1997, Eliopoulos et al., 1999b, Kieser et al., 1999). However, a subsequent study showed that expression of the LMP1 CTAR-1 domain may result in JNK activation in cell lines expressing TRAF-1, and TRAF-1 and TRAF-2 were demonstrated to be critical modulators of JNK signaling by the CTAR-1 region of LMP1 (Eliopoulos et al., 2003b).

Filopodia formation promoted by LMP1 in fibroblasts and cells of epithelial and B-cell origin (reviewed in Eliopoulos & Young, 2001) was shown to be mediated by the small GTPase Cdc42, independently of TRADD and TRAF-2 (Puls et al., 1999). Whereas CTAR-2 mediated NF-κB activation involves TRADD and TRAF-2, LMP1 signaling to JNK1 is independent of TRADD, RIP and the p21 Rho-like GTPases Rac1 and Cdc42 (Kieser et al., 1999, Wan et al., 2004). A recent study employing embryonic fibroblasts from different knockout mice and the small interfering RNA technique revealed that LMP1 activates JNK1 via TRAF-6, the mitogen-activated protein kinase kinase kinase (MAPK3K) TAK1, and the c-jun N-terminal kinase kinases (JNKK) 1 and 2 (Wan et al., 2004). In lymphoid cells, CTAR-2 mediated JNK activation does not involve TRAF-1 but partially depends on TRAF-2 (Eliopoulos et al., 2003b).

Furthermore, LMP1 activates the MAPK p38 through CTAR-1 and -2, which seems to involve TRAF-6 downstream of the P^{204}xQxT motif in CTAR-1 and TRADD (Eliopoulos et al., 1999a, Schultheiss et al., 2001). In epithelial cells, TRAF-6 is recruited to LMP1 complexes in the plasma membrane, but binding to LMP1 seems to be indirect (Schultheiss et al., 2001). p38 has been shown to mediate cytokine induction by LMP1 (Eliopoulos et al., 1999a, Vockerodt et al., 2001). In Rat-1 fibroblasts, LMP1 induces the MAPKs extracellular signal-regulated kinases 1 and 2 (Erk1/2) via Ras, and co-transfection of a dominant negative Ras mutant impaired the ability of LMP1 to induce transformation (Roberts & Cooper, 1998). However, Kieser et al. (1997) did not see any activation of Erk2 by LMP1 in epithelial cells. Eliopoulos et al. (2002) identified the oncogenic serine/threonine kinase Tpl-2 as a component of LMP1-induced NF-κB signaling in epithelial cells. Tpl-2 is activated upon LMP1 expression, interacts with TRAF-2 and expression of a catalytically inactive Tpl-2 mutant inhibited LMP1-induced NF-κB activation (Eliopoulos et al., 2002). Tpl-2 has been shown to interact with and activate NIK (Lin et al., 1999), and is also critical for activation of MAPKs Erk (Dumitru et al., 2000, Hagemann et al., 1999, Patriotis et al., 1994) and JNK (Salmeron et al., 1996).

The region between CTAR-1 and CTAR-2: aa 233-350

The region between CTAR-1 and -2 (aa 233-350) includes four direct imperfect repeats of a conserved PQDPDNTDDNG sequence, a PPQLT sequence (aa 320-324) that resembles a PxQxT/S TRAF binding core but does not function as one, a protease cleavage site (between aa 241 and 242), 19 potential serine or threonine phosphorylation sites and sequences that vary in human isolates and have been reported to affect the ability of LMP1 to transform immortalized rodent fibroblasts (Fennewald et al., 1984, Hu et al., 1991, Li et al., 1996, Mehl et al., 1998). The region encompassing aa 233-350 is not critical for B lymphocyte growth transformation (Izumi et al., 1999b).

LMP1 is phosphorylated at residues serine (S^{313}) and threonine (T^{324}), but not on tyrosine residues, and phosphorylation was shown not to be crucial for the transforming activity of LMP1 (Baichwal & Sugden 1987, Mann & Thorley-Lawson 1987, Moorthy & Thorley-Lawson 1993b). The N-terminus and phosphorylation seem to be important for the degradation of LMP1 by the proteasome (Aviel et al., 2000).

LMP1 interacts with Janus kinase (JAK) 3 and activates STATs

Constitutively active STATs have been found in a variety of human cancers (reviewed in Bowman et al., 2000) as well as in a variety of EBV-associated malignancies (Weber-Nordt et al., 1996, Chen et al., 2001, Kube et al., 2001). In epithelial cells, LMP1 expression was associated with an increase in activated STAT-3 and -5, and expression of constitutively activated STAT-3 upregulated LMP1 protein expression, suggesting a positive feedback loop between LMP1 and STAT-3 (Chen et al., 1999, 2001a, 2003).

One group demonstrated that LMP1 interacts with the Janus kinase (JAK) 3 in epithelial and EBV immortalized B-cells via the region between CTAR-1 and CTAR-2 and activates JAK 3 and STAT-1 and -3 (Gires et al., 1999). Another group did confirm JAK3 binding to LMP1, but not via aa 233-352, and did not find LMP1 induced activation of JAK3 or STAT-3 in B lymphoma or LCLs (Higuchi et al., 2002).

LMP1 signaling leads to activation or repression of several factors implicated in the control of cellular proliferation and apoptosis

The suppression of apoptotic death is a function of LMP1 that contributes to its oncogenicity. One well characterised mechanism by which LMP1 protects against apoptosis is the upregulation of the expression of several antiapoptotic proteins such as Bcl-2, A20 and Mcl-1 (Fries et al., 1996, Henderson et al., 1991, Gregory et al., 1991, Martin et al., 1993, Laherty et al., 1992, Milner et al., 1992, Rowe et al., 1994, Wang et al., 1996). The promoter activity of the Bcl-2 family member Bfl-1, which has been shown to possess cell proliferation

and transforming activities in vitro, is stimulated by LMP1 in EBV-negative BL-derived cell lines through TRAF-2 and NF-κB (D´Souza et al., 2004).

Transforming growth factor (TGF) β, a tumour suppressor cytokine that inhibits cell proliferation due to cell cycle arrest in the G_1 phase (reviewed in Massague 2000), as well as Smad-mediated transcriptional responses are inhibited by LMP1 in epithelial cells and fibroblasts, depending on NF-κB induction by LMP1 (Prokova et al., 2002). However, whereas one study showed that LMP1 also causes loss of TGF β-mediated growth inhibition in B lymphocytes (Arvanitakis et al., 1995), this observation was not confirmed by another study (Inman & Allday, 2000).

LMP1 represses the expression of E-cadherin, an invasion-suppressor gene, and triggers the invasive potential of cells (Fahraeus et al., 1992, Kim et al., 2000). The repression of E-cadherin gene expression seems to be mediated by activation of cellular DNA methyltransferases by LMP1 (Tsai et al., 2002).

Furthermore, LMP1 induces the antiapoptotic PI3K/Akt pathway to promote cell survival and to induce actin remodelling via its P^{204}xQxT motif (Dawson et al., 2003), downregulates transcriptional expression of the metastasis suppressor gene RECK via the MAPK Erk in an EBV negative nasopharyngeal carcinoma cell line (Liu et al., 2003), prevents Ras-induced senescence in human fibroblasts and blocks expression of the $p16^{INK4a}$ tumour suppressor gene (Yang et al., 2000b).

The $p16^{INK4a}$-Retinoblastoma protein pathway plays a critical role in preventing inappropiate cell proliferation, and recently it has been shown that LMP1 inactivates the transcription factor Ets2, known to induce $p16^{INK4a}$ expression in Ras-induced senescence (Ohtani et al., 2001), by promoting the intracellular redistribution of Ets2 from the nucleus into the cytoplasm (Ohtani et al., 2003). In addition, LMP1 inactivates the downstream mediators of the $p16^{INK4a}$-RB growth arrest pathway, E2F4 and E2F5 (Gaubatz et al., 2000, Ohtani et al., 2003). Manipulation of E2F4 seems to depend on both CTAR regions and involves the MAPK Erk pathway.

The LMP1 transmembrane domains are essential for signaling and localisation to lipid rafts

Besides the C-terminal domain of LMP1, its aminoterminal and transmembrane regions play a pivotal role in efficient signaling. The LMP1 N-terminus is crucial for the correct orientation of the transmembrane domains in the membrane (Coffin et al., 2001). LMP1 is able to form aggregates via its transmembrane domains, apparent by the formation of patches in the plasma membrane (Hennessy et al., 1984, Liebowitz et al., 1986, 1987). LMP1 mutants lacking parts of the N-terminal transmembrane domains localise to the plasma membrane in Balb/c 3T3 cells or LCLs, but do not form aggregates, show no transforming activity and are not able to induce cellular gene expression (Baichwal & Sugden et al., 1989, Wang et al., 1988a, Martin & Sugden, 1991, Kaye et al., 1993, Liebowitz et al., 1992, Devergne et al., 1998).

A chimeric protein composed of the six transmembrane domains of LMP2A (see 1.3.1.2) and the C-terminal domain of LMP1 was not able to activate NF-κB (Kaykas et al., 2002). The capacity of LMP1 to signal constitutively in the absence of any ligand is mediated by its transmembrane domains, since a chimeric protein composed of the N-terminus and transmembrane domains of LMP1 and the C-terminal part of CD40 can signal in the absence of CD40 ligand (Floettmann & Rowe, 1997, Gires et al., 1997, Hatzivassiliou et al., 1998).

LMP1 also localises to intracellular membranes and the cytoskeleton and is associated with lipid rafts (Ardila-Osorio et al., 1999, Liebowitz et al., 1986, 1987, Mann & Thorley-Lawson, 1987, Moorthy & Thorley-Lawson, 1990, 1993b, Clausse et al., 1997, Kaykas et al., 2000, Higuchi et al., 2001). Transmembrane domains 1 and 2 were shown to be sufficient for lipid raft association (Coffin et al., 2003).

CD40, which translocates to lipid rafts upon activation with CD40 ligand, as well as LMP1 recruit TRAF-3 to lipid rafts, and efficient signaling of LMP1 from lipid rafts is only achieved by the full length LMP1 protein (Kaykas et al., 2001, Brown et al., 2001). Interestingly, TRAF-3 was found to be degraded after CD40 signaling, but not after LMP1 signaling (Brown et al., 2001). However, whereas activated CD40 signals as a trimeric form, neither the structure nor the extent to which LMP1 aggregates is known (Kaykas et al., 2001).

Lam & Sugden (2003) observed that the majority of LMP1 is localised to and signals from lipid rafts of intracellular membranes in the EBV-immortalized lymphoblastic cell line 721 and 293 cells, and is only detected at low levels at the plasma membrane. In intracellular compartments, LMP1 was shown to associate with TRADD and to actively recruit TRAF molecules (Lam & Sugden 2003). LMP1 protein expression was also observed in extracellular vesicles (Vazirabadi et al., 2003, Flanagan et al., 2003).

When LMP1 is expressed in a variety of cells it inhibits their proliferation by the induction of cytostasis (Cuomo et al., 1992, Floettmann et al., 1996, Hammerschmidt et al., 1989), and this ability has been attributed to its amino terminus and its transmembrane domains (Kaykas & Sugden 2000).

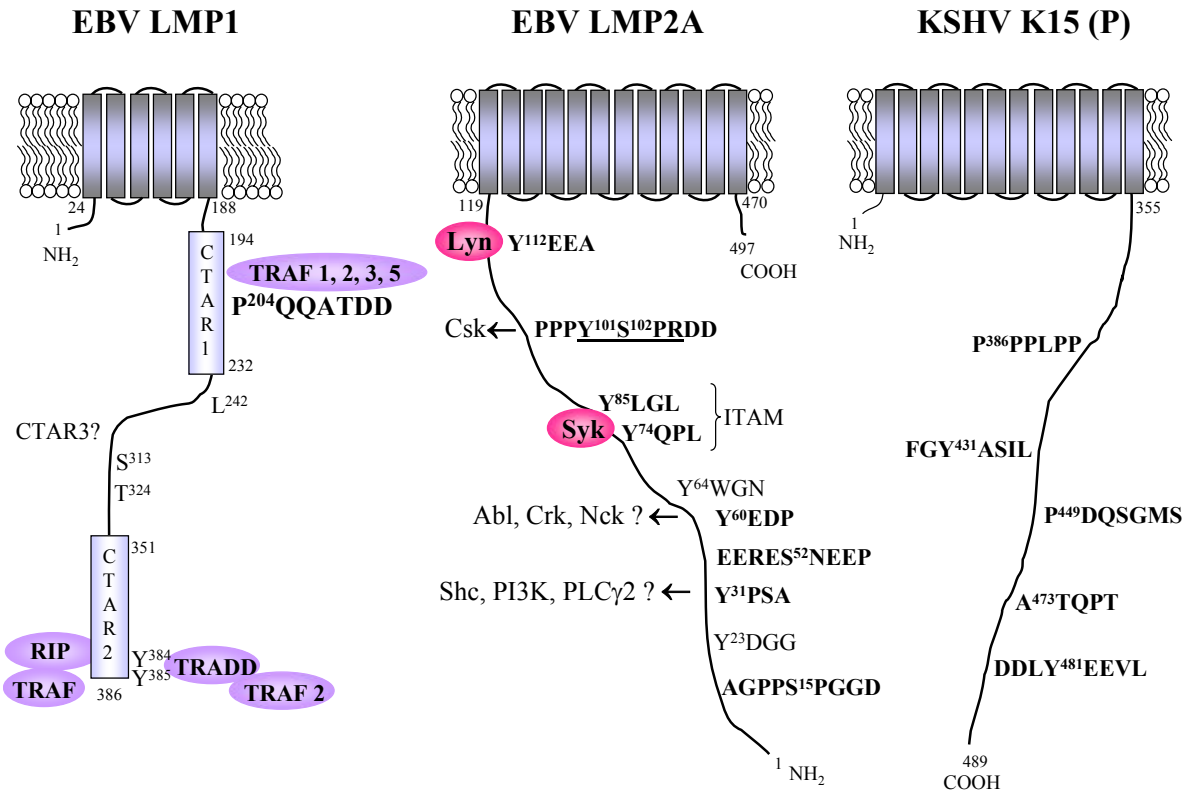

Figure 3: Structures of viral terminal membrane proteins LMP1, LMP2A and K15. EBV LMP1 is a potent inducer of the NF-κB and MAPK pathways and has transforming properties. It interacts via its C-terminal activator regions (CTAR-1 aa 194-232, CTAR-2 aa 351-386) with a variety of cellular proteins, including TRAFs, TRADD and RIP (see text and figure 6). Both regions activate the IκB kinases causing phosphorylation of IκB, IκB degradation and NF-κB activation, and also activate MAPKs JNK1 and p38 (see figure 35). The six transmembrane domains enable LMP1 to aggregate in the plasma membrane. Both the transmembrane domains and the cytoplasmic C-terminus are essential for primary B lymphocyte growth formation. EBV LMP2A contains 12 transmembrane domains and interacts with protein tyrosine kinases Lyn and Syk via SH2-B domains located in its amino-terminal cytoplasmic tail, thereby blocking signaling of the B-cell antigen receptor in vitro. KSHV K15 is, in terms of structural organization and genomic localisation (see figure 5), very similar to the EBV LMP2A protein and contains, as LMP2A, putative SH2-B motifs. The presence of motifs that are reminiscent of TRAF binding sites in the K15 cytoplasmic C-terminus indicate that K15 could share functional features with EBV LMP1.

1.3.1.2 LMP2A

The LMP2 genes code for proteins with multiple transmembrane domains

The two LMP2 genes LMP2A and LMP2B are transcribed into two mRNAs across the circularized viral genome (i.e. across the terminal repeats) from two spatially distinct promoter elements. Both transcripts are multiply spliced, and exons 2-9 are shared by both mRNAs (see figures 2 and 5). Exon 1 of LMP2A codes for a 119 aa hydrophilic N-terminal cytoplasmic domain, whereas exon 1 of LMP2B is noncoding with translation beginning in the common exon 2 before the first transmembrane sequence (figures 2 and 5; Laux et al., 1988, 1989, Sample et al., 1989). The remaining exons are encoding twelve transmembrane

domains and a 27 aa hydrophilic C-terminus (figure 3). LMP2A (497 aa) and LMP2B (378 aa) form patches in the plasma membrane of latently EBV infected B lymphocytes, and LMP2A patches colocalise with LMP1 (Longnecker et al., 1991, Longnecker & Kieff 1990). In transfected B-cells and epithelial cells LMP2A and B have been described to colocalise in perinuclear regions/the trans-Golgi network (Lynch et al., 2002).

The LMP2A N-terminus contains potential SH2-B motifs, two of which compose an ITAM

The LMP2A 119 aa N-terminal cytoplasmic domain includes eight tyrosines (depicted in figure 3), some of which are constitutively phosphorylated (Longnecker et al., 1991). Each of these phosphorylated tyrosines is situated in a context suitable for interaction with Src-homology 2 domain (SH2) containing proteins (depicted in figure 3; reviewed in Longnecker 2000). Many cellular signaling proteins (e.g. lymphocyte receptors, adaptor proteins, protein kinases, transcription factors) contain SH2-binding (SH2-B) domains of the consensus sequence YXXL/I/V. When these domains are tyrosine phosphorylated, direct binding of SH2 domain containing proteins such as non-receptor protein tyrosine kinases (PTKs) and phosphatidylinositol-3 kinase (PI3K) can occur (reviewed in Pawson & Scott 1997). Motifs of the consensus YXXA/P/T also have been described as being SH2-B sites, and the Y^{112}EEA motif, the site of Lyn PTK binding in LMP2A (Fruehling et al., 1998), is clearly homologous to the Src family PTK preferred SH2-B motif YEEI (Songyang et al., 1993, 1994). Except for Y^{64} and Y^{23}, contained in tyrosine motifs that have no predicted specificity to any identified SH2 domain, all tyrosines were found to be highly conserved between LMP2A genes of different virus isolates (reviewed in Longnecker 2000). Tyrosine residues Y^{74} and Y^{85} (Y^{74}QPL and Y^{85}LGL) of LMP2A form an immunoreceptor tyrosine-based activation motif (ITAM; consensus sequence: stretch of negatively charged aa followed by two SH2-B motifs spaced 7-10 aa apart [$(D/E)X_7(D/E)X_2YX_2LX_{7\text{-}10}YX_2L/I$], figure 3).

ITAMs are present in a variety of cellular immunoreceptors such as the B-cell and T-cell antigen receptors (BCR, TCR), and it has been shown that ITAMs play a central role in signal transduction of these receptors. In primary B lymphocytes, activation of the BCR leads to an intricate signal cascade: initially, Src family PTKs are recruited and activated, followed by recruitment and activation of Syk PTK and binding of the B-cell linker protein SLP-65, the phospholipase PLCγ, the Vav guanine nucleotide exchange factor, PI3K, and the Grb2 and Nck adaptor proteins (Fu et al., 1998, Ishiai et al., 1999, Wienands et al., 1998). These initial interactions lead to further downstream signals such as mobilization of calcium and activation of the Ras/MAPK pathway and protein kinase C (PKC), subsequently resulting in transcriptional activation of genes associated with B-cell activation (Buhl et al., 1997, reviewed in Cambier et al., 1994 and Benschop & Cambier 1999).

Furthermore, serine residues in the amino terminal domain of LMP2A are situated in contexts that could serve as potential recognition motifs for serine-threonine kinases (Songyang et al., 1996): AGPPS^{15}PGGD and PPPYS^{102}PRDD for MAP kinases and

EERES^{52}NEEP for Casein kinase II. Indeed, LMP2A has been shown to be phosphorylated in vivo on serine and threonine residues (Longnecker et al., 1991), and to be associated in vivo with the MAPK Erk1, which can phosphorylate LMP2A at residues S^{15} and S^{102} in vitro (Panousis & Rowe 1997).

LMP2A blocks BCR signaling in LCLs and maintains viral latency

Normal BCR signal transduction following BCR cross-linking is blocked in LCLs generated with wildtype EBV as measured by calcium mobilization, cellular kinase activation, induction of tyrosine phosphorylation and activation of gene transcription. In contrast, BCR signal transduction was found to be normal in LCLs infected with a recombinant EBV from which LMP2A had been deleted (Miller et al., 1993, 1995b). From these experiments it is concluded that LMP2A is sufficient to block BCR signaling in LCLs.

In these LCLs, the N-terminal region of LMP2A was found to be constitutively tyrosine phosphorylated and to be stably associated with Src family PTKs (Lyn and Fyn) and the Syk PTK (Burkhardt et al., 1992, Miller et al., 1995b). The Y^{112} of the SH2-B motif Y^{112}EEA essential for Lyn binding, and Y^{74} and Y^{85} of the ITAM mediating Syk binding, were both required for blocking BCR signaling (Fruehling et al., 1996, 1998, Fruehling & Longnecker 1997). In contrast, tyrosine residues Y^{23}, Y^{31}, Y^{60}, Y^{64} and Y^{101} were shown to be not required for this purpose (Fruehling et al., 1996, Swart et al., 1999).

LMP2A/B do not affect EBV transformation of primary B lymphocytes into LCLs, LCL survival or viral replication (Kim & Yates 1993, Longnecker et al., 1992, 1993a,b, Rochford et al., 1997, Speck et al., 1999). These studies with EBV recombinants revealed that BCR cross-linking on LCLs with null mutations in LMP2A results in normal BCR signal transduction and activation of the lytic viral life cycle of EBV, whereas in the presence of LMP2A, lytic infection is blocked. This block can be bypassed by raising intracellular free calcium levels by phorbol ester treatment (Miller et al., 1994a, b). Hence, since LMP2A is expressed in most latently infected B lymphocytes in vivo, it is postulated to have a role in maintaining viral latency.

LMP2A interacts with ubiquitin ligases via its PPPPY motifs and localises to lipid rafts

The N-terminal domain of LMP2A includes several proline-rich motifs reminiscent of SH3-binding (SH3-B) domains (reviewed in Pawson & Gish 1992) and WW domain interaction sites (reviewed in Sudol 1996). SH3-B domains are proline-rich regions recognized by proteins carrying noncatalytic SH3 domains. Many cellular kinases and adaptor proteins that are essential for diverse signal transduction pathways linking cellular receptors to downstream signaling events carry such SH3 domains. WW domains consist of paired tryptophane residues separated by 20-22 aa and specifically bind to the motif XPPXY (reviewed in Sudol 1996), of which LMP2A has two (PPPPY^{60} and PPPPY^{101}). However, no SH3 domain

containing proteins have been reported to interact with LMP2A via its potential SH3-B domain so far, but LMP2A has recently been shown to bind to several members of the Nedd4-like ubiquitin protein ligase family via its PPPPY motifs. This interaction results in ubiquitination and degradation of LMP2A and LMP2A-associated proteins such as Lyn and Syk (Longnecker et al., 2000, Ikeda et al., 2000, 2001, 2002, Winberg et al., 2000).

One model proposes that LMP2A, acting as an activated BCR, exerts its dominant negative effect on BCR signaling by withdrawing Src family PTKs and Syk from the BCR and targets them for degradation by its association with ubiquitin ligases. However, the PPPPY motifs of LMP2A do not seem to be essential for blocking BCR signaling in LCLs (Ikeda et al., 2001), which argues against this model. The dominant negative effect of LMP2A on BCR signaling could be mediated by its localisation to lipid rafts in LCLs: LMP2A was shown to exclude the BCR from entering lipid rafts where the BCR would otherwise initiate normal B-cell signaling (Dykstra et al., 2001). A C-terminal motif of LMP2A seems to mediate physical interaction of LMP2A with heterologous transmembrane molecules or between LMP2A molecules (Matskova et al., 2001), but the relevance of this observation for LMP2A function has not been investigated so far.

LMP2A drives B-cell development in vivo

In strong contrast to the data obtained with EBV transformed LCLs, LMP2A was shown to provide survival and development signals in an LMP2A transgenic mouse cell line with B-cell specific expression of LMP2A (Caldwell et al., 1998). Interestingly, this LMP2A transgenic mouse line showed a reduction in the number of BCR-positive B-cells. Contrary to expectations, even BCR-negative cells were capable of progressing out of the bone marrow and entering the peripheral immune system where they subsequently persist. Further, LMP2A is able to drive B-cell development when this LMP2A mouse line is crossed into a recombinase-activating gene (RAG) null background (Caldwell et al., 2000). In wild type mice, cells either lacking the BCR or B-cells of RAG knockout mice would not be able to proceed with normal B-cell development. The ITAM motif was proven to be critical for this LMP2A function (Merchant et al., 2000).

One in vivo downstream effector of LMP2A in B-cells of LMP2A transgenic mice was identified to be the adaptor protein SLP65 (SH2-domain containing leukocyte protein) (Engels et al., 2001). Studies with LMP2A transgenic mice indicate that Nedd4 ubiquitin ligases downregulate LMP2A activity in B-cells in vivo (Ikeda et al., 2003).

DNA microarrays of primary B-cells from LMP2A transgenic mice, LMP2A-expressing human B-cell lines and LMP2A-positive and -negative LCLs revealed that LMP2A has multiple effects on global gene expression. It increases expression of genes associated with cell cycle induction and inhibition of apoptosis, alters the expression of genes involved in DNA and RNA metabolism and decreases expression of B-cell specific factors and genes associated with immunity (Portis & Longnecker 2003, 2004, Portis et al., 2003). Notably,

these alterations mirror those described for Hodgkin/Reed-Sternberg cells present in Hodgkin lymphoma, in which LMP2A transcripts have been identified (Portis et al., 2003, reviewed in Thorley-Lawson 2001).

The function of LMP2A in epithelial cells differs from its function in B-cells

In epithelial cells, LMP2A function might differ from that in B-cells. Tyrosine phosphorylation of LMP2A in epithelial cells was triggered by cell adhesion to extracellular matrix proteins and was not mediated by Src PTKs but by the C-terminal Src kinase (Csk, a negative regulator of Src) in vivo and in vitro, with the ITAM being the major site of in vitro phosphorylation (Scholle et al., 1999, 2001). Most notably, LMP2A has transforming capabilities and inhibits cell differentiation in the human keratinocyte cell line HaCaT (Scholle et al., 2000). In HaCaT cells and in telomerase-immortalized human foreskin fibroblasts (HFK), LMP2A activated the serine/threonine kinase Akt (but not MAPK activity) (Scholle et al., 2000, Morrison et al., 2003). Akt is implicated in the inhibition of apoptosis and is physiologically activated upon BCR crosslinking via the PI3K signaling pathway. Activation of Akt seemed to be responsible for cellular transformation induced by LMP2A in HaCaT cells (Scholle et al., 2000).

In HFK cells, Akt activation by LMP2A leads to phosphorylation and inhibition of the pro-apoptotic forkhead transcription factor (FKHR) and of the glycogen synthase kinase 3 β (GSK-3β). Inhibition of GSK-3β by LMP2A results in the stabilization of the proto-oncogene β-catenin (Morrison et al., 2003). In B-cells, LMP2A expression also mediates constitutive activation of Akt via PI3K, depending on Syk and Lyn, but in the absence of a survival phenotype (Miller et al., 1995b, Swart et al., 2000). However, transgenic expression of LMP2A in mouse epithelium showed no effect on epithelial differentiation and survival (Longan & Longnecker 2000).

In 293 epithelial cells stably transfected with LMP2A, MAPKs Erk2 and JNK, but not p38 were found to be activated, and activation of the Erk pathway was implicated in LMP2A-mediated cell migration (Chen et al., 2002). Interestingly, cross-linking of the BCR of EBV transformed LCLs failed to induce MAPK activity, but treatment with phorbol esters could bypass this block (Panousis & Rowe, 1997). In epithelial cells, LMP2A localised to internal membranes but did not colocalise with LMP1 (Dawson et al., 2001). LMP2A, but not LMP2B, was able to augment LMP1-mediated signal transduction by prolonging its half-life in epithelial cells (Dawson et al., 2001).

1.3.2 R1 and R15 of Rhesus rhadinovirus (RRV)

RRV has been isolated three years after the discovery of KSHV (Desrosiers et al., 1997) and two viral isolates have been completely sequenced, RRV 17577 (Searles et al., 1999, AF083501) and RRV 26-95 (Alexander et al., 2000, AF210726). RRV belongs to the old world RV-2 lineage of γ_2-herpesviruses and has been predominantly detected in B lymphocytes (Mansfield et al., 1999). Genomic analysis revealed the existence of an ORF at the left hand side of the long unique region that codes for a membrane protein which was termed R1 due to its resemblance to KSHV K1 (see 1.3.5; Alexander et al., 2000, Searles et al., 1999).

The right hand side of the long unique region of RRV, between ORF75 and the terminal repeat region, has the potential to encode an ORF reminiscent of EBV LMP2A and KSHV K15 (see figure 2, 1.3.1.2 and 1.3.6). This ORF was therefore termed R15 for RRV 26-95 by Alexander et al. (2000). R15 has not been experimentally analysed, but computational analysis of the region between ORF75 and the terminal repeats revealed an ORF with a potential splicing pattern strikingly similar to K15 and LMP2A (our observations, see figure 2). This ORF has the potential to encode a transmembrane protein composed of 11 transmembrane domains joined to a cytoplasmic C-terminus (our observations, see chapter 3.1 and figure 9). The cytoplasmic domain would be predicted to contain several SH3-B motifs and motifs suitable for phosphorylation by cellular kinases (our observations).

R1 is a type I transmembrane protein

The ORF R1, located at the left side of the RRV genome (figure 2), codes for a type I transmembrane protein of 423 aa (figure 4) with a predicted molecular mass of 48 kDa (Damania et al., 1999). R1 has an apparent mass of 70 kDa in SDS-PAGE and is glycosylated, most likely at its N-terminal extracellular domain (aa 1-224) where it carries eight potential N-linked glycosylation sites (NXT or NXS). With respect to its N-terminal extracellular domain, R1 shares 27% identity (40% similarity) with the K1 protein of KSHV (see 1.3.5) and shows homology to a human immunoglobulin G receptor CD16 (Damania et al., 1999). The extracellular domains of K1 and R1 contain cysteine residues that may form disulfide linkages similar to members of the immunoglobulin receptor superfamily.

Immunofluorescence studies with C-terminally tagged full length R1 protein revealed that it localises to the cytoplasm, and the authors proposed a possible endosomal localisation since R1 contains Y-X_2-hydrophobic motifs that have been shown to serve as internalization signals of plasma membrane proteins (reviewed in Trowbridge et al., 1993), and a dileucine repeat (aa 318 and 319) which may also act as an endocytosis signal (Damania et al., 1999).

R1 contains several potential SH2-binding motifs and elicits B-cell activation signals

The single transmembrane domain of R1 is succeeded by a long cytoplasmic C-terminal domain of 170 aa (aa 253-423), which contains a number of potential SH2-binding (SH2-B) domains (depicted in figure 4). The five distal SH2-B motifs are of the consensus sequence YXXL and of these, motifs Y^{394}HGL and Y^{407}NHL or Y^{407}NHL and Y^{419}DWL could potentially resemble an ITAM motif, but there is no evidence so far for this potential ITAM to be functional. The five membrane proximal motifs are of the consensus YXXA/P/T/V, which also have the potential to bind to SH2 domain containing proteins (Damania et al., 1999). Full length R1 directly interacts with the PTK Syk but not Src, and is in vitro and in vivo phosphorylated by Syk (Damania et al., 2000a).

A chimeric protein consisting of the extracellular and transmembrane domain of the CD8 receptor fused to the cytoplasmic tail of R1 is capable of eliciting intracellular calcium mobilization in B-cells and cellular tyrosine phosphorylation upon stimulation with an α-CD8 antibody (Damania et al., 2000a). Furthermore, this chimera induces the activity of the B- and T-cell specific transcription factor NFAT (nuclear factor of activated T-lymphocytes) upon α-CD8 stimulation in reporter assays in stably transfected and sorted B-cells, but also full length R1 was able to do so without stimulation in transiently transfected B-cells, but to a lower extent (Damania et al., 2000a). These results show that R1 is capable of inducing events leading to B-lymphocyte activation, however, attempts to define the domains in the cytoplasmic tail of R1 being crucial for these activities failed so far.

R1 shows oncogenic properties

The oncogenic potential of R1 was shown in two different systems: Expression of R1 in rodent fibroblasts (Rat-1) induces morphological changes and focus formation, and injection of R1 expressing Rat-1 cells into nude mice results in formation of multifocal tumours (Damania et al., 1999). When the Stp (saimiri-transforming protein, see 1.3.3) gene in the HVS genome was replaced with either the R1 or K1 (see 1.3.5) gene under control of the Stp promoter, these recombinant viruses could immortalize T lymphocytes from common marmosets to IL-2 independent growth, similar to wildtype HVS containing the oncogenic Stp protein (see 1.3.3; Damania et al., 1999).

1.3.3 Saimiri transforming protein (Stp) and tyrosine kinase interacting protein (Tip) of Herpesvirus saimiri (HVS)

The simian herpesviruses HVS and Herpesvirus ateles (see 1.3.4) are unique in their ability to induce T-cell lymphomas and leukemias in several primate species (Daniel et al., 1974, Melendez et al., 1969a, b, reviewed in Fickenscher & Fleckenstein 2001). HVS, a T-cell specific virus, naturally persists in squirrel monkeys without causing disease (Melendez et al., 1968, Falk et al., 1972). The far left end of the HVS genome was found to be highly variable, and HVS strains were therefore classified into the three subgroups A, B and C which differ with respect to their oncogenic potential (Medveczky et al., 1984, 1989, Desrosiers & Falk 1982). Strains of all subgroups are able to induce T-cell lymphomas in cottontop marmosets, but only members of subgroup A and C cause disease in common marmosets (Duboise et al., 1998a).

HVS strains A and C immortalize common marmoset T-lymphocytes to IL-2 independent growth, and the most highly oncogenic HVS strain C can also immortalize human, rabbit and rhesus monkey lymphocytes and cause fulminant lymphoma in rhesus monkeys and New World primates (Desrosiers et al., 1986, Szomolanyi et al., 1987, Broker et al., 1993, Biesinger et al., 1990, 1992). Among HVS C strains, isolate HVS C-488 is more transforming than isolates HVS C-484 and C-139 (Fickenscher et al., 1997).

These biological differences have been assigned to the genes encoded at the left end of the long unique regions of HVS, localised at the equivalent position as EBV LMP1, KSHV K1 and RRV R1. The HVS TMPs encoded by this region were termed saimiri transforming proteins (Stp) A, B or C (figure 2). HVS strain C encodes an additional TMP at the left end of its genome termed Tyrosine kinase interacting protein (Tip) (figure 2). A TMP encoded at the far right end of the HVS genome has not been described.

StpA and StpC-Tip are recquired for the oncogenic potential of HVS strains A and C

At the left end of the HVS genome, ORF 1 of strain A11 codes for the oncogenic StpA protein (164 aa) (Murthy et al., 1989) and of strain B (SMHI) for the StpB protein (171 aa, Choi et al., 2000b, Hor et al., 2001), whereas two highly oncogenic proteins are derived from a bicistronic transcript of HVS strain C-488 termed StpC (ORF2) and Tip (ORF1; Biesinger et al., 1990, 1995, Jung et al., 1991, Fickenscher et al., 1997, Lund et al., 1995, 1996; figure 2). StpA has been shown to be required for in vitro T-cell transformation and in vivo leukemogenesis (Desrosiers et al., 1985, 1986, Murthy et al, 1989). StpC and Tip have clearly been shown to be responsible for the oncogenic potential of HVS strain C (Medveczky et al., 1993b, Duboise et al., 1998a). Recombinant HVS either lacking StpC or Tip are neither able to immortalize T lymphocytes in vitro to IL-2 independent growth nor to produce fatal lymphomas in infected common marmosets as wildtype HVS, but StpC and Tip are dispensible for replication and persistence (Duboise et al., 1998a). However, Tip expression

alone is not sufficient for oncogenic transformation in rodent fibroblasts (Jung et al., 1991), but it induces T-cell lymphomas in transgenic mice (Wehner et al., 2001) and rabbits infected with a HVS Tip-484 deletion mutant survive (Lund et al., 1997a). In contrast to StpB, StpA and StpC transform rodent fibroblasts (Jung et al., 1991) and transgenic mice expressing StpC-488 or StpA-11 develop tumours (Murphy et al., 1994, Kretschmer et al., 1996).

StpA and StpC are structurally similar

Although StpA, B and C show an extensive sequence divergence (StpB is 28% identical to StpA and 22% identical to StpC), they show structural similarities. The structure of both StpA and C comprises a highly acidic N-terminus followed by collagen-like repeats (Gly-X-Y, with X or Y being a proline residue) and a hydrophobic membrane anchor, whereas StpB is lacking the collagen-like cluster (figure 4; Jung & Desrosiers 1991, 1994, Lee et al., 1997). The net negative charge in the first 17 aa of the N-terminus of StpC-488 was found to be important for protein structure and transformation (Jung & Desrosiers 1994).

StpC-488 is membrane bound and localises primarily to perinuclear compartments in rodent fibroblasts, and the hydrophobic C-terminal region has been shown to be critical for membrane localisation (Jung & Desrosiers 1991, 1994). Whereas the predicted mass for StpC (102 aa) is 9.9 kDa, it has an apparent mass of 20 kDa and 22 kDa, with the 22 kDa form being phosphorylated in vivo at serine residue S^3 (Jung & Desrosiers, 1991, 1992, Jung et al., 1991). While StpC has 18 direct uninterrupted repeats of a collagen motif (G-P-P or G-P-Q encompassing 54 aa) in its N-terminus, StpA has only nine that are not directly repeated (figure 4; Biesinger et al., 1990, Geck et al., 1990, Lee et al., 1997).

Several lines of evidence point to an important role of the collagen repeats of StpA and StpC in transformation. First, StpB, which is not capable to transform rodent fibroblasts, lacks collagen repeats, but when 18 collagen repeat sequences are introduced into its N-terminus, it is able to oligomerize, activate NF-κB and transform rodent fibroblasts (Choi et al., 2000b). Second, a mutation disrupting the collagen repeats has been shown to abolish the transforming activity of StpC-488 (Jung & Desrosiers 1994).

Stp A, B and C interact with TRAFs, but only StpA and StpB bind PTKs

StpA and B both contain SH2-B motifs of the consensus YAEV/I and all three Stp proteins have TRAF-binding sites (consensus PXQXT/S, see below). The SH2-B motif Y^{115}AEV of StpA is preceded by negatively charged aa, matching well with the consensus binding sequence for SH2 domains for Src family PTKs (EEXXYEEV/I) (Songyang et al., 1993, 1994). Y^{115} of the StpA Y^{115}AEV motif has been shown to be crucial for binding to Src and was reported to be phosphorylated by Src in vitro (Lee et al., 1997). Tyrosine phosphorylation of StpA by Src (in vivo) leads to subsequent binding of Lck and Fyn in vitro (Lee et al., 1997). The SH2-B motif Y^{118}AEI of Stp-B is not preceeded by negatively charged residues,

and substitution to negatively charged amino acids resulted in stronger binding to Src, but activation of Src kinase activity by StpB in 293-T cells was not observed by Choi et al. (2000b). In contrast, another group reported that StpB was, like StpA, phosphorylated in vitro and in vivo in the presence of Src in cos cells (Hor et al., 2001). Furthermore, Hor et al. (2001) showed that Src binding to StpB was abolished when Y^{118} was mutated, and that Src binding to StpA and StpB seems to occur via the SH2 domain of Src.

StpC activates the transcription factor NF-κB and interacts with cellular Ras

Although StpA-11 and StpC-488 were shown to bind to TRAFs-1, -2 and -3 via their TRAF binding sites (see below), and StpB to interact with TRAF-1 and -2, StpA and StpB were not able to activate the transcription factor NF-κB (Lee et al., 1999, Choi et al., 2000b). In contrast, activation of NF-κB by StpC in epithelial cells is dependent on an intact TRAF binding motif (residues P^{10} or I^{11}, Lee et al., 1999) and the presence of functional TRAFs (Sorokina et al., 2004).

TRAF-binding motif:	P XQXT/S
StpA-11	P^{60} VQES
StpB SMHI	P^{41} TQHT and P^{84} VQET
StpC-488	P^{10} IEET
LMP1	P^{204}QQAT
CD40	P VQET

Interestingly, studies with recombinant HVS carrying the StpC gene with a $P^{10}\rightarrow R^{10}$ point mutation showed that loss of TRAF interaction and NF-κB activation by StpC is not essential for transformation of common marmosets T lymphocytes in vitro and in vivo, but crucial for immortalization of primary human T lymphocytes (Lee et al., 1999). Stable expression of StpC-488 and a dominant negative TRAF-2 mutant in Rat-1 cells drastically suppressed NF-κB activity and the transformation of Rat-1 cells by StpC (Lee et al., 1999). These data suggest that binding to TRAFs seems to be a major component of the oncogenic potential of StpC, reminiscent of the LMP1 protein of EBV, but TRAFs seem not to be the only effectors for StpC-associated oncogenicity.

As an additional interaction partner of StpC, cellular Ras has been identified. StpC is able to activate the Ras signaling pathway, indicated by a 2-4 fold increase in the ratio of Ras-GTP (active form) to Ras-GDP and constitutive activation of the MAPK Erk2 (Jung & Desrosiers 1995). Ras binding to StpC was reported to be abolished with StpC mutants showing no or reduced transforming potential (Jung & Desrosiers 1994, 1995). In addition, StpC-488 is capable of competing with Raf-1, the downstream effector of Ras, for binding to Ras (Jung & Desrosiers 1995). Experiments with recombinant HVS in which the StpC gene was replaced

by cellular or viral oncogenic Ras showed that Ras could substitute the StpC-488 protein in lymphocyte transformation, but with lower efficiency (Guo et al., 1998).

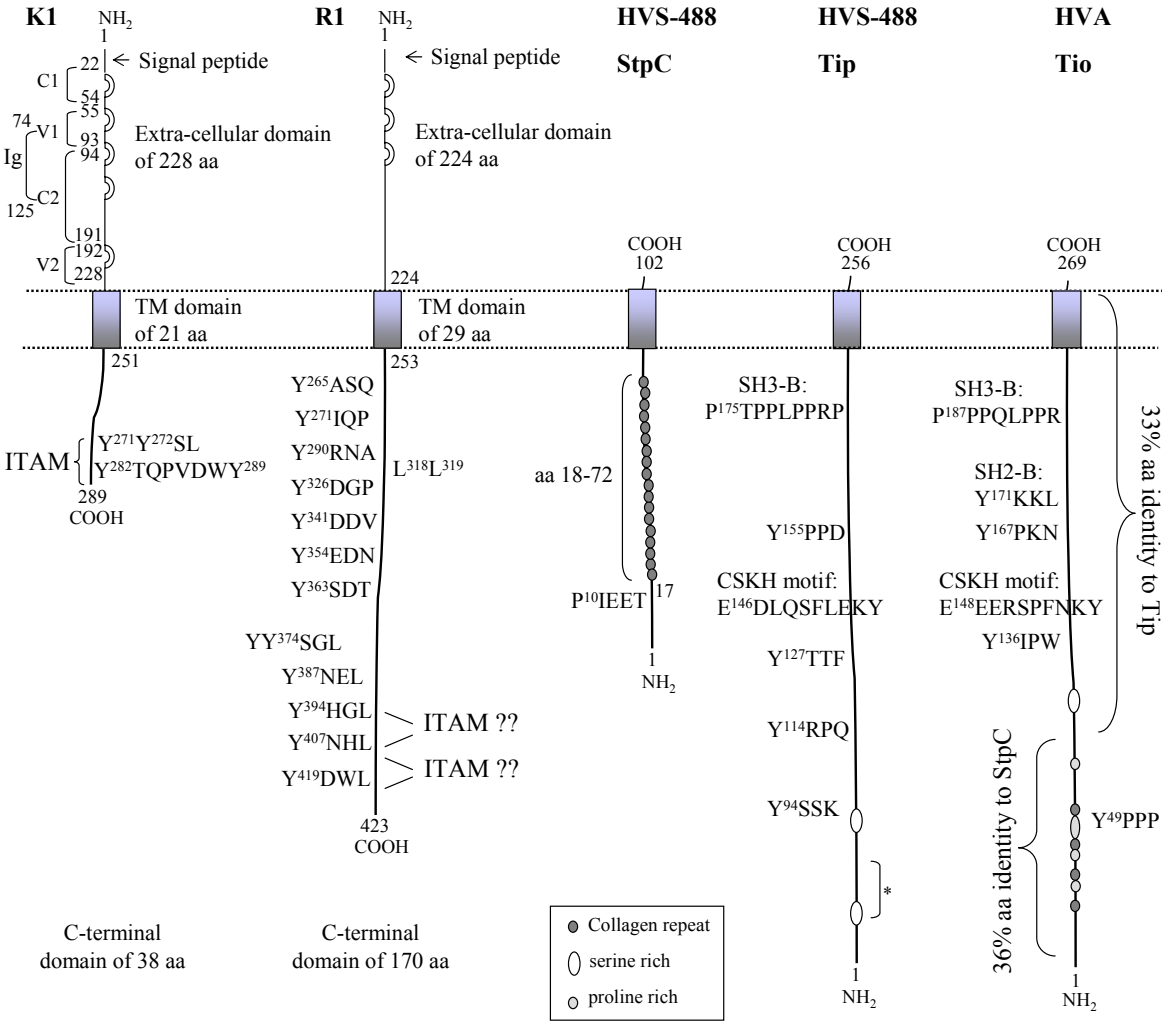

Figure 4: Structure of viral terminal membrane proteins K1, R1, StpC, Tip and Tio. The type I membrane proteins K1 and R1 consist of an N-terminal extracellular domain, one transmembrane domain and a cytoplasmic C-terminal domain with potential SH2-B motifs. StpC, Tip and Tio are type II membrane proteins with their N-terminus located in the cytoplasm. The Tio protein of HVA is 33% identical to Tip in its C-terminal part, whereas it shares 36% identity with StpC in its N-terminal part. The consensus motif for an ITAM is $(D/E)X_7(D/E)X_2YX_2LX_{7\text{-}10}YX_2L/I$ and for TRAF binding PXQXT/S.
(ITAM = immuno receptor tyrosine-based activation motif, X = any amino acid, TRAF = tumour necrosis factor receptor-associated factor, TM= transmembrane, C1, C2 = conserved regions 1 and 2, V1, V2 = variable regions 1 and 2, * = aa 37-79 of Tip-488 are absent in Tip-484, CSKH = C-terminal Src-related kinase homology).

The Tip protein interacts with Lck, a major T-cell protein tyrosine kinase

Two different variants of the Tip protein have been described in the literature, Tip-484 of HVS strain 484 (ORF2, 214 aa; Geck et al., 1990, Lund et al., 1995) and Tip-488 of HVS strain 488 (ORF1, 256 aa; Biesinger et al., 1990, 1995). They show 71% aa identity, with Tip-484 lacking 42 aa (aa 37-79 of Tip-488) in its N-terminal domain (figure 4). Both Tip proteins can form stable complexes with Lck, a major T-cell kinase that physiologically interacts with the T-cell antigen receptor (TCR), CD4, CD8 and IL-2 receptors (Biesinger et al., 1995, Lund et al., 1996).

The binding domain for the Lck kinase has been mapped to (i) a region encompassing the potential Tip SH3-B motif (10 aa) that has been shown to bind to the SH3 domain of Lck, (ii) a CSKH (C-terminal Src related kinase homology) domain (10 aa) which mediates binding to the C-terminal half of Lck and (iii) the 18 aa region between those two motifs (figure 4; Jung et al., 1995b, Lund et al., 1996, Hartley et al., 2000, further details in Schweimer et al., 2002). The Lck binding domain of Tip-484 is sufficient for activation of Lck in vitro and in vivo and also for in vitro STAT-3 binding and activation if expressed in T-cells (Lund et al., 1999). Maximal activation of Lck was shown to require simultaneous binding of both Lck domains to Tip-484 (Hartley et al., 2000).

Furthermore, Tip can be phosphorylated in vitro by Lck (Biesinger et al., 1995, Jung et al., 1995a, b). Further evidence for Tip interaction with PTKs was provided by fluorescence spectroscopy studies showing that Tip-peptides bound to the SH3 domains of Src, Lck, Hck, Lyn, Fyn and Yes, with highest affinity for Lyn, Hck and Lck (Schweimer et al., 2002).

The effect of Tip on Lck kinase activity

It is a contentious issue whether Tip binding to Lck results in an increase or decrease of Lck kinase activity (reviewed in Isakov & Biesinger 2000). In T-cells and 293 cells transfected with Tip-484 (Lund et al., 1997a, Hartley et al., 1999, 2000) and in HVS-484 infected human peripheral blood T lymphocytes (Lund et al., 1997a), Lck kinase activity was found to be elevated. Expression of Tip-488 was also reported to enhance Lck kinase activity in T-cells (Wiese et al., 1996). Interestingly, in vivo and in vitro activation of Lck kinase activity by Tip-484 seemed not to involve the known regulatory sites within Lck (Hartley et al., 1999).

Others observed downregulation of cellular tyrosine phosphorylation and suppression of Lck and Zap-70 activity in Tip-488 stably transfected T-cells (Jung et al., 1995a). In addition, the transformed phenotype of NIH 3T3 fibroblasts expressing activated Lck kinase was suppressed by coexpression of Tip 488 (Jung et al., 1995a). However, in one study (Kjellen et al., 2002) Tip-484 and -488 were analysed in parallel and both were able to stimulate Lck kinase activity in vivo and in vitro. Mutation of Y^{114} in Tip-488 was found to enhance the suppression of cellular tyrosine phosphorylation and to increase Lck binding activity

compared to wildtype Tip (Guo et al., 1997). In contrast, Kjellen et al. (2002) found that mutant Tip-488 $Y^{114}F$ could stimulate Lck activity as well as wildtype Tip.

Studies with Tip-488 in the context of the complete HVS genome showed that a Tip protein in which the prolines in the SH3-B motif have been substituted by alanines (HVS-TipΔSH3-B) was unable to bind Lck but was still able to immortalize common marmoset T lymphocytes in vitro and in vivo (Duboise et al., 1998b, Yoon et al., 1997), suggesting that Lck binding to Tip is not essential for immortalization. However, abrogation of Lck binding to Tip resulted in altered characteristics of the transformed cells/lymphomas (Duboise et al., 1998b). T-cells transformed with HVS-TipΔSH3-B also showed an increased NF-κB activity and upregulated expression of TRAFs-1,-2 and -3, but the relevance of this observation is not yet clear.

Tip activates the transcription factors NFAT, NF-κB, STAT-1 and -3

Tip-484 induction of DNA-binding of STAT-1 and -3 was shown to be dependent on Lck in T-cells (Lund et al., 1997b, 1999). Tip-484 is phosphorylated by Lck at Y^{72} (= Y^{114} in Tip-488) of the Y^{72}XPQ motif, and subsequently STAT-1 and -3 are phosphorylated and STAT dependent transcription is induced in 293-T cells (Hartley & Cooper 2000, Kjellen et al., 2002). STAT-3 can be phosphorylated in vitro by a complex of GST-Tip and Lck, and T-cells infected with recombinant HVS or expressing recombinant Tip showed significant increase of DNA-binding activity of STAT-1 and -3 and increased in vivo phosphorylation of STAT-3 in the presence of Lck (Lund et al., 1997b). Transient expression of Tip-484 in T-cells was found to stimulate STAT-3- and NFAT-dependent transcription, and this required both Lck binding domains of Tip (Hartely et al., 2000). Tip-484 and -488 were shown to stimulate NFAT and STAT-3 dependent transcription in T-cells (Kjellen et al., 2002).

Furthermore, Tip-488 interacts with the nuclear RNA export factor Tap (Tip-associated factor) and co-expression of Tip and Tap in T-cells results in upregulated surface expression of adhesion molecules and activation of NF-κB. However, the role of Tap in Tip signaling is not clear yet (Yoon et al., 1997).

Tip has an effect on the TCR and localises to lipid rafts

Tip-488 interacts with a WD repeat domain containing endosomal protein termed p80. This interaction was reported to lead to lysosomal vesicle formation and subsequent targeting of the Lck kinase into lysosomes for degradation. Furthermore, Tip interaction with p80 and Lck resulted in the downregulation of TCR and CD4 surface expression, respectively (Park et al., 2002).

Tip localises to lipid rafts in transfected T-cells and HVS-C488 transformed common marmoset T-cells (Park et al., 2003). While lipid raft association of p80 depended on co-expression of Tip in transfected 293 cells, interaction of Tip and Lck was required for the

recruitment of the TCR to lipid rafts (Park et al., 2003). Based on these results and the observation that expression of Tip in human T-cells suppresses cellular tyrosine phosphorylation and surface expression of lymphocyte antigens (Jung et al., 1995a), Park et al. (2003) postulate that Tip might mediate TCR downregulation and thereby interfere with the host´s immune control in the following scenario: Upon Tip and Lck interaction, TCR complexes would be recruited to lipid rafts and subsequently, Tip would interact with p80 and initiate aggregation and internalization of the lipid raft domain, leading to downregulation of the TCR complex.

1.3.4 The Herpesvirus ateles (HVA) two-in-one (Tio) protein

Herpesvirus ateles (HVA) causes fulminant lymphomas in various New World primates and is most closely related to Herpesvirus saimiri (Melendez et al., 1972a). The natural host of HVA is the spider monkey (Melendez et al., 1972b). HVA isolates from two strains (810 and 73) have been described to transform monkey T-cells to permanent growth in vitro and in vivo (Hunt et al., 1972, Laufs & Melendez, 1973, Melendez et al., 1973).

Tio shares sequence similarity with StpC and Tip of HVS

In transformed monkey T-cells, a single spliced mRNA derived from the highly variable left region of the HVA genome (strain 73) is transcribed and gives rise to a protein of 269 aa with a predicted mass of 29 kDa (Albrecht et al., 1999, 2000). The term “Two-in-one” (Tio) for this protein is derived from its sequence similarity to HVS strain C oncogenic proteins StpC and Tip (figure 4). Tio shares 36% aa identity in its N-terminal third with StpC, whereas its C-terminal two thirds are 33% identical to Tip (figure 4; Albrecht et al., 1999). However, the collagen repeats (Gly-X-Y, with X or Y being a proline residue) of which StpC has 18 in a perfect repetetive order are fewer in number (4) and interrupted by proline rich regions in the Tio protein (figure 4).

Tio and Tip share a CSKH motif which is homologous to the αI helix of Src (Xu et al., 1997), a conserved SH3-B domain (P^{187}PPQLPPR) and a serine rich motif of unknown function (figure 4; Albrecht et al., 1999). Tyrosine residues of motifs Y^{136}IPW (Y^{127}TTF in Tip) and Y^{167}PKN (Y^{155}PPD in Tip) are conserved between Tip and Tio, whereas the tyrosine residue of the putative SH2-B motif of Tio, Y^{171}KKL, is not conserved (figure 4).

Tio interacts with and is phosphorylated by PTKs

In lysates of transformed monkey T-cells and in 293-T cells transfected with recombinant Tio, protein bands of 43 and 46 kDa are detected. Additionally, a homodimeric form of Tio is observed in 293-T cells (Albrecht et al., 1999). When co-transfected in 293-T cells with Src family members of PTKs Lck, Src and Fyn, a tagged Tio protein is in vivo phosphorylated on

tyrosine and directly binds to Lck, Src and Fyn. Fluorescence spectrometry assays performed with a Tio peptide encompassing its SH3-B domain revealed that this binds to GST-SH3 domain fusion proteins of Lyn, Hck, Lck, Fyn, Src and Yes, but not of Abl, the p85α subunit of PI3K or Grb2 (Albrecht et al., 1999). However, a direct binding assay with the complete Tio protein was only performed with the SH3 domain of Lck and confirms the peptide approach.

Direct binding of Tio to the SH2 domains of Lck, Src and Fyn is only observed when Tio is tyrosine phosphorylated (Albrecht et al., 1999). Interaction of Tio with SH2-domains seems to be specific for members of the Src familiy of PTKs, since binding of Tio to SH2 domains of Abl, Vav, Grb2 and phospholipase γ was not observed.

Thus, Tio combines functions of Tip regarding its interaction with PTKs of the Src family via its SH3-B motif and with StpA/B with respect to binding to Lck, Src and Fyn via its SH2-B motif in a phosphotyrosine dependent manner. However, despite of the structural similarities of Tio and the oncoprotein StpC, no functionally related features have been identified so far. The only data indicating that Tio might be an oncoprotein is its similarity to the oncoproteins StpC and Tip of HVS regarding its structure and genomic localisation, its ability to interact with members of the Src familiy of PTKs and its expression in virus-transformed monkey T-cells.

1.3.5 The KSHV K1 protein

KSHV encodes a 46 kDa type I transmembrane glycoprotein (289 aa) known as K1 at the left end of its genome (Russo et al., 1996, Lagunoff & Ganem 1997, Lee et al., 1998a) in a position similar to that of the Stp gene of HVS, the R1 gene of RRV and Tio of HVA (figures 1 and 2).

The extracellular domain of K1 is structurally similar to that of the R1 protein, but shows no similarity to Stp, Tip or Tio regarding aa sequence or structure (figure 4). The K1 protein has transforming capabilities in so far as it can induce morphological changes and focus formation in rodent fibroblasts (Lee et al., 1998a). In addition, K1 can functionally substitute the StpC gene in the context of the HVS genome with regard to immortalization of common marmoset T-lymphocytes to interleukin-2-independent growth and the induction of lymphomas (Lee et al., 1998a).

K1 displays high sequence divergence in its extracellular domain

K1 is composed of an N-terminal domain exposed to the extracellular matrix, a single transmembrane domain and a cytoplasmic C-terminal domain of 38 aa (figure 4). The N-terminal domain of K1, especially the variable regions 1 and 2 (V1, V2), displays high levels of genetic variability between different KSHV isolates (except for 12 conserved cysteine

residues), with 15-30% divergence at the aa level. This led to the definition of four to five major subtypes of K1 (A-E) and 13 distinct variants plus several clades (Nicholas et al., 1998, Cook et al., 1999, Cook et al., 2002, Hayward 1999, Lacoste et al., 2000, Zong et al., 1999). Different V1 and V2 regions seem to correspond to different geographic areas. For example, K1 subtype B is found in KS patients from Africa, whereas subtype C2 is found in classic KS in the Middle East, Asia, Europe and USA, and AIDS KS samples from USA predominantly have A1, A4 and C3 K1 variants (Cook et al., 1999, Hayward 1999, Kasolo et al., 1998, Lacoste et al., 2000, Zong et al., 1999). Notably, the R1 protein of different macaque species shows much less amino acid sequence divergence (1-7%) than K1 (Damania et al., 1999). K1 has been shown to oligomerize, most probably via disulfide linkage of its N-terminal domain (figure 6; Lee et al., 1998a, Lagunoff et al., 1999) and contains several N-glycosylation sites in its extracellular domain.

K1 is a lytic protein

K1 is predominantly expressed during the lytic phase of the viral life cycle (Lagunoff & Ganem 1997). A 1.3 kb K1 transcript was detected in BCBL-1 cells induced with TPA (Lagunoff & Ganem, 1997), whereas a 1.3 kb and 3 kb K1 transcript were expressed in uninduced BC-3 cells, with both transcripts being upregulated in TPA-induced BC-3 cells (Samaniego et al., 2001). However, K1 transcripts detected during latency could represent K1 transcription from the ~5% of BCBL-1 cells undergoing spontaneous lytic replication (Renne et al., 1996, 1998), and gene array studies indicate that K1 is a lytic rather than a latent gene (Jenner et al., 2001, Paulose-Murphy et al., 2001, Nakamura et al., 2003). It is nevertheless possible that there is minimal K1 expression during the latent viral life cycle. Studies with monoclonal antibodies raised against the N-terminal domain of K1 showed that K1 protein is expressed during the early lytic viral life cycle in PEL cell lines BCBL-1, BC-1 and Jsc-1 (with little if any expression in unstimulated cells) and MCD tissue but not in KS lesions (Lee et al., 2003). By RT-PCR, Samaniego et al. (2001) identified K1 transcripts in KS lesions.

The K1 promoter element from BCBL-1 cells contains binding sites for transcription factors SP-1, NF-1, AP-2 and myc-max and seems to be conserved between different K1 subtypes (Bowser et al., 2002). The K1 promoter was proven to be active in 293, KSHV negative (BJAB) and positive (BCBL-1) B-cells and KS tumour-derived endothelial cells (SLK-KS$^-$). Ectopic expression of the major lytic switch protein of KSHV, ORF50/RTA, could further activate the K1 promoter element in 293, BJAB and BCBL-1, but not in SLK-KS$^-$ cells (Bowser et al., 2002), suggesting that K1 expression may be regulated differently in endothelial cells.

K1 contains a functional ITAM and signals B-cell activation

The cytoplasmic tail of K1 contains an immunoreceptor tyrosine-based activation motif (ITAM), which is highly conserved between different K1 subtypes and is also present in LMP2A, but with the rightmost leucine of the second SH2-B motif (consensus YXXL/I) being substituted by proline in the K1 ITAM (Lee et al., 1998b):

LMP2A: **DY**^{74} QP**L**GTGDQSL**Y**^{85} LGL
K1: **DY**^{271}YS**L**HDLCTED**Y**^{282}TQP

Studies in KSHV negative B-cells (BJAB cells) stably transfected with a chimeric protein consisting of the extracellular and transmembrane domain of CD8 fused to the cytoplasmic C-terminus of K1 showed that the CD8-K1 chimera induced cellular tyrosine phosphorylation and calcium mobilisation upon stimulation with a α-CD8 antibody (Lee et al., 1998b). In this system, a single motif of the ITAM (Y^{271}YSL or Y^{282}TQP) was shown to be sufficient for induction of cellular tyrosine phosphorylation, but both were important for mobilisation of intracellular calcium.

K1 binds several kinases and is tyrosine phosphorylated at its ITAM motif

In BJAB cells, the CD8-K1 chimera is predominantly phosphorylated upon α-CD8 stimulation at Y^{271} of K1, and also but to a lesser extent at Y^{282} of the ITAM motif (see figure 4). Co-transfection studies in cos1 cells indicate that Syk could be a kinase responsible for this phosphorylation (Lee et al., 1998b). Phosphorylation of the CD8-K1 ITAM allowed subsequent binding of SH2 proteins Syk, Vav and PI3K. Phosphorylated forms of Syk, Cbl and PI3K, but not of Vav and Blk, were detected in antibody stimulated CD8-K1 expressing BJAB cells. Phosphorylated Syk kinase and phosphorylated phosholipase C-γ2 (PLC-γ2) were also detected in KSHV negative/EBV positive B-cells (Raji cells) transfected with full length K1, depending on an intact ITAM (Lagunoff et al., 1999).

Co-transfection experiments in cos1 cells demonstrated that phosphorylated Syk but not Src interacted with CD8-K1, however, both kinases could phosphorylate the K1 ITAM motif, whereas only a weak phosphorylation was observed with Lyn and ZAP70 and none with Lck and Fyn (Lee et al., 1998b). Syk interaction was also observed with a K1 ITAM peptide phosphorylated on both tyrosines, but interaction of Syk with full length K1 has not been demonstrated yet (Lagunoff et al., 1999). In line with these data, signal transduction of full length K1 is impaired in a Syk deficient cell line, pointing to a role of this PTK in downstream signaling events of K1 (Lagunoff et al., 1999).

Interestingly, K1 signaling was found to be quite different in KSHV positive BCBL-1 cells versus KSHV negative B-cells. In BCBL-1 cells, transfected K1 was no longer able to induce intracellular calcium mobilization or NFAT activation upon antibody stimulation and was

impaired in its ability to induce cellular tyrosine phosphorylation (Lee et al., 2002). However, Syk was activated, and Syk and Lyn expression levels were equal in both cell lines, but expression of PLC-γ2 and Cbl was weak in BCBL-1-K1 compared to BJAB-K1 cells (Lee et al., 2002).

K1 activates the transcription factor NFAT and the PI3K/Akt pathway

Full length K1 is able to activate the transcription factor NFAT in KSHV negative B-cells (Raji). This occurred in the absence of any cross-linking ligand, and was not completely abolished with a K1 double mutant (ITAM: $Y^{271}F$, $Y^{282}F$), indicating that flanking sequences of the two SH2-B motifs of the K1 ITAM are important for efficient signal transduction (Lagunoff et al., 1999). Constitutive signaling of K1 is attributed to its extracellular domain, that, when transferred to other consensus ITAMs, was able to induce constitutive signaling (Lagunoff et al., 1999). K1 signal transduction induced by antibody stimulation with K1 monoclonal antibodies raised to the N-terminal domain required both the ITAM and the authentic conformation of the extracellular domain (Lee et al., 2003). K1 monoclonal antibodies recognizing aa 92-125 (encompassing the C2 and Ig-like region, see figure 4) could efficiently induce an increase in intracellular calcium concentration and cellular tyrosine phosphorylation in B-cells stably transfected with K1 (Lee et al., 2003).

In B-cells, K1 was found to enhance the phosphorylation of the p85 subunit of PI3K and the kinase Akt, thereby activating them, and to enhance the phosphorylation of the regulator of the PI3K/Akt pathway, PTEN, thereby inactivating it (Tomlinson & Damania 2004). Therefore, K1 seems to signal via the PI3K/Akt pathway, and the K1 ITAM was shown to be essential for this feature. Activated Akt phosphorylates and thereby inactivates pro-apoptotic factors such as caspase 9, GSK3-β, Bad and members of the FKHR family of transcription factors, which results in cell survival. K1 expressing cells showed increased phosphorylation of FKHR, but not of Bad, caspase 9 or GSK3-β, and K1 was shown to be able to protect cells from FKHR- and Fas-mediated apoptosis (Tomlinson & Damania 2004).

K1 activates the transcription factors NF-κB and AP-1 and affects cytokine expression

In the context of KSHV tumourgenicity, it has been postulated that lytic viral proteins (e.g. vGPCR) may contribute to tumourigenicity by exerting paracrine effects. In reporter assays, K1 was reported to activate the transcription factor AP-1 eight fold in BJAB cells (Lagunoff et al., 2001) and to activate the transcription factor NF-κB four fold and AP-1 two fold when transiently expressed in cos1 cells (Samaniego et al. 2001). In our hands, K1 did not activate the AP-1 transcription factor in reporter assays in 293-T cells (unpublished results).

In KS endothelial cells and B-cells transfected with K1, NF-κB-dependent promoter activity was induced. In addition, in KS cells expressing K1, the induction of secretion of inflammatory cytokines implicated in KS lesion formation such as IL-6, IL-12 and

granulocyte macrophage colony stimulating factor was observed, but not of RANTES, MIP-I or –II (Samaniego et al., 2001, Prakash et al., 2002). This would indicate that K1 could contribute to spindle cell formation in KS lesions, but further experiments are needed to support this notion.

However, in K1 transgenic mice, serum IL-12 levels were severely impaired, and basic fibroblast growth factor (bFGF) expression was upregulated in lymphocytes and tumours (2 of 13 mice developed tumours) of K1 mice (Prakash et al., 2002). bFGF is an autocrine growth factor for endothelial cells that promotes growth and angiogenesis of AIDS-KS cells (Samaniego et al., 1995). B lymphocytes of K1 transgenic mice showed constitutive activation of transcription factors NF-κB and Oct-2, increased tyrosine phosphorylation and activity of the B-cell specific PTK Lyn (Prakash et al., 2002).

K1 can downregulate BCR surface expression

Apart from the induction of signaling events from the plasma membrane, full length K1 was reported to downregulate the expression of the BCR complex at the cell surface of BJAB cells, thereby potentially inhibiting B-cell activation and allowing a long term survival advantage for KSHV infected cells (Lee et al., 2000). Based on studies with different CD8-K1 chimeric proteins, the N-terminal domain of K1 was proven to be required for BCR surface downregulation, and not an intact ITAM. The N-terminal domain of K1 was shown to interact with the μ chains of the BCR complex, which probably leads to the retention of BCR subunits in the ER (Lee et al., 2000). The physiological interaction of BCR subunits Igα and Igβ with μ chains results in the direction of the BCR to the cell surface, so it seems that K1, showing structural homology to Igα and Igβ, may act as a dominant negative protein (Lee et al., 2000). Inhibition of BCR signaling is reminiscent of the LMP2A protein of EBV, which also contains an ITAM motif and interferes with BCR signaling.

K1 has an effect on the viral life cycle

K1 expression cannot by itself initiate viral replication (Lukac et al., 1998), but recent data suggest that K1 may augment reactivation of KSHV from its latent state and play a role in lytic gene expression (Lagunoff et al., 2001). When dominant negative K1 mutants (lacking the ITAM motif and shown to inhibit K1, Syk and PLC-γ2 phosphorylation) were expressed in the KSHV positive PEL cell line BCBL-1 together with an expression vector for the viral transactivator ORF50/RTA, gene expression of ORF59, which is an early lytic gene, was reduced by 80%. However, a mild decrease of ORF59 expression was also observed when K1 wildtype was expressed instead of K1 dominant negative mutants (Lagunoff et al., 2001). Notably, the block in lytic replication induced by K1 dominant negative mutants could be overcome by TPA treatment (Lagunoff et al., 2001). This result would argue for the notion that K1 might signal via a pathway that can be bypassed by TPA treatment. TPA has

pleiotropic effects on B-cells, e.g. the induction of AP-1 activity via the Ras-Raf-MEK-Erk pathway. Whereas the calcineurin inhibitor FK506 could efficiently block NFAT activation by wildtype K1 in BJAB cells, and a dominant negative Ras mutant (Ras N17) could block K1 induced AP-1 activity, both FK506 and RasN17 did not have any effect on ORF59 expression in BCBL-1 cells transfected with ORF50/RTA. This would suggest that K1, if it augments lytic reactivation, does not achieve this via these two pathways (Lagunoff et al., 2001).

In contrast to the observations made by Lagunoff et al. (2001), Lee et al. (2002) observed that K1 was able to suppress lytic KSHV reactivation induced by TPA but not by ORF50 ectopic expression. A KSHV microarray (established by Paulose-Murphy et al., 2001) showed that the majority of viral genes was downregulated in BCBL-1-K1 cells treated with TPA (exceptions: levels of ORF48, K1 and K15 were upregulated, Lana and vFLIP not affected), including the viral transactivator ORF50/RTA (Lee et al., 2002). Expression of the late lytic glycoprotein K8.1 was not enhanced in BCBL-1-K1 cells treated with TPA, and this depended on a functional ITAM of K1 (Lee et al., 2002). Furthermore, TPA-induced activation of transcription factors AP-1, NF-κB and Oct-1 activities were diminished in BCBL-1 cells stably transfected with the CD8-K1 chimera, but not of NFAT, AP-2 and SP-1 (Lee et al., 2002).

Whereas the results by Lee et al. (2002) would suggest that K1, as EBV LMP2A and HVS Tip, may play a role in maintaining viral latency, the observations made by Lagunoff et al. (2001) would rather point to a role of K1 in augmenting the viral lytic cycle.

1.3.6 The K15 open reading frame of KSHV

The K15 ORF shows striking similarities to the EBV ORF LMP2A (see figure 5, K15 ex1-8 M- and P-type). Both genes are located at exactly the same genomic position between the viral terminal repeat region and ORF75 (ORF75/BNRF1 in EBV) (see figures 2 and 5). K15 and LMP2A genes show a complex, very similar splicing pattern concerning number and length of introns and exons (figure 5) and structural similarities (figure 3), although they are not homologous at the aa level. Furthermore, both ORFs code for membrane proteins with up to 12 transmembrane domains and a cytoplasmic domain (see figure 3; Glenn et al., 1999, Poole et al., 1999, Choi et al., 2000a). Whereas LMP2A has a long amino-terminal domain encoded by exon 1 and 2 with signaling motifs such as SH2-B and SH3-B sites and an ITAM motif, putative signaling motifs of K15 are located in its cytoplasmic C-terminus encoded by exon 8 (figures 3 and 5).

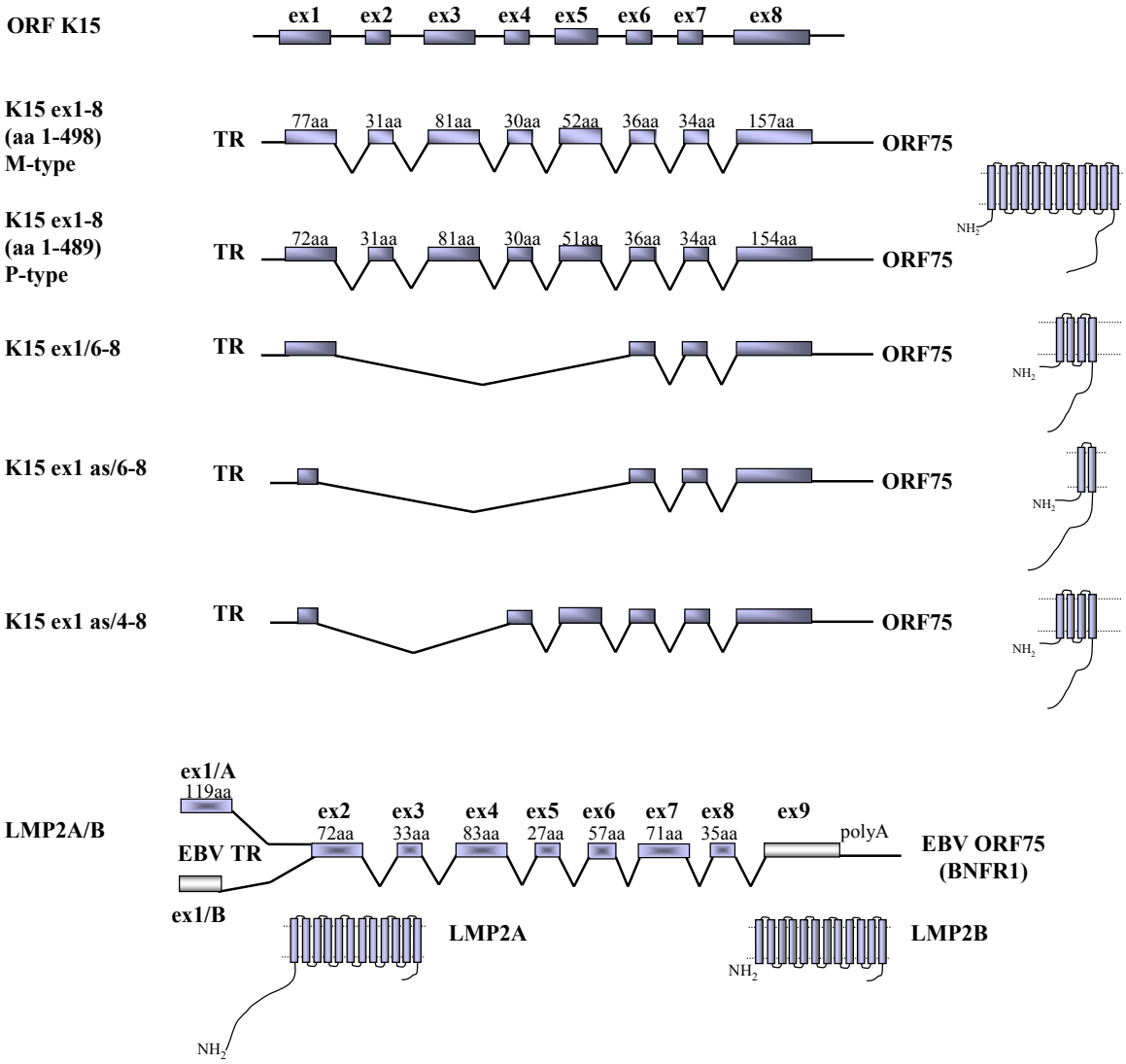

Figure 5: Splicing pattern of KSHV ORF K15 and EBV ORF LMP2A/B. Two K15 alleles, termed K15-P (predominant) and K15-M (minor) have been identified in different KSHV isolates. K15-P, K15-M and LMP2A/B show a highly similar splicing pattern and are both localised at the "right" end (in the orientation of the genome usually used in the γ_2-herpesvirus field) of the respective viral genomes upstream of ORF75 (BNFR1 in EBV). Whereas LMP2A has a long amino terminal domain encoded by exon 1 and 2 with signaling motifs such as SH2-B and SH3-B sites, putative signaling motifs of K15 are located in its cytoplasmic C-terminus encoded by exon 8. Splicing forms of K15 identified to date vary in the number of transmembrane domains, but all code for the cytoplasmic domain. The white/grey boxes indicate non-coding exons of LMP2 (ex1 of LMP2B, ex9 of LMP2A/B). as = alternative splice (see text for further details).

K15 is multiply spliced and gives rise to proteins with different numbers of transmembrane domains and a putatively cytoplasmic C-terminus

Expression of K15 transcripts was identified in unstimulated KSHV positive PEL cells (K15 P-type: in BCP-1 and BCBL-1 cells; K15 M-type in Hbl-6 cells) and found to be upregulated upon lytic cycle induction (Glenn et al., 1999, Poole et al., 199, Choi et al., 2000a). Multiple alternatively spliced transcripts are generated from the K15 gene (exemplary transcripts are depicted in figure 5) with the most prominent transcript containing eight exons (figure 5, K15

ex1-8). The sequences of all K15 cDNA clones isolated so far are predicted to contain a common C-terminal cytoplasmic region (encoded by exon 8) linked to a variable number of transmembrane domains (figure 5). The eight exons are positioned such that any combination of exons identified to date would be in the same open reading frame (e.g. K15 ex1/6-8 depicted in figure 5). Several splice variants identified (e.g. K15 ex1 as/4-8 and K15 ex1 as/6-8) use an alternative splice donor and start codon in exon 1, which would be predicted to join a part of exon 1 out of frame with the other exons, resulting in an alternative six aa at the N-terminus of the resulting protein (figure 5; Glenn et al., 1999, Choi et al., 2000a). This is reminiscent of LMP2, which also alternatively uses exon 1 resulting in two proteins LMP2A and LMP2B (see 1.3.1 and figure 5; Sample et al., 1989).

K15 contains signaling motifs in its C-terminus: potential binding sites for SH2 and SH3 domain-containing proteins and for TRAFs

Two different forms of the K15 ORF, K15-P (predominant, found in the majority of KSHV genomes tested) and K15-M (minor) have been identified (Poole et al., 1999), which are almost identical concerning splicing pattern (figure 5) and protein structure, but show as little as 33% aa identity (Glenn et al., 1999, Poole et al., 1999, Choi et al., 2000a).

The putative signaling motifs in the cytoplasmic C-terminus of these two K15 variants are highly conserved (see below), suggesting the conservation of associated functional properties. The cytoplasmic domain of K15 contains proline-rich domains that could potentially serve as SH3-B domains (K15-P: PP^{387}PLPP, K15-M: P^{396}PLPS, P^{480}PPFQP, and T^{452}PPPT) and a motif that is reminiscent of a TRAF binding site (consensus PxQxT/S) present in LMP1 (K15-P: ATQ^{475}PTDD, K15-M: PFQ^{484}PADE). Furthermore, two potential highly conserved SH2-B sites are present in the cytoplasmic domains of K15-P and K15-M (K15-P: VFGY^{431}ASIL and DDLY^{481}EEVL, K15-M: TVTY^{444}ASIL and DEVY^{490}EEVL). However, since the YASI motif is not proceeded by negatively charged aa in either K15 type, it may not serve as an SH2-B motif but rather as an internalization motif (Bonifacino & Dell´Angelica 1999). Since most K15 studies published so far have been performed with the P-type of K15, only signaling motifs of K15-P are depicted in figure 3.

K15-M:	**P^{396}PLP**S	**Y^{444}ASIL**	IN**Q^{464}SG**I**S**	PP**PF**Q^{484}**P**A**DE**	**Y^{490}EEVL**
K15-P:	**P^{387}PLP**P	**Y^{431}ASIL**	PD**Q^{451}SG**M**S**	QAAT**Q^{475}PTDD**	**Y^{481}EEVL**
LMP1:				**PQQ^{206}ATDD**	
LMP2A:					**Y^{112}EE**A

A CD8-K15 chimera is tyrosine phosphorylated and can downregulate BCR signaling

Studies with BJAB cells stably transfected with a CD8-K15 chimera, in analogy to CD8-K1 (see 1.3.5), revealed that the K15 cytoplasmic domain was not able to induce intracellular calcium mobilization and intracellular tyrosine phosphorylation upon α-CD8 antibody stimulation when compared to BJAB cells expressing the CD8-K1 chimera (Choi et al., 2000a). In this system, the cytoplasmic tail of K15 was found to be constitutively phosphorylated at Y^{481} of the YEEV motif (Choi et al., 2000a).

CD8-K15 seems to be capable of downregulating BCR signaling in B-cells, since stimulation of B-cells with an anti-IgM (BCR) antibody, which normally leads to BCR crosslinking and subsequent B-cell activation, resulted in a reduction of cellular tyrosine phosphorylation and levels of free calcium concentration in CD8-K15 expressing B-cells. This effect of CD8-K15 was abolished by mutating the prolines in the putative SH3-B motif (PPPLPP) to glycines in addition to point mutating Y^{481} to phenylalanine, indicating that both motifs could be crucial for blocking BCR signaling (Choi et al., 2000a). However, it has not been demonstrated yet that full length K15 can block BCR signaling as described for LMP2A and K1, and the mechanism by which K15 may be exerting this dominant negative effect on BCR signaling has not been investigated so far.

K15 interacts with TRAFs and Hax-1

The cytoplasmic domain of K15-P and K15-M can interact in vitro and in vivo with TRAFs -1, -2 and -3, reminiscent of EBV LMP1 which induces multiple signaling cascades via its interaction with TRAFs (Glenn et al., 1999, Brinkmann et al., 2003, see 1.3.1.1). In contrast to TRAF-1 and TRAF-3, TRAF-2 was no longer able to bind to a K15 deletion mutant lacking aa 473-489, which include the Y^{481}EEV motif and the TRAF-like binding site ATQ^{475}PT (Brinkmann et al., 2003). Furthermore, the C-terminus of K15 interacts with Hax-1, which partly seems to involve the Y^{431}ASI motif of K15 (Sharp et al., 2002). Hax-1 was shown to inhibit Bax-induced apoptosis (Sharp et al., 2002), but the relevance of its interaction with K15 is not clear.

K15 expression in vivo

In uninduced primary effusion lymphoma (PEL) cell lines, a 23 kDa protein was detected by by Western blotting with a monoclonal antibody (mab) raised to the C-terminal domain of K15 (Sharp et al., 2002). Upon TPA induction, expression of this 23 kDa protein decreased over time, suggesting latent kinetics for this protein. Immunofluorescence analysis of uninduced PEL cells with the K15 mab showed a cytoplasmic staining pattern in the majority of cells (Sharp et al., 2002). These observations contradict results obtained by RT-PCR by Glenn et al. (1999) and Choi et al. (2000a), who detected very low expression of K15

transcripts in uninduced PEL cells and a strong increase of K15 transcript expression upon induction with TPA, which would suggest K15 to be a lytic transcript.

Since serum of some KS patients reacted with the cytoplasmic domain of K15-M and K15-P by Western blotting, K15 expression in KS seems likely (Glenn et al., 1999), but so far, K15 expression has not been shown directly in KS lesions. K15 expression has been observed in MCD plasmablasts by immunofluorescence (Sharp et al., 2002). Reports about the intracellular localisation of transiently transfected K15 observed by immunofluorescence describe the formation of large patches on external and cytoplasmic membranes in 293 cells (Glenn et al., 1999), cytoplasmic, plasma membrane and perinuclear localisation in cos-1 and 293 cells (Choi et al., 2000a, Sharp et al., 2002), and localisation to the endoplasmatic reticulum in Hela cells (Sharp et al., 2002).

The high GC-rich terminal repeat region complicates the identification of the K15 promoter region, but 5´ RACE and primer extension studies indicate that the transcriptional start site of K15 might be located to the terminal repeat region (Lucille Rainbow, personal communication). A proximal TATATAA box motif and probable associated lytic cycle promoter elements are present just upstream of ORF K15-M exon 1 (BC-1 DNA), but not in K15-P (Poole et al., 1999).

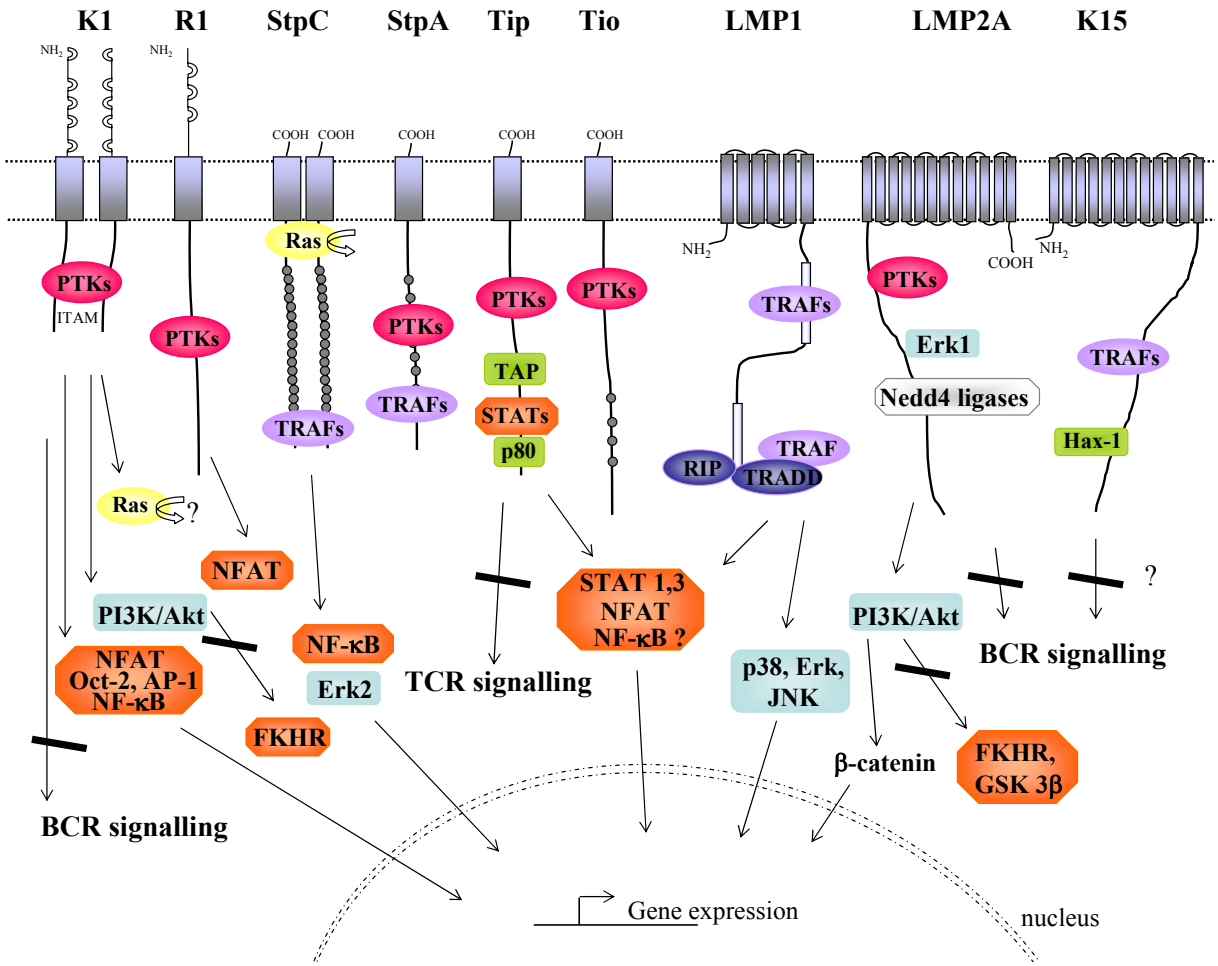

Figure 6: Summary of the identified cellular interaction partners of viral TMPs of γ-herpesviruses and downstream signaling events. For many of the discussed viral terminal membrane proteins, the exact binding site via which interaction with the cellular effector molecules takes place is not determined yet. If the exact binding site is known, this is indicated in the text or in figures 3 and 4.

characteristics	R1	K1	STP	LMP1	TIO	TIP	LMP2A	K15
Direct interaction with	Syk, but not Src	- N-terminus with μ chains of BCR in the ER - Syk - Vav, PI3K, Cbl (CD8-K1)	- Ras (StpC) - TRAF 1,2,3 (StpA, StpC) - TRAF 1,2 (StpB) - Src (StpA,B) - Fyn, Lck (StpA)	-TRAF 1,2,3,5 via CTAR-1 -TRADD, RIP via CTAR-2 -JAK3 via CTAR-3	- Via SH3-B site with Lyn, Hck, Lck, Src, Fyn, Yes but not Abl, PI3K, Grb2 - Via SH2-B site with Lck, Src, Fyn but not phospholipase γ, Abl, Grb2, Vav	- Lck, TAP, p80 STAT 1,3 - in vitro with Lyn, Hck, Lck weaker with Src, Fyn, Yes	- Csk (in epithelial cells) - Nedd4-like ubiquitin ligases - Erk1 - Lyn (via Y^{112}EEA), Syk (via ITAM Y^{74}, Y^{85}), Fyn	- TRAF 1, 2, 3 (LMP1-K15 chimera) - Hax-1
Phosphorylated by	Syk, Src (full length R1)	Syk, Src at Y^{271}, Y^{282}, weakly by Lyn and ZAP70 (CD8-K1)	Src (StpA in vitro at Y^{115})	not known	In vivo by Lck, Src, Fyn	Lck on Y in vitro	Lyn, Syk, Erk1	phosphorylated at Y^{481}
Activated by	Not known, maybe by oligomerisation	Signals constitutively; maybe by oligomerisation	Oligomerisation?	Self-multimerisation, no ligand needed	not known	not known		not known
Induction of Ca-mobilization	CD8-R1 chimera upon α-CD8 stimulation	K1 in B cells upon α-CD8 stimulation	-	-	n.d.		CD8-LMP2A N-terminal chimera	No (CD8-K15 chimera)
Induction of cellular tyrosine phosphorylation	CD8-R1 chimera in B cells upon α-CD8 stimulation	K1 in B cells upon α-CD8 stimulation	-	-	n.d.	Tip-488 suppresses Y~P	-	No (CD8-K15 chimera)
Induction of the activation of	NFAT (by CD8-R1 chimera upon α-CD8 stimulation and full length R1 without stimulation in B cells)	- NFAT, NF-κB, AP-1, Oct2, Lyn, Syk, PLC-γ2 Ras (?) - p85 of PI3K, Akt - inhibits PTEN and FKHR - secretion of inflammatory cytokines	- NF-κB via TRAFs (StpC) - Erk2 (StpC)	-NF-κB and p38 via CTAR-1,-2 -JNK via CTAR-2 - JAK3 and STAT 1,3 - induces expression of: a) IL-6 in epithelial cells via TRAFs (NF-κB dependent) b) Fas, ICAM-1, CD40, LFA-3 c) TRAF1 in B cells via CTAR-1 d) A20, EGFR in epithelial cells via CTAR-1	n.d.	-STAT 3 when Lck present (Tip-484) -Activation or suppression of Lck activity (see text) - NF-κB (?), NFAT	- Erk2, JNK1 in epithelial cells - PI3K/Akt in B cells and epithelial cells - β-catenin signaling in epithelial cells	n.d.

characteristics	R1	K1	STP	LMP1	TIO	TIP	LMP2A	K15
Self oligomerisation	Little, likely via disulfide bonding of extracellular domain	likely via disulfide bonding of extracellular domain	Likely via collagen repeats (StpA, StpC)	Yes, multimerizes via its membrane domains	Homodimers	n.d.	Aggregation (?), clustering via C-terminus (?)	n.d.
Transformation of rodent fibroblasts	When cloned into HVS genome	Yes, but with low efficiency	StpA and StpC, but not StpB		n.d.	no	-	n.d.
In vivo cell growth transformation	When cloned into HVS genome	When cloned into HVS genome	StpA and StpC, but not StpB		n.d.	Induces T cell lymphomas in transgenic mice	-	n.d.
Transformation of T-lymphocytes from common marmosets	yes	yes	StpA and StpC, but not StpB		n.d.	no	Transforming in keratinocyte cell line HaCaT	n.d.
Localization in lipid rafts	n.d.	yes (unpublished results)	n.d.	yes	n.d.	yes	yes	n.d.
Effect on viral replication and interference with host immune control	n.d.	- inhibits lytic cycle in BCBL-1 - dom.neg. K1 mutants inhibit lytic cycle in BCBL-1 - downregulates BCR surface expression -downregulation of KSHV genes - inhibition of B cell activation	n.d.		n.d.	TCR and CD40 down-regulation via p80 and Lck in human T cells?	- Inhibits lytic cycle induction by inhibiting BCR signalling in vitro - Induces B cell survival in transgenic mice	Downregulation of BCR signalling?

Table 1: Functional features of γ-herpesvirus terminal membrane proteins. Besides structural commonalities (see figures 3 and 4), the viral terminal membrane proteins (TMPs) LMP1 and LMP2A of EBV, R1 of RRV, K1 and K15 of KSHV, Stp and Tip of HVS and Tio of HVA share functional features. The cellular signaling cascades initiated by these TMPs are summarised in figure 6.

1.4 Objectives

Because of the resemblance of K15 to EBV latent membrane proteins LMP1 (with respect to TRAF binding) and LMP2A (with respect to the presence of SH2-B and SH3-B sites as well as structural similarities), we asked whether K15 is also able to elicit cellular signaling cascades. Since LMP1, StpC and K1 were shown to induce the activity of transcription factors, and K15 proteins could bind TRAFs which were proven to be essential for NF-κB activation by LMP1 and StpC, we investigated whether K15 could activate the NF-κB transcription factor.

Another transcription factor, AP-1, is a target of several terminal membrane proteins of γ-herpesviruses. LMP1 for example induces AP-1 via activation of the MAPKs p38 and JNK1, and StpC activates the MAPK Erk2, possibly through its interaction with and activation of cellular Ras. We therefore examined whether K15 has regulatory effects on one of the three MAPK pathways that lead to activation of AP-1 family members of transcription factors. Furthermore, we wanted to identify the site of tyrosine phosphorylation and the kinases phosphorylating K15 proteins - members of the Src family of non-receptor protein tyrosine kinases were potential candidates due to their role in signaling of viral TMPs LMP2A, K1, R1, StpA, Tip and Tio.

In order to define the intracellular distribution of K15 proteins, immunofluorescence studies and cellular fractionation studies of transiently transfected cells were carried out. In addition, we investigated the in vivo expression of K15 proteins in several KSHV cell culture systems.

Studies with the EBV LMP2A and the KSHV K1 protein indicated that they may play a role in the maintenance of viral latency, and we were therefore interested whether K15 proteins could also have a regulatory effect on the viral life cycle of KSHV.

2. Material and Methods

2.1 Reagents and Chemicals

Chemicals were purchased from the following companies: Amersham, AppliChem, Biomol, BioRad, Boehringer Mannheim, Difco, Eurogentech, Fluka, Gibco, ICN, Invitrogene, Life Technologies, Merck, Molecular probes, New England Biolabs, Pierce, Promega, Riedel-deHaën, Roche, Roth, Santa Cruz, Seromed, Serva, Sigma and Stratagene.
Consumables came from Amersham, Beckman, Biozym, Costar, Eppendorf, Falcon, Gilson, Greiner, Kodak, Macherey-Nagel, Pharmacia, Robbins, Qiagen, Sarstedt, Schleicher&Schuell and Whatman.
Radionucleotides were purchased from Hartmann Analytics and restriction enzymes came from Amersham, New England Biolabs and Life Technologies. Oligonucleotides were purchased from MWG Biotech.

2.1.1 Antibodies

α-K15:

Generated by M. Glenn (Glenn et al., 1999), rabbit polyclonal antibody, used in a dilution of 1:1000. GST-K15$^{355-489}$ fusion protein was prepared as described in 2.6.7. The K15 portion of the protein was cleaved by incubating in the presence of PreScission protease while still bound to GST beads according to the manufacturer´s instructions (Amersham Pharmacia). The cleaved C-terminal cytoplasmic domain of K15 (aa 355-489) was eluted with PBS and used to immunize two rabbits according to standard protocols.

α-K15 C12C4:

Mouse monoclonal, see 2.3.8. Tissue culture supernatant used in a 1:4 dilution.

α-JNK1 C-17:

Santa Cruz, rabbit polyclonal affinity-purified, used in a 1:1000 dilution.
Raised against a peptide at the C-terminus of JNK1 of human origin.
Molecular weight of JNK-1: 46 kDa

α-Erk2 D-2:

Santa Cruz, mouse monoclonal IgG_{2b}, used in a 1:2000 dilution.
Raised against a peptide at the C-terminus of human Erk2-encoded MAP kinase.
Molecular weight of Erk2: 42 kDa

α-p38 MAPK H-147:

Santa Cruz, rabbit polyclonal, used in a 1:200 dilution.
Raised against a recombinant protein corresponding to aa 213-360 at the C-terminus of human p38.
Molecular weight of p38: 38 kDa

α-Caveolin-1 (N-20):

Santa Cruz, rabbit polyclonal affinity-purified, used in a 1:200 dilution.
Raised against a peptide at the N-terminus of human caveolin-1. MW: 21-24 kDa

α-c-myc 9E10:
Biomol, mouse monoclonal, protein A purified IgG_1, used in a 1:1000 dilution.
Immunogen: human pp62 c-myc (408-432) peptide. Targets the c-myc epitope EQKLISEEDL.

α-phosphotyrosine P-Thyr-100:
Cell Signaling, mouse monoclonal, used in a 1:2000 dilution.
Binds phospho-tyrosine in a manner largely independent of the surrounding aa sequence.

α-Flag M2:
Sigma, mouse monoclonal, purified IgG_1, used in a 1:2000 dilution.
Recognizes the Flag epitope sequence DYKDDDDK.

α-HA antibody 12CA5:
Boehringer Mannheim, mouse monoclonal, $IgG_{2b}\kappa$, used in a 1:4000 dilution for Western Blotting. Recognizes the HA peptide sequence YPYDVPDYA derived from the human influenza hemagglutinin protein.

α-Calnexin:
Hammond et al., 1994, rabbit polyclonal, used in a 1:1000 dilution.
Calnexin is a 64 kDa type I membrane protein with chaperone-like function in the ER.

α-K8.1 A/B:
Zhu et al., 1999, mouse monoclonal, IgG_{2a}, tissue culture supernatant used in a 1:2 dilution.
Reacts with KSHV virion envelope-associated glycoproteins.

2.2 Vectors and Primers

If not otherwise indicated, all vectors listed code for resistance to Ampicillin.

2.2.1 Eucaryotic expression vectors

pFJEA:
Eucaryotic expression vector containing a SRα-O promoter. Provided by J. Jung (Takebe et al., 1988).

pcDNA3:
T7 and SP6 promoter for in vitro transcription, CMV promoter for expression in mammalian cells. Bovine growth hormone polyadenylation signal. Amp^r and $Neomycin^r$. Invitrogen.

pcDNA3.1(+):
Derived from pcDNA3, with differences in the MCS and lack of the SP6 promoter. Amp^r and $Neomycin^r$. Invitrogen.

pcDNA3.1 Myc-His (-) A:
Derived from pcDNA3.1. With a C-terminal peptide containing the c-myc epitope and a polyhistidine metal-binding tag. Invitrogen.

pEF C-X:
pEF BOS (Mizushima & Nagata, 1990) with 5´*Cla*/*Sal*/*Bam*/*Xba* polylinker, EF-1 α Promoter. Invitrogen.

pEGFP-N1:
N-terminal enhanced fluorescent protein (EGFP) vector suitable for generation of GFP fusion proteins for expression and localisation studies or expression of GFP in mammalian cells. Gene of interest will be inserted into the MCS and expressed as a fusion to the N-terminus of EGFP. CMV promoter, Kan^r, Neo^r. Clontech.

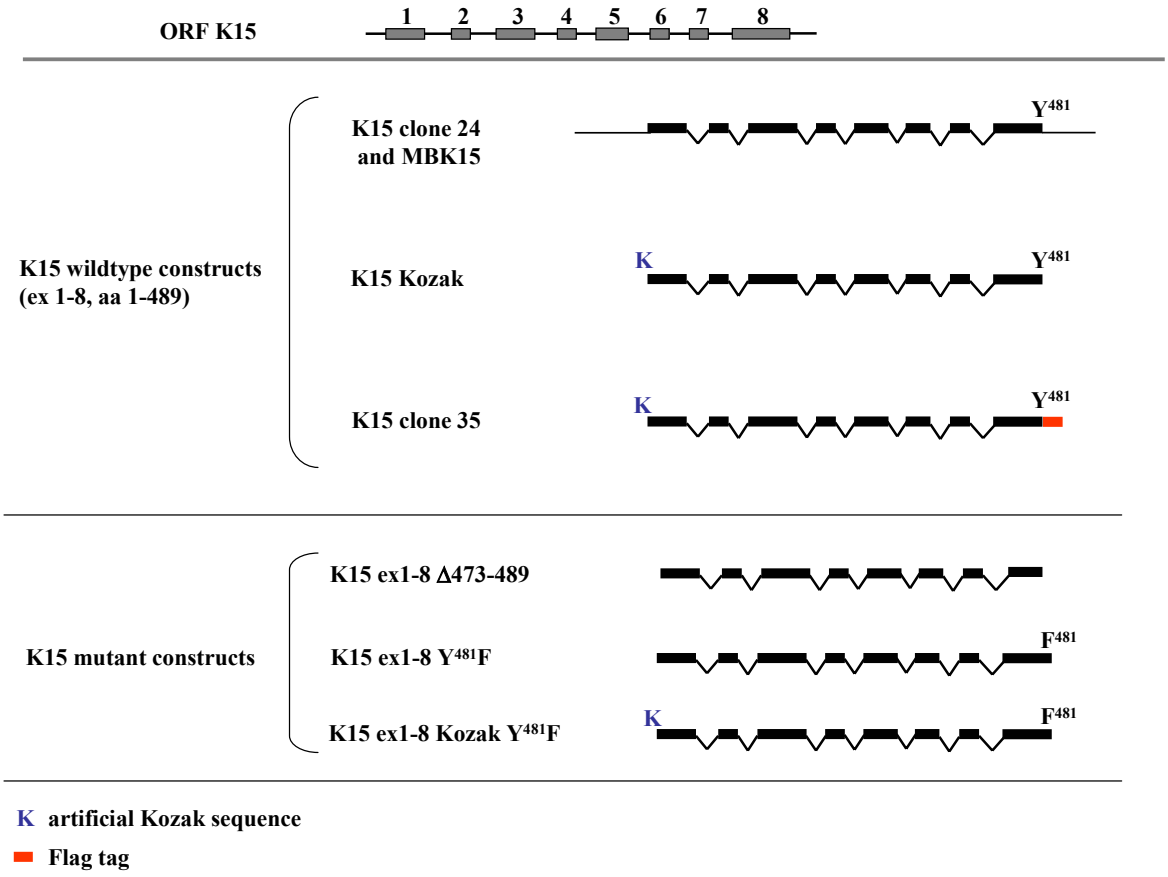

Figure 7: Expression constructs of K15 wildtype and C-terminal K15 mutants used in this study. See text (2.2.1) for further details.

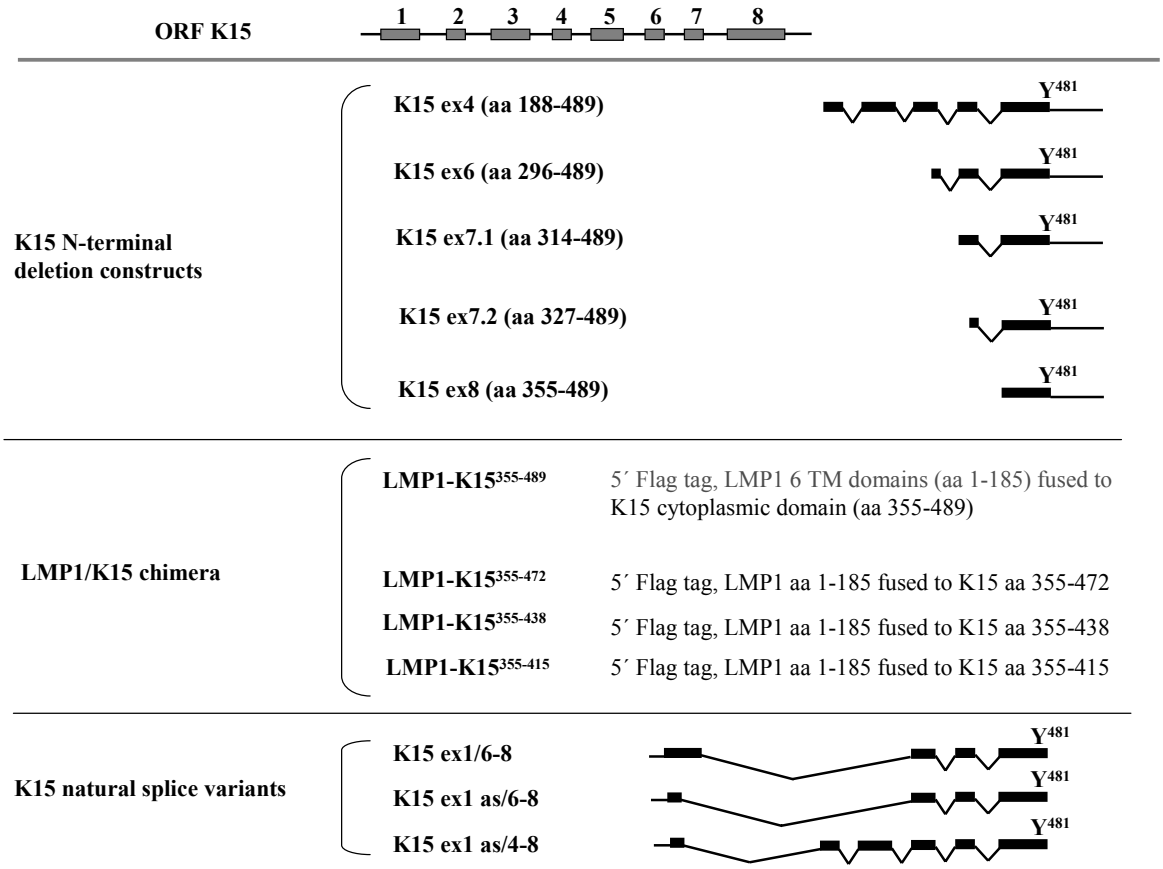

Figure 8: K15 N-terminal deletion constructs, LMP1-K15 chimera constructs and natural splice variants used in this study. See text (2.2.1) for further details. TM = transmembrane, as = alternative splice. For a detailed map of the deletion constructs of the LMP1-K15 chimera, see also figure 19.

K15 expression constructs (see figures 7 and 8):

pK15 clone 35:

Contains a full length cDNA (exons 1-8) of K15 from the BCBL-1 PEL cell line (see 2.3.2) cloned into the *Eco*RI/*Xba*I sites of pFJEA. Contains an artificial Kozak sequence, begins at the putative start codon of K15 in exon 1, and contains a Flag epitope tag at its C-terminal end. Provided by J.-K. Choi (Choi et al., 2000a).

pK15 ex1-8 (aa Δ473-489):

Lacks the C-terminal 17 aa of K15. Generated by PCR amplification of K15 clone 35 with the upstream primer LAMPB5´ and reverse primer ex8ad1. PCR product was cloned into pGEM-T and subsequently cloned into the *Not*I site of pFJEA (M. Glenn).

pK15 ex1-8 $Y^{481}F$:

Carries the $Y^{481} \rightarrow F^{481}$ point mutation in the Y^{481}EEV motif of K15. Generated by PCR amplification of K15 clone 35 with the upstream primer LAMPB5´for and the reverse primer LAMPaY:Frev. PCR product was cloned into pGEM-T and subsequently cloned into the *Not*I site of pFJEA (M. Glenn).

pK15 clone 24:

Full length K15 cDNA clone (K15 aa 1-489) from the BCP-1 KSHV isolate. Generated by RT-PCR amplification of the K15 region using primer LRH6for (binding 192 bp upstream of

the putative start codon of K15) and primer ex8arev (binding to the start region of ORF75 245 nucleotides downstream of the K15 stop codon). The resulting PCR product was cloned into pGEM-T (L. Rainbow, Glenn et al., 1999).

pMBK15:

pK15 clone 24 was digested with *EcoR*I and cloned into pFJEA.

pMBK15 Kozak:

Full length K15 with an artificial Kozak sequence at the ATG in exon 1 but without any tag. Generated by PCR on pMBK15 using primers K15*Eco*RIKozakfor and reverse primer FlagLAMPa3´. Cloned *EcoR*I in pFJEA.

pMBK15 Kozak $Y^{481}F$:

Generated as pMBK15 Kozak but with reverse primer LAMPaY:Frev introducing the aa substitution $Y^{481} \rightarrow F^{481}$.

pMBK15 Kozak on pcDNA3.1:

pMBK15 Kozak was digested *Eco*RI and the insert cloned *Eco*RI into pcDNA3.1.

pK15 splice variants K15 ex1/6-8, K15 ex1 as/6-8 and K15 ex1 as/4-8:

The cDNAs were generated by RT-PCR amplification of the K15 region (BCP-1 KSHV isolate, see 2.3.2) using primers LR65for (binding 192 bp upstream of the ATG in exon 1) and ex8arev, followed by a nested PCR with forward primer FJLampfor (binding 45 nucleotides upstream of the K15 start codon), and reverse primer FJLamprev (binding at the K15 stop codon). PCR products were cloned into pGEM-T, and subsequently into the *Eco*RI and *Kpn*I sites of pFJEA (L. Rainbow).

K15 N-terminal deletion constructs:

pK15 ex4-8:

Initiates at the ATG in exon 4 and codes for aa 188-489 of K15. The PCR product amplified with primers MBexon4for and FlagLAMPa3´ from pK15-24 was cloned in pGEM-T and subsequently into the *Psp*AI/*Spe*I sites of pFJEA.

pK15 ex6-8 on pFJEA or pcDNA3.1:

Begins at the ATG in exon 6 and codes for aa 296-489 of K15. The PCR product was amplified with primers MBexon6for and FlagLAMPa3´ from pK15-24 and cloned *Kpn*I/*Eco*RI in pcDNA3.1 and subsequently *Kpn*I/*Not*I in pFJEA.

pK15 ex7.1-8 on pFJEA:

Begins at the first ATG in exon 7 and codes for aa 314-489 of K15. The PCR product was amplified with primers MBexon7.1for and FlagLAMPa3´ from pK15-24 and cloned in pGEM-T and subsequently *Kpn*I/*Not*I in pFJEA.

pK15 ex7.2-8 on pFJEA or pcDNA3.1:

Begins at the second ATG in exon 7 and codes for aa 327-489 of K15. The PCR product amplified with primers MBexon7.2for and FlagLAMPa3´ from pK15-24 was cloned *Kpn*I/*Eco*RI in pcDNA3.1 and subsequently *Kpn*I/*Not*I in pFJEA.

pK15 ex8:
Codes for the putative C-terminal domain of K15 (aa 355-489). PCR was performed with primers ex8forVNSYRQ and FlagLAMPa3´ on pMBK15, and the amplified fragment was cloned *Kpn*I/*Eco*RI in pcDNA3.1.

pLMP1-K15$^{355-489}$:
Chimera consisting of the six N-terminal transmembrane domains of LMP1 (aa 1-185) and the cytoplasmic region of K15 (aa 355-489). Constructed by amplification of the transmembrane domain of LMP1 from plasmid pSG5-LMP1 using primers LMPLAMPa5´ (introduces the Flag epitope tag) and LMPLAMPa3´ (the first 25 nucleotides are homologous to a region in the C-terminus of K15). The resulting amplicon was purified and used as a primer together with primer FlagLAMPa3´ in a PCR using genomic BCP-1 DNA (see 2.3.2) as template. The resulting product was cloned *Kpn*I/*Eco*RI into pcDNA3 (M. Glenn). N-terminally Flag-tagged.

pLMP1-K15$^{355-489}$ deletion constructs (see also figure 8):
Generated by PCR on plasmid pLMP1-K15$^{355-489}$ with forward primer LMPLampa5´ and reverse primers ex8aD1rev, ex8aD2rev, ex8aD3rev to generate pLMP1-K15$^{355-472}$, pLMP1-K15$^{355-438}$, pLMP1-K15$^{355-415}$, respectively. Cloned *Kpn*I/*Eco*RV in pcDNA3. All are N-terminally Flag-tagged. M. Glenn.

pSV-LMP1:
Expression vector based on pHEBO (Sugden et al., 1985) in which LMP1 is expressed from a subgenomic EBV fragment under transcriptional control of the SV40 promoter/enhancer (Kieser et al., 1997). Provided by A. Kieser.

pSG5-LMP1:
LMP1 wildtype cloned in pSG5 (Huen et al., 1995, Liebowitz et al., 1992). pSG5 (Stratagene) contains the SV40 early promoter and a β-globulin intron upstream of the cloning site. Provided by A. Eliopoulos.

pTRAF-1, -2, -3:
cDNA plasmids expressing Flag-tagged human TRAF-1, -2, -3. Provided by M. Rothe.

pcSrc, pcFyn, pEFYes:
C-terminally myc-tagged protein tyrosine kinases. Src (full length chicken Src, aa 1-533) and Fyn (full length, human, aa 1-537) are both cloned *Eco*RI/*Bam*HI into pcDNA3.1 Myc-His (-) A. Yes was cloned in pEF C-X. Constructed and provided by S. Lang.

pEFLck, pEFHck:
C-terminally myc-tagged full length PTKs, both cloned into pEF C-X. Constructed by A. Baur, provided by S. Lang.

pSRα-HA-JNK1:
HA-tagged MAPK JNK1 (Minden et al., 1994, Derijard et al., 1994). Provided by A. Kieser.

pSRα-HA-Erk2:
HA-tagged MAPK Erk2 (Minden et al., 1994). Provided by A. Kieser.

pCMV-HA-p38:
HA-tagged MAPK p38α (Minden et al., 1994). Provided by A. Kieser.

pRKH5:
Expression vector containing a CMV promoter. Provided by A. Kieser.

pRK-TRAF-2(87-501):
Dominant negative mutant of TRAF-2 lacking aa 1-86 (comprising the N-terminal RING finger domain) cloned into pRKH5 (Hsu et al., 1996, Natoli et al., 1997, Rothe et al., 1995). Provided by A. Kieser.

pTRAF-6(300-524):
Dominant negative mutant of human TRAF-6. Lacks aa 1-299 including the RING finger domain. Cloned into pcDNA3.1 (Schultheiss et al., 2001). Provided by A. Kieser.

pCis2:
Expression vector provided by A. Kieser.

pRas N-17:
Dominant negative mutant of Ras with a single point mutation (Asparagine 17) cloned into pCis2 (Stacey et al., 1991). The aa substitution is localised to the putative Mg^{2+} binding site of Ha-Ras. Provided by A. Kieser.

pKRSPA:
Expression vector containing the Rous sarcoma virus promoter and the SV40 polyadenylation signal cloned into the distal ends of the MCS of the pBluescript-KS^{+} vector from Stratagene (Dorn et al., 1990). Provided by S. Ludwig.

pErk2 C3 ($Y^{185}\rightarrow F^{185}$):
Dominant negative mutant of Erk2 in the vector background pKRSPA with one single aa substitution ($Y^{185}\rightarrow F^{185}$) (Robbins et al., 1993, Ludwig et al., 1996). Provided by S. Ludwig.

pRaf C4B:
Dominant negative mutant of c-Raf-1. Carboxy-terminal deletion mutant which contains the Ras binding domain (Bruder et al., 1992) fused to HA and cloned into pKRSPA (Flory et al., 1996, Ludwig et al., 1998). Provided by S. Ludwig.

pRTA:
RTA (ORF50) expressing plasmid with a Flag peptide sequence at the N-terminus. Contains the cDNA sequence of RTA following the CMV enhancer-promoter sequence cloned *Eco*RI/*Xba*I into pFlagCMV2 (Song et al., 2002). Provided by Ren Sun.

pCaveolin-1-GFP:
C-terminally GFP-tagged canine caveolin-1. Vector backbone is pEGFP-N1, Kan^{r} (Pelkmans et al., 2001). Provided by A. Helenius.

2.2.2 Reporter vectors

pRTU14:

AP-1 reporter construct with the luciferase reporter gene under the control of a minimal promoter and four TREs (TPA response elements) (Kieser et al., 1996). Provided by A. Kieser.

pRTU1:

pRTU14 lacking the TREs (Kieser et al., 1996). Provided by A. Kieser.

p3EnhκBconA-Luc:

NF-κB reporter plasmid. Comprises the firefly luciferase gene cloned downstream of a minimal promoter into which three κB elements derived from the immunoglobulin kappa chain enhancer are inserted (Arenzana-Seisdedos et al., 1993, Eliopoulos et al., 1997). Provided by A. Eliopoulos.

pGL2basic:

Luciferase reporter vector (Promega). Lacks eucaryotic promoter and enhancer sequences. Expression of luciferase activity depends on insertion and proper orientation of a functional promoter upstream of the luciferase coding region.

p3kbORF50P:

3 kb promoter region of ORF50 amplified with primers *Nhe*IRTAfor and *Bgl*IIRTA2 from HBL-6 DNA (KSHV positive PEL cell line) and cloned *Nhe*I/*Bgl*II upstream of the luciferase cDNA of pGL2basic (Deng et al., 2000). Generated by A. Viejo-Borbolla.

2.2.3 Procaryotic expression vectors

pGEM-T easy:

System for cloning of PCR products with single 3´ thymidine overhangs at the insertion site (Promega). Contains T7 and SP6 RNA polymerase promoters flanking a multiple cloning region within the α–peptide coding region of β–galactosidase.

pGEX-6P-1, pGEX-3X:

GST fusion vectors (Amersham Pharmacia). Contain a tac promoter for chemically inducible expression (IPTG) and an internal $lacI^q$ gene. pGEX-6P-1 encodes the recognition sequence for site-specific cleavage by PreScission protease and pGEX-3X the factor Xa protease recognition site between the GST domain and the MCS.

GST-K15 fusion proteins (see figure 19):

pGST-$K15^{355-489}$:

Entire predicted cytoplasmic domain (aa 355-489) of K15 (BCP-1 derived, see 2.3.2) fused to GST, cloned into pGEX-6P-1 (Glenn et al., 1999).

pGST-K15$^{355-472}$:
GST fusion plasmid in which the carboxy terminal 17 aa of K15 were deleted. Generated by PCR on pGST-K15$^{355-489}$ using the 5´ primer GSTex8afor and the 3´ primer ex8aD1rev, cloned into pGEX-3X (M. Glenn).

pGST-K15$^{355-438}$:
Generated using plasmid pGST-K15$^{355-489}$ as template together with primer GSTex8afor and reverse primer ex8aD2rev, cloned into pGEX-3X (M. Glenn).

pGST-K15$^{355-373}$:
Generated using plasmid pGST-K15$^{355-489}$ as template together with primer GSTex8afor and reverse primer ex8aD4rev, cloned into pGEX-3X (M. Glenn).

pGST-c-Jun:
c-Jun-GST fusion protein (Kieser et al., 1997). Provided by A. Kieser.

2.2.4 Primers

Table 2 summarises the primers being used for reverse transcriptase reactions and PCR.

Table 2: Primers used for RT-PCR and PCR. The primer sequences are shown in 5´ to 3´ direction. Primer LMPLAMPa5´ introduces the Flag epitope tag DYKDDDDK (sequence underlined), whilst the first 25 nucleotides of LMPLAMPa3´ are homologous to a region within the carboxy terminus of K15 (sequence underlined). Substituted bases are marked in bold.

Name	5´-3´ sequence
LR65for	ACGATCTAGATCCGGAATATTTATGAGC
LRH6for	ATCCGGAATATTTATGAGCC
LAMPB5´for	ATCGGATCCAAAATGAAGACACTCATATTCTTCTGG
MBK15Bfor	CTCCCCGGGCATTTACAACAACTCTATTG
FJLAMPfor	ATCGAATTCCATTTACAACAACTCTATTG
K15*Eco*RIKozakfor	TATGAATTCGCCACCATGAAGACACTCATATTCTTCTGG
LR65for	ACGATCTAGATCCGGAATATTTATGAGC
MBexon4for	CTCCCCGGGGCTTGGTCATGGGTTACCCTGTATCC
MBexon6for	ATCGGTACCATGCTGCATTTAATTG
MBexon7.1for	ATCGGTACCATGCTTCTCCCTAGTG
MBexon7.2for	ATCGGTACCATGATCATCTGCATCAG
MBexon8forVNSY	ATCGGTACCGCCACCATGGTAAATAGTTACCGACAG
GSTex8afor	CAGGGATCCTAAATAGTTACCGACAGAGAAGGGG
ex8aD4rev	ACTCCCGGGTGTGGTGTAAGTTCTGGTCCC
ex8aD3rev	ACTCCCGGGTCGTTCAGTAGTTGGCTCCCG
ex8aD2rev	ACTCCCGGGACCGGACACTAAAATACTGGC
ex8aD1rev	ACGCCCGGGTTAGGCTTGGGCGGTGTCTATACGGAAGGC
FlagLAMPa3´	TATGAATTCCTAGTTCCTGGGAAATAAAAC
LAMPaY:Frev	TATGAATTCCTAGTTCCTGGGAAATAAAACCTCCTC**AAA**CAGGTC
FJLAMPrev	ATCGGTACCTAGTTCCTGGGAAATAAAAC
LRR6rev	CATGTAGCCATGTCACTAACCTC
ex8arev	CTCCAACCACAGCCCAGTGACG
LMPLAMPa5´for	GACGGTACCATGGACTACAAGGACGATGACGACAAGGAACAC GACCTTGAGAGGGGCCCACCG
LMPLAMPa3´rev	CCTTCTCTGTCGGTAACTATTTACTTCATCACTGTGTCGTTGTCCATGG
*Nhe*IRTAfor	ACGCTAGCGCTCCTTCAATTGGAAGCA
*Bgl*IIRTA2rev	ACAAGATCTTTGTGGCTGCCTGGACAGTATTC

2.3 Eucaryotic cell culture methods

2.3.1 General components for cell culture

DMEM (Gibco)	+ 0.11 g/l Sodiumpyruvate, with Pyridoxine
MEM (Biochrom)	+ Eagle´s BSS, NEAA, L-Glutamine, 2.2 g/l $NaHCO_3$
RPMI 1640 (Gibco)	+ L-Glutamine
RPMI 1640 (Cytogen)	+ Glutamine, Hepes
Grace´s Insect medium (Gibco)	+ L-amino acids
Penicillin, Streptomycin (Cytogen)	10.000 U/ml, 10 mg/ml
L-Glutamine (Cytogen)	200 mM
NEAA (Gibco)	100x
Pyruvate (Gibco)	100 mM
β-mercaptoethanol (Gibco)	50 mM
Trypsin/EDTA (Cytogen)	0,05/0,02% in PBS
FCS (Gibco)	heat-inactivated for 30 min at 56°C
Puromycin (Sigma)	5 mg/ml stock
G418 (Sigma)	67 mg/ml stock
Neomycin (Amimed)	10.000 µg/ml
Amphotericin B (PAN Systems)	250 µg/ml
FCS hybridoma grade (PAA lab.)	heat-inactivated for 30 min at 56°C
HAT Media supplement (Sigma)	50x
PBS (1x)	137 mM NaCl 2.7 mM KCl 6.6 mM Na_2HPO_4 x $2H_2O$ 1.5 mM KH_2PO_4

2.3.2 Eucaryotic cell lines

Adherent cell lines:

HEK 293:

With Adenovirus Type 5 (Ad 5) DNA transformed human embryonic kidney epithelial cell line (ACC 305 from the German Collection of Microorganisms and Cell Cultures).

293-T:

The 293-T cell line is a highly transfectable derivative of the 293 cell line, into which the temperature sensitive gene for SV40 T-antigen was inserted. Expresses the SV40 T antigen. (ATCC CRL-11268).

Cos7:

Kidney fibroblasts, isolated from the African green monkey (*Cercopithecus aethiops*). SV40 transformed, expresses the SV40 T antigen (ATCC CRL-1651). Derived from the CV-1 cell line (ATCC CCL-70) by transformation with an origin defective mutant of SV40 which codes for wildtype T antigen.

Ptk2:
Epithelial cell line (kidney) isolated from *Potorous tridactylis* (ATCC CCL-56).

DU145:
Human epithelial cell line isolated from a prostate carcinoma (ATCC HTB-81).

T24:
Human epithelial cell line isolated from a bladder carcinoma (ATCC HTB-4).

Vero:
Epithelial cell line (kidney) isolated from the African green monkey (*Cercopithecus aethiops*) (ATCC CCL-81).

Insect cells SF9:
Cells isolated from *Spodoptera frugiperda* (ATCC CRL-1711).

Adherent cell lines carrying a recombinant KSHV genome:
DU145 rKSHV:
DU145 cells stably transfected with rKSHV.152 (Vieira et al., 2001). In rKSHV (derived from BCBL-1, see 2.3.2), a GFP/*neo* cassette was inserted between the polyadenylation sites for ORFs 57 and K9 (see figure 1). The GFP gene is expressed from the elongation factor 1-α promoter. The *neo* gene (RSV promoter) confers resistance to G418.

T24 rKSHV:
T24 cells stably transfected with rKSHV.152 (Vieira et al., 2001).

Vero rKSHV:
Vero cells stably transfected with recombinant KSHV (rKSHV.219) with a cassette inserted between ORF K9 and 57 (see figure 1) that contains the red fluorescent protein under the control of the lytic PAN RNA promoter along with GFP being expressed by the human elongation factor 1-α promoter and the PAC gene for resistance to puromycin expressed by the RSV promoter. Kindly provided by J. Vieira.

Suspension cells:
PEL cell lines:
BCBL-1:
Body cavity lymphoma cell line, established in vitro from a malignant effusion. $KSHV^+$, EBV^- (Renne et al., 1996).

BCP-1:
Established from peripheral-blood mononuclear cells of a HIV seronegative patient with PEL who previously had KS. $KSHV^+$, EBV^-, HIV^- (Boshoff et al., 1998).

CroAP-3:
Human B-cell lymphoma cells, established from the malignant PEL of a 42-year-old HIV^+ man at diagnosis without a previous history of KS. $KSHV^+$, EBV^-, HIV^- (ACC 275; Carbone et al., 1998).

CroAP-5:
Human B-cell lymphoma cells, established in 1998 from the pleural effusion of a 35-year-old HIV^+ man with PEL and a sarcoma. $KSHV^+$, EBV^+, HIV^- (ACC 215; Carbone et al., 1998).

CroAP-6:
Derived from the pleural effusion of a 26-year-old man with a 2 year history of HIV infection. Cell phenotype: lymphoid, non-B non-T-cell phenotype. Approximate copy number of KSHV: 20-80 copies of KSHV DNA per cell. $KSHV^+$, EBV^-, HIV^- (Carbone et al., 2000).

Jsc-1:
Established from the ascites fluid of a HIV^+ patient. Low level of EBV latent gene expression. Lytic and latent KSHV gene expression. Produces more infectious virus than BCP-1 (see above) upon induction with TPA (Cannon et al., 2000).

ISI:
Established in 1996 from a PEL related to AIDS. $KSHV^+$, EBV^- (Oksenhendler et al., 1998).

BBG-1:
Established from an AIDS patient with a cutaneous lymphoma from the patient´s peripheral blood mononuclear cells. Spontaneously expresses KSHV lytic antigens and EBV transforming latent antigen EBNA2. $KSHV^+$, EBV^+, HIV^- (Morand et al., 1999).

B-cell lines:
DG75:
Derived from the pleural effusion of a child with a primary abdominal lymphoma, which resembled Burkitt´s lymphoma. $KSHV^-$, EBV^- (Ben Bassat et al., 1977).

Raji:
B-lymphocytes established from a Burkitt´s lymphoma. $KSHV^-$, EBV^+ (ATCC CCL-86).

BJAB:
Continuous lymphoma cell line, derived from the tumour of an exceptional African case of Burkitt´s lymphoma. Contains no detectable amount of EBV (Clements et al., 1975).

Myeloma cell line P3X63Ag8.653:
Isolated from BALB/c mice. HAT sensitive (ATCC CRL-1580). Used for fusion of spleen cells from immunized Balb/c mice to generate hybridoma cell lines. See also 2.3.8.

2.3.3 Cell culture conditions

All cell culture media contained Penicillin (50 U /ml), Streptomycin (50 µg/ml) and glutamine (300 µg/ml).

Cos7, 293, 293-T, T24, DU145:	DMEM with 10% (v/v) FCS
B-cells, PEL cells:	RPMI 1640 with 10% (v/v) FCS
BCP-1 and CroAP-3 cells:	RPMI 1640 with 20% (v/v) FCS
Vero, PtK2:	MEM with 10% (v/v) FCS
SF9 insect cells:	Grace´s insect medium with 10% (v/v) FCS

Hybridoma cells:	RPMI 1640 with: 1% (v/v) NEAA, 0.1% (v/v) β–Mercaptoethanol, 0.5% (v/v) Neomycin, 1% (v/v) Amphotericin, 10% (v/v) FCS, 2% (v/v) HAT
Vero rKSHV:	MEM with 10% (v/v) FCS, Puromycin 5µg/ml
DU145rKSHV, T24 rKSHV:	DMEM with 10% (v/v) FCS, G418 250 µg/ml

Cells were kept in humified air with 5% CO_2 at 37°C. Insect cells were cultured at 27°C and split at 100% confluency. All cell lines were split at 80% confluency.

2.3.4 Cryoconservation

For conservation, cells were resuspended in 1 ml of the appropriate cell culture medium with 20% FCS and 8 % DMSO, transferred in a cryo tube and frozen in a polystyrene box at -20°C. After 4 h, the cells were transferred to -80°C for 24 h and then stored in liquid nitrogen. PEL cell lines were frozen in FCS containing 8% DMSO. For recovery, cells were thawn for 10 min at 37°C, washed with 10 ml medium and transferred to a tissue culture flask.

2.3.5 Lytic cycle induction, preparation of rKSHV.219 and infection of epithelial and B-cells with rKSHV.219

TPA (Sigma, in DMSO) was added to the cells at 20 ng/ml, and n-butyrate (Sigma, in H_2O) at 1 mM final concentration for induction of the lytic viral life cycle.
Suspension cells were split to a density of 2.5 x 10^5 cells/ml at 12-20 h before induction with TPA or n-butyrate and were lysed 48 h later.
Vero rKSHV.219 cells were induced with 1 mM n-butyrate and Baculovirus ORF50 (prepared as described in 2.3.6) diluted 1:20 in fresh medium at 80% confluency. In order to produce rKSHV.219 for infection studies, MEM medium without puromycin was added to the cells before induction containing n-butyrate and Baculovirus ORF50. One day after induction, medium was replaced with fresh medium without puromycin. The medium containing free rKSHV.219 was collected 3 days after induction, centrifuged for 15 min at 3.000 x g, filtered through a 0.45 µm filter and stored at 4°C.
Epithelial cell lines 293-T, 293 or Vero were plated to be 50% confluent at the time of infection with rKSHV.219 prepared as described above and B-cell lines BCBL-1, BJAB and Raji were infected at a cell density of 2.5 x 10^5 cells/ml. In order to determine the infectivity of rKSHV.219 (infectious units per ml, IU/ml), a serial dilution of rKSHV.219 was applied to the epithelial cell lines. rKSHV.219 was added at 1:2 dilution to the B-cell lines. After a 12 h incubation, virus containing medium was removed and fresh medium was added to the epithelial cells. B-cells were left in rKSHV.219 containing medium for the entire time. IU/ml were determined by counting GFP expressing cells.

2.3.6 Production of Baculovirus ORF50/RTA

Baculovirus ORF50 was kindly provided by J. Vieira. For production of new Baculovirus ORF50, insect cells cultured in suspension at 27°C were infected at a cell density of 1 x 10^6 cells/ml with Baculovirus ORF50 directly added to the cells (1:20 dilution). When a cytopathic effect was observed (usually two days post infection), the medium was collected, cleared from cells by centrifugation at 3.000 x g and stored at 4°C.

2.3.7 Transient transfection

Electroporation of suspension cells was carried out with the Biorad Gene pulser Xcell Electroporation system. Cells were split one day prior transfection. At the day of transfection, cells were pelleted by centrifugation, washed once with RPMI 1640 medium without FCS [RPMI (-)] and resuspended to a cell density of 1.5-2.5 x 10^7 cells/ml in RPMI (-). DNA was added to 200 µl of cell suspension in an eppendorf tube and mixed by carefully pipetting up and down once. During a 10 min incubation at RT, 0.2 cm cuvettes (Biorad) were prepulsed with RPMI (–) at 100 Volts and 975 µF. Then, the DNA/cell suspension mix was added to a prepulsed cuvette and pulsed at 100 Volts and 975 µF in the Biorad Gene pulser. Immediately after the pulse, 200 µl of RPMI containing 30% FCS were added to the cuvette and the cells were transferred to a 6 well plate already containing 2 ml of RPMI with 10% FCS. The length of the pulse should not vary more than 2-3 msec between samples that are to be compared.

293, 293-T and Vero cells were transfected using the Fugene 6 transfection reagent (Roche) according to the manufacturer´s instructions. Fugene 6 is a lipid-based transfection reagent, and usually a transfection efficiency of ~40% was reached. The DNA:Fugene 6 ratio was kept constant at 1µg:3µl throughout all experiments. Usually, cells were plated one day prior transfection and were 50% confluent at the day of transfection. Vero rKSHV cells were plated at a cell density of 0.8 x 10^5cells/ml (= 1.6 x 10^5 cells per well of a six well plate) the day prior transfection and transfected with Fugene at 80% confluency. For reporter assays using the AP-1 reporter plasmid pRTU14 and for the Erk2 Kinase assay, 293-T cells were transfected at 80% confluency and the medium was replaced with fresh medium containing 1% FCS prior addition of the DNA-Fugene 6 mix.

Cos7 cells were transfected with the Effectene transfection reagent (Qiagen), which is based on a non-liposomal lipid. For six well plates, 400 ng DNA were diluted with the DNA condensation (EC) buffer to a total volume of 100 µl. 1.6 ml of fresh growth medium were added to each well of the six well plate. To the DNA, 3.2 µl Enhancer and 5 µl Effectene were added according to the manufacturer´s instructions. After a 10 min incubation at RT, 600 µl of medium containing 10% FCS were added to the complex, mixed by pipetting up and down twice and added dropwise to the cells.
Total amounts of transfected DNA were adjusted using salmon testis DNA (Sigma) for all transfection methods.

2.3.8 Generation of mouse monoclonal antibodies to the C-terminal K15 domain

In order to generate antibodies directed against K15 in its native form, Balb/c mice were immunized with purified K15-GST fusion protein (GST-K15$^{355-489}$, see 2.6.7). The protein concentration was adjusted to 300 µg/ml and each mouse was immunized with 40 µg of antigen three times over a time period of four months and boosted once three days before sacrificing the mice (=160 µg protein total per mouse). For the first immunisation, the antigen was mixed 1:1 with complete Freunds Adjuvans (Sigma) and injected intraperitoneally. For the following immunisations, incomplete Freunds Adjuvans was used (Methods Enzymol., 1986, 121, Hybridoma techniques and monoclonal antibodies). Spleens were removed and spleen cells fused with the P3X63Ag8.653 myeloma cell line to generate antibody secreting hybridoma cell lines. Fused cells were seeded into dishes to derive clonal colonies. After fusion and single-cell cloning, each hybridoma supernatant was tested for reactivity against GST and GST-K15 protein by ELISA as follows:
96 well plates were coated overnight at RT with 200 ng purified GST-K15$^{355-489}$ diluted in 0.1 M $NaHCO_3$ pH 8.5 per well. The following day, plates were washed six times with PBS-T

(see 2.6.3) and incubated for 2 h at RT with blocking buffer (see 2.6.3). After washing once with PBS-T, plates were incubated with hybridoma culture supernatants diluted 1:1 in blocking buffer for 1 h at RT. Plates were then washed six times with PBS-T and incubated with anti-mouse AP-conjugated secondary antibody diluted 1:1000 in blocking buffer for 1 h at RT. After six washes with PBS-T, AP-substrate (1 mg/ml p-Nitrophenyl phospate in AP substrate buffer) was added for 1 h at 37°C and plates were analysed photometrically in an ELISA plate reader (Anthos reader 2001) at 405 nm.
The monoclonal antibodies were further characterized by immunoblotting or in a peptide array as described in 2.6.3 or 2.6.6, respectively.

AP-substrate buffer: 0.75% glycine
1 mM $MgCl_2$
1 mM $ZnCl_2$
pH 10.4 with NaOH

2.4 Procaryotic culture methods

2.4.1 Culture media and growth conditions

LB-medium:
1% (w/v) Trypton (Becton Dickinson)
0.5% (w/v) Yeast extract (Difco)
1% (w/v) NaCl
pH 7.0 with NaOH

2YT-medium:
1.6% (w/v) Peptone (Difco)
1% (w/v) Yeast extract
0.5% (w/v) NaCl
pH 7.0 with NaOH

Agar-plates:
LB-Medium with 1.5% (w/v) Bacto-Agar (Becton Dickinson)

Overnight cultures were usually grown in LB medium at 37°C and 220 rpm. The medium was inoculated with bacteria kept on agar plates at 4°C or from cryoconserved cultures (2.4.3). The medium/agar plates, according to the properties of the plasmid being introduced, were supplemented with a final concentration of:

Ampicillin	100 µg/ml
Kanamycin	25 µg/ml
Chloramphenicol	20 µg/ml
IPTG	0.5 mM
X-Gal	100 mM

2.4.2 Bacterial strains

E. coli BL21:
hsdS gal (λ*c* I*ts*857 *ind*1 *S*am7 *nin*5 *lac*UV5-T7 gene *1*)

E. coli TG-2:
*supE hsd*Δ5 *thi* Δ(*lac-proAB*) Δ(srl-recA)306::Tn*10*(tet^r)F´[*traD*36 $proAB^+$ $lacI^q$ *lacZ*ΔM15]

2.4.3 Cryoconservation of bacteria

800 µl of overnight culture were added to 75 µl DMSO in a cryo tube and stored at -80°C.

2.4.4 Preparation of competent cells and transformation

Competent bacteria were prepared using the rubidium chloride method. An overnight culture was diluted 1:100 in LB medium and grown at 37°C and 200 rpm to an OD_{600} between 0.6 and 0.8. From now on, all steps were performed at 4°C and buffers were ice cold. Cells were kept on ice for 15 min, centrifuged at 1.000 x g for 10 min and cell pellets were resuspended gently and thoroughly in 20 ml RF1 buffer per 50 ml of starting culture. After a 15 min incubation on ice, cells were centrifuged as above, resuspended in 2 ml RF2 per 50 ml of starting culture and aliquoted à 200 µl. After 15 min incubation on ice, cells were competent and were used for transformation or stored at -80°C.
For each transformation, 200 µl of competent bacteria were mixed with DNA (e.g. 100 ng plasmid DNA) in a 1.5 ml tube, incubated on ice for 1 h and subsequently heat shocked for 45 sec at 42°C and put on ice for 5 min. After addition of 800 µl LB medium prewarmed to 42°C and an incubation period of 45 min at 37°C and 200 rpm, 100 µl of cell suspension was plated onto LB agar plates containing the appropiate antibiotic for selection. Plates were incubated overnight at 37°C.

RF1:		RF2:	
	100 mM $RbCl_2$		10 mM MOPS
	30 mM K acetate		75 mM $CaCl_2$
	10 mM $CaCl_2$		10 mM $RbCl_2$
	50 mM $MnCl_2$		
	15 % (v/v) glycerol		15% (v/v) glycerol
	pH 5.8 with acetic acid		pH 6.5 with KOH

2.5 Molecular biological methods

2.5.1 Isolation of plasmid DNA

Plasmid DNA was isolated with the QIAprep Spin Miniprep Kit from Qiagen or with the Nucleobond AX Maxiprep Kit from Machery & Nagel according to the manufacturer´s instructions.

2.5.2 Enzymatic modification of DNA

Digestion of DNA with specific restriction endonucleases, dephosphorylation with alkaline phosphatase and ligations were performed with enzymes and the suitable provided buffers from Roche, Boehringer Mannheim, New England Biolabs or Life Sciences according to the manufacturer´s instructions or to Sambrook *et al.* (1989).

2.5.3 Amplification of DNA

Standard PCR reactions were carried out in a final volume of 50 µl with the following components: 200 ng of template DNA, two specific primers (5 pmoles each), 200 µM dNTPs, 3 mM $MgCl_2$, 1x polymerase buffer, 5 U Taq/Pfu polymerase and H_2O in a 0.2 ml PCR tube. DNA fragments were amplified with the appropriate oligonucleotide primers listed in table 2 in a Perkin Elmer GeneAmp PCR System 2400 thermocycler. The length of denaturation, annealing and elongation were dependent on the characteristics of the DNA template (e.g. genomic DNA or plasmid DNA, GC-content of the fragment), the primers (the optimal annealing temperature was usually investigated experimentally starting with a value calculated according to the formula 4x (G/C) + 2x (A/T) - 5) and the length of the amplified PCR product.

2.5.4 Preparation of RNA and RT-PCR

Total RNA was prepared with the RNeasy Mini Kit from Qiagen according to the manufacturer´s instructions. DNase digestion was carried out during the RNA purification step using the RNase-free DNase set from Qiagen. To ensure purity and RNA concentration, it was analysed spectrometrically and an aliquot was run on a 1% agarosegel.
For reverse transcription reactions, the Expand reverse transcriptase from Roche was used. Expand reverse transcriptase is a RNA directed DNA polymerase and is a genetically engineered version of the moloney murine leucaemia virus reverse transcriptase. This enzyme synthesizes a complementary cDNA strand (cDNA) with mRNA or single-strand DNA as substrate in the presence of an oligo (dT) or a specific primer.
First-strand cDNA synthesis: 1-1.5 µg of total RNA and 10 picomoles specific reverse primer were pipetted in a 0.2 ml PCR tube and filled up with H_2O to give a final volume of 11.5 µl. RNA and primer were denatured at 65°C for 10 min in a thermocycler, immediately cooled on ice and the following components were added to give a final volume of 20 µl: 1 x Expand buffer, 10 mM DTT, 2.5 mM dNTPs, 20 Units RNase Inhibitor and 50 Units Expand reverse transcriptase. The tubes were incubated at 42°C for 1 h in a thermocycler and stored at -20°C.
For the subsequent PCR, 6-10 µl of cDNA were mixed with two specific primers (10 pmoles each), 200 µM dNTPs, 1x polymerase buffer, 3 mM $MgCl_2$, 5 U of Taq/Pfu polymerase and filled up with H_2O to a final volume of 50 µl. Cycling conditions were determined experimentally.

2.5.5 Electrophoresis of DNA and extraction from agarose gels

DNA loading buffer (5x) was added to plasmid DNA or DNA fragments and the DNA was separated electrophoretically with 0.5-1.5 % agarosegels in TAE running buffer. DNA-fragments were purified with the QIAquick Gel Extraction Kit from Qiagen according to the manufacturer´s instructions.
Molecular weight marker: 1 kb plus DNA ladder (Invitrogen)

DNA-loading buffer (5x):
100 mM Tris-HCl, pH 7.4
10 mM EDTA, pH 8.0
45% (v/v) Glycerol
Orange G

TAE buffer (1x):
40 mM Tris-acetate
1 mM EDTA

2.5.6 DNA sequencing

All fragments, which were amplified by PCR and subsequently cloned into eucaryotic or procaryotic vectors, were fully sequenced with the ABI Prism dRhodamine terminator cycle sequencing ready reaction kit (Applied Biosystems). Per sequencing reaction, 500 ng of plasmid DNA were added to 4 µl terminator ready reaction mix and 1.6 pmole specific primer and filled up with H_2O to give a final volume of 10 µl. Thermal cycling was performed with the following parameters, with the annealing temperature depending on the specific sequencing primer: 96°C for 10 sec, 56°C (variable) for 10 sec, 60°C for 4 min, for 25 cycles. Afterwards, excess of dye terminators was removed by ethanol precipitation as follows:
10 µl of the PCR-product was added to 37 µl precipitation mix (70% EtOH, 0.5 mM $MgCl_2$) in a 1.5 ml high yield nucleic acid recovery tube (Robbins), vortexed and incubated for 15 min at RT. After centrifugation (14.000 x g, 15 min) the supernatant was removed and the pellet was dried at 95°C for 1 min. The sample pellet was resuspended in 6 µl of template suppression reagent, heated for 2 min at 95°C, cooled on ice, centrifuged and transferred to a 0.5 ml sequencing sample tube (Applied Biosystems). Sequencing was carried out with the ABI Prism 310 Genetic Analyzer.

2.6 Biochemical and cell biology methods

2.6.1 Preparation of cell lysates

Cells were washed once with PBS (adherent cells) or medium without FCS (suspension cells) and lysed on ice with lysis buffers (see below) for 10 min. Lysates were cleared from cell debris by centrifugation at 14.000 x g for 10 min at 4°C.
For the analysis of proteins of cell lines or transiently transfected cells, the following lysis buffers containing protease inhibitors were used for different applications:

1% NP40 Lysis Buffer:	50 mM Tris-HCl pH 7.4 150 mM NaCl 0.5 mM EDTA 1% NP40
TNE:	10 mM Tris-HCl pH 7.4 150 mM NaCl 5 mM EDTA
TBS:	20 mM Tris-HCl pH 7.4 150 mM NaCl 1 mM EDTA
TBS-T:	TBS and 1% Triton X-100
Protease inhibitors:	1 mM phenylmethylsulfonyl fluoride (PMSF) 50 µM leupeptin 100 U/ml aprotinin 200 µM benzamidine 1 µM pepstatin A (in DMSO)

To ensure that equal amounts of proteins were loaded per lane, the protein concentration of crude cell extracts was determined using the Bradford reagent (Biorad) according to the manufacturer´s instructions. This test is based on binding of Coomassie brillant blue G-250 to proteins, which alters the maximum of absorption of the dye from 465 nm without protein to 595 nm with protein (Bradford 1976). BSA served to generate the standard curve.

2.6.2 SDS-polyacrylamide gelelectrophoresis (SDS-PAGE)

For detection of proteins by Western blot, cleared cell lysates or fractions of the sucrose gradient containing K15 proteins were not boiled prior to SDS-PAGE. Cell lysates were diluted with 5x protein loading buffer and 20 µl were loaded per lane. According to the size of the protein of interest, the separation gel contained 10-12% and the stacking gel 4% polyacrylamide. Gels were run at 25 mA each in a Hoefer mighty small electrophoresis chamber (Amersham).

Protein loading buffer (5x):	Protein loading buffer (1x):
300 mM Tris-HCl, pH 6.8	50 mM Tris-HCl, pH 6.8
50 % (v/v) glycerol	10% (v/v) glycerol
10% (w/v) SDS	2% (w/v) SDS
0.1% (w/v) BPB	0.05% (w/v) BPB
300 mM β-Mercaptoethanol	100 mM DTT

Electrophoresis buffer:

25 mM Tris-Base

250 mM glycine
0.1% (w/v) SDS
pH 8.3

Molecular weight standard: 10.000 - 200.000 Da, prestained (Biorad)

For detection of proteins after SDS-PAGE, gels were blotted (see 2.6.3) or stained. For staining, gels were washed once in H_2O, stained for 1 h in Coomassie blue staining solution (Biorad) and destained with H_2O for 1 h. For storage, gels were put on Whatman paper and dried for 1 h at 80°C.
In order to estimate the protein concentration of purified proteins expressed in bacteria, different amounts of BSA protein were run in parallel with SDS-PAGE and the colour intensities of the purified protein and the known amount of BSA protein were compared.

2.6.3 Immunoblotting

After separation by SDS-PAGE, the protein gel, Whatman filter paper, porous pads and a nitrocellulose membrane (Hybond ECL, Amersham) were soaked in blotting buffer. The gel and membrane were sandwiched between Whatman 3MM paper, two porous pads and two plastic supports and immersed in a blotting tank containing blotting buffer. The membrane was placed toward the anode.
The protein transfer to nitrocellulose membranes took place in ice cold blotting buffer at 350 mA for 1 h in a Mini Trans Blot Cell (Biorad). To check for the efficiency of the blotting process, membranes were stained with Ponceau S for 1 min and destained with PBS for 10 min. Saturation of the protein binding surface of the membranes (blocking) was carried out at

RT for 1 h in blocking buffer or overnight at 4°C. Subsequently, proteins of interest were visualized with specific primary antibodies and a secondary antibody recognizing the primary antibody and being covalently coupled to the enzyme horseradish peroxidase (HRP). When HRP converts a substrate containing cumaric acid, luminol and H_2O_2, a fluorescence signal is emitted which can be detected by autoradiography.
The primary antibodies with the according dilutions used for immunostaining of immunoblots are listed in 2.1.1. Blots were probed for 1 h at RT with the primary antibody diluted in blocking buffer (see2.1.1), followed by three washing steps (10 min each) with PBS-T. Subsequently, membranes were incubated with the HRP-coupled secondary antibodies (DAKO) in blocking buffer for 45 min at RT followed by three washes with PBS-T. For detection, a standard enhanced chemiluminescence (ECL) reaction kit (Perkin Elmer) was used. The signal was visualised by exposing the membranes for different time intervals (10 sec – 15 min) to Hyperfilm ECL (Amersham).
In order to reprobe Western blots, nitrocellulose membranes were stripped for 30 min at 50°C in stripping buffer. Afterwards, the membranes were washed several times in PBS-T and blocked for 1 h at RT or at 4°C overnight in blocking buffer.

Blotting buffer: 25 mM Tris base
250 mM glycine (pH 8.3)
20% (v/v) Methanol

Blocking buffer: PBS-T
5% (w/v) nonfat dried milk

PBS-T: PBS
0.1% (v/v) Tween 20

Ponceau S staining solution:
3% (w/v) TCA
0.2% (w/v) Ponceau S

Stripping buffer: 62.5 mM Tris-HCl, pH 6.8
2% SDS
100 mM β-mercaptoethanol

2.6.4 Luciferase Reporter Assay

A commonly used method to examine effects of a certain protein on transcription factors or promoters is to clone the regions of interest (e.g. promoter regions, transcription factor binding sites) upstream of a reporter gene (e.g. firefly luciferase), whose expression and activity will be regulated by the upstream region. Increased transcription of the luciferase cDNA correlates with an increased luciferase activity in the cell lysate (Nordeen, 1988).
In order to check expression of the transfected proteins, a Western blot was performed with the cell lysates.
To assay NF-κB activity, 293-T cells were transiently co-transfected with 50 ng of the NF-κB luciferase reporter plasmid p3EnhκBconA-Luc containing three tandem repeats of the NF-κB sites from the IgGκ promoter and the indicated amounts of K15 expression constructs or LMP1, as mentioned in the figure legends, per well of a 6 well plate. At 29 h post-transfection, cells were washed once with PBS and incubated for 10 min on ice with 300 µl 1x

Reporter Lysis Buffer (Promega) per well of a 6 well plate and transferred in a 1.5 ml tube. Lysates were cleared by centrifugation for 10 min at 14.000 x g at 4°C and the supernatant was transferred to a new tube. Lysates were assayed immediately for luciferase activity in a luminometer (Berthold Lumat LB9501) or stored at -20°C. For measurement of luciferase activity, 20 µl of cleared lysate was added to 100 µl luciferase assay buffer and light emission was measured for a time period of 10 seconds. NF-κB activity was calculated as fold induction compared to mock (=empty expression vector) transfected controls.
For analysis of AP-1 activity, 50 ng of the reporter plasmid pRTU14 or the negative control reporter pRTU1 were co-transfected with different amounts of K15 or LMP1 expression constructs as indicated in the figure legends. Dominant negative mutants of TRAF-2, TRAF-6, Ras, Raf, Erk2 or the respective empty expression vectors were co-transfected as indicated in the figures. After transfection, cells were maintained in medium containing 1% FCS to downregulate serum-activated signaling pathways. Cells were lysed 24 h post-transfection in reporter lysis buffer and the luciferase activity assayed as mentioned above.
For ORF50 reporter assays, 293-T cells were co-transfected with 50 ng of the p3kbORF50P reporter plasmid and different amounts of K15 expression constructs. Cells were lysed 40 h after transfection.
Suspension cells (BCBL-1) were transfected by electroporation as described in 2.3.7 with 5 µg of luciferase reporter plasmid and 10 µg of expression constructs. 24 h post-transfection, cells were washed twice with PBS and lysed in 50 µl of luciferase assay buffer.

Luciferase Assay Buffer:
40 mM Tricine pH 7.8
10 mM $MgSO_4$
0.5 mM EDTA
0.5 mM ATP
10 mM DTT
0.5 mM Coenzyme A
0.5 mM D-Luciferin

2.6.5 Immunofluorescence and fluorescence microscopy of adherent cells

Ptk2 cells were plated for transient transfection onto 20x20 mm glass coverslips in a six well plate. 48 h after transfection, cells were washed once with PBS and fixed for 20 min at RT with 3% paraformaldehyde (PFA) in PBS. Cells were washed three times with PBS and residual PFA was inactivated with 50 mM NH_4Cl in PBS for 10 min. Subsequently, cells were permeabilised with 0.1-0.2% Triton X-100 in PBS for 5-10 min. After three washing steps with PBS, unspecific protein binding sites were blocked with blocking solution (0.2% gelatine in PBS) for 30 min at RT. The primary antibody was diluted in blocking solution and incubated with the cells for 1 h at RT (100 µl per cover slip). Afterwards, cells were washed three times with blocking solution and incubated with the secondary antibody (see below) diluted in blocking solution for 30 min at RT, subsequently washed three times with blocking solution and once with PBS. Finally, the DNA was stained with Hoechst 33258 in PBS (1 µg/ml, 5 min, RT) and cells were washed three times with PBS. PBS was removed by a short washing step in distilled water and the cover slips were mounted in 30 µl Mowiol containing 25 mg/ml DABCO.
Vero cells carrying the recombinant KSHV.219 genome, which express GFP constitutively and RFP if induced (see 2.3.5), were plated onto 20x20 mm glass cover slips in six well plates. 48 h after induction, cells were washed twice with PBS, fixed with 3% PFA for 20 min at RT, washed three times with PBS, coated with 30 µl Mowiol/DABCO for 1 h or overnight and analysed by fluorescence microscopy.

Blocking solution: 0.2% (w/v) gelatine in PBS
3% (w/v) Paraformaldehyde in PBS with 0.1 mM $CaCl_2$ and 0.1 mM $MgCl_2$, pH 7.4
0.1-0.2% (v/v) Triton X-100 in PBS
Mowiol 4-88 (Calbiochem), DABCO (Sigma) 25 mg/ml, Hoechst 33258 (1 mg/ml stock)
Secondary antibodies: donkey α-rabbit IgG Cy3 (1:200), donkey α-mouse IgG Cy3 (1:200) (both Dianova Immunotech GmbH), swine anti-rabbit FITC (1:40) (DAKO).

2.6.6 Peptide array

In order to characterize the epitope recognised by the monoclonal K15 antibodies (see 2.3.8) the full length K15 protein was synthesized as peptides of 15 aa on Whatman filter paper with the SPOT-technique by Ronald Frank at the GBF in Braunschweig (R. Frank, 2002). Each step was carried out with 10 ml of solution on a rocking platform at RT, and all washing steps lasted 10 min.
For the antibody binding test, the dried filter was moistened with EtOH, washed 3 times with TBS and blocked overnight with Genosys blocking buffer at 4°C. The following day, the filter was washed once with TBS-T and incubated with the secondary antibody conjugated with the enzyme alkaline phosphatase (AP) in order to test the background binding caused by the secondary antibody. The AP conjugate was diluted 1:500 in Genosys blocking buffer and incubated with the filter for 90 min. Afterwards, the filter was washed twice with TBS-T, PBS and CBS each. Then, the staining solution was added to the filter and incubated for a maximum of 30 min under slow agitation. After washing with PBS, the background staining was documented by scanning the filter (HP Scanjet 5370C).
If the secondary antibody used caused significant background staining, the filter was stripped as follows (all steps carried out with 15 ml of solution): The filter was washed twice with H_2O, once with DMF, then with DMF in a sonication bath at RT until the background staining vanished, three times with buffer A (with 5 min on a rocking platform and 5 min in the sonication bath at 40°C), three times with buffer B and three times with EtOH.
After stripping, the blocking step was repeated as described above followed by a washing step with TBS-T and incubation with the primary specific K15 monoclonal antibody diluted 1:2 in Genosys blocking buffer for 3.5 h. Afterwards, the filter was washed three times with TBS-T and incubated with the secondary antibody and stained as described above. For long term storage, the filter was stripped, dried, sealed in plastic foil and kept in -20°C.

Peptide TBS: 50 mM Tris-HCl pH 7.0
137 mM NaCl
2.7 mM KCl

Peptide TBS-T: peptide TBS pH 7.0 for washing, pH 8.0 for blocking
0.05% Tween 20

Peptide PBS: 137 mM NaCl
2.7 mM KCl
8 mM $Na_2HPO_4x2H_2O$
1.5 mM KH_2PO_4
pH 7.0 with HCl

CBS: 137 mM NaCl
2.7 mM KCl
50 mM Citric acid-1-hydrate
pH 7.0 with NaOH

Buffer A:
8 M Urea
1% (w/v) SDS
pH 7.0 with acetic acid
0.5% (v/v) β-mercaptoethanol

Buffer B:
10% (v/v) acetic acid
50% (v/v) EtOH
40% H_2O

Genosys blocking buffer:
20% (v/v) Genosys buffer (Sigma)
5% (w/v) Saccharose
in TBS-T pH 8.0
pH 7.0

Staining solution for AP conjugates:
For 10 ml CBS:
5 mM $MgCl_2$
2.4 mg BCIP
3 mg Methylthiazoletetrazolin

2.6.7 Purification of GST-fusion proteins

An overnight culture of *E. coli* strain BL21 transformed with expression plasmids of the GST-fusion proteins GST-c-Jun, GST-K15$^{355-489}$ or GST-K15$^{355-472}$ was diluted 1:20 in 1 litre of LB-Amp medium, grown at 37° C to a density of OD_{600} = 0.4, induced with 0.5 mM IPTG and grown for another 4 hours at 30° C in an orbital shaker at 220 rpm. Cultures were harvested by centrifugation (1.000 x g, 30 min, 4°C) and each pellet was resuspended in 20 ml of GST lysis buffer. After a 10 min incubation on ice, the cell suspension was sonicated on ice (3 x 10 sec with one minute pauses inbetween, 50% duty cycle, Branson sonifier 250), centrifuged for 10 min at 17.000 x g and the supernatant was divided into two 15 ml tubes (Falcon). 700 µl of glutathione-sepharose beads (Amersham) were washed three times with PBS and were added to each 10 ml of supernatant. Binding of the GST-fusion proteins to the beads was carried out for 30 min at 4°C on a roller. Then, samples were centrifuged for 1 min (500 x g), the supernatant was removed and each bead pellet was washed four times with 10 ml of GST-lysis buffer and twice with 10 ml of TBS (see 2.6.1). To elute the fusion proteins, each bead pellet was resuspended in 300 µl of GST-elution buffer, transferred to a 1.5 ml tube and rotated for 30 min at RT. The beads were pelleted (10.000 x g , 30 sec) and the supernatant transferred to a new tube. Elution was repeated twice, supernatants pooled, aliquoted and stored at -80°C.
The eluted GST fusion proteins were analysed by SDS-PAGE using BSA as standard to estimate the protein concentration.

GST lysis buffer:
PBS
1% (v/v) Triton X-100
10 mM DTT
1 mM PMSF

GST-elution buffer:
50 mM Tris-HCl pH 8.0
1% Triton X-100
10 mM glutathione

2.6.8 Pulldown assay with GST fusion proteins

For GST-pulldown experiments, BL21 *E. coli* cultures transformed with the GST-K15 expression plasmids or GST alone were grown at 37°C in 2YT medium plus ampicillin, induced at OD_{600} of 0.3-0.4 with 1 mM IPTG and grown for 6 h at 30°C. Cells were harvested by centrifugation (1.000 x g, 30 min, 4°C) and the pellet was resuspended in 1000 µl PBS

(containing protease inhibitors) per 10 ml of culture and an OD_{600} of 2.5. After sonication on ice (as in 2.6.7, but 3x 1 min), Triton X-100 was added to 1% final concentration, cells kept on ice for 10 min and then centrifuged for 15 min at 14.000 x g at 4°C. The supernatant was adsorbed onto 20 µl of glutathione sepharose beads prepared as described in 2.6.7 for 1 h at 4°C, after which beads were washed twice in PBS, followed by washing once in 1% NP40 lysis buffer.
HEK 293-T cells were transfected (as described in 2.3.7) with 1 µg of cDNA expression construct per well of a 6 well plate of myc-tagged Src kinases Src, Lck, Yes, Fyn or Hck. 48 h after transfection, cells were washed once on ice with PBS and lysed in 1% NP40 lysis buffer containing protease inhibitors for 10 min on ice. Cell lysates were centrifuged at 14.000 x g for 10 min at 4° and precleared by incubating with 50 µl of glutathione beads for 1 h at 4°C. Cleared lysates were then incubated for 1 h or overnight at 4°C with either GST control protein or GST-K15 fusion protein immobilised to glutathione beads. The beads were washed three times in 1% NP40 lysis buffer and proteins adsorbed to beads were boiled in 50 µl of 1x SDS electrophoresis sample buffer (see 2.6.2) and analysed by SDS-PAGE and Western blotting.

2.6.9 Cellular fractionation

B-cells and transiently transfected cos7 cells (three 75 cm^2 flasks) were washed once with RPMI without FCS or with PBS, respectively, counted, and cell pellets were resuspended in the appropiate volume of ice cold HB-T buffer to adjust the cell concentration to 3 x 10^7 cells/ml. For transiently transfected cos7 cells, transfected cells were filled up with untransfected cos7 cells to give 3 x 10^7 cells/ml. Cells were incubated on ice for 20 min and then pipetted in a “cell cracker” provided by Robert Lindner and Ernst Ungewickell, Institute of Cell Biology, MHH. In the cell cracker, the cells are passaged through a tube of 8.02 mm in diameter with a total volume of 0.5 ml, in which metallic spheres of different diameters can be inserted. For cos7 and B-cells, a sphere with a diameter of 8.01 mm was used. After passaging the cell suspension 10 times on ice through the cell cracker with one 1 ml syringe on each side of the sphere, the degree of homogenisation was checked by comparing intact cells to the homogenate with Trypan blue staining (cells were incubated 1:1 with a 0.4% trypan blue solution for 2 min) under the light microscope. Nuclei should only be stained blue if the cells are cracked, and usually over 50% of the cells were successfully cracked. After homogenisation, the suspension was incubated in ice for 1 h with 100 µg/ml DNaseI.
Afterwards, the homogenate was centrifuged for 10 min at 1.000 x g at 4°C to pellet nuclei and non broken cells. The supernatant was transferred to a new tube and centrifuged again for 10 min at 1.000 x g. To avoid cross-contamination of the pellet and supernatant fraction after ultracentrifugation, the supernatant was layered on top of a 10% sucrose cushion (10% w/v sucrose in HB-T) of 200 µl in a polycarbonate centrifuge tube (11x34 mm, Beckman) and subjected to centrifugation at 100.000 x g for 1.5 h in a Beckman table top ultracentrifuge TL-100 in a TLA 100.2 rotor. The supernatant after ultracentrifugation was transferred to a new tube and the pellet resuspended in HB-T buffer in 1/8 of the volume undergoing ultracentrifugation. All fractions were shock frozen in liquid nitrogen and stored at -80°C.
The supernatant after ultracentrifugation was subject to an acetone precipitation. The supernatant was mixed thoroughly with 5 volumes of acetone (stored at -20°C), incubated at -20°C for 30 min, centrifuged at 14.000 x g for 15 min at 4°C and the pellet resuspended in HB-T buffer.

HB-T:	10 mM triethanolamine 10 mM acetic acid 1 mM EDTA 250 mM sucrose pH 7.4 protease inhibitors	DNase I:	10 mg/ml DNaseI (Calbiochem) 5 mM Na-acetate pH 4-5 1 mM $CaCl_2$

2.6.10 Lipid raft preparation by sucrose density centrifugation

One day prior to transfection, cos7 cells were plated out in 75 cm^2 tissue culture flasks (Costar) and were transfected the following day at ~50% confluency with Effectene (3.1 µg DNA per 75 cm^2 flask) according to the manufacturer´s instructions (Qiagen). 48 h post-transfection, cells were washed once with PBS, trypsinised, resuspended in PBS, centrifuged (10 min 1.000 x g), washed with 10 ml PBS, counted and pelleted (10 min 1.000 x g). The cell pellets were resuspended in the appropriate volumes of ice cold TNE buffer (see 2.6.1) containing 1% Triton X-100 to adjust the cell concentration to 10^7 cells/ml for all samples. Cells were lysed for 30 min on ice, homogenised with a 200 µl pipette (10 strokes) and centrifuged for 10 min at 900 x g at 4°C. 1 ml of the supernatant was mixed with 1 ml of 85% sucrose in TNE and pipetted on the bottom of an ultracentrifuge tube (14x95 mm, Beckmann). 6 ml of a 35% sucrose solution in TNE were layered on top followed by 3.5 ml of a 5% sucrose solution in TNE. The samples were subjected to ultracentrifugation at 200.000 x g (40.000 rpm) in a SW40 rotor for 22 h at 4°C and subsequently, 1 ml fractions were collected starting at the top of the gradient. The pellet was resuspended in 200 µl of TNE buffer containing 1% Triton X-100. Equal amounts of each fraction 1-12 (20 µl) were analysed by SDS-PAGE and Western blotting (of the pellet fraction, only 4 µl were loaded). Fractions 4-5 of the gradient contain lipid rafts and the proteins associated with them. Fractions 9-12 contain soluble and solubilised proteins of the non-raft membrane.

2.6.11 Immunoprecipitation and Immunocomplex Kinase Assay

As indicated in the figure legends, 293-T cells were co-transfected with 1 µg of HA-tagged MAP kinase and 1 µg of K15 cDNA expression constructs as described in 2.3.7. Where indicated, 700 ng of dominant negative mutants or their respective empty expression vectors were co-transfected. After transfection, cells were maintained in medium containing 1% FCS to downregulate serum-activated signaling pathways. 24 h after transfection, cells were washed once with PBS and lysed in 400 µl of TBS-T buffer (see 2.6.1) containing protease and phosphatase inhibitors per well of a 6 well plate.

The monoclonal α-HA antibody 12CA5 was immobilized to Protein G sepharose beads (Amersham) as follows: 80 µl of resuspended beads were washed twice with 1 ml PBS and twice with 1ml TBS-T (15.000 x g, 30 sec). 200 µg of α-HA antibody were dissolved in 500 µl PBS containing 4% sucrose and 0.02% Na-azide, incubated on ice for 15 min and added to the beads. After a 2 h incubation on a roller at 4°C, beads were pelleted (15.000 x g, 30 sec), washed three times in TBS-T and finally resuspended in 1.2 ml PBS containing 4% sucrose and 0.02% Na-azide and stored at 4°C.

Cleared cell lysates were incubated overnight on a roller at 4°C with 12 µl of HA-beads to immunoprecipitate HA-tagged MAP-kinases. Afterwards, samples were centrifuged (30 sec, 15.000 x g) and supernatants transferred to a new tube to be analysed for expression of K15 constructs by Western blot. Beads with bound MAP kinase were washed twice with TBS-T, twice with kinase reaction buffer, adjusted to 25 µl and kept on ice.

In vitro kinase reactions to assay the activity of immunoprecipitated HA-MAPK were performed as follows: Kinase reactions were started with the addition of the immunoprecipitated MAP-kinase bound to HA-beads to 10 µl of a kinase reaction mix containing 10 µCi of [γ-^{32}P] ATP (3000 Ci/mmol, 10 mCi/ml, Hartmann Analytics) per reaction sample and 200 ng of either purified bovine myelin basic protein (MBP; Upstate Biotechnology), ATF2 fusion protein (34 kDa; Cell Signaling) or purified GST-c-Jun (2.6.7) as a substrate in kinase reaction buffer. The samples were incubated for 30 min at 25°C and kinase reactions were stopped by putting the samples on ice and adding 4 µl of 4 x stop buffer. Samples were then heated for 5 min at 100°C, cooled on ice for 2 min, separated by SDS-PAGE (15 µl per lane), blotted onto Hybond-C nitrocellulose membranes (Amersham) and analysed by autoradiography. Immunoblots were performed with the same membranes used for autoradiography to check for equal expression levels of the immunoprecipitated MAP kinases.
For the Src kinase assay, 293-T cells were transfected with either 1 µg of expression plasmids for myc-tagged Src kinases Src, Hck, Lck, Yes or Fyn or empty expression vector. After transfection, cells were kept in complete medium with 10% FCS and cells were lysed 24 h post-transfection in TBS-T as mentioned above. Immunoprecipitation of the myc-tagged Src kinase was carried out overnight with 12 µl of anti-c-myc (clone 9E10) coated protein A agarose beads (Clontech) per sample. The in vitro kinase reaction was done as described above, but with 200 ng of purified GST-K15$^{355\text{-}489}$ or GST-K15$^{355\text{-}472}$ fusion protein (see 2.6.7) as substrate. Immunoblots were performed with the same membranes used for autoradiography to check for equal amounts of purified GST-K15 fusion protein.

Kinase reaction buffer:
20 mM Tris-HCl pH 7.4
20 mM NaCl
1 mM DTT
10 mM $MgCl_2$
2 µM ATP
0.5 mM β-glycerophosphate
0.5 mM sodium-orthovanadate

4 x stop buffer:
200 mM Tris-HCl pH 6.8
4 mM EDTA
100 mM DTT
40% glycerol
8% SDS
0.1% bromphenolblue

Phosphatase inhibitors:
0.5 mM sodium-orthovanadate
0.5 mM β-glycerophosphate
0.5 mM sodium-molybdate
0.5 mM sodium-fluoride
0.5 mM sodium-pyrophosphate

Protease and phosphatase inhibitors were added to TBS-T. The specific MEK1/2 inhibitors PD98059 and UO126 (both Calbiochem) were used at a concentration of 50 µM from a 50 mM stock solution in dimethyl sulfoxide (DMSO). UO126 was prepared fresh for every experiment. Inhibitors were added to the medium 14 h after transfection and cells were incubated for a further 8 hours before being extracted as described above.

2.6.12 Coupled *in vitro* transcription/translation

In vitro translated proteins were prepared non-radioactively with the TNT-System following the manufacturer´s instructions (Promega: TNT coupled reticulocyte lysate system). 5 µl per reaction were analysed by SDS-PAGE and immunoblotting.

3 Results

3.1 Characterisation of the K15 proteins of KSHV

3.1.1 Expression and cellular localisation of K15 proteins

When we started our work on K15, the most common KSHV cell culture system were cell lines etablished from patients with primary effusion lymphoma (PEL) that carry and maintain KSHV genomes. These PEL cell lines are either co-infected with KSHV and EBV, or with KSHV alone. Three independent groups identified differentially spliced transcripts derived from ORF K15 of KSHV by RT-PCR on RNA extracted from PEL cell lines BCBL-1, BCP-1 and Hbl-6 (for details see 2.3.2; Glenn et al., 1999, Poole et al., 1999, Choi et al., 2000a). The most prominent transcript that was identified in these cell lines is multiply spliced, consists of eight exons and encompasses ~1500 bp. Of these PEL cell lines, Hbl-6 codes for the K15-M (minor) variant that shares only 33% amino acid identity with the K15-P (predominant) variant that is found in the majority of KSHV genomes. Despite their low similarity at the amino acid level, the eight exon transcripts of K15-M and K15-P are almost identical in their splicing pattern (see figure 5 in 1.3.6; Glenn et al., 1999, Poole et al., 1999). Furthermore, the splicing pattern of the K15-P and K15-M variants shows striking similarity in number and length of exons to the EBV LMP2A transcript (figure 5 in 1.3.6), which localises to the far right end of the EBV genome as K15-M and K15-P in KSHV (figure 2 in 1.3 and 1.3.1.2).

As a first approach to characterise the protein derived from ORF K15, we analysed the protein sequences of the EBV membrane proteins LMP1 and LMP2A in parallel to the two K15 variants K15-P and K15-M with the membrane protein topology prediction programme TMHMM at http://www.cbs.dtu.dk, which is one of the most reliable topology prediction programme available today (Melén et al., 2003). As shown in figure 9 and as expected from the literature, 12 transmembrane domains and an N-terminal cytoplasmic domain were predicted for LMP2A (aa 1-497, pI 4.8, NCBI # CAD53382), and 6 transmembrane domains joined to a cytoplasmic C-terminus were predicted for LMP1 (aa 1-386, pI 4.0, NCBI #CAD53472) (see 1.3.1 and figure 3). The K15-M protein (aa 1-498, pI 8.0, NCBI accession #AAD45296) was predicted to consist of 12 transmembrane domains followed by a cytoplasmic C-terminal domain (figures 9 and 15). The K15-P protein (aa 1-489, pI 8.6, NCBI accession #AAD45297) was similarly predicted to contain 12 hydrophobic regions (figure 9). Of these, the third did not quite reach significance in the prediction algorithm for a transmembrane domain. However, based on the otherwise similar arrangement as in K15-M, it is likely that it also contains 12 transmembrane domains, joined to a cytoplasmic C-terminal domain encoded by exon 8 (figures 9 and 15).

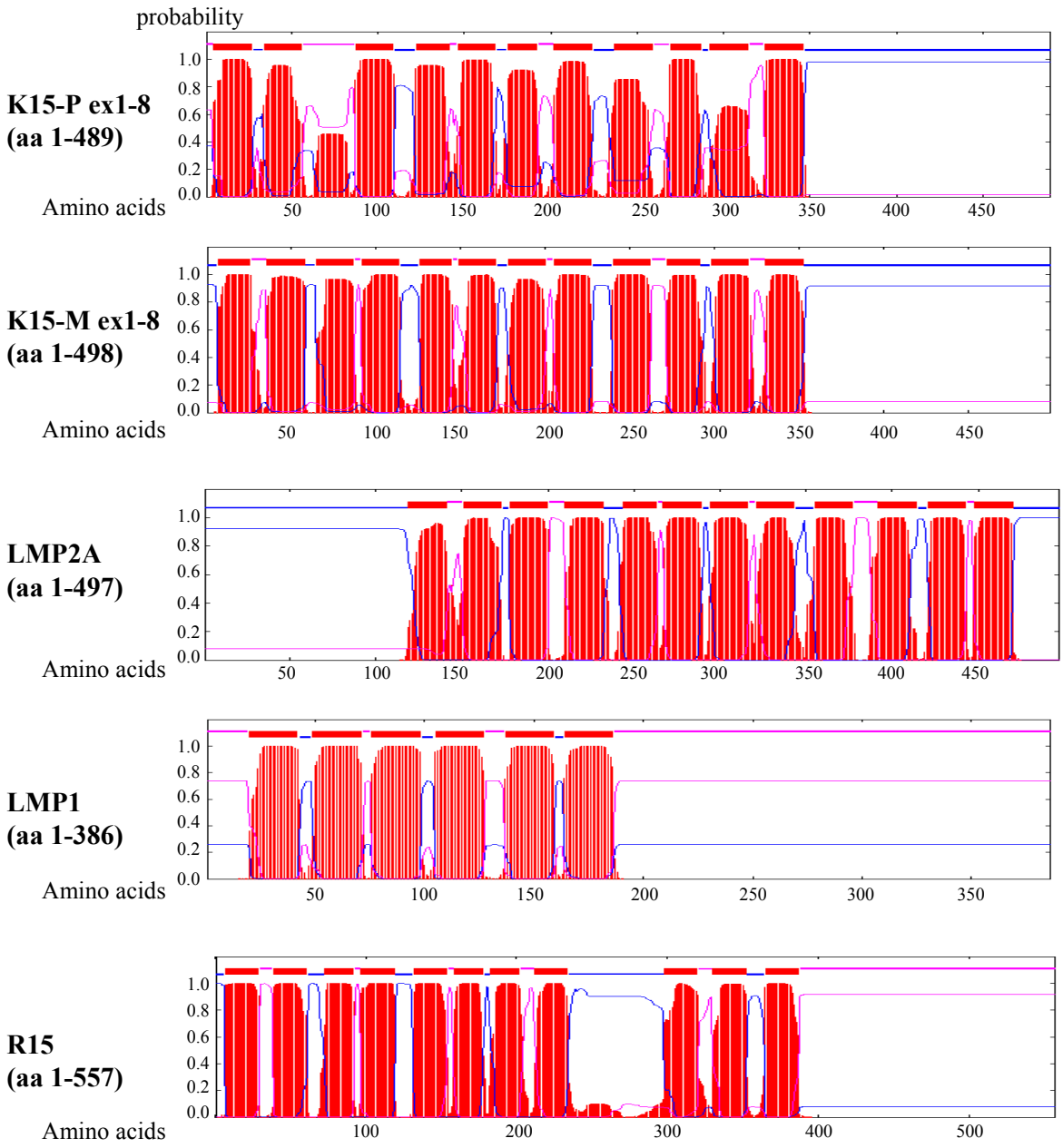

Figure 9: Predicted transmembrane topology of viral terminal membrane proteins EBV LMP1 and LMP2A, RRV R15 and the two KSHV K15 variants K15-P and K15-M. The membrane topology was predicted with the TMHMM programme at http://www.cbs.dtu.dk. The x-axis shows the number of amino acids, the y-axis the relative probability of a potential transmembrane domain. Red lines = transmembrane domain, blue lines = inside, pink lines = outside. See text for further details.

When we analysed the region at the far right end of the RRV strain 17577 genome (accession number #NC_003401, Searles et al., 1999) between the terminal repeats and ORF75, we found that this region has the potential to encode a transcript with an exon/intron pattern similar to ORF K15 and EBV LMP2A. This potential ORF R15 would hypothetically encode a transcript of 1674 bp that could give rise to a protein of 557 aa (pI 8.389). Analysis of the R15 protein sequence with the TMHMM programme revealed that the R15 protein would consist of 11 transmembrane domains and a cytoplasmic C-terminal domain (figure 9).

Hence, the two K15 variants K15-P and K15-M and the hypothetical R15 protein are very similar to the EBV LMP2A protein concerning their membrane topology. Furthermore, the EBV TMPs LMP1 and LMP2A, RRV R15 and KSHV K15 contain hydrophilic N- (LMP2A) or C-termini (K15, R15, LMP1) that are between 119 and 198 aa in length (aa 1-119 for LMP2A, aa 188-386 for LMP1, aa 388-557 for R15, aa 348-489 for K15-P, aa 353-498 for K15-M) (see figures 9 and 15).

In addition to the full length eight exon transcript, three K15-P splice variants identified by RT-PCR in BCP-1 cells by Glenn et al. (1999) were examined in this study. Splice variant K15-P ex1/6-8 uses exons 1, 6, 7 and 8, and would therefore lack exons 2-5 compared to the K15 exon 1-8 transcript (figure 5 in 1.3.6). This splice variant could potentially give rise to a protein with 3-4 transmembrane domains joined to a cytoplasmic C-terminus.

The splice variants K15-P ex1 as/6-8 and K15-P ex1 as/4-8 use an alternative ATG codon and splice donor in exon 1 together with exons 6, 7, 8 or exons 4, 5, 6, 7, 8, respectively (figure 5 in 1.3.6; as = alternative splice). The use of this alternative splice donor in exon 1 would imply the use of a different reading frame in exon 1, resulting in an alternative six aa at the N-terminus of the resulting proteins compared to the full length eight exon transcript or splice variant K15-P ex1/6-8. The subsequent sequence of these two K15 splice variants would be in the same frame as K15-P ex1-8 or K15-P ex1/6-8. Splice variant K15-P ex1 as/6-8 would be predicted to encode a protein with two transmembrane domains, whereas splice variant K15-P ex1 as/4-8 could potentially be composed of three transmembrane domains followed by a cytoplasmic C-terminus (data not shown). Since the K15-P variant is detected in the majority of KSHV genomes (see 1.3.6), the experiments of this study were performed with this K15 variant.

The first step in order to characterise proteins encoded by the KSHV K15 ORF was to transiently express the eight exon K15 transcript (K15 ex1-8, aa 1-489) and the three splice variants (K15 ex1/6-8, K15 ex1 as/4-8, K15 ex1 as/6-8) in different cell lines and to analyse protein expression with a polyclonal antibody generated against the putatively cytoplasmic domain of K15 (Material and Methods, 2.1.1). We then investigated the subcellular localisation of ORF K15 derived proteins by biochemical subcellular fractionation assays and by immunofluorescence studies.

Proteins of 45, 34 and 23 kDa are expressed from the K15 ex1-8 expression construct

The longest of the K15-encoded proteins, containing all 8 exons, is predicted to give rise to a membrane protein of 489 amino acids with a molecular weight of 54 kDa. However, when we transiently transfected cos7 cells with the K15 ex1-8 expression construct, a major protein of ~45 kDa was detected by immunoblotting with a polyclonal antiserum raised against the cytoplasmic domain of K15 (figure 10 A lane 1). In addition, two minor protein bands were detected with molecular weights of ~34 and ~23 kDa, which may be the result of alternative splicing, proteolytic processing or internal initiation of translation (figure 10 A, lanes 1 and 2). Upon heat treatment (5 min, 100° C) of the cos7 lysates, the 45 kDa K15 protein was not detected anymore (figure 10 A, compare lanes 1 and 2). This may be caused by aggregation of the multiple transmembrane domains upon heat treatment, which would prevent the protein to enter the SDS gel. This notion was supported by the presence of the ~34 and ~23 kDa proteins after heat treatment, which would both be predicted to have fewer transmembrane domains (figure 10 A, lanes 1 and 2). The results shown in figure 10 A were also obtained with 293-T and Vero cells transiently transfected with the K15 ex1-8 expression construct (data not shown).

In vitro transcription/translation of the K15 exon 1-8 construct gave rise to a protein of ~45 kDa (figure 10 B, lane 1), that migrated as fast as the 45 kDa protein transiently expressed in cos7 cells (figure 10 B, compare lanes 1 and 3). A 34 kDa protein was weakly expressed in vitro, whereas the 23 kDa protein was not detectable in vitro (figure 10 B, lane 1). This may be due to the absence of cellular factors in the reticulocyte lysate used for the in vitro assay, that are required for the posttranslational processing of the 45 kDa protein.

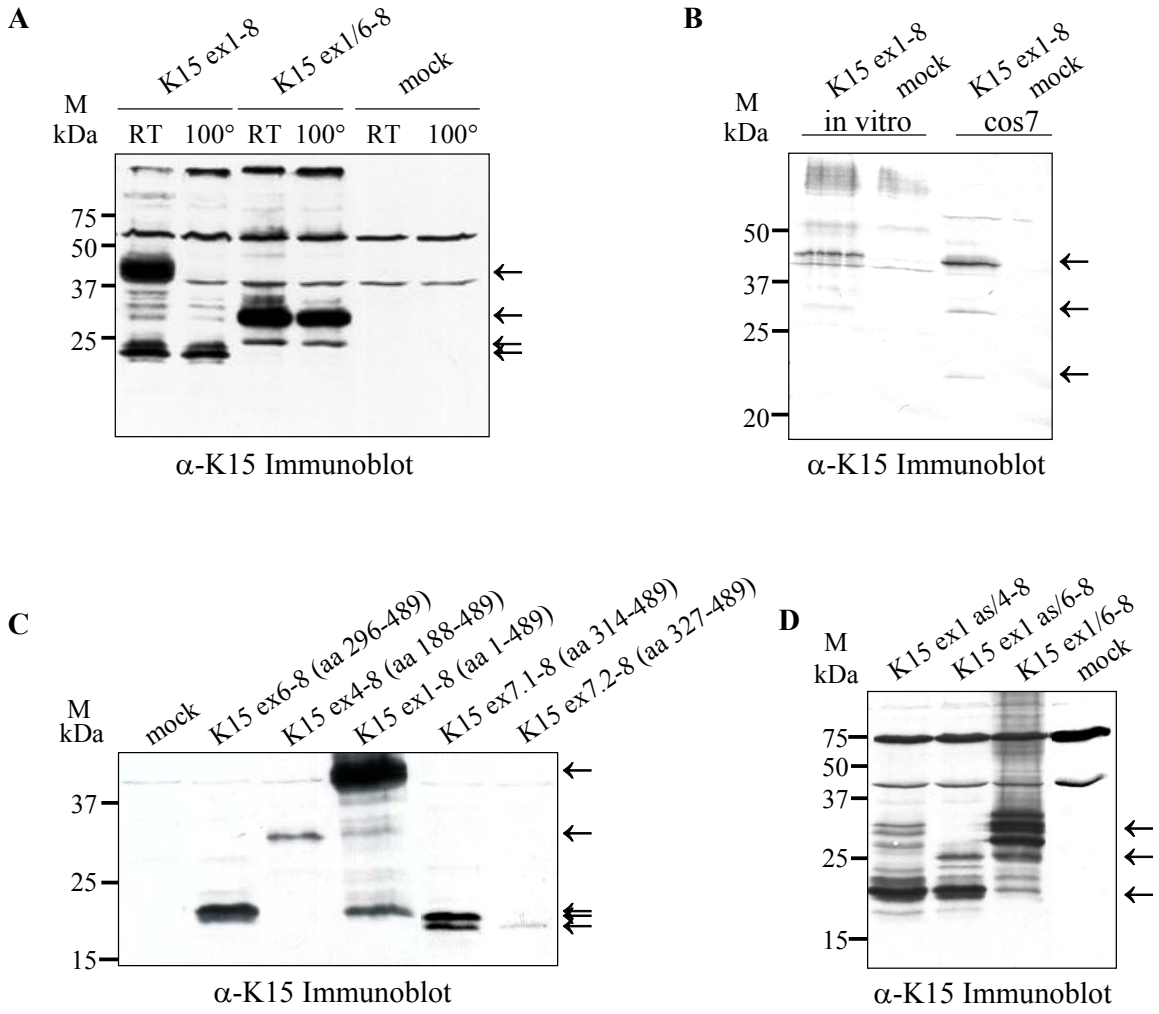

Figure 10: A protein of 45 kDa was expressed in vivo and in vitro from a K15 cDNA expression construct containing all eight exons. The K15 ORF is multiply and alternatively spliced. The major transcript identified by RT-PCR in PEL cell lines is fully spliced and contains all 8 exons (K15 ex1-8; aa 1-489). It encodes a membrane protein with up to 12 transmembrane domains and a putatively cytoplasmic C-terminal domain (aa 348-489). Splice variants K15 ex1/6-8, K15 ex1 as/6-8 and K15 ex1 as/4-8, also identified in PEL cell lines by RT-PCR, differ in number of transmembrane domains but all contain the C-terminal domain encoded by exon 8. Western blots A-D were probed with a polyclonal K15 rabbit antibody raised to the K15 C-terminal domain.
(A) Transient expression of K15 ex1-8 and splice variant K15 ex1/6-8 in cos7 cells. The K15 ex1-8 cDNA expression construct, predicted to encode a protein of 54 kDa, gives rise to a major protein with an apparent mass of 45 kDa and two minor proteins of 23 and 34 kDa in SDS-PAGE (lane 1). The 45 kDa protein is sensitive to heat treatment (lane 2). The K15 splice variant K15 ex1/6-8 gives rise to a protein of the predicted mass of 34 kDa and a minor protein of 25 kDa, which both can be detected with or without heat treatment of the lysate (lanes 3 and 4). (B) The K15 ex1-8 expression construct was in vitro transcribed/translated and analysed by Western blotting. In vitro transcribed/translated K15 ex1-8 protein (lane 1) was run in parallel to a cos7 lysate expressing K15 ex1-8 (lane 3). (C) K15 ex1-8 and N-terminal deletion constructs starting at internal ATG codons (K15 ex4-8, K15 ex6-8, K15 ex7.1-8, K15 ex7.2-8) were transiently expressed in cos7 cells and analysed by Western blotting. (D) Several protein bands were detected by Western blotting in cos7 lysates transiently expressing K15 natural splice variants K15 ex1 as/4-8, K15 ex1 as/6-8 and K15 ex1/6-8. See text for details.

To address the question whether the smaller K15 proteins of 23 and 34 kDa expressed from the K15 ex1-8 construct were derived from internal initiation, and since the K15 ORF contains several internal in frame ATG codons, we constructed K15 N-terminal deletion

mutants beginning at the internal ATG in exon 4 [K15 ex4-8, aa 188-489 (predicted mass of 33 kDa)], the ATG in exon 6 [K15 ex6-8, aa 296-489 (predicted mass of 22 kDa)] or at the ATGs in exon 7 [K15 ex 7.1-8, aa 314-489 (predicted mass of 20 kDa) and K15 ex7.2-8, aa 327-489 (predicted mass of 18.5 kDa)]. The resulting recombinant expression constructs K15 ex6-8, K15 ex7.1-8 and K15 ex7.2-8 were predicted to encode proteins with one transmembrane domain, whereas the protein derived from K15 ex4-8 could potentially be composed of three transmembrane domains.

As shown in figure 10 C (lane 2), the K15 exon 6-8 construct gave rise to a protein of ~23 kDa, suggesting that the 23 kDa expressed from K15 ex1-8 may be derived from internal initiation at the ATG in exon 6 (figure 10 C, compare lanes 2 and 4). Expression of construct K15 exon 7.1-8 gave rise to a doublet of ~20 and ~18 kDa, and K15 ex7.2-8 expressed a protein of ~18 kDa (figure 10 C lanes 5 and 6). The K15 ex4-8 construct gave rise to a protein of the predicted mass of ~34 kDa, corresponding in size to the 34 kDa protein expressed from the K15 ex1-8 construct (figure 10 C, compare lanes 3 and 4). This indicates that the 34 kDa, as well as the 23 kDa protein, may be derived from the full length K15 cDNA by internal initiation at ATGs in exon 4 and exon 6, respectively.

When the smaller K15 splice variants were transiently expressed in cos7 cells, proteins of approximately ~34 kDa and ~25 kDa (K15 ex1/6-8; figure 10 A lanes 3 and 4 and figure 10 D lane 3), ~34 kDa and ~21 kDa (K15 ex1 as/4-8; figure 10 D lane 1), and ~26 and ~21 kDa (K15 ex1 as/6-8; figure 10 D lane 2) were detected by immunoblotting with polyclonal K15 antiserum. The ~34 kDa protein seen with K15 ex1/6-8 corresponds to the size expected for this cDNA, as do the ~34 kDa and ~26 kDa proteins seen with K15 ex1 as/4-8 and K15 ex1 as/6-8, respectively. However, multiple protein bands were derived from all three splice variants (figure 10 D, lanes 1-3), and the additional 21 kDa protein seen with K15 ex1 as/4-8 and K15 ex1 as/6-8 was more abundantly expressed than the 34 and 26 kDa proteins. These smaller proteins may, as well as the 34 and 23 kDa proteins expressed from the K15 ex1-8 expression construct, be derived from additional splicing events or internal initiation.

K15 proteins are membrane associated

In order to analyse whether the proteins derived from the full length K15 expression construct are membrane proteins as was predicted by the TMHMM programme (figure 9), subcellular fractionation experiments were performed as described in Material and Methods (2.6.9). The K15 ex1-8 construct was transiently expressed in cos7 cells and 48 h after transfection, cells were resuspended in hypotonic buffer and mechanically lysed. After a 1.000 x g centrifugation step to deplete lysates from cell debris and nuclei, the cleared lysates were subjected to an ultracentrifugation step at 100.000 x g to pellet cellular membranes and proteins associated with them. The supernatant after high speed ultracentrifugation corresponds to the cytosolic fraction containing soluble proteins.

As depicted in figure 11 A (upper panel, lane 4), the 45 kDa K15 protein could be pelleted with cellular membranes after high speed centrifugation (100.000 x g). Upon longer exposure, the 34 and 23 kDa protein species were also detectable in the membrane fraction (not shown). As a positive control for the subcellular fractionation method, the different fractions of cos7 lysates (supernatant after 1.000 x g, supernatant and pellet after ultracentrifugation) were probed with an antibody to endogenous calnexin. Calnexin is a type I transmembrane protein with a predicted mass of 64 kDa and an apparent mass of 88 kDa, which was reported to have chaperone-like functions in the ER (Hammond et al., 1994 and references therein). As expected, Calnexin was detected in the membrane fraction after ultracentrifugation (figure 11 A, lower panel lanes 3 and 4) and not in the cytosolic fraction (figure 11 A, lower panel lanes 1 and 2).

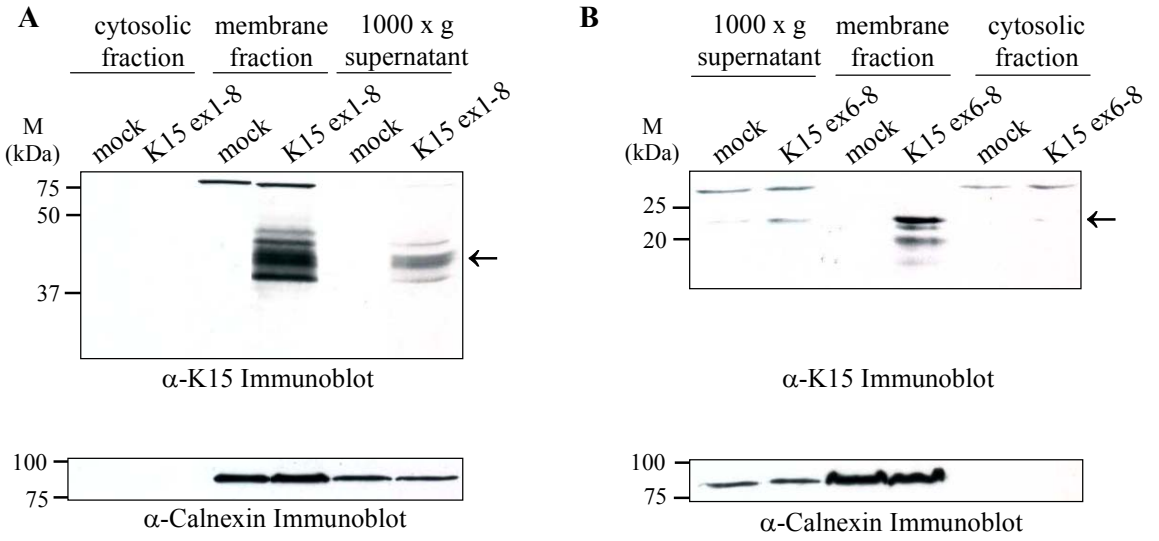

Figure 11: K15 derived proteins transiently expressed in cos7 cells could be pelleted with cellular membranes in a subcellular fractionation assay. Cos7 cells were lysed as described in Material and Methods (2.6.9) and nuclei and non-broken cells were pelleted by centrifugation at 1.000 x g. The resulting supernatant was subjected to ultracentrifugation at 100.000 x g. The pellet after high speed ultracentrifugation contains cellular membranes and membrane proteins, while the supernatant contains the cytosolic fraction and soluble proteins. Subcellular fractionation assay fractions were analysed by SDS-PAGE, and Western Blots were probed with an antibody to K15 (upper panels in A and B). Endogenous Calnexin, a type I membrane protein in the ER, served as a positive control and was detected, as expected, in the pellet (membrane) fraction with a Calnexin antibody (lower panels in A and B). K15 ex1-8 (aa 1-489) could be pelleted with cellular membranes (A, lane 4), as well as the 23 kDa protein derived from the recombinant expression construct K15 ex6-8 that starts at the in frame ATG in exon 6 (B, lane 4).

Lysates of cos7 cells transiently transfected with the recombinant K15 expression construct K15 ex6-8 were also subjected to subcellular fractionation. K15 ex6-8, beginning at the internal ATG in exon 6 and giving rise to a 23 kDa protein with one putative transmembrane domain and a cytoplasmic C-terminus, was also found to be membrane-associated (figure 11 B upper panel lane 4) as Calnexin (figure 11 B lower panel lanes 3 and 4).

K15 proteins are localised in lipid rafts

Many cellular and viral membrane proteins have been reported to be associated with membrane microdomains termed “lipid rafts”. Examples include the viral membrane proteins LMP1 and LMP2A of EBV and the cellular B- and T-cell antigen receptors. Lipid rafts have been proposed to function as platforms for receptor signaling and trafficking (reviewed in Brown & London 2000). Lipid rafts are membrane microdomains rich in cholesterol and sphingolipids that are resistant to solubilisation with non-ionic detergents such as Triton X-100 at 4°C. Hence, lipid rafts and proteins associated with them float up to a position of lower density (5-35%) in a sucrose gradient in the presence of 1% Triton X-100, whereas soluble proteins and solubilised membrane proteins remain at the bottom of the gradient at the higher sucrose concentration (35-42.5%) (see figure 12 A, left panel).

The K15 isoforms, i.e. full length K15 ex1-8 and splice variants K15 ex1/6-8, K15 ex1 as/4-8 and K15 ex1 as/6-8, were transiently expressed in cos7 cells and cell lysates were subjected to a sucrose density fractionation as described in Material and Methods (2.6.10) and figure legend 12. In addition, a chimeric protein composed of the six transmembrane domains of the EBV LMP1 protein and the K15 cytoplasmic C-terminus (LMP1-K15$^{355-489}$) was analysed for lipid raft localisation. After the overnight ultracentrifugation step, 1 ml fractions were collected from the top of the gradient (see figure 12 A, left panel) and equal volumes of fractions 1-12 were analysed by Western blotting with the polyclonal K15 antibody. As a positive control for successful lipid raft preparation, Western blots were routinely stripped and reprobed with an antibody to endogenous Caveolin-1. The 21-24 kDa membrane protein Caveolin-1 is a component of Caveolae which represent a specialized subset of lipid rafts (Simons & Toomre 2000, Galbiati et al., 2001), and therefore Caveolin-1 served as a marker protein for lipid rafts (shown for K15 ex1-8 in figure 12 A, not shown for K15 splice variants and LMP1-K15$^{355-489}$ in figure 13).

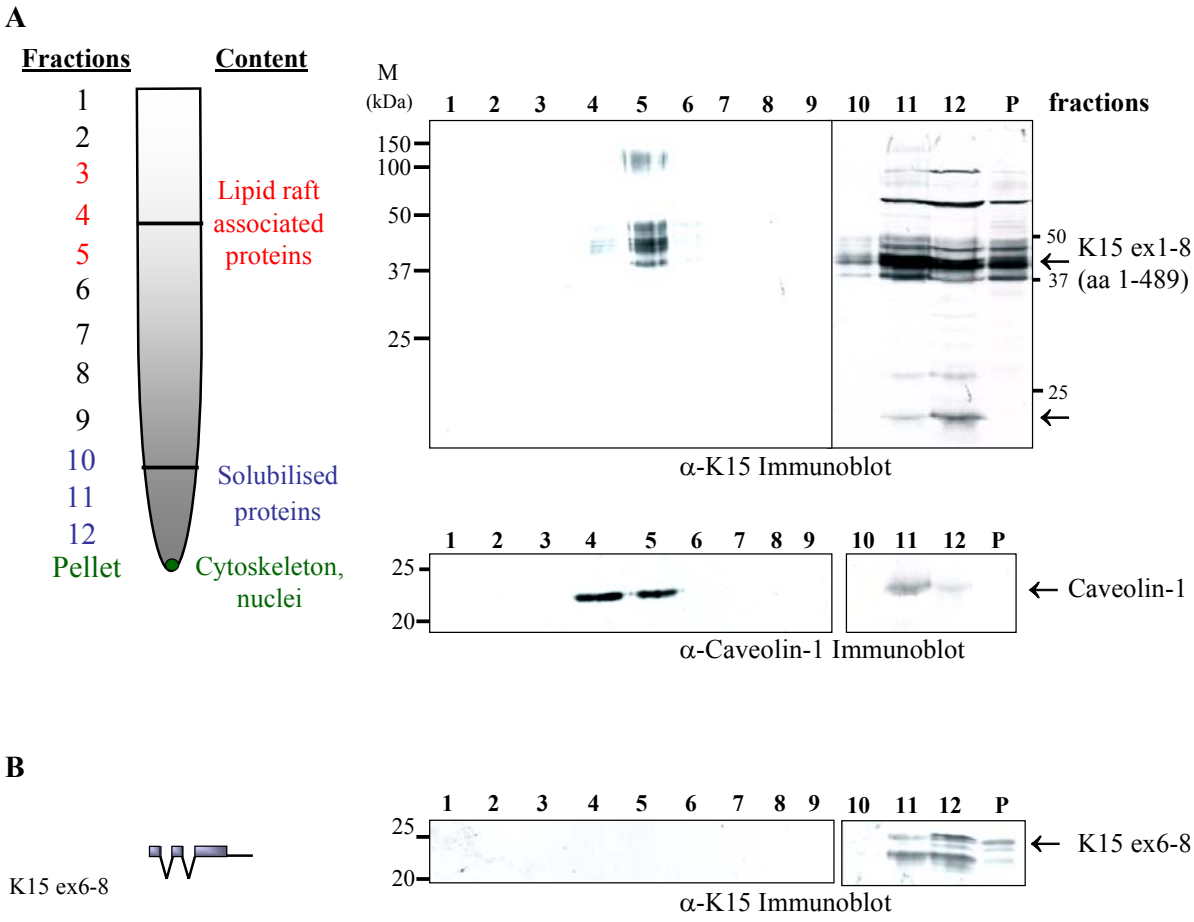

Figure 12: The 45 kDa K15 protein derived from the K15 ex1-8 expression construct localised to lipid rafts. Cos7 cells transiently transfected with the (A) K15 ex1-8 construct or (B) K15 ex6-8 construct (see Material and Methods 2.2.1, figure 8) were lysed 48 h after transfection in TNE buffer and cell extracts were analysed on a flotation sucrose gradient as described in Material and Methods (2.6.10). After ultracentrifugation, 1 ml fractions were collected starting at the top of the gradient and analysed on Western blots with a rabbit polyclonal antibody to the C-terminal domain of K15.
(A) Left panel: After ultracentrifugation, lipid rafts and lipid raft-associated proteins localise at the interface of 5 and 35% sucrose (fractions number 3-5). Solubilised membrane proteins of the non-raft plasma membrane and soluble proteins localise to the higher density sucrose fractions (35-42.5% sucrose) corresponding to fractions 10-12. The pellet fraction (P) contains proteins associated with the cytoskeleton. (A) Right upper panel: The 45 kDa K15 protein is found in fractions 4 and 5 of the sucrose gradient which correspond to the lipid raft containing fractions. The 45 kDa K15 protein is also found in fractions 10-12 and in the pellet fraction (P). Right lower panel: Western blot membranes shown in the upper panel were stripped and reprobed with an antibody to endogenous Caveolin-1, which served as a marker protein for lipid rafts and mainly localised, as expected, to lipid raft containing fractions 4 and 5. (B) The 23 kDa protein expressed from the recombinant K15 ex6-8 construct was shown to be membrane associated (see figure 11 B), but did not localise to lipid raft fractions. The 23 kDa protein localised to the fractions corresponding to soluble and solubilised proteins (fractions 11-12) and the pellet fraction after sucrose density centrifugation.

As shown in figure 12 A (right upper panel), the 45 kDa protein derived from the 8 exon K15 cDNA expression construct (K15 ex1-8; aa 1-489) could be detected in fractions 4 and 5 of the sucrose gradient which represent the interface of 5 and 35% sucrose. These fractions correspond to the position of lipid rafts, as indicated by the presence of caveolin-1 (figure 12 A, right lower panel). The 8 exon 45 kDa K15 protein also localised to non-raft membranes (fractions 10, 11 and 12, sucrose concentration of 35-42.5%) of the sucrose gradient, where

solubilised membrane proteins and soluble proteins would be expected (figure 12 A, right upper panel). This result is reminiscent of LMP1 and LMP2A, which both localise to lipid rafts and also to non-raft cell membranes in EBV-transformed B-cells (LCLs) (Higuchi et al., 2001). The 45 kDa K15 protein was also detected in the pellet fraction containing cytoskeleton-associated proteins (figure 12 A, right upper panel), which is also observed for the LMP1 protein, but not for LMP2A (Higuchi et al., 2001).

K15 proteins of ~34 kDa (splice variant K15 ex1/6-8, figure 13 A) and ~21 kDa (splice variants K15 ex1 as/4-8, figure 13 B and K15 ex1 as/6-8, figure 13 C) floated to the lipid raft fractions of the sucrose gradient as the 45 kDa K15 protein (figure 12 A). In contrast, the ~34 kDa protein derived from splice variant K15 ex1 as/4-8 (figure 13 B) and the ~26 kDa protein derived from splice variant K15 ex1 as/6-8 (figure 13 C) did not float up to the lipid raft fractions in the sucrose gradient. This could be due to the different use of exon 1 of these two splice variants, since the ~34 kDa protein derived from splice variant K15 ex1/6-8, which encodes the complete exon 1 as the K15 ex1-8 construct, did localise to lipid rafts. This is reminiscent of the LMP1 protein: an LMP1 deletion mutant lacking the N-terminus and the first transmembrane domain does not localise to lipid rafts (see discussion).

Only a portion of the K15 proteins was incorporated into lipid rafts (figures 12 and 13). On the basis of densitometry scanning of the blots shown in figures 12 and 13, approximately 21% of the 45 kDa immunoreactive K15 protein (K15 ex1-8) (excluding the material in the pellet fraction) was present in lipid rafts. For the smaller ~34 kDa K15 ex1/6-8 splice variant, a comparable amount (26%) was found in lipid rafts, in contrast to only 5% in the case of K15 ex1 as/4-8 and a similar small proportion in the case of K15 ex1 as/6-8. It thus appears that the K15 ex1 as/4-8 and K15 ex1 as/6-8 derived ~21 kDa proteins were incorporated less efficiently than the 45 kDa (K15 ex1-8) or ~34 kDa (K15 ex1/6-8) isoforms.

The LMP1-K15$^{355\text{-}489}$ chimeric protein, which had an apparent mass of 37 kDa as predicted, localised to lipid rafts and non-raft cell membranes (figure 13 D). This would be expected, since the transmembrane domains of LMP1 have clearly been shown to be crucial for lipid raft localisation.

The 34 and 23 kDa proteins that were expressed from the full length K15 cDNA expression construct K15 ex1-8 (see figure 10 A) were not present in the lipid raft fractions (not shown). In accordance with this observation, the 23 kDa protein expressed from the recombinant K15 ex6-8 construct was not localised to lipid rafts (figure 12 B). This would point to an important role of the N-terminal transmembrane domains of K15 for its localisation to lipid rafts.

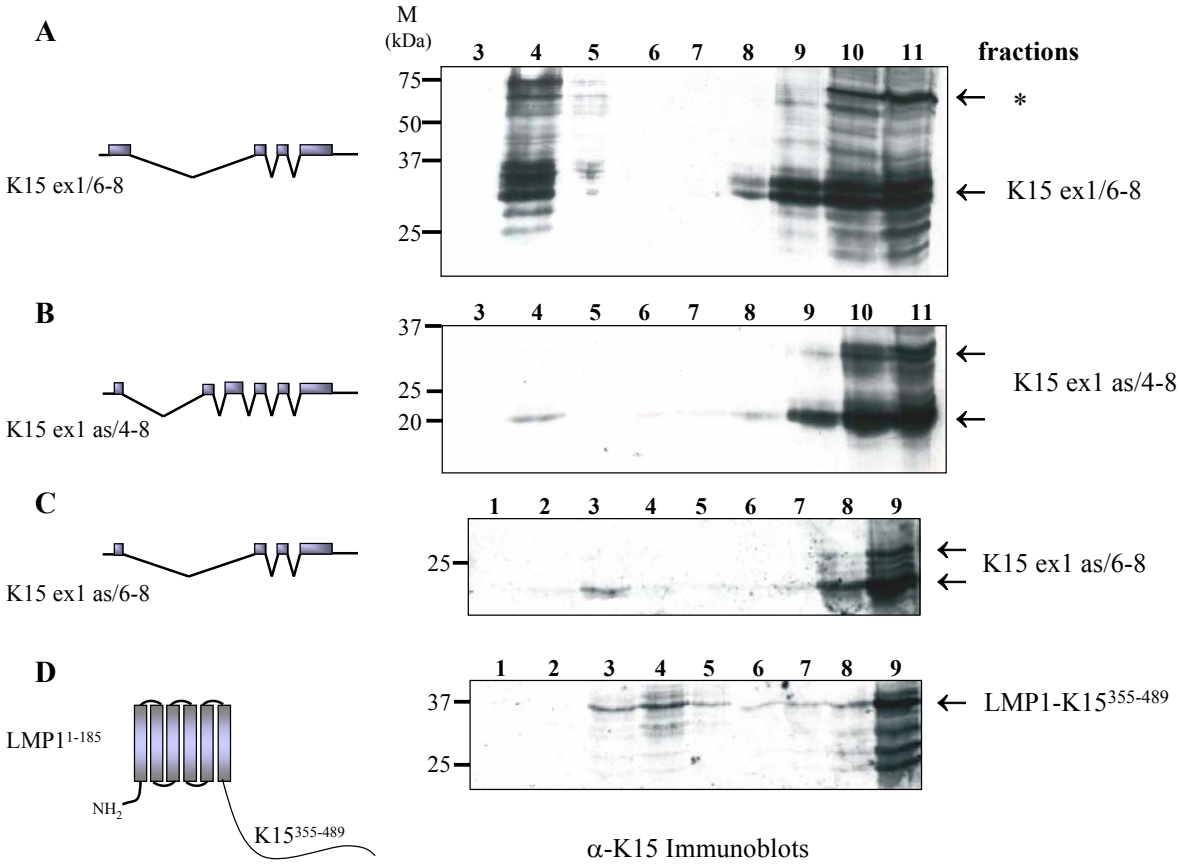

Figure 13: Analysis of lipid raft localisation for K15 splice variants and an LMP1-K15 chimeric protein by sucrose density centrifugation. Cos7 cells were transiently transfected with expression constructs for the natural splice variants K15 ex1/6-8 (A), K15 ex1 as/4-8 (B), K15 ex1 as/6-8 (C) or the LMP1-K15$^{355-489}$ chimera (D). Cell lysates were subjected to a sucrose density centrifugation as described in figure legend 12 and Material and Methods (2.6.10). Fractions of the sucrose gradient were analysed by SDS PAGE, and Western blots were probed with the polyclonal K15 antibody. (A) The ~34 kDa protein derived from splice variant K15 ex1/6-8 localised to the lipid raft fraction and fractions of high density sucrose. The asterisk (*) indicates a possible dimeric form of the ~34 kDa protein. (B) The ~21 kDa protein derived from splice variant K15 ex1 as/4-8 was found in lipid rafts and fractions of high density sucrose, while the ~34 kDa protein did not float up to the lipid raft fractions. (C) The ~21 kDa protein derived from K15 ex1 as/6-8 localised to lipid rafts and to fractions of high density sucrose, while the ~26 kDa protein was not associated with lipid rafts. (D) The LMP1-K15$^{355-489}$ chimera was found in lipid rafts and fractions of high density sucrose.

Caveolin-1 interacts with a variety of lipid-modified signaling molecules including G-proteins, H-Ras and protein tyrosine kinases of the Src family via its scaffolding domain (reviewed in Galbiati et al., 2001). Using a peptide approach, Couet et al. (1997) identified a motif (consensus Φ-x-Φ-x-x-x-x-Φ or Φ-x-x-x-x-Φ-x-x-Φ, with Φ being W, F or Y) via which proteins interacted with a Caveolin-1 scaffolding domain peptide. The K15-P variant contains four such potential caveolin-binding sites (depicted in table 3). One is present in exon 1 (F^{6}FWNLWLW), another in exon 3 (W^{148}IFFPISF) and two in exon 6 (F^{227}LWCLYVW, W^{279}CLYVWQSF). Notably, the K15-M variant also contains four caveolin-binding sites, one in exon 1 (Y^{3}KKYLWGTW) and three in exon 6 (F^{282}LLYCFFCW, F^{285}YCFFCWQSF and F^{302}LFLFLAW). Three of these sites are present at

similar positions in both variants (underlined), which could point to an important functional role of these regions.

Exon 1 of the two splice variants K15 ex1 as/4-8 and K15 as/6-8 encodes only six aa (M^1ALGPT^6) in contrast to 72 aa (M^1KTLIF^6FWNLWLW……PSSWHLGII^{72}) encoded by exon 1 from K15 ex1-8 or splice variant K15 ex1/6-8. Hence, these two splice variants would not contain the potential caveolin-binding site present in exon 1 in K15 ex1-8 and K15 ex1/6-8, which might explain their absence in lipid rafts. The K15 ex6-8 construct, which does not localise to lipid rafts, would also lack this site and additionally the site in exon 6. The less efficient incorporation of the 21 kDa protein derived from splice variants K15 ex1 as/4-8 and K15 ex1 as/6-8 in lipid rafts could also be explained by the lack of exon 1 in these K15 isoforms. To explain the residual incorporation of these proteins into lipid rafts one could hypothesise that this 21 kDa protein is palmitoylated or myristoylated, which would allow lipid raft localisation.

Subcellular localisation of K15 membrane proteins by microscopy

The biochemical analysis of the subcellular localisation of the K15 variants indicated that individual K15 proteins may localise to different cellular compartments. Therefore, we investigated the localisation of full length K15 ex1-8, K15 splice variants K15 ex1/6-8 and K15 ex1 as/4-8 and K15 ex6-8 by immunofluorescence microscopy (figures 14, 16). For a comparative analysis between K15 ex1-8 and viral TMPs K1 and LMP1, we analysed the protein expression pattern of these proteins, as well as of the LMP1-K15$^{355-489}$ chimeric protein composed of the six transmembrane domains of LMP1 (aa 1-185) fused to the cytoplasmic domain of K15 (aa 355-489) (figures 15, 17).

When the epithelial cell line Ptk2 was transiently transfected with the K15 ex1-8 expression construct giving rise to a major 45 kDa and two minor proteins of 34 and 23 kDa (figure 10 C), and K15 expression was analysed with K15 antiserum, K15 showed a distinct punctate expression pattern that was equally distributed over the entire cell (figure 14 A, B). K15 partially accumulated in the plasma membrane, and could as well localise to intracellular membranes or endosomes. K15 was concentrated in a perinuclear region, reminiscent of Golgi or late endosome localisation. However, since we did not perform cycloheximide experiments to synchronise protein expression, the strong perinuclear staining may arise from overexpression of the K15 protein, and may not reflect its physiological localisation.

We have shown that K15 localised to lipid rafts and contains putative caveolin binding sites that are partially conserved between the two K15 variants K15-P and K15-M (table 3). Therefore, we investigated whether K15 and Caveolin-1 showed a similar subcellular expression pattern. As depicted in figure 14 C and D, a fusion protein composed of GFP fused to the C-terminus of Caveolin-1 (Caveolin-1-GFP) transiently expressed in Ptk2 cells showed a punctate expression pattern and partly formed larger spots. These larger spots were particularly conspicuous in some regions of the plasma membrane (indicated by arrows in

figure 14 C), but were also distributed in the cytoplasm. In live cell microscopy of cells expressing Caveolin-1-GFP, Pelkmans et al. (2001) described small scattered spots on the plasma membrane, and they suggest that these spots may represent individual caveolae. They also described larger, more brightly stained intracellular organelles scattered through the cytoplasm, which is consistent with our data.

In order to analyse whether K15 and Caveolin-1 co-localised, Ptk2 cells were co-transfected with the Caveolin-1-GFP fusion protein and the K15 ex1-8 expression construct. As depicted in figure 17 G and H, both proteins were found at the plasma membrane where they partially formed larger spots. However, when the two images were merged, there was no obvious co-localisation between the two proteins (figure 17 I).

For further analysis of the subcellular distribution of K15, we double-labelled Ptk2 cells transiently expressing K15 ex1-8 with an antibody recognizing endogenously expressed Calnexin and a K15 antibody. Calnexin is a type I transmembrane protein and localises to the ER (Hammond et al., 1994). As expected for an ER marker, a perinuclear and reticulated distribution pattern was observed with the Calnexin antibody (figure 17 E). K15 ex1-8 showed an equal overall distribution pattern (figure 17 D), and when the two images were merged it became obvious that the majority of K15 did not co-localise with Calnexin/the ER with the exception of the perinuclear region (figure 17 F).

In contrast, the K15 splice variant K15 ex1/6-8 showed a cellular distribution pattern characteristic of the ER (figure 16 E and F). The expression pattern of this protein was not punctate as that observed for K15 ex1-8, but clearly reticulated as seen with the ER marker Calnexin (figure 17 E).

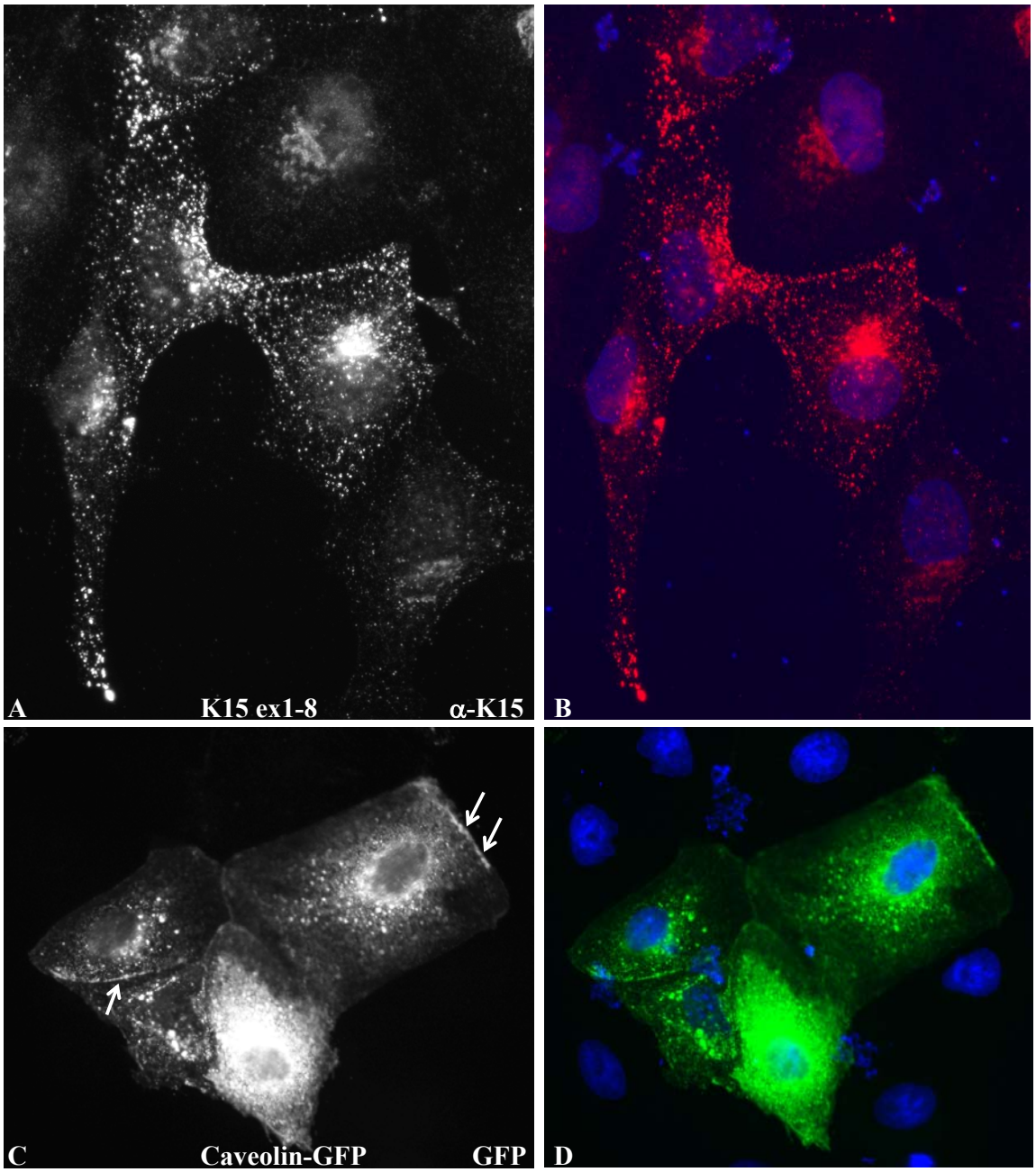

Figure 14: Subcellular localisation of K15 ex1-8 and Caveolin-1-GFP by immunofluorescence microscopy. Ptk2 cells were transiently transfected with 1 µg of the respective expression constructs as indicated in the figures with the Fugene transfection method. 48 h post transfection, cells were fixed with PFA and analysed for protein expression by fluorescence microscopy as described in detail in Material and Methods (2.6.5). Nuclei were stained with the Hoechst dye as described in 2.6.5. (A) The K15 ex1-8 construct coding for the major 45 kDa and minor 34 and 23 kDa K15 proteins was transiently expressed in Ptk2 cells and K15 proteins were localised with K15 antiserum and a secondary Cy3 conjugated antibody. (B) Overlay of image A with Hoechst stain. (C) Transient expression of a chimeric protein composed of GFP fused to the C-terminus of Caveolin-1 in Ptk2 cells. (D) Overlay of image C with Hoechst stain.

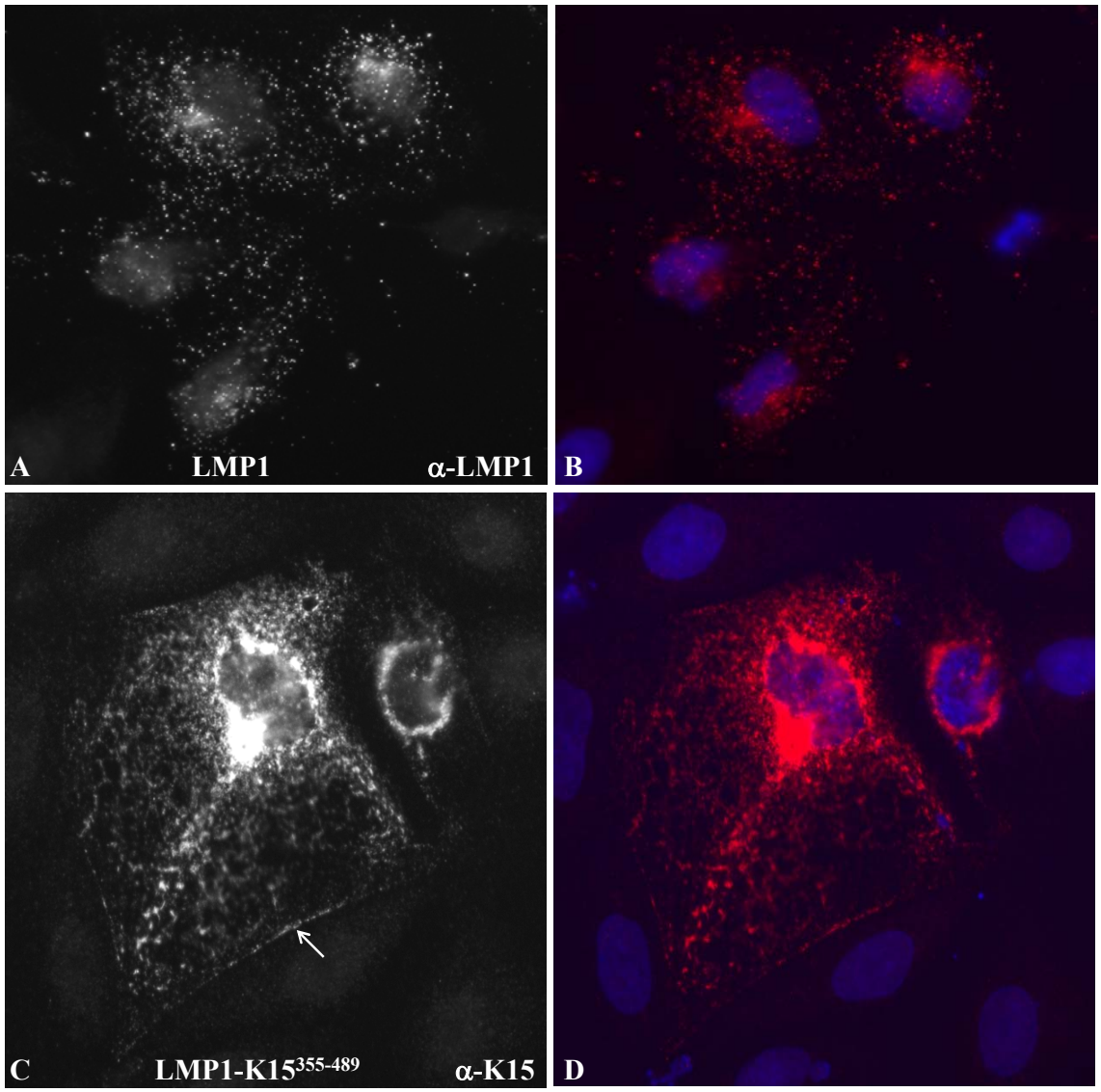

Figure 15: Ptk2 cells transiently expressing the EBV LMP1 protein or the LMP1-K15$^{355-489}$ chimera. Ptk2 cells were transiently transfected with 1 µg of the respective expression constructs as indicated in the figures with the Fugene transfection method. 48 h post transfection, cells were fixed with PFA and analysed for protein expression by fluorescence microscopy as described in detail in Material and Methods (2.6.5). Nuclei were stained with the Hoechst dye as described in 2.6.5. (A) The EBV LMP1 protein was detected with an LMP1-antibody and a secondary Cy3 conjugated antibody. (B) Overlay of image A with Hoechst stain. (C) The chimeric protein composed of the six transmembrane domains of LMP1 fused to the C-terminal domain of K15 was transiently expressed in Ptk2 cells and detected with K15 antiserum and a secondary Cy3 conjugated antibody. (D) Overlay of image C with Hoechst stain.

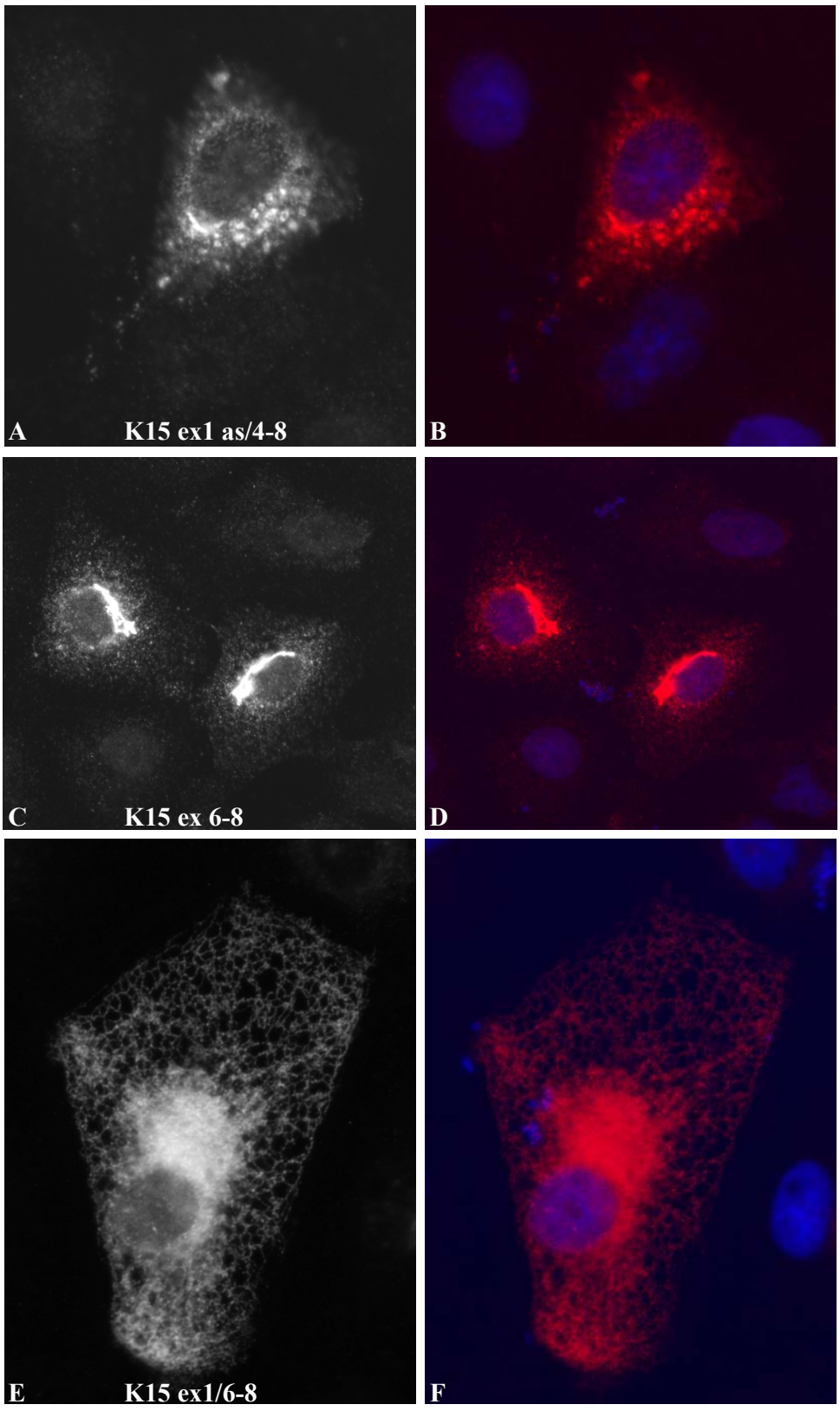

Figure 16: Ptk2 cells transiently expressing the K15 splice variants K15 ex1 as/4-8, K15 ex1/6-8 or the recombinant K15 ex6-8 construct. Ptk2 cells were transfected and fixed as described in figure legend 15. (A) The localisation of the K15 splice variant K15 ex1 as/4-8 was analysed with K15 antiserum and a secondary Cy3 conjugated antibody. (B) Overlay of image A with Hoechst stain. (C) Expression of the 23 kDa protein derived from the recombinant K15 ex6-8 construct was detecetd with K15 antiserum and a secondary Cy3 conjugated antibody. (D) Overlay of image C with Hoechst stain. (E) Expression of splice variant K15 ex1/6-8 was analysed with K15 antiserum and secondary Cy3 conjugated antibody (F) Overlay of image E with Hoechst stain.

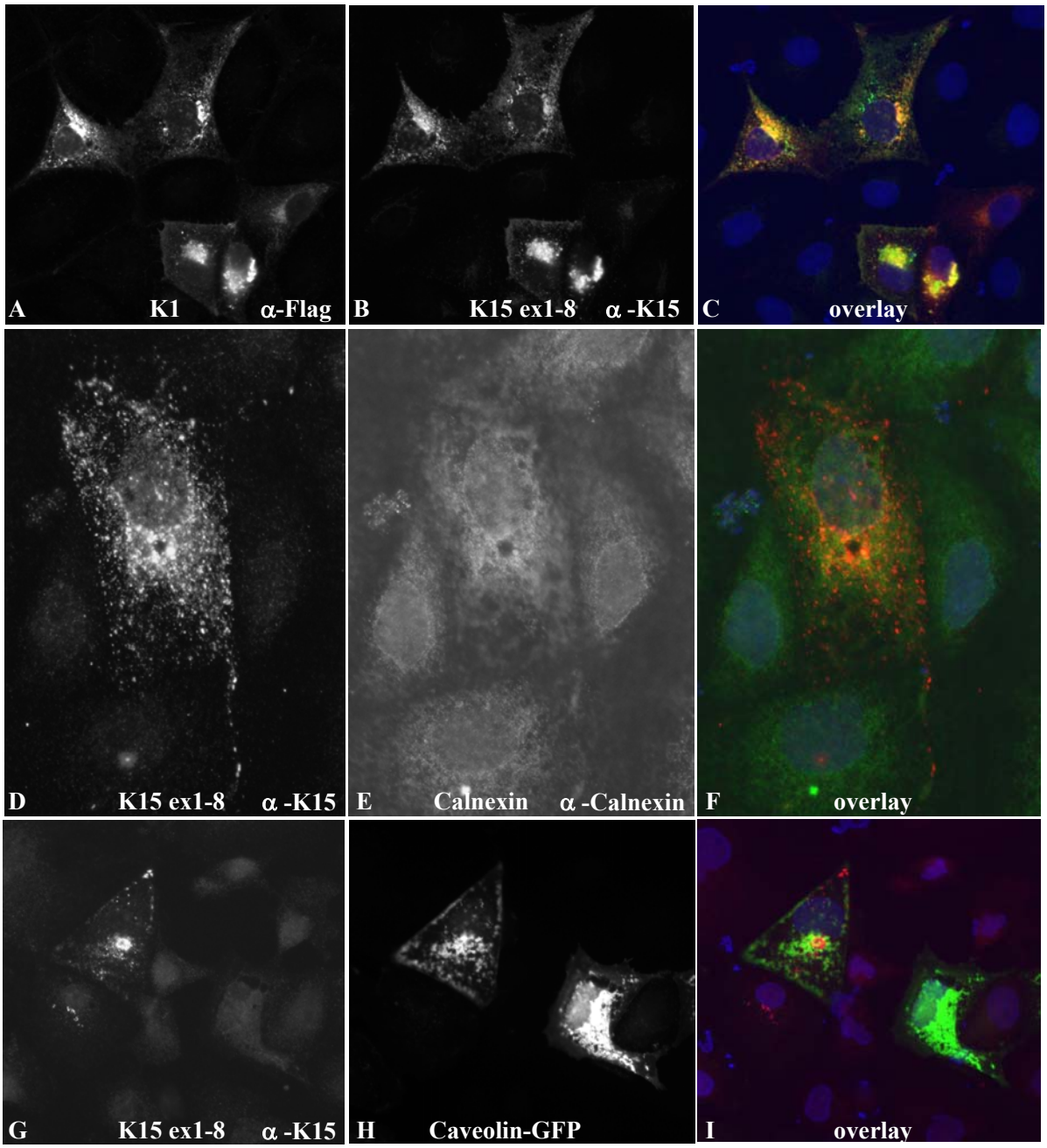

Figure 17: Co-localisation studies of transiently transfected Ptk2 cells. Ptk2 cells were transiently transfected with 1 µg of the respective expression constructs as indicated in the figures with the Fugene transfection method. 48 h post transfection, cells were fixed with PFA and analysed for protein expression by fluorescence microscopy as described in detail in Material and Methods (2.6.5). Nuclei were stained with the Hoechst dye as described in 2.6.5. Images A-C: Ptk2 cells were co-transfected with expression constructs for the Flag-tagged K1 type I transmembrane protein and K15 ex1-8 (without any tag) and cells were double-labelled with a Flag antibody and K15 antiserum. As secondary antibodies, anti-mouse Cy3 for Flag-K1 (A) and anti-rabbit FITC for K15 (B) were used. (C) Overlay of images A and B and Hoechst stain. Images D-F: Ptk2 cells transiently expressing the K15 ex1-8 expression construct were double-labelled with the K15 monoclonal antibody (see 3.2) and an anti-rabbit antibody for endogenous Calnexin. As secondary antibodies, anti-mouse Cy3 for K15 (D) and anti-rabbit FITC for Calnexin (E) were used. (F) Overlay of images D and E and Hoechst stain. Images G-I: K15 ex1-8 and Caveolin-GFP (see also figure 14) were coexpressed in Ptk2 cells and labelled with a K15 monoclonal antibody (see 2.3.8) and anti-mouse Cy3 conjugated secondary antibody (G). (I) Overlay of images G and H and Hoechst stain.

The EBV LMP1 protein has been reported to localise to the plasma membrane, intracellular membranes and lipid rafts (see 1.3.1.1). When we immunolabelled Ptk2 cells transiently transfected with LMP1 with an LMP1 antibody, LMP1 was equally distributed over the entire cell in a distinct punctate pattern and localised to a perinuclear region (figure 15 A and B). Interestingly, the LMP1-K15$^{355\text{-}489}$ chimeric protein showed a subcellular distribution pattern very different from that of LMP1 (figure 15 C and D). LMP1-K15$^{355\text{-}489}$ did not show a punctate pattern as K15 ex1-8 or LMP1, but rather a reticulated distribution reminiscent of the ER. The LMP1-K15 chimera also localised to the perinuclear region and to the plasma membrane (figure 15 C). At the plasma membrane, the chimera was partially present in larger spots as seen with the Caveolin-1-GFP fusion protein (figure 15 C, indicated by an arrow, compare with figure 14 C).

Since K1 and K15 transcripts are both present in latently KSHV infected B-cells and upregulated upon TPA treatment which induces lytic viral gene expression (see 1.3.5 and 1.3.6), we wondered whether these two proteins may co-localise. This idea was also supported by our observation that K1 localised to lipid rafts (data not shown). As depicted in figure 17 A, the KSHV K1 type I transmembrane protein was mainly localised to the perinuclear region, with a less distinct punctate but more diffuse staining pattern when compared to K15 or LMP1. K1 staining was partially reminiscient of ER localisation, and K1 was not found to form larger spots at the plasma membrane as does K15 ex1-8 (figure 17 A and B). This result would be consistent with observations by Lee et al. (2000), who described that K1 directly interacts with the μ chains of the BCR, thereby leading to the retention of B-cell antigen receptor subunits in the ER (see 1.3.5).

In Ptk2 cells transiently expressing the K1 and K15 ex1-8 protein and labelled with Flag-antibody recognising Flag-tagged K1 and K15 antibody, these two proteins were found to co-localise (figure 17 C). However, co-localisation was rather observed in the cytoplasm and in a perinuclear region, and not at the plasma membrane.

The K15 splice variant K15 ex1 as/4-8 did clearly not localise to the plasma membrane but rather to a perinuclear region, where it formed clusters (figure 16 A and B). The staining pattern of this splice variant appeared more diffuse than that of K15 ex1-8 (figure 14 A and B) and was also very different than that of splice variant K15 ex1/6-8 (figure 16 E and F). Expression construct K15 ex6-8, which was biochemically shown to localise to cellular membranes (figure 11 B) but not to lipid rafts (figure 12 B), mainly localised to the perinuclear region, and clearly not to the plasma membrane (figure 16 C and D). The staining pattern of K15 ex 6-8 was composed of small spots in the perinuclear region and stronger staining close to the nucleus reminiscent of Golgi localisation. Its staining pattern seemed diffuse-punctate but clearly not reticulated as that of K15 ex1/6-8 (figure 16 E and F) and was more reminiscent of the staining pattern obtained with splice variant K15 ex1 as/4-8 (figure 16 A and B).

In summary, the full length K15 isoform and K15 splice variants were shown to localise to different subcellular compartments as judged by biochemical subcellular fractionation assays (figures 12 and 13) and immunofluorescence microscopy (figures 14-17). Only the K15 ex1-8 protein formed larger spots in the plasma membrane that could represent caveolae/lipid rafts, but further co-localisation experiments are needed to underline this observation. The splice variant K15 ex1/6-8, lacking exons 2-5 and thereby being composed of fewer transmembrane domains than K15 ex1-8, shows a very different subcellular localisation by immunofluorescence microscopy. This does not contradict the flotation experiments that showed that this protein localised to lipid rafts, since lipid rafts are also present in intracellular membranes. Interestingly, the splice variant K15 ex1 as/4-8, that uses exon 1 differently, showed a subcellular distribution clearly different from K15 ex1-8 and K15 ex1/6-8, which indicates that the protein sequence encoded by exon 1 may be important for the subcellular localisation.

Since the K15 ex1-8 construct was clearly shown to localise to lipid rafts that are important sites for receptor signaling, we next investigated whether the K15 protein might exert signaling activity.

3.1.2 Signaling activities of K15 membrane proteins

Many cellular proteins such as adaptor proteins and protein kinases (e.g. protein tyrosine kinases of the Src family or PI3 kinase) contain non-catalytic domains termed SH2 or SH3 domains, via which they can bind to proteins having SH2-binding (SH2-B) or SH3-binding (SH3-B) motifs. The consensus motif for SH2-B domains is YXXL/I/V, that, when tyrosine phosphorylated, allows binding of SH2 domain containing proteins. SH2-B motifs of the consensus YXXA/P/T have also been reported. Different SH2 domains have differing preferences for hydrophobic or hydrophilic residues immediately carboxyl prime to the tyrosine residue (Songyang et al., 1993, 1994). The C-terminal putatively cytoplasmic domain of K15, common to all splice variants identified so far, contains motifs that could function as SH2-B and SH3-B motifs and contains tyrosine, serine and threonine residues that are potential phosphorylation sites for cellular kinases (shown in figure 18 and table 3).

Analysis of the twelve tyrosines of K15 ex1-8 and their surrounding motifs reveals that Y^{481}, located to the C-terminal putatively cytoplasmic domain of K15, is situated in a context that would be suitable for optimal binding to identified proteins involved in signal transduction (table 3). The Y^{481}EEV motif in the K15 cytoplasmic domain is preceded by negatively charged aa (see figure 18) and resembles an SH2-B site similar to the preferred SH2-B site for Src family non-receptor protein tyrosine kinases (PTKs) YEEI. An analysis with the programme Motif Scan at http://scansite.mit.edu revealed that the Y^{481}EEV motif of K15 would be a suitable docking site for SH2 domain containing proteins such as the Src family members of PTKs Src, Fyn, Fgr and Lck, the adaptor protein Nck and the receptor tyrosine kinase fibroblast growth factor receptor (FGFR) (table 3).

Tyrosine motifs Y^{52}TQA, Y^{90}ACL, Y^{163}AFA, Y^{190}PVS, Y^{213}LGF and Y^{282}VWQ are located to regions with low surface accessibility according to the membrane topology prediction (figure 9). Of these motifs, Y^{163}AFA could represent an SH2-B site and the Y^{90}ACL motif bears some resemblance to an immunoreceptor tyrosine-based inhibitory motif (ITIM). It has been demonstrated that the phosphatase SHP-1 binds to the ITIM within the cytoplasmic domain of the Fc receptor. This interaction is important in the negative regulation of the BCR (Benschop & Cambier, 1999, Cambier et al., 1994, Weiss & Littman, 1994). The consensus ITIM binding motif for SHP-1 is T/S-X-X-X-X-X-L, which is very similar to the K15 Y^{90} motif SVTY^{90}ACL and to the LMP2A Y^{85} motif SLY^{85}LGL. Notably, this motif is also present in the K15-M variant (SVY^{46}YQL).

Tyrosine motifs Y^{345}LYK and Y^{347}KEK are located to the very membrane proximal part of the cytoplasmic domain. Similar motifs are present at equivalent positions in the K15-M variant (Y^{351}LYR and Y^{353}RES), but no interaction partners were predicted for these motifs (figure 18, table 3). Y^{358}RQR and Y^{366}TRD are located to the putatively cytoplasmic region of K15, but are not reminiscent of SH2-B domains. However, a motif similar to Y^{366}TRD is present in the K15-M variant (Y^{371}TPH). The Y^{431}ASI motif in the cytoplasmic domain of K15 could serve as an SH2-B motif, and the PTK C-terminal Src kinase (Csk), which is a negative regulator of Src family kinases, may be an interaction partner for K15 via this motif (table 3). The Y^{431}ASI motif is also reminiscent of an internalization motif found in plasma membrane proteins with the consensus Y-X-X-hydrophobic, with leucine being the preferred residue at the hydrophobic position, although isoleucine, phenylalanine, methionine and, to a lesser extent, valine are tolerated (Bonifacino & Dell´Angelica 1999).

According to phosphorylation site prediction programmes at http://scansite.mit.edu and http://cbs.dtu.dk, the tyrosine residue of the Y^{481}EEV motif can potentially be phosphorylated by the receptor tyrosine kinases FGFR and platelet-derived growth factor receptor (PDGFR), and PTK Src family members Src and Lck. In addition, several serine and threonine residues of the K15 cytoplasmic domain would be situated in a context suitable for phosphorylation by serine/threonine kinases such as MAPKs p38 and Erk1 (S^{385}), glycogen synthase kinase 3 (GSK3; S^{433}, S^{442}, S^{446}), the calcium/calmodulin-dependent protein kinase II (CaMII; S^{446}, T^{367}), the cAMP dependent protein kinase A (PKA; S^{446}, T^{367}), the calcium-dependent protein kinase C (PKC; T^{404}) and the protein kinase Akt (T^{367}) (see table 3 and figure 18).

A comparison between the two K15 variants, K15-P and K15-M that share only 33% aa identity, points to a functional role of several signaling motifs (table 3 and figure 18): Tyrosine motifs YEEV and YASI are strictly conserved between the K15-P (Y^{481}EEV, Y^{431}ASI) and K15-M variant (Y^{490}EEV, Y^{444}ASI) (figure 18 and table 3). Tyrosine motifs $\underline{Y^{345}LY}$K/$\underline{Y^{347}}$K$\underline{E}$K/$\underline{Y^{366}T}$RD in K15-P and $\underline{Y^{351}LY}$R/$\underline{Y^{353}}$R$\underline{E}$S/$\underline{Y^{371}T}$PH in K15-M are also partly conserved between the two variants. The proline-rich motif in the K15 C-terminal domain (P^{387}PLPP) may recruit SH3 domain containing proteins such as the adaptor protein Crk and the PTK Src (table 3). Notably, this motif is strictly conserved between K15-P (P^{387}PLP) and K15-M (P^{396}PLP) (figure 18 and table 3).

K15-P (489 aa)				K15-M (498 aa)			
K15 tyrosine	**K15 tyrosine motif**	**Potential function and binding partners**	**Potential kinase**	**K15 tyrosine**	**K15 tyrosine motif**	**Potential function and binding partners**	**Potential kinase**
Y52	YTQA	?	-	Y3	YKKY	?	-
Y90	YACL	SH2-B; SHP	-	Y6	YLWG	?	-
Y163	YAFA	SH-2B ?	-	Y46	**YYQL**	?	-
Y190	YPVS	?	-	Y47	YQLF	?	-
Y213	YLGF	?	-	Y57	YVQS	?	-
Y282	YVWQ	?	-	Y146	YNNW	?	-
				Y285	YCFF	?	-
				Y322	YTDG	?	-
Y345	YLYK	?	-	Y351	**YLYR**	?	-
Y347	YKEK	?	-	Y353	**YRES**	?	-
Y358	YRQR	?	-				
Y366	YTRD	?	-	Y371	**YTPH**	?	-
Y431	YASI	SH2-B or internalization signal; Csk kinase	-	Y444	**YASI**	as for K15-P	-
Y481	YEEV	SH2-B; Src, Lck, Fyn, FGFR, Nck, Fgr	Lck, Src, PDGFR, FGFR	Y490	**YEEV**	SH2-B; Lck, Src, Fyn, Fgr	Src, EGFR, Lck
K15 serine	**K15 serine motif**			**K15 serine**	**K15 serine motif**		
S385	HLGNNVI**S**PPPLPPF	-	Erk1, p38	S360	YRESRLV**S**FNNVTT	-	Akt
S433	GYA**S**ILVS	-	GSK3				
S442	AEE**S**REPS	-	GSK3				
S446	AEESREP**S**PQPDQSG	-	GSK3, CaMII, PKA				
K15 threonine	**K15 threonine motif**			**K15 threonine**	**K15 threonine motif**		
T367	QRRRRIY**T**RDQNLHH	-	Akt, CaMII, PKA	T452	ASILGDN**T**PPPTRA	-	GSK3
T404	SHV**T**DRG	-	PKC	T372	TTRLPIY**T**PHDTPH	-	GSK3
K15 proline	**K15 proline rich**			**K15 proline**	**K15 proline rich**		
P387	PPLPP	SH3-B; Crk, Src	-	P396	**P**PLP	SH3-B; p85, Crk, Grb2, Src	-
				P399	PPL**P**SRN	SH3-B; p85	-
K15 caveolin-binding site				**K15 caveolin-binding site**			
F6	FFWNLWLW	?	-	Y3	YKKYLWGTW	?	-
W148	WIFFPISF	?	-	F282	FLLYCFFCW	?	-
F277	FLWCLYVW	?	-	Y285	YCFFCWQSF	?	-
W279	WCLYVWQSF	?	-	F302	FLFLFLAW	?	-
TRAF-binding site				**TRAF-binding site**			
P449	PDQSGMS	TRAFs ?	-	I462	INQSGIS	TRAFs ?	-
A473	ATQPT	TRAFs ?	-	P482	PFQPAD	TRAFs ?	-

Table 3: Potential signaling motifs of KSHV terminal membrane proteins K15-P (aa 1-489) and K15-M (aa 1-498). See text and figure 18 for further details.

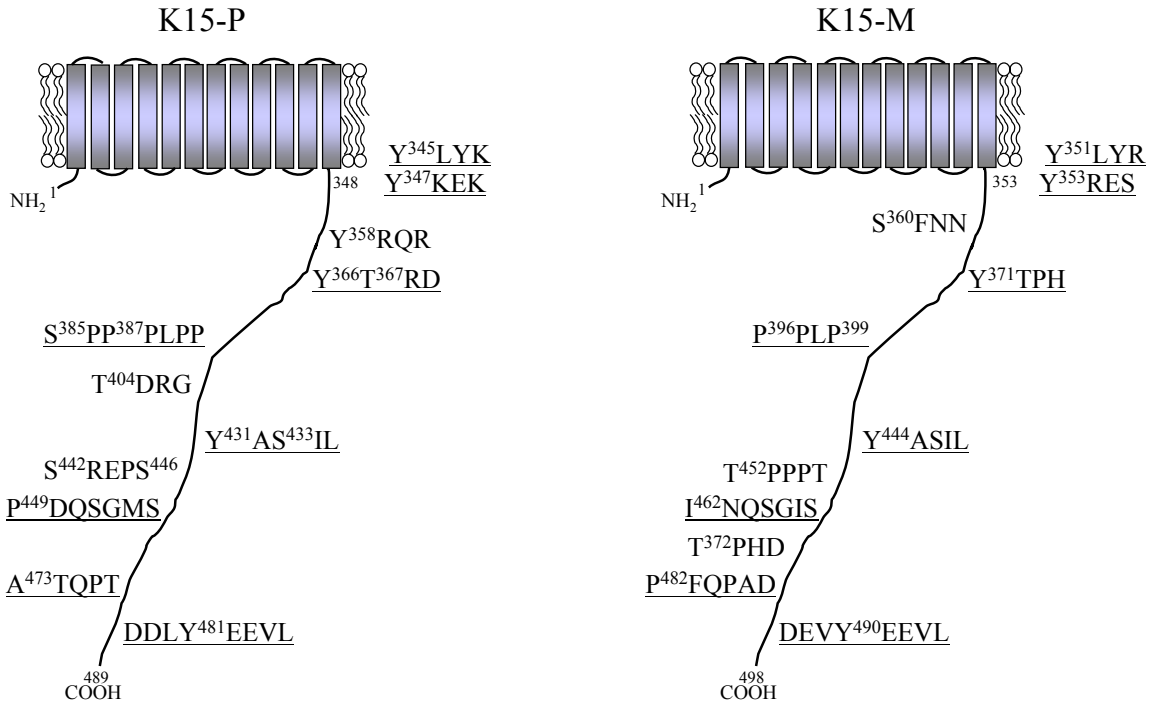

Figure 18: Potential interaction motifs of the KSHV terminal membrane proteins K15-P and K15-M. The cytoplasmic domain of K15 contains motifs reminiscent of SH2-B (YASI, YEEV) and SH3-B (PPLP) sites that are conserved between the K15-P and K15-M variant. In addition, certain tyrosine, serine and threonine residues are situated in a context suitable for phosphorylation by cellular kinases as e.g. Src family PTKs and MAPKs (see text). Possible cellular interaction partners for the two K15 variants are listed in detail in table 3. Similar or conserved motifs of the two K15 variants are underlined.

SH2 and SH3 domain containing proteins have been shown to be crucial downstream effectors of LMP2A signaling activities. The PTKs Lyn and Syk are crucial interaction partners of the LMP2A protein and mediate its downstream signaling. The Y^{481}EEV motif of K15 is reminiscent of the SH2-B motif Y^{112}EEA of LMP2A, which is the docking site for the PTK Src family member Lyn (see figure 3 in 1.3.1.1 and 1.3.1.2). Therefore, we investigated whether K15 is able to bind to members of the Src family of PTKs.

The K15 C-terminal domain binds to members of the Src family of PTKs

To investigate the binding of K15 to members of the Src family of PTKs, a GST-pulldown approach was used. A fusion protein composed of GST fused to the C-terminal, putatively cytoplasmic domain of K15 (GST-$K15^{355-489}$) was expressed in *E. coli* and used to bind the myc-tagged PTKs Src, Hck, Fyn, Lck and Yes from transiently transfected 293-T cells (see figure 19 and 2.6.8). GST alone served as negative control. As shown in a Western blot probed with anti-c-myc antibody, all PTKs examined could be precipitated with the GST-$K15^{355-489}$ protein (figure 19, lane 3) but not with GST alone (figure 19, lane 2). In order to identify the binding site of the PTKs within the K15 cytoplasmic domain, serial deletion

mutants of GST-K15$^{355-489}$, depicted in the upper panel of figure 19, were used in a GST pulldown experiment.

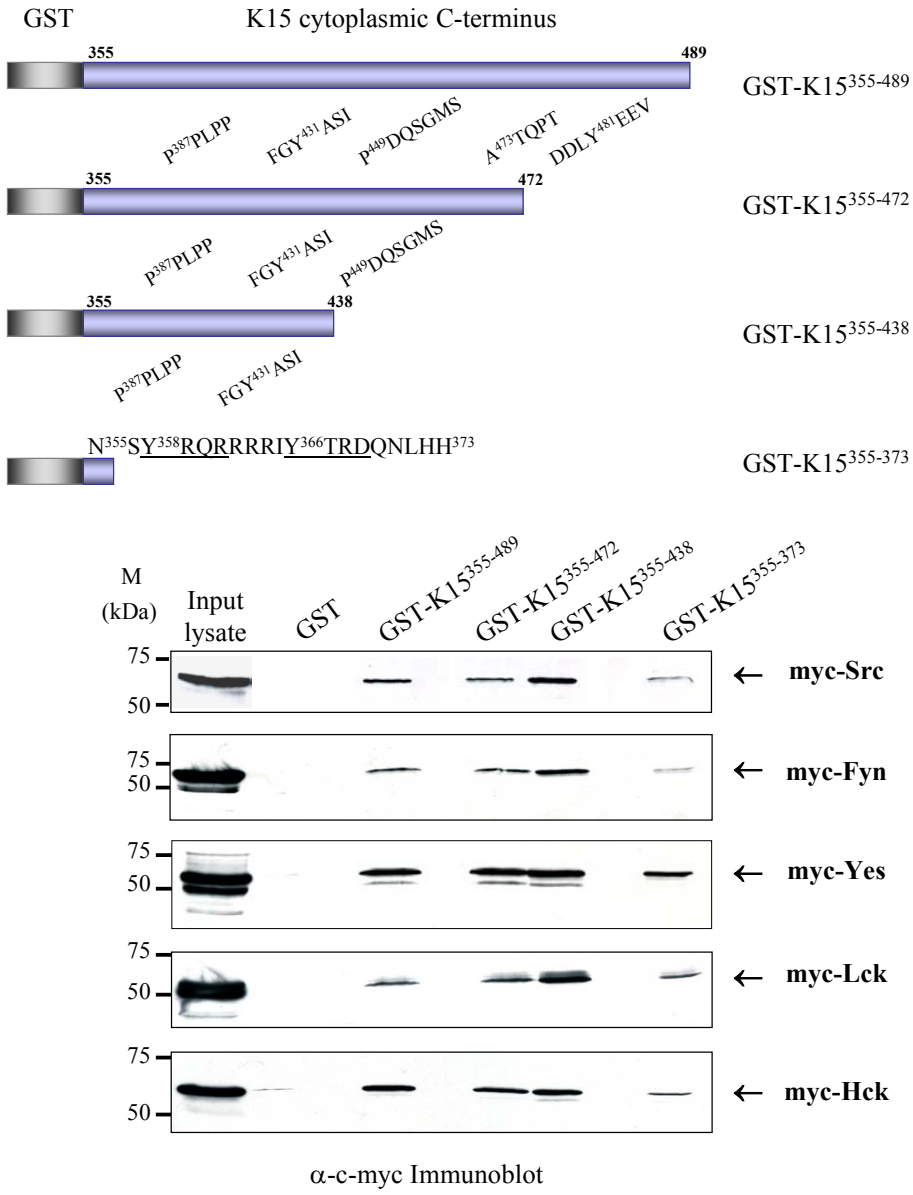

Figure 19: The non-receptor protein tyrosine kinases (PTKs) Src, Fyn, Yes, Lck and Hck bind to the C-terminal domain of K15. The C-terminus of K15 (aa 355-489) was fused to the GST protein and a GST-pulldown experiment was performed with myc-tagged PTKs transiently expressed in 293-T cells. In order to map the PTK binding region in the C-terminal domain of K15, serial C-terminal deletion constructs were used in the GST-pulldown assay. GST-K15$^{355-472}$ lacks the putative SH2-B motif Y^{481}EEV, and GST-K15$^{355-373}$ additionally lacks the putative SH2-B motif Y^{431}ASI and the putative SH3-B motif P^{387}PLPP (see also table 3 and figure 18). Bound PTKs were detected by Western blotting and an antibody to c-myc.

As shown in figure 19, all analysed PTKs still bound to all deletion mutants lacking, respectively, the distal SH2-binding motif Y^{481}EEV (GST-K15$^{355-472}$), the region of aa 439-489 (GST-K15$^{355-438}$), and the P^{387}PLP motif together with the Y^{431}ASI motif (GST-K15$^{355-373}$). Motifs Y^{481}EEV, Y^{431}ASI and P^{387}PLPP are conserved between the K15-P and K15-M

variants, and could be candidates for SH2- and SH3-binding motifs (figure 18 and table 3). The GST-pulldown results suggest that the most proximal region of the cytoplasmic domain of K15 (aa 355-373) contributes to the binding of Src kinases, but do not exclude a role for the P^{387}PLP or Y^{431}ASI motif in this interaction. The region of aa 355-373 encompasses two tyrosine motifs, Y^{358}RQR and Y^{366}TRD, which do not represent typical SH2-B motifs. The K15-M variant has a similar motif at the equivalent position in its cytoplasmic C-terminus, Y^{371}TPH (figure 18), which indicates that this motif might play a role in K15 signaling. However, point mutations in this region would be needed to assure whether the Y^{366}TRD motif is indeed a docking site for PTKs of the Src family.

K15 is phoyphorylated by Src family PTKs at Y^{481}

It has previously been shown that a chimeric protein composed of the extracellular and transmembrane domain of the CD8 receptor fused to the cytoplasmic domain of K15 is constitutively phosphorylated on the tyrosine within the distal putative SH2-binding motif Y^{481}EEV independent of antibody stimulation (Choi et al., 2000a). Since LMP2A is phosphorylated at its ITAM motif by members of the PTK family (see 1.3.1.2), we investigated whether K15 was a substrate for these kinases. The cytoplasmic C-terminal domain of K15 fused to GST (GST-$K15^{355-489}$) and the deletion mutant GST-$K15^{355-472}$ lacking the potential SH2-binding and phosphorylation motif Y^{481}EEV were expressed in *E. coli* and purified as described in Material and Methods (2.6.7). The purified fusion proteins were analysed by SDS-PAGE and equal amounts of protein were used as a substrate in an in vitro kinase assay with immunoprecipitated myc-tagged PTKs Src, Fyn, Lck, Hck and Yes from transiently transfected 293-T cells (see 2.6.11).

Figure 20 shows that all kinases examined phosphorylated the C-terminal domain of K15 (GST-$K15^{355-489}$, 42 kDa, figure 20 A, left top panel), whereas the GST-$K15^{355-472}$ fusion protein lacking the Y^{481}EEV motif was not phosphorylated (40 kDa, figure 20 A, right top panel), nor was unfused GST protein (27 kDa, figure 20 A, left and right top panels). Expression of the immunoprecipitated myc-tagged PTKs was examined with an anti-c-myc antibody (figure 20 A, left middle panel and figure 20 A, right lower panel). The polyclonal K15 antibody, which also recognizes the GST protein, was used to detect the GST-$K15^{355-489}$ fusion protein and GST (figure 20 A, left lower panel).

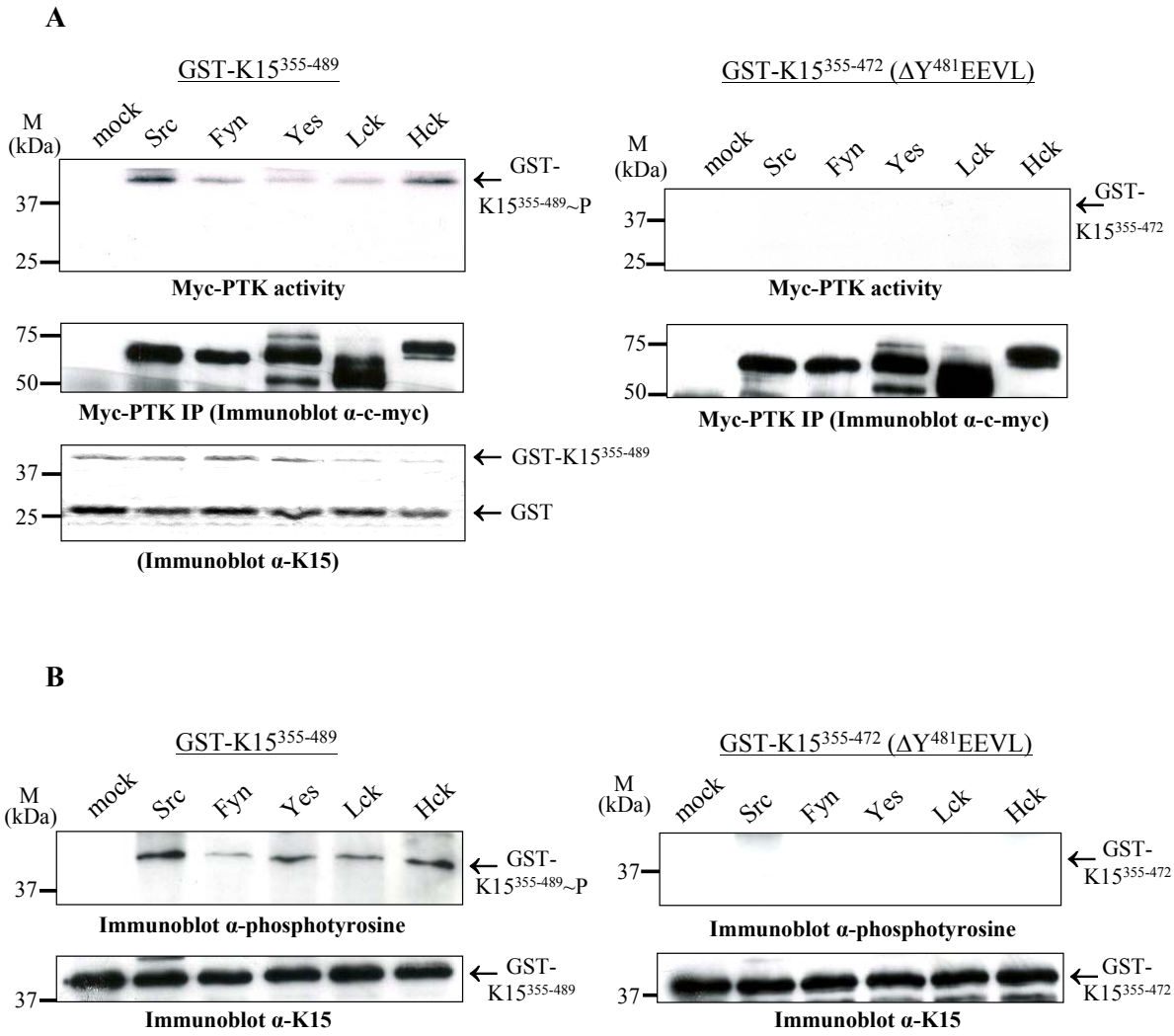

Figure 20: The tyrosine residue of the distal SH2-binding motif (Y^{481}EEV) of the K15 C-terminal domain is phosphorylated by members of the Src kinase family of protein tyrosine kinases. Purified GST-$K15^{355-489}$ and GST-$K15^{355-472}$ protein was used as a substrate in an in vitro kinase assay with immunoprecipitated myc-tagged Src kinases and [γ-^{32}P] ATP. (A) The Src kinase family members Src, Fyn, Yes, Lck and Hck phosphorylate the C-terminal domain of K15 in an in vitro immunocomplex kinase assay (left top panel). If the last 17 aa encompassing the SH2-binding motif (Y^{481}EEV) of the C-terminus were deleted (GST-$K15^{355-472}$), no phosphorylation was observed (right top panel). The expression level of the myc-tagged immunoprecipitated Src kinases was detected with an anti-c-myc antibody (left middle panel and right lower panel). The amount of GST-$K15^{355-489}$ fusion protein and nonfused GST protein used in the in vitro kinase reactions was analyzed by Western Blotting and probed with K15 antiserum (left lower panel). (B) The kinase reactions shown in (A) were analysed by Western blotting with an anti-phosphotyrosine antibody. Expression of the GST-K15 fusion proteins GST-$K15^{355-489}$ and GST-$K15^{355-472}$ was detected with K15 antiserum.

Since the sequence deleted in mutant GST-$K15^{355-472}$ contains two threonine residues (T^{474}, T^{478}), which theoretically could be targets for phosphorylation by other cellular kinases, the immunoblots of the kinase assay reactions were probed with an anti-phosphotyrosine antibody (figure 20 B). The result shows that GST-$K15^{355-489}$ (figure 20 B, left top panel), but not GST-$K15^{355-472}$ (figure 20 B, right top panel), was phosphorylated on tyrosine, indicating that Y^{481} in the Y^{481}EEV SH2-binding motif of K15 was phosphorylated by the Src kinases

examined. However, assuming that other protein kinases bound to the immunoprecipitated Src kinases, the question whether K15 is solely phosporylated at Y^{481} in the region encompassing aa 473-489 could only be addressed with a GST-$K15^{355-489}$ fusion protein carrying the point mutation $Y^{481} \rightarrow F^{481}$.

Activation of the NF-κB pathway by the 45 kDa K15 protein involves Y^{481}

NF-κB is a dimeric transcription factor that activates transcription from a large number of target genes that play key roles in cell growth and death, as well as in immune and inflammatory responses. NF-κB activity is frequently increased in human tumours; it is essential for growth and survival of tumour cells. Cells tightly regulate NF-κB activity by expression of a family of inhibitory proteins, IκBs, that bind to NF-κB sequestering it in the cytoplasm (reviewed in Pomerantz & Baltimore 2002, Gosh & Karin 2002). One prominent example of bypassing this control mechanism is the EBV LMP1 protein, which is a potent inducer of the NF-κB pathway. LMP1 activates IκB kinases (IKK) that subsequently phosphorylate IκB on serines. Phosphorylated IκB is then recognized by WD40 domains of ubiquitin ligase receptors, ubiquitinated by E3 ubiquitin protein ligases at lysine residues and targeted for degradation by the 26 S proteasome, which relieves inhibition of NF-κB-dependent transcription (see 1.3.1.1 and figure 35 in 4.1).

The ability of TRAF-1, -2 and -3 to interact with K15 (Glenn et al., 1999, Brinkmann et al., 2003) resembles their binding to the CTAR-1 region of LMP1, where they provide a link to the downstream events that result in activation of the NF-κB pathway (see 1.3.1.1, 1.3.6, figure 3 in 1.3.1.1 and figure 35 in 4.1). Therefore, we investigated whether the different K15 isoforms could activate NF-κB by co-transfecting corresponding expression vectors (figures 7 and 8 in 2.2.1) together with a luciferase reporter plasmid containing three NF-κB sites into 293-T cells (2.2.2).

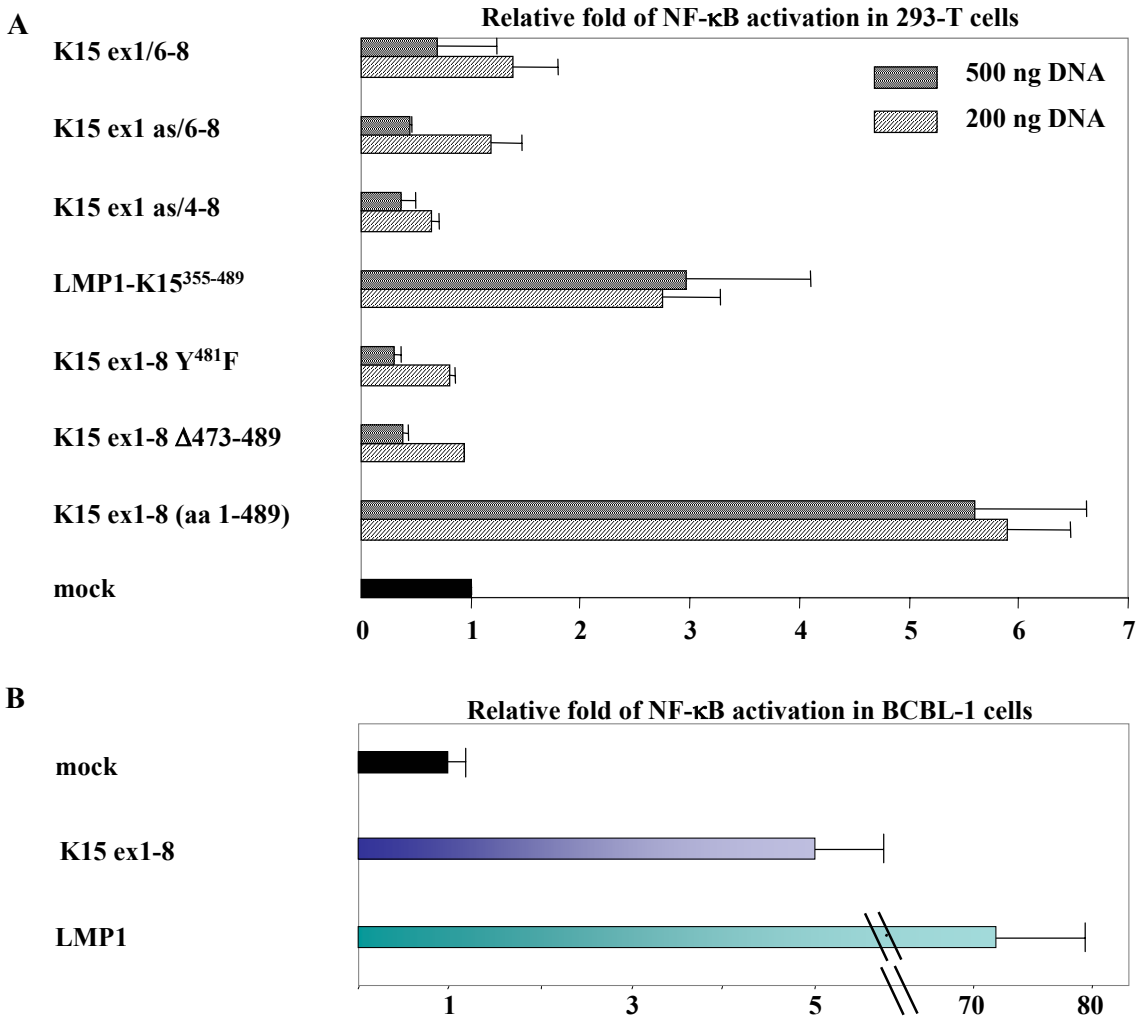

Figure 21: The 45 kDa K15 protein activates the transcription factor NF-κB in a luciferase based reporter assay. (A) 293-T cells were transiently co-transfected with 50 ng of the luciferase reporter plasmid p3EnhκBconA-Luc containing three NF-κB binding sites upstream of the luciferase gene and different amounts of K15 expression constructs (200, 500 ng DNA). 24 h after transfection, cells were lysed and analysed for luciferase activity. Shown is the relative fold of activation compared to empty vector (mock) transfected (200, 500 ng DNA) cells based on triplicate samples. Equal expression levels of K15 proteins were analysed by Western blot with a K15 antiserum (not shown). (B) BCBL-1 cells were transfected with 5 µg of the NF-κB luciferase reporter p3EnhκBconA-Luc and 10 µg of expression constructs for either K15 ex1-8, LMP1 or mock DNA by electroporation as described in Material and Methods (2.3.7), lysed 24 h after transfection and analysed for luciferase activity as described in 2.6.4. Shown is the relative fold of NF-κB activation compared to mock transfected BCBL-1 cells.

As shown in figure 21 A, K15 ex1-8, expressing the longest K15 isoform (aa 1-489), showed a 5-6 fold activation of the NF-κB transcription factor, whereas the smaller K15 isoforms (K15 ex1/6-8, K15 ex1 as/6-8 and K15 ex1 as/4-8) did not significantly increase basal NF-κB activity. As a positive control, pSV-LMP1 coding for the LMP1 protein was transfected, which induced an approximately 100 fold activation of this reporter (not shown). In comparison, only a moderate three fold NF-κB activation was observed with the LMP1-K15$^{355-489}$ chimeric protein (figure 21 A). Protein expression of the different constructs in 293-T cells was comparable on Western blots (not shown).

These results indicate a contribution of the transmembrane regions of K15 to NF-κB activation, which can also partly be provided by the LMP1 transmembrane regions. A deletion construct lacking aa 473-489, including the Y^{481}EEV motif, and the K15 $Y^{481}\rightarrow F^{481}$ point mutant did not activate NF-κB (figure 21 A), indicating that phosphorylation of Y^{481}, most likely by members of the PTK family, is required for initiating NF-κB signaling.

The ability of K15 ex1-8 to induce the NF-κB transcription factor was also analysed in the naturally KSHV-infected PEL cell line BCBL-1. As depicted in figure 21 B, transiently expressed K15 ex1-8 induced NF-κB up to five fold in BCBL-1 cells, whereas LMP1 showed a much stronger activation of the NF-κB reporter.

The activity of the AP-1 transcription factor is induced by K15

The mitogenic transcription factor AP-1 is a dimer of Jun-Jun or Jun-Fos family proto-oncoproteins and it has been shown that LMP1 is an inducer of AP-1 activity in 293 cells (Kieser et al., 1997). To test whether K15 can activate the AP-1 transcription factor, HEK 293-T cells were transiently co-transfected with 50 ng of the reporter plasmid pRTU14, which consists of a luciferase reporter gene under the control of a minimal promoter and four AP-1 binding sites [TPA responsive elements (TREs), consensus 5´-TGA(G/C)TCAG-3´], and increasing amounts of different K15 expression constructs or plasmid pSV-LMP1 as a positive control (figures 7 and 8 in 2.2.1).

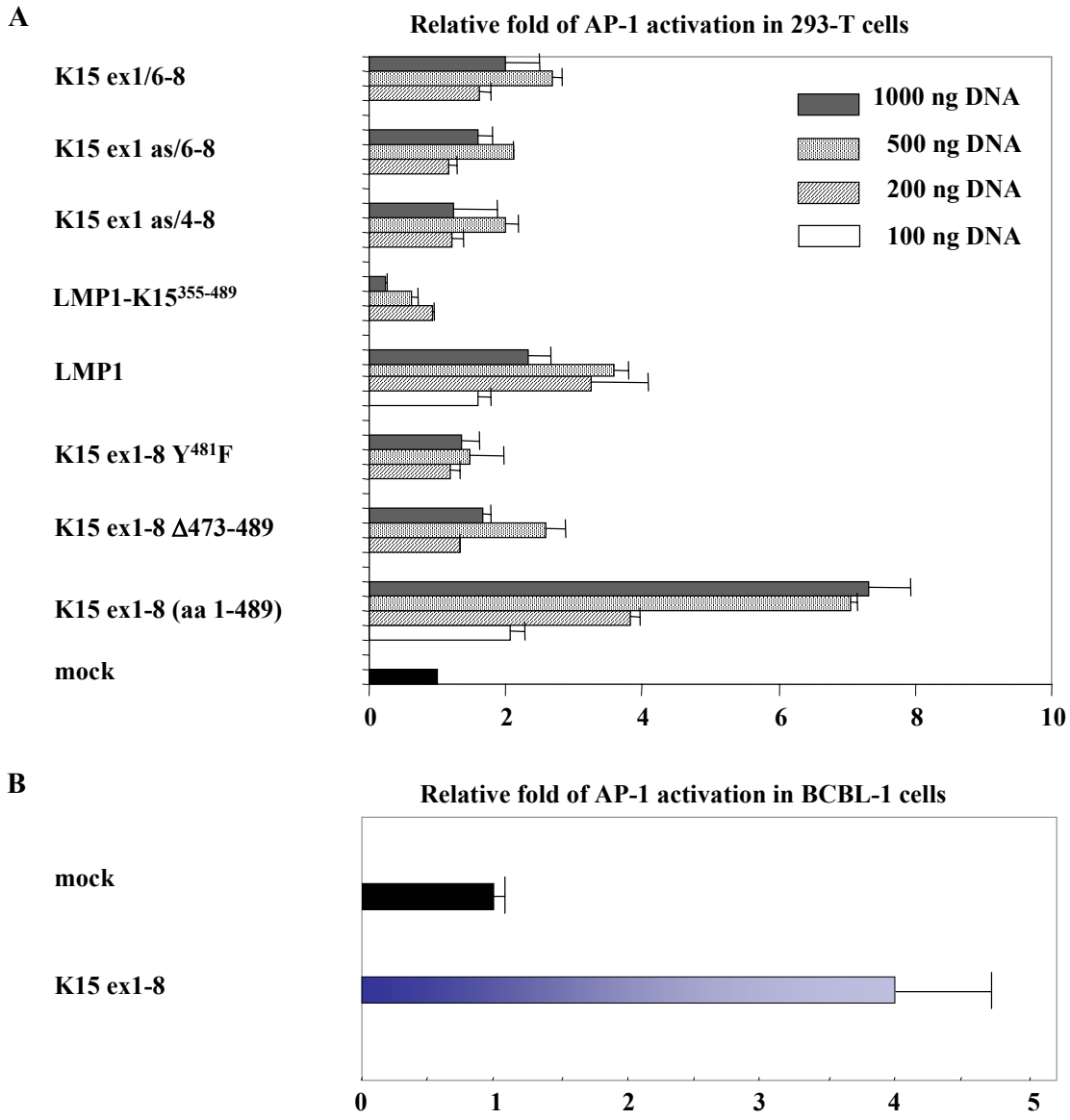

Figure 22: The transcription factor AP-1 is activated by K15. (A) 293-T cells were transiently co-transfected with the AP-1 luciferase reporter plasmid pRTU14 containing four AP-1 binding sites upstream of the luciferase gene, and different amounts of K15 expression constructs (100, 200, 500 1000 ng). After transfection, cells were grown in medium containing 1% FCS, lysed after 24 h and analysed for luciferase activity. Shown is the relative fold of activation compared to mock transfected (100, 200, 500, 1000 ng) cells based on triplicate samples. Equal expression levels of K15 proteins were analysed by Western blot with K15 antiserum (not shown). (B) BCBL-1 cells were transfected with 5 µg of the AP-1 luciferase reporter pRTU14 and with 10 µg of either K15 ex1-8 or mock DNA by electroporation as described in Material and Methods (2.3.7), lysed 24 h after transfection and analysed for luciferase activity as described in 2.6.4. Shown is the relative fold of AP-1 activation compared to mock transfected BCBL-1 cells.

The results depicted in figure 22 A show that full length K15 ex1-8 (aa 1-489) was a more potent inducer of AP-1 activity than LMP1, with K15 activating AP-1 up to 7-8 fold and LMP1 activating AP-1 up to 3-4 fold in a dose-dependent manner compared to cells transfected with control plasmids. Transiently expressed full length K15 ex1-8 is also able to induce the AP-1 transcription factor in the naturally KSHV infected PEL cell line BCBL-1 up to four fold (figure 22 B).

AP-1 activation of the K15 deletion mutant lacking the Y^{481}EEV motif (K15 ex1-8 Δ473-489) and the point mutant K15 ex1-8 Y^{481}F was significantly reduced (figure 22 A). This result indicates that phosphorylation of tyrosine Y^{481} of the Y^{481}EEV motif was important for K15-induced AP-1 activation. Interestingly, the LMP1-$K15^{355-489}$ chimera did not induce AP-1 activity. The three K15 splice variants (K15 ex1/6-8, K15 ex1 as/6-8 and K15 ex1 as/4-8) showed no clear-cut activation although they contain the entire K15 cytoplasmic domain (figure 22 A). This might suggest that the regions encoded by exons 2-5 are also important for induction of AP-1 activity.

K15 induces the kinase activity of the MAP kinases Erk2 and JNK1, but not of p38

After we established that K15 was able to induce the AP-1 transcription factor, the next step was to elucidate the signaling pathways that are mediating the signaling effects of the K15 protein. Three major MAP kinase pathways have been described to date that regulate AP-1 activity in the cell: the Ras-Raf-MEK1/2-Erk1/2 pathway, the MKK4/7(SEK1)-JNK1 cascade and the MKK3/6-p38 pathway (Chang & Karin 2001, Pearson et al., 2001). LMP1 induces the activity of the transcription factor AP-1 specifically via the c-Jun N-terminal kinase 1 (JNK1) pathway (Kieser et al., 1997, Eliopoulos & Young 1998, Eliopoulos et al., 1999). Furthermore, LMP1 induces the activity of the MAP kinase p38 (Schultheiss et al., 2001). In order to investigate the ability of the longest K15 isoform to induce any of these pathways, the activation of the MAP kinases Erk2, JNK1 or p38 was examined in in vitro immunocomplex kinase assays (see Material and Methods 2.6.11). LMP1 was included in the JNK1 and p38 kinase assay as a positive control.

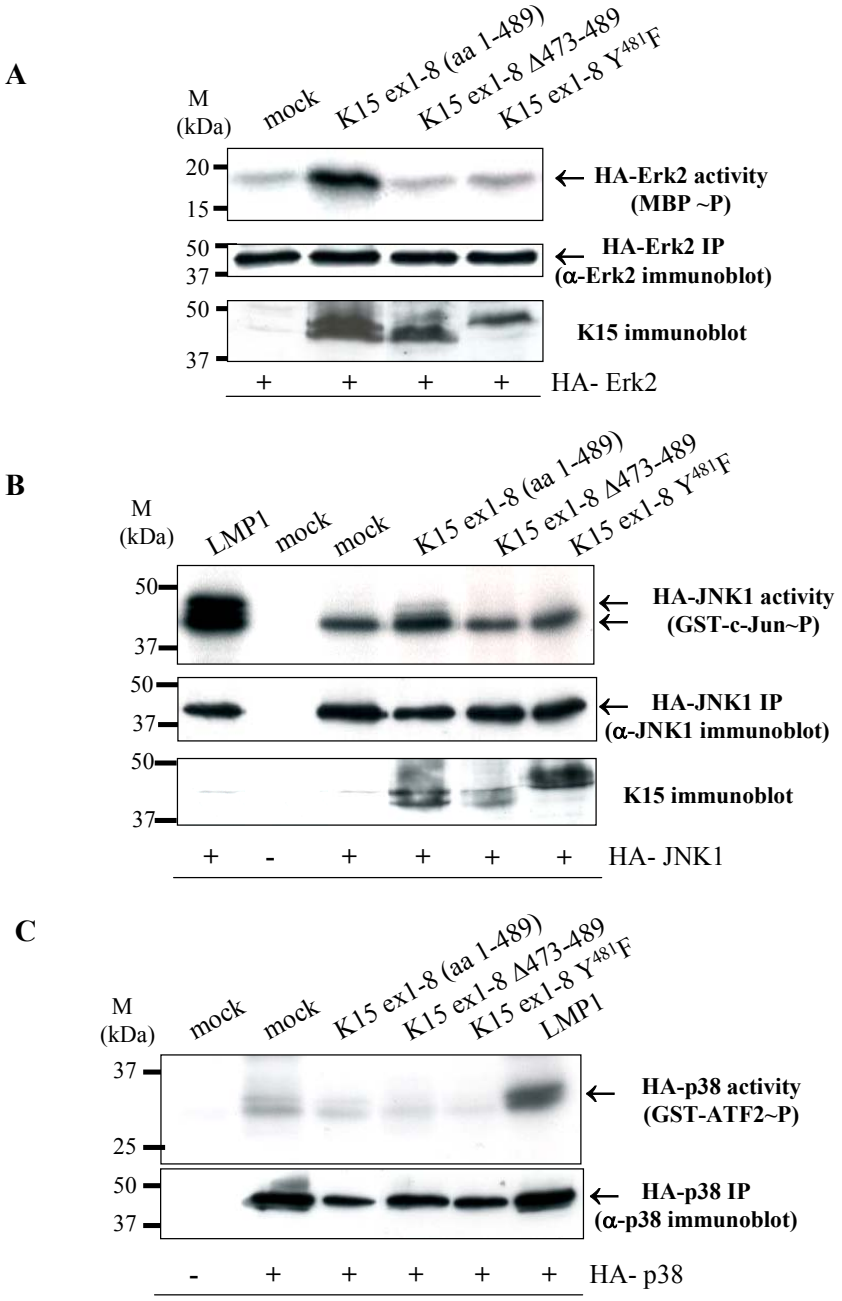

Figure 23: Immunocomplex kinase assays with MAP kinases Erk2, JNK1 and p38. 293-T cells were transiently co-transfected with 1 µg of the HA-tagged MAP kinases Erk2, JNK1 or p38, and 1 µg of the K15 or LMP1 expression constructs. After transfection, cells were grown in medium containing 1% FCS and lysed after 24 h in TBS-T buffer containing phosphatase inhibitors. The cell lysates were then subjected to an immunoprecipitation with HA-antibody 12C5 coupled to protein G beads overnight. Myelin basic protein (MBP), purified GST-c-Jun fusion protein (see 2.6.7) or GST-ATF2 served as substrates in the in vitro kinase reactions with Erk2 (A), JNK1 (B) or p38 (C), respectively. The immunoprecipitated kinase was incubated with its substrate and [γ-^{32}P] ATP for 30 min at 25°C in kinase reaction buffer and subsequently analysed by autoradiography (upper panel A, B, C). Western blots of the kinase reactions were probed with specific Erk2, JNK1 or p38 antibodies to assure equal expression levels of the MAP kinases (middle panel A, B, lower panel C). Cell lysates were analyzed for equal expression of K15 constructs by Western blot probed with a K15 antibody (lower panel A, B).

As depicted in figure 23 A, the 45 kDa K15 protein (K15 ex 1-8; aa 1-489) was able to induce the kinase activity of co-transfected hemagglutinin (HA)-tagged Erk2 kinase in transiently transfected 293-T cells as measured by phosphorylation of the myelin basic protein (MBP). In contrast to the strong activation of Erk2 kinase by K15 ex1-8, we only observed a weak activation of JNK1 in co-transfected 293-T cells (figure 23 B) as monitored by phosphorylation of the JNK1 substrate GST-c-jun. The activity of the p38 MAPK was not induced by K15, since phosphorylation of the GST-ATF2 protein by p38 was not increased when K15 ex1-8 was co-expressed compared to mock infected cells (figure 23 C, compare lanes 2 and 3). As expected, the positive control LMP1 induced the kinase activity of co-transfected HA-JNK1 and HA-p38 in 293-T cells (figure 23 B and C; Kieser et al., 1997, Schultheiss et al., 2001). Equal amounts of HA-tagged MAPKs Erk2, JNK1 and p38 being immunoprecipitated and used for the kinase assay reactions were confirmed by Western blot with antibodies to Erk2, JNK1 or p38 protein (figure 23 A-B, middle panels, C lower panel).

The activation of the Erk2 and JNK1 kinase activities in 293-T cells induced by the K15 protein depended on its intact cytoplasmic domain (figure 23 A, B), since no Erk2 or JNK1 activities were observed upon co-transfection with either the deletion construct K15 ex1-8 Δ473-489 or the point mutant K15 ex1-8 $Y^{481}F$. Cell lysates were also analysed for equal expression levels of K15 proteins by Western Blotting with K15 antiserum (figure 23 A, B lower panels, not shown for figure 23 C).

These findings demonstrate that the 45 kDa K15 protein specifically induced the MAP kinases Erk2 and JNK1, but not p38 (summarised in figure 36 in 4.1). Furthermore, phosphorylation of Y^{481}, presumably by members of the PTK family, seemed to be crucial for K15 signaling activity in these two MAPK pathways.

Dominant negative mutants of TRAF-2, Ras, Raf, Erk2 and MEK1/2-specific inhibitors PD98059 and UO126 reduce K15-induced activities of Erk2 and AP-1

We have shown that K15 bound TRAF-2 via aa 472-489 of its C-terminal domain (Brinkmann et al., 2003), and this region was shown to be crucial for induction of NF-κB and AP-1 activity by K15 (figures 21 A and 22 A). Therefore, it was elucidated whether a dominant negative TRAF-2 mutant could block K15-induced Erk2 and AP-1 activation. In order to further examine the downstream signaling routes linking K15 to Erk2, it was also tested if co-expression of dominant negative mutants of Ras (Ras N17), Raf or Erk2 could inhibit K15-induced Erk2 and AP-1 activation in immunocomplex kinase assays (figure 24 A) and luciferase-based AP-1 reporter experiments (figure 25). In addition, the effects of two chemical MEK1/2 specific inhibitors, PD98059 (Alessi et al., 1995, Dudley et al., 1995) and UO126 (Favata et al., 1998), were tested on K15 induction of Erk2 and AP-1 (figure 24 B). MEK1/2 is the upstream kinase which phosphorylates and thereby activates Erk1/2 (see figure 36 in 4.1).

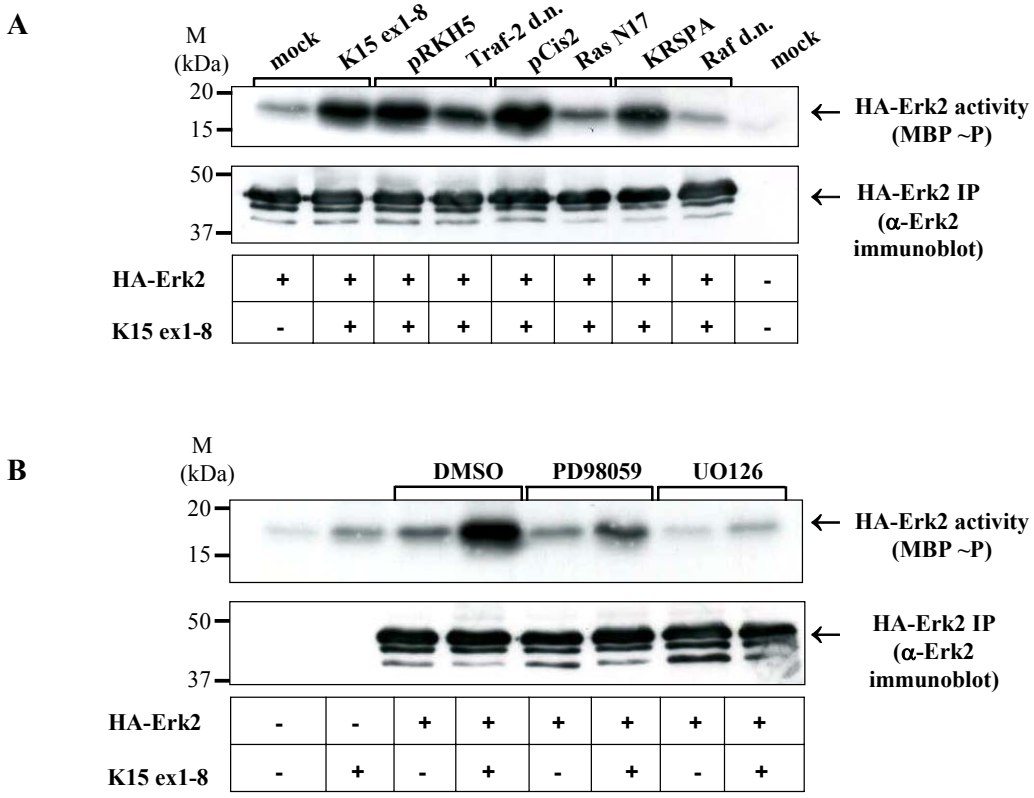

Figure 24: Dominant negative mutants of TRAF-2, Erk2, Raf and Ras and the MEK1/2 inhibitors UO126 and PD98059 reduce the Erk2 and AP1 activation induced by K15. (A) 700 ng of dominant negative mutants of TRAF-2, Ras, Raf or Erk2 or their respective empty expression vectors pRKH5, pCis2 or pKRSPA were co-transfected with 1 µg of HA-Erk2 and 1 µg of K15 ex1-8 (aa 1-489) or empty K15 expression vector (mock) where indicated. Erk2 kinase activity was monitored by phosphorylation of MBP (upper panel). The Western blot probed with anti-Erk2 antibody shows equal expression levels of the Erk2 kinase for all samples. (B) 293-T cells were co-transfected with 1 µg of HA-Erk2 and 1 µg of K15 ex1-8 (aa 1-489) expression construct or empty K15 expression vector. 14 h after transfection, DMSO alone or the MEK1/2 inhibitors PD98059 or UO126 were added to the medium at 50 µM from a 50 mM stock solution in DMSO. Cells were incubated for a further 8 hours before protein extraction. In vitro kinase assays were performed as described in Material and Methods (2.6.11). The Western blots were probed with anti-Erk2 antibody to show equal expression levels of the Erk2 kinase for all samples.

Transient co-expression of dominant negative TRAF-2 with HA-Erk2 and full length K15 reduced K15-induced Erk2 activity as shown by decreased phosphorylation of the Erk2 substrate MBP compared to co-expression with the empty TRAF-2 vector pRKH5 in 293-T cells (figure 24 A, compare lanes 3 and 4). An even more marked inhibition by dominant negative TRAF-2 was seen in the AP-1 luciferase based reporter assay (figure 25). In order to show the specificity for TRAF-2 and since TRAF-6 is involved in LMP1-induced activation of the p38 MAP kinase pathway (Schultheiss et al., 2001), the effect of a dominant negative TRAF-6 mutant on K15-induced AP-1 activation was also examined. The result in figure 25 shows that dominant negative TRAF-6 had no effect on AP-1 induction by K15 compared to co-transfected pcDNA3.1 vector. Dominant negative Ras (Ras N17) inhibited K15-induced Erk2 and AP-1 activation as shown in the immunocomplex kinase assay (figure 24 A,

compare lanes 5 and 6) and the reporter assay (figure 25) compared to the empty expression vector pCis2. The dominant negative Raf mutant reduced MBP phosphorylation by Erk2 in the immunocomplex kinase assay (figure 24 A, compare lanes 7 and 8), but showed only a moderate inhibition in the AP-1 reporter assay compared to the empty expression vector KRSPA (not shown). In the AP-1 reporter assay, the dominant negative Erk2 mutant (Erk C3, $Y^{185}\rightarrow F^{185}$) was able to inhibit AP-1 activation by K15 compared to KRSPA (figure 25).

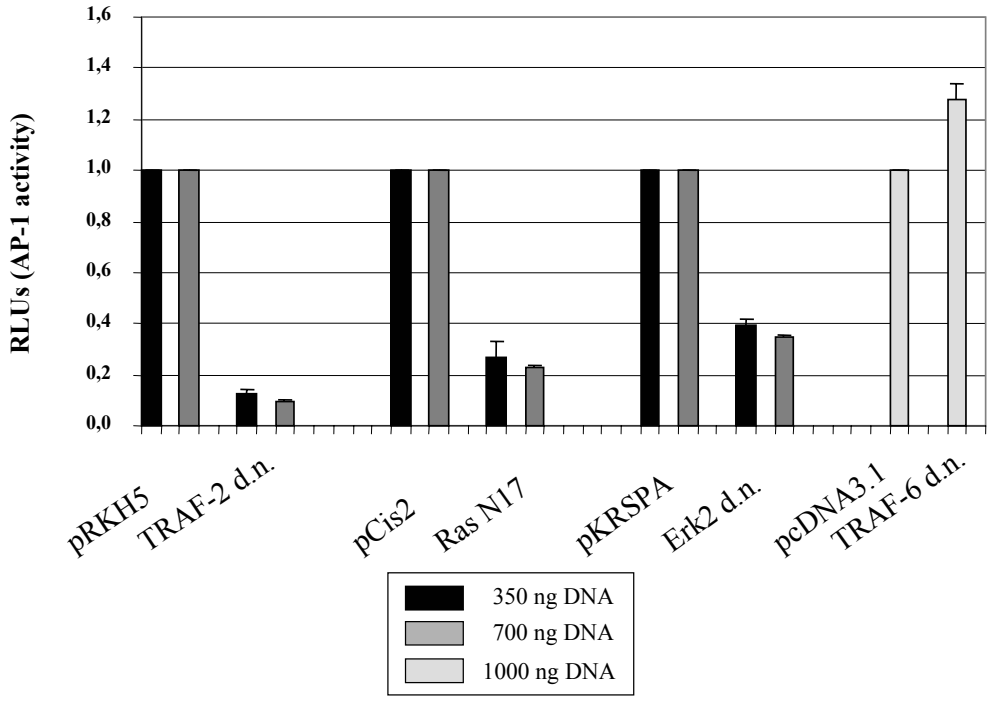

Figure 25: Dominant-negative TRAF-2, Ras and Erk2 mutants inhibit K15-induced AP-1 activity in an AP-1 luciferase-based reporter assay. 293-T cells were transiently co-transfected with 50 ng of the AP-1 reporter plasmid (pRTU14), 500 ng of the K15 ex1-8 (aa 1-489) expression construct and 350, 700 or 1000 ng of dominant negative mutants of Ras, TRAF-2, TRAF-6, Erk2 or their respective empty expression vectors pCis2, pRKH5, pcDNA3.1, pKRSPA. Shown are relative light units (RLU) with the luciferase values of the corresponding empty expression vectors of the different dominant negative mutants set at 1.

In addition to dominant negative mutants of the components of the Ras-Raf-MEK-Erk pathway, the two chemical inhibitors of MEK1/2, PD98059 and UO126, inhibited K15-induced Erk2 activity in an immunocomplex kinase assay (figure 24 B). Likewise, in the AP-1 reporter assay, both PD98059 and UO126 at 50 µM inhibited K15 induced AP-1 activity by approximately 50-60% (not shown). These results suggest that K15 activates the AP-1 transcription factor via the Ras-Erk pathway involving the components Ras, Raf, MEK, Erk2, and that TRAF-2 may be involved in linking this pathway to K15 phosphorylated on Y^{481} (summarised in figure 36 in 4.1).

3.2 Physiological (in vivo) expression of K15

KSHV shows a broad in vitro tropism: it has been shown to infect human B, endothelial, epithelial and fibroblast cells (see 1.1 and 1.2). In addition, KSHV infects a variety of animal cells, such as owl monkey kidney cells, baby hamster kidney fibroblast cells, Chinese hamster ovary cells, and primary embryonic mouse fibroblast cells (Akula et al., 2002, 2003, Bechtel et al., 2003, Dourmishev et al., 2003, Naranatt et al., 2003). In vivo, KSHV DNA and transcripts have been detected in human B-cells, macrophages, keratinocytes, endothelial cells, and epithelial cells (reviewed in Schulz 2001). Only a very small subset of KSHV genes is expressed during the latent viral life cycle, namely LANA-1 and LANA-2, kaposin, vFLIP and vcyclin (see figure 1 in 1.2). A variety of cell lines have been established from patients with primary effusion lymphoma (PEL) that are latently infected with EBV and KSHV or with KSHV alone (see 2.3.2 for references and details). In these cell lines, the lytic viral life cycle can be artificially induced by the addition of phorbol esters such as TPA or n-butyrate. Viral genes transcribed early after induction are referred to as immediate early/early lytic genes, followed by lytic genes and late genes (see figure 1 in 1.2). The viral glycoprotein K8.1 is such a late gene, and K8.1 protein can be detected 48-72 h after induction. During latent infection, PEL cells can also spontaneously undergo lytic replication (1-5% of the cell population, depending on the cell line).

Our group and others identified K15 transcripts in the latently infected PEL cell lines BCP-1 and BCBL-1, that are upregulated upon TPA treatment (Glenn et al., 1999, Choi et al., 2000a). This expression pattern indicates that K15 may be expressed during latency and during the lytic viral life cycle. However, the transcripts identified by RT-PCR in latently infected, non-induced cells, may be derived from the small subset of cells undergoing spontaneous lytic replication. We sought to identify the in vivo expression of K15 protein and analysed several PEL cell lines using the polyclonal antibody raised against the K15 C-terminus, and additionally generated a monoclonal antibody.

Epitope mapping of the monoclonal K15 antibody

The monoclonal K15 antibody, raised against the putatively cytoplasmic domain of K15 (aa 355-489), was generated as described in Material and Methods (2.3.8). The epitope in the K15 aa sequence recognized by this antibody was analysed with a peptide array (figure 26 A, see Material and Methods 2.6.6). The complete aa sequence of K15 (aa 1-489) was synthesized as peptides of 15 aa on a filter by Ronald Frank (GBF Braunschweig). Each peptide was shifted by three aa, resulting in a total of 159 K15 peptide spots on the filter. First, the filter was incubated with the secondary alkaline phosphatase conjugated antibody to measure the background reactivity (figure 26 A, upper panel). Subsequently, the filter was incubated with the K15 monoclonal antibody C12C4 as described in 2.6.6. As depicted in figure 26 A (lower

panel), this antibody strongly bound to three spots of the peptide array (spots 118, 119 and 120), and the aa sequence of K15 corresponding to these spots is depicted in the figure (23 A lower panel). Common to all spots was the aa sequence Y^{358}RQRRRRIY (underlined in figure 26).

This monoclonal antibody was further characterised by immunofluorescence on K15 ex1-8 transfected cos7 cells (data not shown) and by Western blotting (figure 26 B), and was found to be suitable for both applications. The monoclonal K15 antibody still recognized the shortest C-terminal GST-K15 (GST-$K15^{355-373}$, figure 26 B, left panel, see also figure 19) and LMP1-K15 deletion mutant (LMP1-$K15^{355-415}$, figure 26 B, right panel) by Western Blot analysis, which confirms the data obtained with the peptide array.

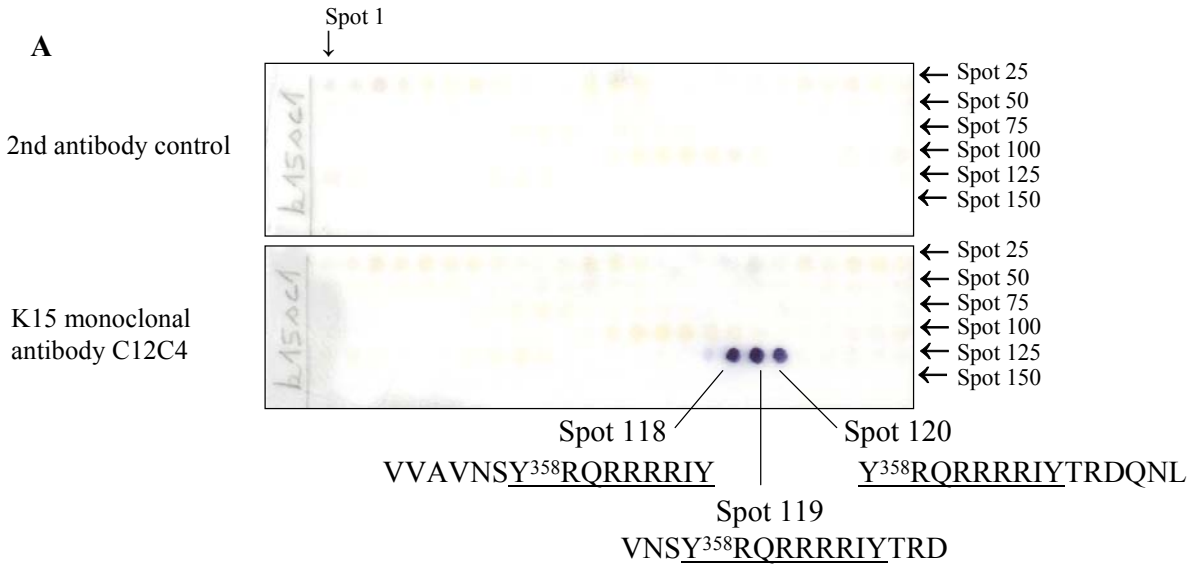

Figure 26: The K15 monoclonal antibody recognizes the epitope Y^{358}RQRRRRIY of the K15 C-terminal domain. The K15 monoclonal antibody C12C4 was generated as described in Material and Methods (2.3.8) and analysed by a peptide array (A) and by Western Blot (B). The epitope recognized by the antibody is localised to the beginning of the putative cytoplasmic domain of K15: the antibody detects the shortest C-terminal deletion constructs LMP1-$K15^{355-415}$ and GST-$K15^{355-373}$ in SDS-PAGE (B) and binds strongly to peptide spots 118, 119 and 120 of the peptidearray (A), which all contain the aa sequence Y^{358}RQRRRRIY.

A protein of 23 kDa was detected in PEL cell lines with a polyclonal K15 antibody

Various latently infected PEL cell lines (described in detail in Material and Methods, 2.3.2) were analysed by Western Blot for in vivo expression of K15 protein with K15 antibodies. Cells were either left untreated, or the viral lytic cycle was induced with TPA and cells were lysed 72 h after induction. In order to check whether the lytic cycle was successfully induced, the lysates were analysed for the expression of the late lytic K8.1 glycoprotein, which would only be expected to be expressed after TPA treatment. The B-cell line DG75, negative for both EBV and KSHV, served as a negative control. As shown in figure 27 (upper panel), a ~23 kDa protein was detected in PEL cell lines CroAP-5, CroAP-6, Jsc-1 and BCBL-1, that was absent in DG75 cells. In addition, a protein of ~40 kDa was detected in PEL cell lines CroAP-5, CroAP-6 and Jsc-1. However, this ~40 kDa protein was not reproducibly seen in PEL lysates, whereas the 23 kDa protein was always detected. Both proteins were present in unstimulated and TPA stimulated cells, suggesting that both protein forms may be expressed during the latent and lytic viral life cycle. Expression of the 23 kDa protein seemed to be slightly upregulated upon lytic cycle induction with TPA (figure 27 upper panel).

The same PEL cell lysates were analysed for protein expression of the late lytic glycoprotein K8.1 with a K8.1 monoclonal antibody (figure 27, lower panel). Multiple bands were detected by Western Blot with this antibody due to the heavy glycosylation of this protein. Weak K8.1 expression was found in non-induced Jsc-1, CroAP-6 and BCBL-1 cell lines, suggesting that a subset of the cell population undergoes spontaneous lytic replication (figure 27, lower panel). In non-induced CroAP-5 cells, K8.1 was not detected, indicating that this cell line is strictly latent. However, K8.1 expression was significantly upregulated in all four PEL cell lines treated with TPA, indicating that the lytic cycle was induced (figure 27, lower panel).

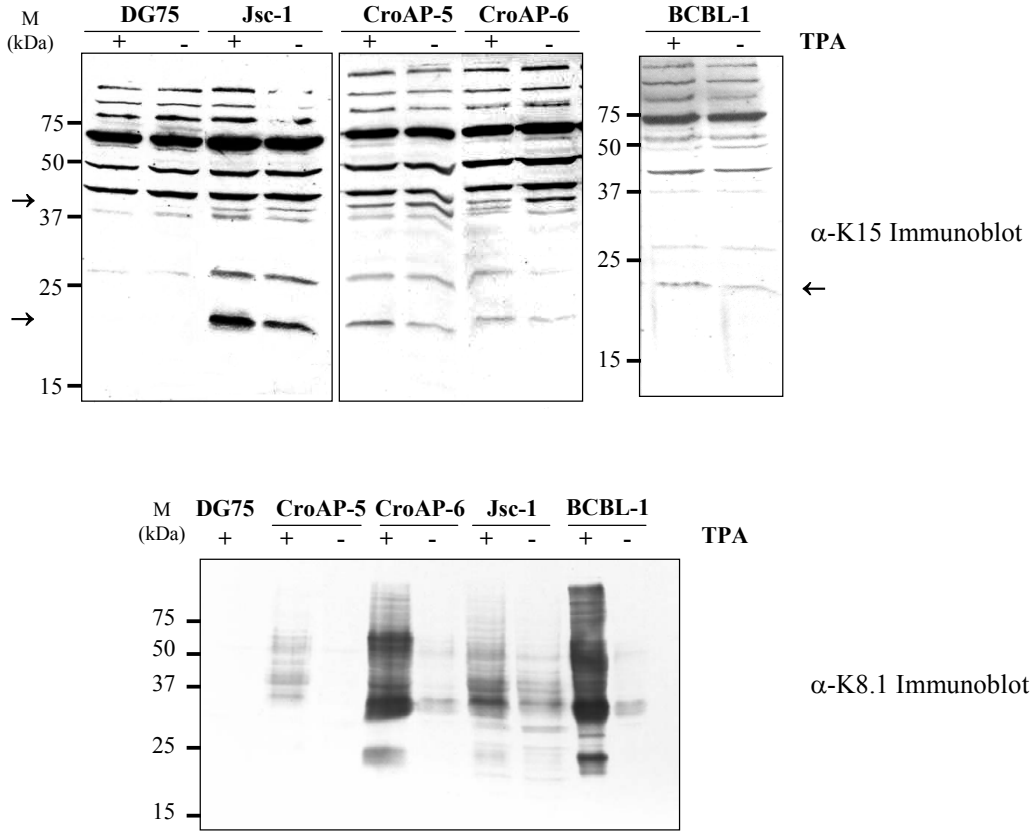

Figure 27: A protein of 23 kDa was detected in PEL cell lines with a polyclonal antibody to the K15 C-terminus. KSHV-infected PEL cell lines Jsc-1, CroAP-5, CroAP-6 and BCBL-1 were either treated with TPA for lytic cycle induction (+) or left untreated (-). 72 h after induction, cells were lysed in 1% NP40 lysis buffer (Material and Methods 2.6.1) and subjected to SDS-PAGE. Western Blots were probed with the polyclonal K15 antibody (upper panel) or a monoclonal K8.1 antibody (lower panel). The EBV and KSHV negative cell line DG75 served as a negative control.

Since the 23 kDa protein was most strongly expressed in Jsc-1 cells, we continued our analysis with this PEL cell line. Figure 28 B (upper panel) shows that the 23 kDa protein frequently detected in latently infected Jsc-1 cells corresponds in size to the 23 kDa K15 protein derived from the recombinant K15 expression construct that begins at the internal ATG codon in exon 6 (K15 ex6-8). The protein derived from the K15 ex6-8 construct is predicted to encode a protein with one putative transmembrane protein and was shown to be membrane associated (figure 11 B) but does not localise to lipid rafts (figure 12 B). Hence, Jsc-1 cell lysates were subjected to a subcellular fractionation assay as described in Material and Methods (2.6.9) in analogy to cos7 lysates transiently transfected with the K15 ex6-8 construct. Surprisingly, the 23 kDa protein from Jsc-1 lysates was not found to be membrane-associated as the marker protein calnexin, but localised to the soluble fraction (figure 28 A). The same result was obtained for the PEL cell line CroAP-5 (data not shown). Further, the monoclonal K15 antibody did not recognise the Jsc-1 23 kDa protein, whereas it detected the 23 kDa protein expressed from the K15 ex6-8 construct (data not shown).

Since the 23 kDa protein expressed in Jsc-1 cells seemed to be a soluble protein, we analysed whether this protein was encoded by the cytoplasmic domain of K15. Two possible scenarios could explain the origin of the soluble 23 kDa protein: (i) the Jsc-1 23 kDa protein may be derived from an additional splice event not identified so far, that splices directly in exon 8, or (ii) it could result from cleavage in the cytoplasmic domain of a precursor K15 protein. This would be reminiscent of the EBV LMP1 protein, which is cleaved in its cytoplasmic domain resulting in a 25 kDa protein (see 1.3.1.1).

Assuming that a K15 precursor protein would be cleaved at the junction between the last predicted transmembrane domain and the cytoplasmic domain, the resulting protein would be predicted to have a molecular weight of 15 kDa and to be a soluble protein. Since the predicted mass of a protein does not necessarily resemble its apparent mass in SDS-PAGE, we constructed an expression vector coding for the cytoplasmic domain of K15 (K15 ex8, aa 354-489). When the K15 ex8 construct was in vitro transcribed/translated and run in parallel to a Jsc-1 cell lysate and in vitro transcribed/translated K15 proteins expressed from constructs K15 ex6-8 or K15 ex7.2-8 (figure 28 B, lower panel), it clearly migrated at ~15 kDa and thereby faster than the Jsc-1 23 kDa protein. This would suggest that the 23 kDa protein detected with the K15 polyclonal antibody in Jsc-1 cell lysates was not derived by cleavage in the C-terminal domain of K15.

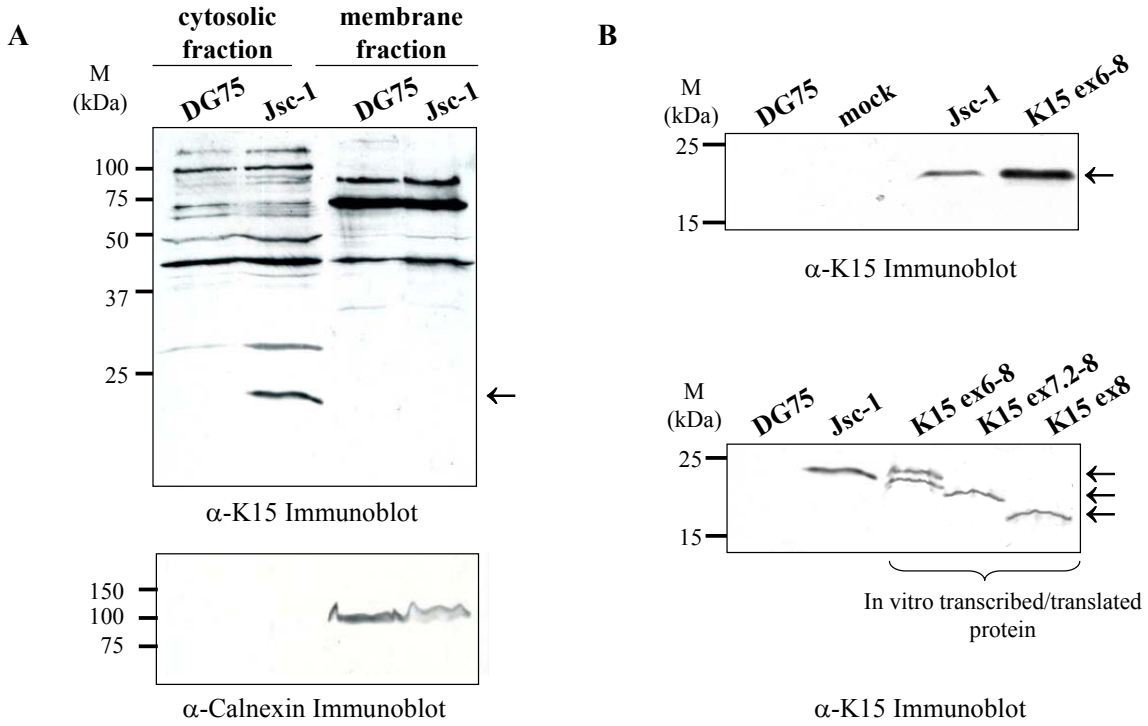

Figure 28: The 23 kDa protein expressed in PEL cell lines was not membrane associated. (A) The 23 kDa protein detected in lysates of latently KSHV-infected Jsc-1 cells did not pellet with cellular membranes (upper panel) as did the calnexin type I transmembrane protein (lower panel). (B) The 23 kDa protein in Jsc-1 cells corresponded in size to a K15 protein beginning at the in frame ATG in exon 6 (K15 ex6-8) transiently expressed in cos7 cells (upper panel). In vitro transcription/translation of K15 constructs K15 ex7.2-8 (beginning at the second in frame ATG in exon 7) and K15 ex8 (beginning at the epitope recognized by the K15 monoclonal antibody, see figure 26 A) showed that the derived proteins migrate faster than the 23 kDa protein of Jsc-1 cells.

Sharp et al. (2002) reported the detection of a ~23 kDa protein in latently infected Jsc-1 cells with a monoclonal K15 antibody. The authors showed that the expression of this Jsc-1 23 kDa protein decreased over time upon TPA induction. This contradicts our results, since we observed a slight upregulation of the 23 kDa protein expression after TPA treatment (figure 27, upper panel). When we examined Jsc-1 cells by immunofluorescence for expression of K15 protein, we obtained negative results with both our polyclonal and monoclonal K15 antibody (data not shown). Sharp et al. (2002) reported a cytoplasmic immunostaining pattern in the majority of Jsc-1 cells with their K15 monoclonal antibody, which would support the idea that the 23 kDa protein is not membrane-associated. The observation that the majority of Jsc-1 cells stained positive for K15 (Sharp et al., 2002) would also suggest that the 23 kDa protein was a truly latent protein, since if it was a lytic protein, it would be expected to be expressed in only a small subset of cells undergoing lytic replication. The observation by Sharp et al. (2002) that K15 is expressed during latency and decreasing upon TPA treatment contradicts data obtained by RT-PCR and viral gene expression arrays that showed low expression of K15 transcripts in latently infected BCP-1 cells and upregulation of expression upon lytic cycle induction (Glenn et al., 1999, Choi et al., 2000a, Paulose-Murphy et al. 2001, Nakamura et al. 2003).

Several K15 transcripts were detected in Jsc-1 cells by RT-PCR

In order to trace the origin of the 23 kDa protein expressed in PEL cell lines, which may originate from splice events that were not identified so far, we performed an RT-PCR on RNA extracted from uninduced Jsc-1 cells with a specific reverse primer annealing 233 bp downstream of the K15 stop codon in exon 8 (exon8arev, see table 2 in 2.2.4 and Material and Methods 2.5.4). The subsequent PCR was performed with primers beginning 25 bp upstream of the ATG in exon 1 (MBK15Bfor, table 2 in 2.2.4) and a reverse primer annealing 51 bp downstream of the stop codon in exon 8 (LRR6rev, table 2 in 2.2.4). The B-cell line Raji, EBV positive but negative for KSHV, served as a negative control. As shown in figure 29, three bands of ~2.2 kb, ~1.6 kb and ~1.4 kb and one weak band of ~1.0 kb could be detected after gel electrophoresis. Jsc-1 transcripts were excised from the gel and cloned into the pGEM-T vector and several clones were sequenced.

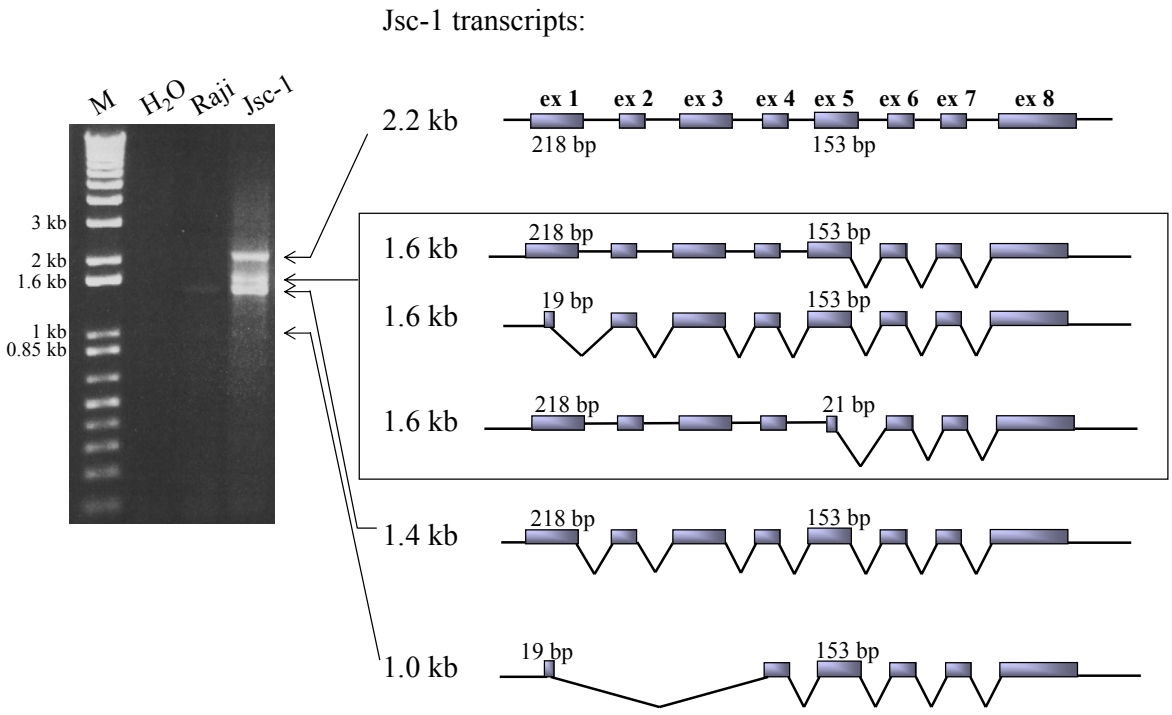

Figure 29: K15 transcripts identified by RT-PCR on Jsc-1 RNA. The reverse transcriptase reaction was performed with a gene specific primer annealing 233 bp downstream of the stop codon of ORF K15 (see text). The subsequent PCR with a K15 forward primer annealing 25 bp upstream of exon 1 and a K15 reverse primer binding 51 bp downstream of the K15 stop codon identified several transcripts with different splicing patterns (see text for details). kb = kilobases, M = 1kb ladder, bp = basepairs.

The ~2.2 kb Jsc-1 transcript corresponded to the genomic, non-spliced K15 ORF, while the 1.4 kb transcript corresponded to the fully spliced eight exon form (figure 29). An alignment with the BCBL-1 K15 sequence (NCBI accession #AAD45297) showed that the BCBL-1 and Jsc-1 ex1-8 sequences were 99% identical, with only three aa substitutions: one in exon 1 ($N^{9}\rightarrow D$), one in exon 3 ($V^{131}\rightarrow M$) and one in exon 5 ($F^{237}\rightarrow L$).

When we cloned the ~1.6 kb band in the expression vector pGEM-T and sequenced several clones, we obtained three different transcripts that are depicted in figure 29. One contained all eight exons but was not completely spliced. The second contained eight exons, was completely spliced, began at an alternative start codon in exon 1 and used a different splice donor in exon 1. The third transcript also contained all eight exons, but was not completely spliced and showed a deletion of 132 bp (44 aa) in exon 5, which did not alter the reading frame.

The 1.4 kb transcript corresponded to the K15 ex1-8 construct first identified in BCP-1 cells and found in this study to induce several signaling pathways. The 1.0 kb transcript began at an alternative start codon in exon 1 and used a different splice donor in exon 1, then spliced in exon 4 and completely spliced exons 5-8 (figure 29). This 1.0 kb transcript corresponded to the splice variant K15 ex1 as/4-8 that was identified in BCP-1 cells by Glenn et al. (1999), which was shown in this study to express proteins of 34 and 21 kDa (figure 10 D). However, none of the transcripts detected in Jsc-1 cells would be predicted to encode a protein with low hydrophobicity.

In summary, we could not clarify the origin of the 23 kDa protein that we detected by Western Blot with the polyclonal K15 antibody in Jsc-1 cell lysates. This suggests that this protein may be derived from a cellular or viral ORF other than K15, with which our polyclonal K15 antibody and the monoclonal K15 antibody from Sharp et al. (2002) do crossreact. The most prominent transcripts that were identified in Jsc-1 and BCP-1 cells encoded all eight exons and were fully spliced, which would suggest that a protein should be expressed from this transcript in KSHV infected B-cells. However, this protein may either be expressed at very low levels in vivo or has a short half life.

Analysis of K15 protein expression in epithelial cell lines T24, DU145 and Vero stably infected with recombinant KSHV

Since KSHV has also been shown to infect epithelial cells, we analysed three epithelial cell lines for K15 protein expression. Epithelial cell lines DU145 and T24 are stably infected with recombinant KSHV derived from virions of BCBL-1 cells (rKSHV.152) (figure 30 A; Vieira et al., 2001; for details see Material and Methods 2.3.2).

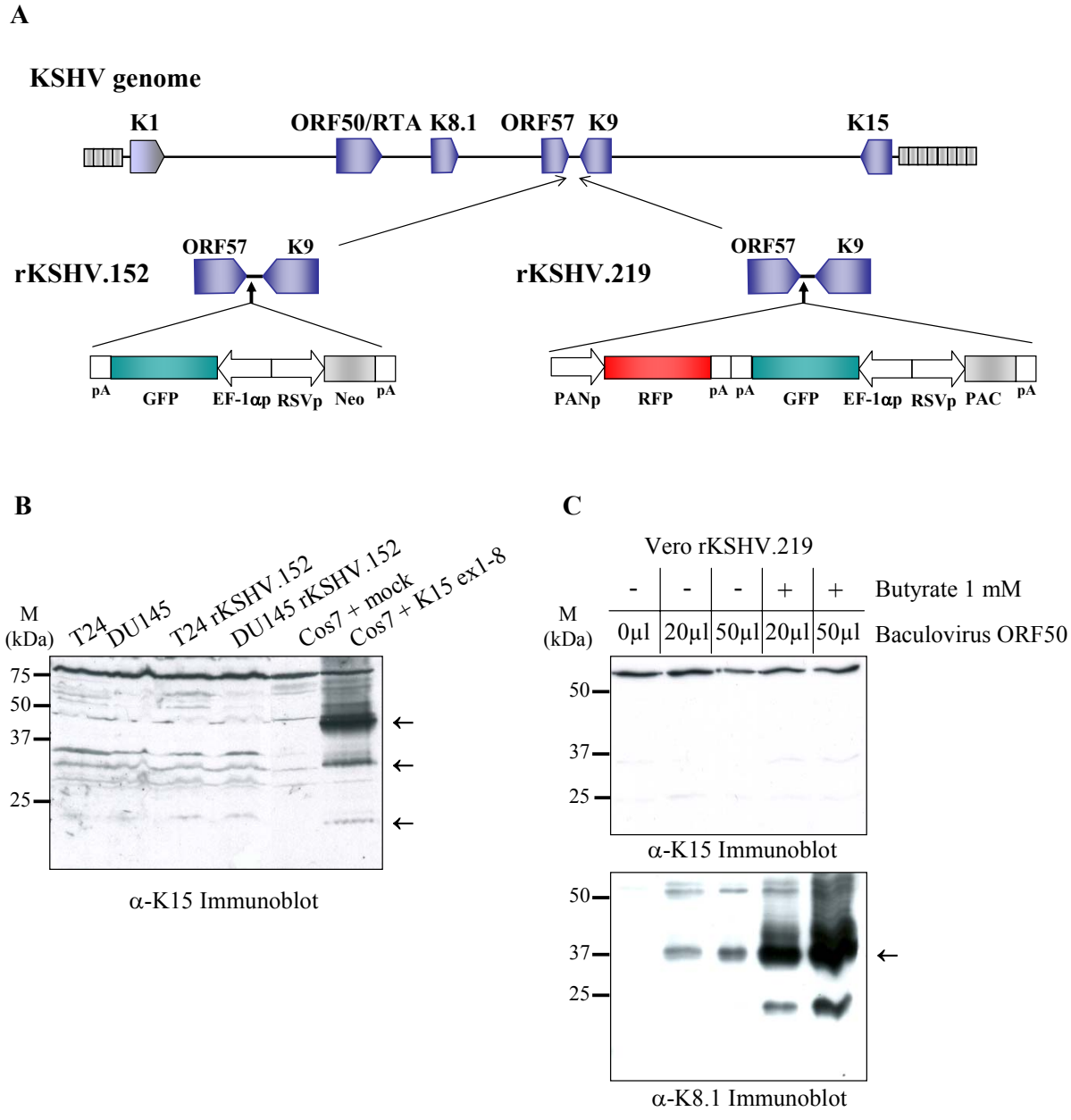

Figure 30: Analysis of in vivo K15 expression in epithelial cell lines stably infected with recombinant KSHV. (A) Epithelial cell lines T24 and DU145, stably infected with recombinant KSHV.152 (rKSHV.152), and Vero cells stably infected with rKSHV.219 were analysed by Western blotting for K15 expression. Both recombinant viruses carry a GFP cassette under control of the human EF-1 α promoter. Both cassettes are inserted between viral ORFs 57 and K9 of the KSHV genome and confer antibiotic resistance. The cassette of rKSHV.219 additionally contains the RFP gene under control of the lytic PAN (polyadenylated nuclear) RNA

promoter. (B) KSHV infection of cell lines T24 rKSHV.152 and DU145 rKSHV.152 is reported to be strictly latent (see text). Lysates of these two cell lines were analysed by Western blot with the polyclonal K15 antibody. Non-KSHV infected cell lines T24 and DU145 served as negative controls. (C) Vero cells stably infected with rKSHV.219 were either left untreated or were infected with different amounts of Baculovirus ORF50/RTA as indicated in the figure (0, 20 or 50 µl) and treated with n-butyrate (1 mM final concentration) to induce lytic viral gene expression. 48 h after induction, cells were lysed and analysed for K15 expression with K15 antiserum (upper panel) or expression of the late lytic viral glycoprotein K8.1 with a K8.1 antibody (lower panel).

Between the polyadenylation sites for ORFs 57 and K9 (figure 1 in 1.2 and figure 30 A) of rKSHV.152, a GFP/*neo* cassette is inserted, with the GFP gene being expressed from the human elongation factor 1-α promoter. The *neo* gene (RSV promoter) confers resistance to the antibiotic G418. Hence, cells stably infected with rKSHV.152 would express the GFP protein. The two cell lines DU145 rKSHV.152 and T24 rKSHV.152 were reported to be strictly latent and the lytic cycle could only be induced by a co-infection with the human cytomegalovirus (Vieira et al., 2001). Lysates of uninduced cell lines DU145 rKSHV.152 and T24 rKSHV.152 were analysed by Western blotting with the polyclonal K15 antibody, and non-infected T24 and DU145 cell lines served as negative control. As shown in figure 30 B, no protein bands were detected in lysates from DU145 rKSHV.152 or T24 rKSHV.152 that were absent in T24 and DU145. These results would suggest that in strictly latent KSHV positive epithelial cells, K15 protein is either not or very weakly expressed.

Since the lytic viral life cycle in cell lines DU145 rKSHV.152 and T24 rKSHV.152 can only be induced by infection with HCMV (Vieira et al., 2001), we did not analyse these cell lines for K15 expression during the lytic viral life cycle. Another epithelial cell line infected with recombinant KSHV, Vero rKSHV.219, became available to us to investigate K15 protein expression during the lytic viral life cycle. This cell line allows lytic cycle induction by phorbol esters and furthermore, the efficiency of lytic cycle induction can be easily monitored by expression of the RFP protein upon lytic cycle induction. The Vero rKSHV.219 cell line is stably infected with recombinant KSHV.219 (rKSHV.219) derived from KSHV produced by the PEL cell line Jsc-1. In rKSHV.219, a cassette is inserted between ORFs 57 and K9 that contains the red fluorescent protein (RFP) along with GFP (under control of the human elongation factor 1-α promoter) and the *pac* gene for resistance to puromycin (figure 30 A).

Besides TPA and n-butyrate, ectopic addition of an expression construct for the KSHV ORF50/RTA protein, which is the major lytic switch protein of KSHV, was shown to be sufficient to induce the lytic cyle of KSHV in several cell lines (see 1.2). Since the expression of RFP is under control of the viral lytic PAN (polyadenylated nuclear) promoter in rKSHV.219, and the PAN gene is a directly responding target for RTA (Wang et al., 2004 and references therein), the efficiency of lytic cycle induction could be monitored by the presence of GFP expressing cells that are also expressing RFP.

We achieved the most efficient induction of the lytic viral life cycle in Vero rKSHV.219 cells upon addition of 1 mM n-butyrate together with infecting the cells with a Baculovirus encoding the lytic switch protein ORF50/RTA (figure 31 A, see Material and Methods 2.3.5 and 2.3.6). Already 24 h post induction, approximately 30% of cells expressed RFP (figure 31 A upper panel). 48 h post induction, ~50% of cells were found positive for RFP expression (figure 31 A lower panel).

We analysed lysates of non-induced Vero rKSHV.219 cells and of cells that were treated with n-butyrate and additionally infected with the ORF50/RTA Baculovirus by Western blotting for K15 protein expression. As depicted in figure 30 C (upper panel), we did not detect K15 protein being expressed in neither uninduced nor induced Vero rKSHV.219 cells with the polyclonal or monoclonal K15 antibody. When the same lysates were analysed for expression of the late lytic viral glycoprotein K8.1 (figure 30 C lower panel), K8.1 was not expressed in non-induced Vero rKSHV.219 cells (lane 1), and K8.1 expression was efficiently induced by infection with Baculovirus ORF50/RTA alone (lanes 2 and 3) and significantly enhanced in the presence of n-butyrate and Baculovirus ORF50/RTA (lanes 4 and 5).

To summarise, K15 protein expression in vivo was not detected in three different epithelial cell lines being infected with recombinant KSHV, indicating that K15 is either not expressed in KSHV positive epithelial cells, or if expressed its expression is too low to be detected with the K15 antibodies. However, in ongoing experiments we detected a ~45 kDa protein in 293 cells stably infected with the KSHV genome cloned into a bacterial artificial chromosome (BAC) vector (data not shown). In this system (provided to us by Zhou et al., 2002), we detected K15 protein expression 15 h post induction with n-butyrate and Baculovirus ORF50/RTA. The K15 45 kDa protein was most strongly expressed at 2 days post induction, and expression decreased three days post induction (data not shown).

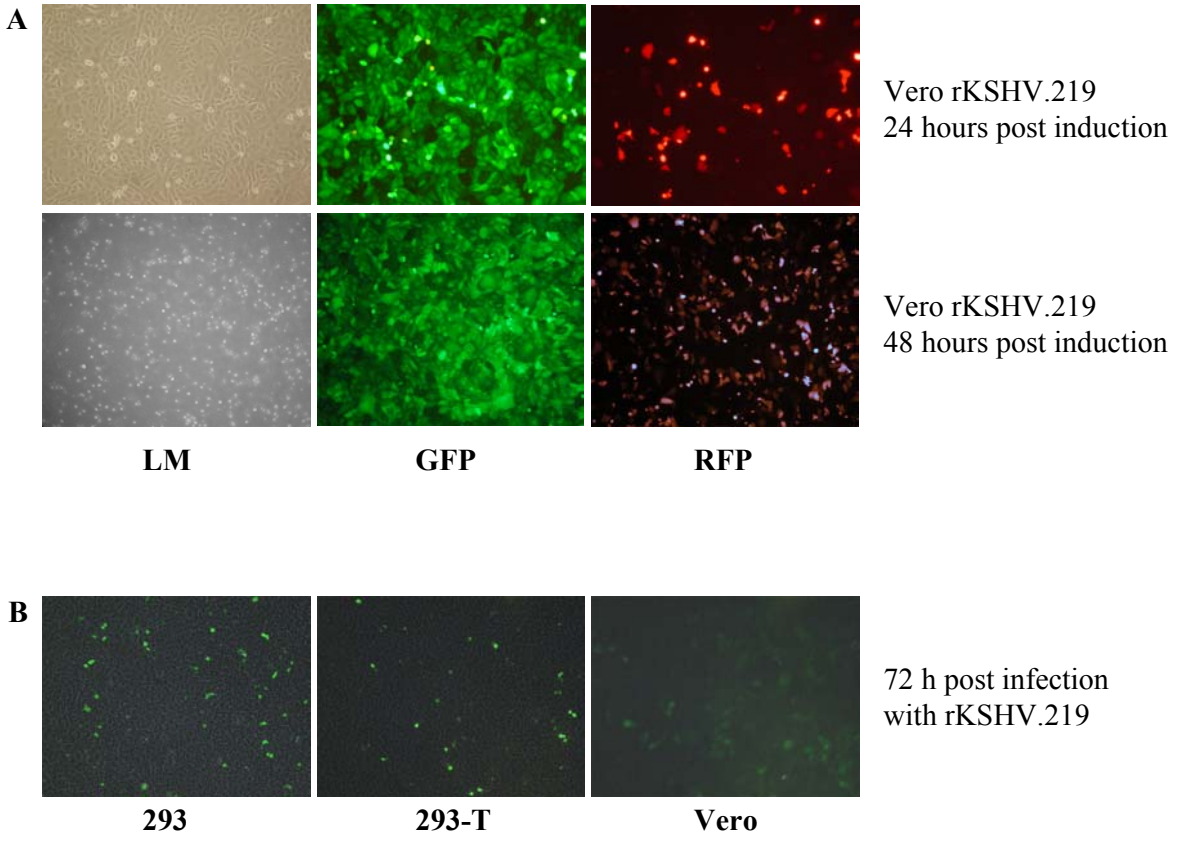

Figure 31: The lytic viral life cycle can be efficiently induced in Vero cells stably transfected with rKSHV.219. (A) Vero rKSHV.219, stably expressing GFP, were infected at 80% confluency with Baculovirus ORF50/RTA and treated with 1 mM n-butyrate to induce the viral lytic life cycle. RFP expression, under the control of the viral lytic PAN promoter (see text), was observed already at 24 h post induction (upper panel). 48 h post induction, more than 50% of Vero rKSHV.219 cells expressing GFP were positive for RFP expression, indicating lytic viral gene expression (lower panel). (B) rKSHV.219 was harvested 48 h post induction from Vero rKSHV.219 cells and added to 293, 293-T or Vero cells. KSHV-infection of these cell lines could be monitored and quantified by the appearance of GFP positive cells. One GFP positive cell was considered as one infectious unit, and infectious units per ml were determined at 72 h post infection for each cell line. LM = light microscopy.

K15 transcripts were identified in rKSHV.219 infected 293-T epithelial cells by RT-PCR

Another timepoint for K15 expression may be immediately after KSHV entry in the target cell. Therefore, we prepared rKSHV.219 from the cell line Vero rKSHV.219 to perform infection studies with rKSHV.219 (see 2.3.5 for details). The day after induction of the lytic cyle in Vero rKSHV.219 cells with n-butyrate and Baculovirus ORF50/RTA, the medium (containing n-butyrate and Baculovirus ORF50/RTA) was replaced. 24 h later, the medium was collected and filtered through a 0.45 µm filter (Material and Methods 2.3.5). The production of infectious rKSHV.219 from Vero rKSHV.219 cells was determined by titering the medium containing rKSHV.219 on epithelial cell lines 293, 293-T or Vero or B-cell lines BCBL-1, BJAB or Raji. The GFP gene carried by rKSHV.219 allowed the detection of rKSHV.219 infected cells, and infectious units could be determined by counting GFP

expressing cells three days post infection. GFP-expressing cells were first observed 48 h post infection in 293, 293-T and Vero cells, and the number of GFP positive cells further increased up to 72 h post infection in these cell lines (figure 31 B). The number of GFP-positive cells produced per ml of rKSHV.219 containing media was used as the number of infectious units (IU) of KSHV per ml. The infectivity of rKSHV.219 (infectious units per ml) was determined to be 2.8 x 10^5 IU/ml for 293 cells, 0.7 x 10^5 IU/ml for 293-T cells and 1.4 x 10^7 IU/ml for Vero cells at 72 h post infection (figure 31 B). We did not detect any GFP positive cells in the B-cell lines BCBL-1, BJAB and Raji infected with rKSHV.219 (data not shown).

In order to analyse rKSHV.219 infected cells for K15 expression, we infected 293-T cells with a rKSHV.219 stock diluted 1:2 in medium. 293-T cells were lysed 24, 48 and 72 h post infection for RNA preparation or Western blotting. As shown in figure 32 A for the timepoint 72 h post infection, 293-T cells infected with rKSHV.219 expressed GFP, indicating successful infection. The reverse transcriptase reaction was performed with a specific K15 reverse primer annealing 233 bp downstream of the ORF K15 stop codon (exon 8arev, table 2 in 2.2.4, see 2.5.4). For the subsequent PCR, a K15 forward primer annealing at the second in frame ATG in exon 7 (MBexon7.2for, table 2) and K15 reverse primer binding at the ORF K15 stop codon (FlagLAMPa3´, table 2) were employed. As a positive control for the PCR, a K15 ex1-8 plasmid (without introns) was used. With these primers, amplification of K15 cDNA and the K15 ex1-8 plasmid would result in a PCR product of 513 bp, whereas amplification of genomic DNA would give rise to a PCR product of 598 bp (intron length between exon 7 and 8 is 85 bp).

As shown in figure 32 B, a band of ~513 bp was detected by PCR on cDNA of 293-T cells at 24, 48 and 72 h post infection (lanes 4-6, indicated by an arrow), that was absent when the PCR was performed on cDNA of uninfected 293-T cells (lane 3). The 513 bp band was absent when the reverse transcription was not performed (-RT, lanes 7-10), showing the specificity of the 513 bp transcript.

When 293-T protein lysates collected at time points 24, 48 and 72 h post infection were analysed by Western blotting with K15 antibodies, no protein band was detected that was not present in uninfected 293-T cells (figure 32 C).

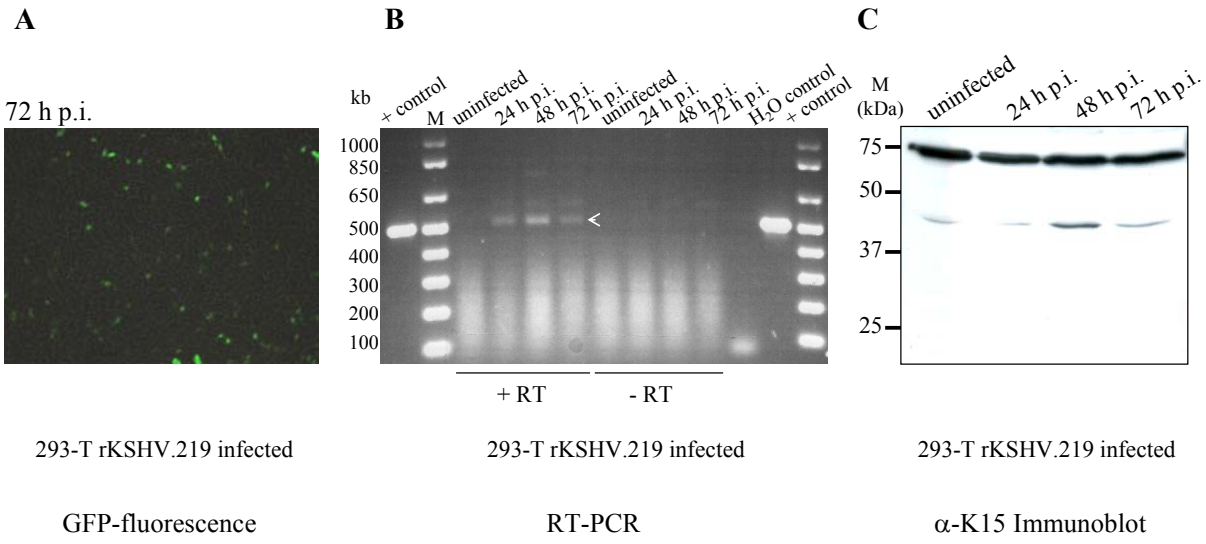

Figure 32: K15 transcripts but no protein expression were detected in 293-T cells at 24, 48 or 72 h post infection with rKSHV.219. 293-T cells were lysed at 24, 48 and 72 h post-infection with rKSHV.219 for analysis of protein expression and RNA preparation for RT-PCR. (A) Infection of 293-T cells with rKSHV.219 prepared from Vero rKSHV.219 cells was monitored by GFP expression 72 h post infection. (B) RNA was prepared from 293-T cells at timepoints 24, 48 and 72 h post infection with rKSHV.219 and used as a template for a reverse transcriptase reaction with a specific reverse primer annealing 233 bp downstream of the ORF K15 stop codon. Uninfected 293-T cells served as negative control. The subsequent PCR was carried out with a reverse primer annealing at the ORF K15 stop codon and a forward primer annealing at the second in frame ATG in exon 7. Plasmid DNA of K15 exon1-8 served as a positive control for the PCR reaction. A transcript of ~513 bp (indicated by an arrow) was detected in 293-T cells at 24, 48 and 72 h post infection, which was absent in uninfected 293-T cells and in the control reactions without RT (-RT). (C) 293-T cells were lysed in TBS-T buffer at timepoints 24, 48 and 72 h post-infection with rKSHV.219 and analysed for protein expression of K15 protein by Western blotting with the polyclonal K15 antibody. Uninfected 293-T cells served as a negative control. p.i. = post infection, M = marker (DNA 1 kb ladder), RT = reverse transcriptase.

3.3 K15: an effect on the viral lytic cycle?

It has been reported for viral terminal membrane proteins EBV LMP2A and KSHV K1 that they may exert an effect on the viral life cycle. LMP2A, which is expressed during latent infection in EBV infected B-cells, seems to have a role in the maintenance of viral latency in B-cells (see 1.3.1.2). This assumption is based upon the observation that in LCLs infected with EBV recombinants lacking LMP2A, BCR crosslinking leads to normal BCR signal transduction and activation of the lytic viral life cycle, whereas lytic infection is blocked in LCLs infected with wildtype EBV. The effect of K1 on viral replication is controversial (see 1.3.5). K1 expression by itself cannot initiate viral replication as the major lytic switch protein ORF50/RTA (Lagunoff et al., 1997), but two recent reports suggest that K1 may (i) augment KSHV reactivation from latency (Lagunoff et al., 2001) or (ii) play a role in maintaining viral latency (Lee et al., 2002). Lee et al. (2002) observed that the majority of KSHV genes was downregulated after induction of the viral lytic life cycle with TPA in the PEL cell line BCBL-1 stably transfected with K1.

Based on our results that K15 activates the AP-1 and NF-κB transcription factors, we analysed whether K15 has an effect on viral gene expression. The KSHV lytic switch protein ORF50/RTA, that is sufficient to activate the viral lytic programme of KSHV, shows several AP-1 binding sites in its promoter region as predicted by the Mat Inspector programme at http://transfac.gbf.de (figure 33, upper panel). We therefore cloned the 3085 bp ORF50 promoter region (figure 33, upper panel) in the promoter-less luciferase reporter plasmid pGL3basic (p3kbORF50P) and transfected it together with different amounts of the K15 ex1-8 expression construct (100, 250, 500, 1000 ng) in 293-T cells. As shown in figure 33 A, when 500 ng of the K15 ex1-8 expression construct were co-transfected with 50 ng of the reporter plasmid p3kbORF50P and cells were analysed for luciferase activity 40 h after transfection, the luciferase activity was enhanced ~4 fold compared to empty vector (mock) transfected cells. This would imply that full length K15 had a positive effect on the ORF50 promoter region.

One pathway via which K15 could activate the ORF50 promoter would be the Ras-Erk2 signaling cascade, which K15 has been shown to activate (see chapter 3.1). We therefore co-transfected 293-T cells with 500 ng of the K15 ex1-8 construct, 50 ng of p3kbORF50P and either 350 or 700 ng of dominant negative mutants of Ras, TRAF-2 or Erk2 or their respective empty expression vectors pCis2, pRKH5 or pKRSPA, and determined the luciferase activity 40 h after transfection. Figure 33 B shows the relative inhibition of K15-induced luciferase activity by dominant negative mutants Ras, TRAF-2 and Erk2. The luciferase activity of 293-T cell lysates transfected with the empty expression vectors of the dominant negative mutants was set at 1. Dominant negative mutants Ras and Erk2 significantly inhibited the effect of K15 on the ORF50 promoter region (Ras 350 ng by 92%, Ras 700 ng by 94%, Erk2 350 and 700 ng by 80%), whereas dominant negative TRAF-2 showed a less significant effect (350 ng

by 30%, 700 ng by 40%). This would suggest that K15 might activate expression of the viral ORF50/RTA gene via the MAPK pathway components Ras and Erk2, but further experiments are needed to underline this observation.

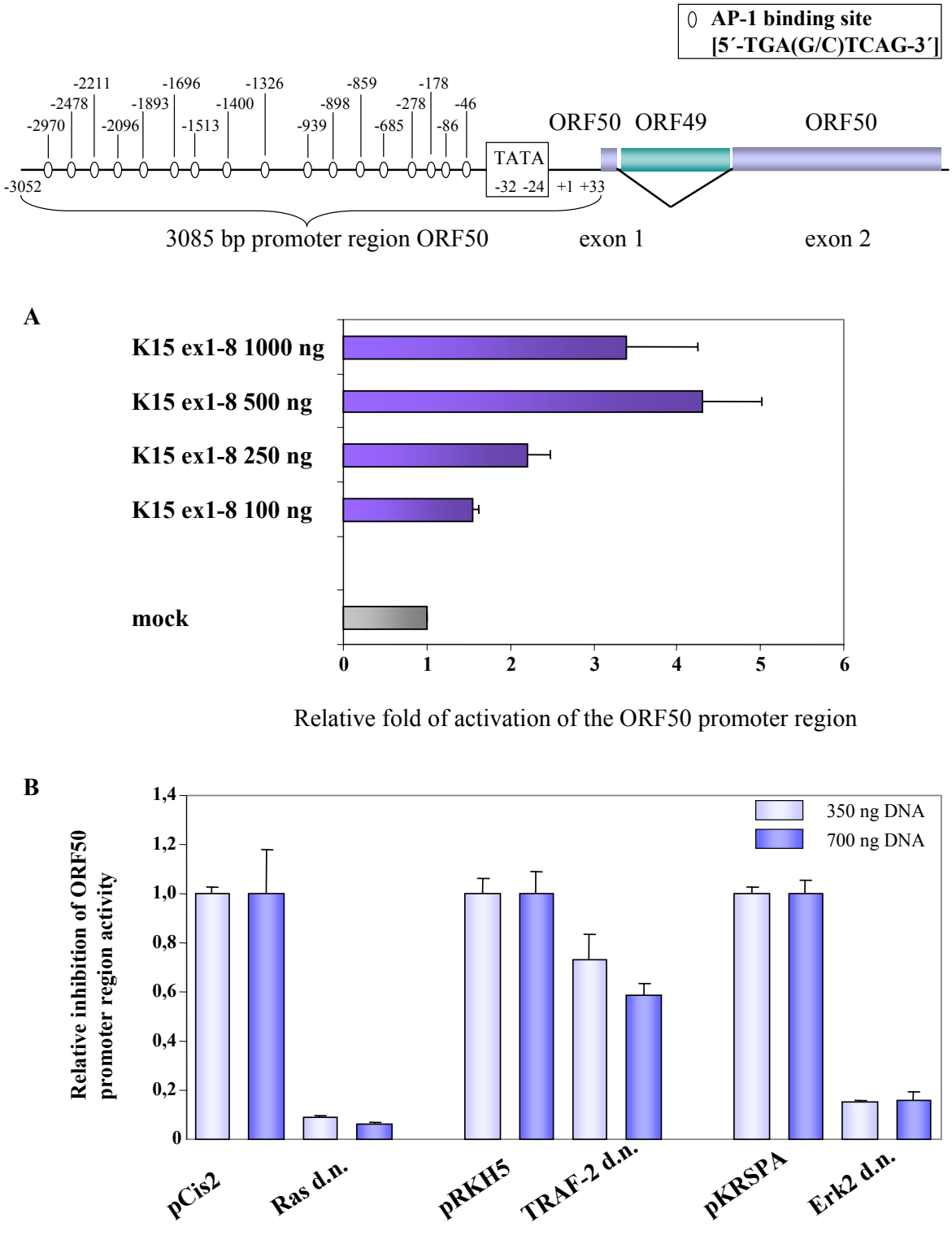

Figure 33: K15 activated a luciferase reporter plasmid containing the ORF50 promoter region. Dominant negative Ras and Erk2 inhibit K15-induced activation of the ORF50 reporter. A region of 3085 bp of the ORF50 promoter region was cloned upstream of a promoter-less luciferase reporter plasmid. The ORF50 promoter region contains several AP-1 binding sites (consensus 5´-TGA(G/C)TCAG-3´) as predicted by the Mat

Inspector programme at http://transfac.gbf.de. (A) 293-T cells were transiently transfected with different amounts of the K15 ex1-8 expression construct (100, 250, 500, 1000 ng) together with 50 ng of a reporter plasmid containing the 3085 bp ORF50 promoter region cloned upstream of the luciferase gene (p3kbORF50P). Cells were lysed 40 h after transfection and analysed for luciferase activity. Shown is the relative fold of activation compared to empty vector (mock) transfected (100, 250, 500, 1000 ng DNA) cells based on two independent experiments each of them performed in duplicate. (B) 293-T cells were transiently co-transfected with 50 ng of the ORF50 luciferase reporter plasmid p3kbORF50P, 500 ng of the K15 ex1-8 expression construct and 350 or 700 ng of dominant negative mutants of Ras, TRAF-2, Erk2 or their respective empty expression vectors pCis2, pRKH5, pKRSPA. Cells were lysed 40 h after transfection and analysed for luciferase activity. The relative fold of activation obtained with K15 ex1-8 co-transfected with the empty expression vectors pCis2, pRKH5 or pKRSPA was set at 1 and compared to the relative fold of activation obtained with K15 ex1-8 and dominant negative mutants of Ras, TRAF-2 and Erk2. Shown is one representative experiment based on duplicate samples.

Ectopic overexpression of the viral lytic switch protein ORF50/RTA induces viral reactivation in a variety of latently KSHV infected cell lines. The ORF50 gene is expressed early in lytic reactivation, and its expression can upregulate several promoters of lytic genes (Lukac et al., 1999). Since K15 had a positive effect on the ORF50 promoter, we asked whether K15 might be able to activate lytic viral gene expression by activating expression of RTA. To address this question, we transfected the Vero rKSHV.219 cell line that is stably infected with recombinant KSHV.219 (see figure 30 A) with the K15 ex1-8 expression construct or empty vector (mock). In addition, Vero rKSHV.219 cells were transfected with an expression construct for the Flag-tagged RTA protein. Induction of the lytic viral life cycle can be monitored by RFP expression in rKSHV.219 infected cells (see figure 31 A).

As depicted in figure 34 C, RFP expressing cells could be observed 48 h after transfection when RTA was transiently expressed in the cell line Vero rKSHV.219. Hence, ectopic expression of the Flag-RTA expression construct lead to the induction of the lytic cycle of rKSHV.219, as has been shown in chapter 3.2 with Baculovirus ORF50/RTA (figure 31 A). As expected, upon transfection with an empty expression vector (mock), no RFP positive cells were observed (figure 34 A). Transient expression of K15 ex1-8 in Vero rKSHV.219 cells did not result in the expression of RFP, indicating that K15 did not induce the lytic viral life cyle in this cell system (figure 34 B). Western blot analysis with a Flag antibody or K15 antiserum showed that both RTA and K15 ex1-8 were expressed in transiently transfected Vero rKSHV.219 cells (not shown).

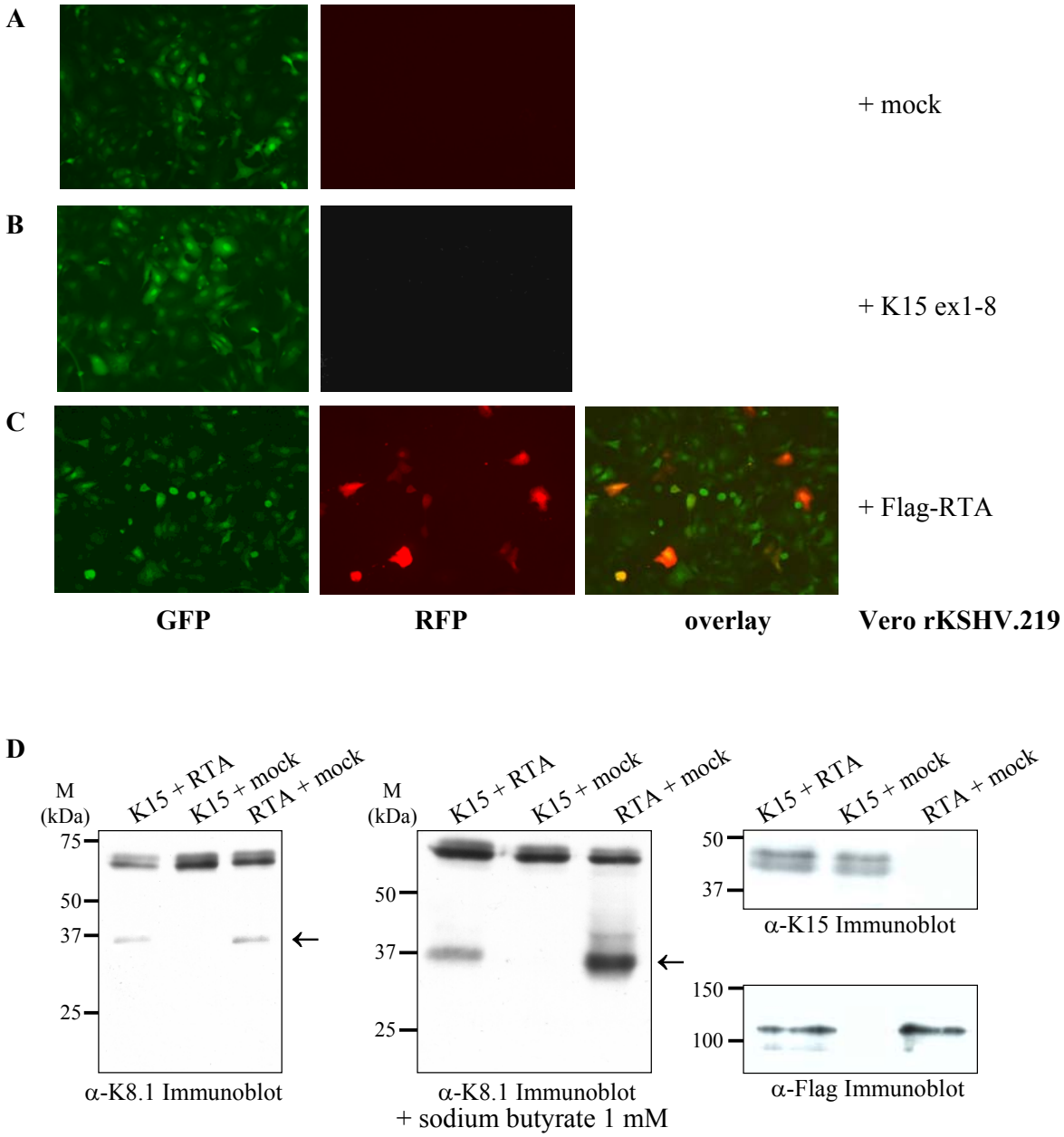

Figure 34: Ectopic expression of K15 ex1-8 in Vero rKSHV.219 cells did not induce viral lytic replication as did ectopic expression of the lytic switch protein RTA. As illustrated in figure 30, Vero cells stably and latently infected with rKSHV.219 express the GFP protein, whereas RFP protein is only expressed in cells undergoing lytic viral replication. Vero rKSHV.219 cells were transiently transfected with 1 µg of either empty expression vector (mock) (A), K15 ex1-8 (B) or Flag-tagged RTA (C) and analysed for RFP expression up to 48 h after transfection. While RTA expression resulted in lytic viral gene expression as judged by the appearance of RFP expressing cells (C), no cells positive for RFP expression were observed in K15 ex1-8 expressing cells (B) as well as for mock transfected cells (A). (D) Vero rKSHV.219 cells, either treated with 1 mM n-butyrate (middle panel) or left untreated (left panel) were co-transfected with expression constructs for K15 ex1-8 and RTA, K15 ex1-8 and mock or RTA and mock. 48 h post transfection, cells were lysed and analysed for expression of the late lytic protein K8.1 with a specific K8.1 antibody (left and middle panel), K15 and RTA expression (right panel).

These results show that ectopic expression of K15 ex1-8 in the epithelial cell line Vero rKSHV.219 did not result in the induction of the viral lytic life cycle as ectopic expression of Flag-RTA under the conditions we used. Hence, K15 was not able to initiate viral lytic replication on its own in Vero rKSHV.219 cells. However, this does not rule out that K15 may augment lytic replication by activating ORF50/RTA expression in cells that already undergo lytic gene expression due to RTA expression or treatment with n-butyrate.

We therefore transfected Vero rKSHV.219 cells with the K15 ex1-8 expression construct alone or together with the RTA expression construct in duplicate and either treated cells with 1 mM n-butyrate to induce the lytic viral life cycle or left cells untreated. Cells were lysed 48 h after transfection/induction and analysed by Western blot for expression of the late lytic KSHV protein K8.1. As depicted in figure 34 D, the K8.1 protein was not expressed in cells that were transfected with K15 ex1-8 alone in the absence (left panel, lane 2) or presence (middle panel, lane 2) of n-butyrate, which confirmed our results shown in figure 34 B. As expected, K8.1 protein was expressed in Vero rKSHV.219 cells transiently transfected with Flag-RTA that were not treated with n-butyrate (figure 34 D left panel, lane 3), and K8.1 expression was further increased in the presence of Flag-RTA and n-butyrate (figure 34 D middle panel, lane 3). In Vero rKSHV.219 cells that were co-transfected with Flag-RTA and K15 ex1-8, we did not see a significant difference in the level of K8.1 expression compared to Vero rKSHV.219 cells transfected with RTA alone (figure 31 D left and middle panels lane 1). Expression of transiently expressed K15 ex1-8 and Flag-RTA was detected with K15 antiserum or a Flag antibody (figure 34 D, right panels).

The fact that we did not see an effect of transiently expressed K15 on the lytic viral life cycle in the Vero rKSHV.219 cell line does however not rule out that K15 has the ability to activate the lytic viral life cycle. The activation of the ORF50 promoter by K15 in 293-T luciferase reporter assays may not represent the in vivo situation as such that the ORF50 promoter is methylated in vivo, and other co-factors might be needed to allow K15 to exert its effect on viral gene expression that are not given in the system we employed.

4 Discussion

4.1 K15 signaling

We have shown that the major isoform of K15-derived proteins, containing all 8 exons and presumably 489 amino acids, activated the Ras-Raf-MEK1/2-Erk2 MAPK pathway as well as the NF-κB pathway and the MAP kinase JNK1 (summarised in figure 36). Activation of these pathways depended on Y^{481} in a carboxyterminal Y^{481}EEV motif that is reminiscent of the Y^{112}EEA motif of EBV LMP2A. In B-cells, Y^{112} of LMP2A is phosphorylated by the Src kinases Lyn and Fyn and important for the recruitment of these kinases. We could show that several members of the Src kinase family of PTKs, including Src, Fyn, Yes, Hck and Lck, bound to the K15 C-terminus and phosphorylated Y^{481} of K15 in vitro (figures 19 and 20). When phosphorylated, the Y^{481}EEV motif would be an optimal SH2-binding site for members of the Src kinase family of PTKs (table 3). The ability of K15 to bind to Src kinase family members of PTKs and to be phosphorylated by those kinases is reminiscent not only of the LMP2A protein, but also of HVS terminal membrane proteins StpA, StpB and Tip, KSHV K1 and the HVA Tio protein (see table 1; Lee et al., 1997, Choi et al., 2000b, Albrecht et al., 1999, Biesinger et al., 1995, Lee et al., 1998b).

Sequences located between aa 355 and 373 at the membrane proximal region of the cytoplasmic domain of K15 appear to contribute to the interaction of Src family PTKs with K15, since a GST-K15 fusion protein containing this region still bound to all the Src kinases tested (figure 19). The two tyrosine motifs in this region, Y^{358}RQR and Y^{366}TRD, are not reminiscent of SH2-B motifs, but the fact that the K15-M variant contains a similar tyrosine motif at the equivalent position (Y^{371}TPH, see figure 18) points to a functional role of the Y^{366}TRD motif of K15-P. Point mutations in this motif would be required to further address its role in PTK interaction. Hypothesising that the interaction of K15 with PTKs is crucial for downstream signaling, a full length K15 ex1-8 construct carrying point mutations in the Y^{366}TRD motif should be analysed for its ability to activate NF-κB and the MAPKs Erk2 and JNK1.

A $Y^{481} \rightarrow F^{481}$ mutant abolished the ability of the full length K15 protein to activate the Ras-Erk2 pathway, as well as JNK1 and NF-κB (figures 21, 22, 23), indicating that phosphorylation of Y^{481}, presumably by members of the Src kinase family of PTKs, represents a first step in the activation of these pathways. Results by Choi et al. (2000a) underline the importance of the the phosphorylation of K15. They found that the K15 C-terminus, when fused to the CD8 receptor, was constitutively phosphorylated at Y^{481} in B-cells (see 1.3.6), although the kinases involved were not identified. When phosphorylated, the Y^{481}EEV motif was predicted to be an optimal binding site for SH2 domain containing proteins such as the FGFR, Src family PTKs and the adapter protein Nck (see table 3), or it

may be a docking site for other not yet identified cellular proteins, which may be crucial for mediating K15 downstream signaling events.

The K15 transmembrane domains appeared to be important for the ability of K15-derived proteins to initiate different signaling pathways, since only the longest isoform K15 ex1-8, containing up to 12 putative transmembrane domains (figures 9 and 18) was capable of initiating efficient signaling (figures 21 and 22). LMP1 induces the NF-κB and AP-1 transcription factors (see 1.3.1.1, figures 21, 22), but the LMP1-K15 chimera, composed of the six transmembrane domains of LMP1 fused to the K15 cytoplasmic domain, was not able to induce activation of an AP-1 reporter (figure 22), and only showed a moderate activation of an NF-κB reporter when compared to the K15 ex1-8 isoform (figure 21).

The six transmembrane domains of LMP1 mediate efficient clustering of LMP1 in the cell membrane, which is a prerequisite for constitutive intracellular signaling of this viral oncoprotein (see 1.3.1.1). A chimeric protein composed of six transmembrane domains of LMP2A follwed by the LMP1 cytoplasmic domain is not able to activate NF-κB (Kayakas et al., 2002), which illustrates that the LMP1 transmembrane domains are not simple membrane anchors, but are crucial for efficient signaling of the LMP1 molecule. This suggests that, concerning the LMP1-K15 chimera, the six LMP1 transmembrane domains might either not allow correct insertion in the membrane that positions the K15 C-terminal domain in a manner that allows efficient signaling, or the LMP1 transmembrane domains might lack motifs that are crucial for the interaction of K15 with cellular proteins. Therefore, the K15 transmembrane domains seem to play a crucial role in efficient K15 signal transduction.

Choi et al. (2000a) found that a CD8-K15 chimeric protein could inhibit B-cell receptor initiated signaling in the B-cell line BJAB, but was unable to initiate Ca^{++} mobilization after cross-linking with an antibody to CD8. Although we did not examine Ca^{++} mobilization as a consequence of K15-initiated signaling, we think that it is possible that the CD8-K15 chimeric protein used by Choi et al. (2000a) may have been unable to trigger Ca^{++} mobilization due to the absence of the K15 transmembrane domains. Chimeric proteins composed of CD8 fused to the cytoplasmic domains of K1 or R1 are both able to elicit intracellular Ca^{++} mobilisation as well as cellular tyrosine phosphorylation upon treatment with an antibody to CD8 (Lee et al., 1998b, Damania et al., 2000a). An explanation could be that these chimeras more likely reflect the natural situation, since K1 and R1 both contain one transmembrane domain as the CD8 receptor, and not 12 transmembrane domains as K15.

Another study identified Hax-1 as an interaction partner of K15 (Sharp et al., 2002, see 1.3.6), but the role of this interaction is not clear. Interestingly, Hax-1 was first identified as a protein that associates with hemopoietic specific protein 1 (Hs1) (Suzuki et al., 1997), which is thought to play a role in signal transduction in B-cells. Upon BCR crosslinking, Hs1 is one

of the earliest proteins to be tyrosine phosphorylated by Syk and Lyn (Ruzzene et al., 1996). Following phosphorylation, Hs1 translocates to the nucleus and induces apoptosis (Yamanashi et al., 1997). However, whether K15 has a role in BCR signal transduction, which involves the Ras/MAPK pathway, is not clear, but it would be reminiscent of the EBV LMP2A protein, which is known to inhibit BCR signal transduction in EBV infected LCLs (see 1.3.1.2), or the Tip protein that may mediate TCR downregulation (Park et al., 2003), as well as K1 that downregulates BCR surface expression (Lee et al., 2000). Furthermore, cellular effector molecules such as the adapter protein Nck and the serine/threonine kinase PKC, which play a role in BCR signal transduction, were identified as putative interaction partners of K15 (see table 3), but whether K15 interacts with Nck via its Y^{481}EEV motif or is phosphorylated by PKC at T^{404} as predicted has not been addressed in this study.

Lipid rafts serve as signaling platforms in cellular membranes that can incorporate and recruit membrane-associated molecules required for the assembly of signaling cascades (reviewed in Simons & Toomre 2000). We therefore examined whether the longest K15 isoform (which is capable of inducing intracellular signaling) differed from the smaller isoforms and the LMP1-K15 chimera (which are not capable of inducing intracellular signaling) with respect to their incorporation into lipid rafts. We found that at least the isoform K15 ex1/6-8, which contains the complete first exon, appeared to be incorporated into lipid rafts to roughly the same extent as the longest K15 isoform (figure 13 A). Therefore, sequences encoded by K15 exons 2-5 may contribute to intracellular signaling by providing sites for post-translational modification, by interacting with other intracellular components or be crucial for correct membrane insertion.

The LMP1-K15 chimeric protein was incorporated into lipid rafts (figure 13 D) as was described for wildtype LMP1 (see 1.3.1.1), indicating that incorporation into lipid rafts was not responsible for the fact that the LMP1-K15 chimera differed in the ability to initiate intracellular signaling compared to the K15 ex1-8 isoform. The notion that lipid raft association is not sufficient for efficient signaling is further supported by data obtained by Kaykas et al. (2001). When they targeted the LMP1 C-terminal domain to lipid rafts by tagging it with the 10 aa myristoylation sequence from the Yes Src family PTK, this molecule activated NF-κB less efficiently than full length LMP1.

In contrast to the K15 ex1-8 and K15 ex1/6-8 isoforms, the 34 and 26 kDa proteins derived from splice variants K15 ex1 as/6-8 and K15 ex1 as/4-8, which show an alternative start codon and splice donor in exon 1 and therefore contain only 6 amino acids derived from the first exon in a different reading frame (figure 5), were not incorporated into lipid rafts (figure 13 B and C). This might point to an important role of exon 1 for lipid raft targeting. As shown in table 3, the K15-P variant contains four potential caveolin-binding sites (exon 1: F^{6}FWNLWLW, exon 3: W^{148}IFFPISF, exon 6: F^{227}LWCLYVW, W^{279}CLYVWQSF; Couet et al., 1997). Splice variants K15 ex1 as/4-8 and K15 ex1 as/6-8 lack the potential caveolin-1-

binding site in exon 1 due to the use of a different reading frame in exon 1 (M^1ALGPT^6 compared to M^1KTLIF^{6}FWNLWLW……PSSWHLGII^{72} for K15 ex1-8 and K15 ex1/6-8). Further, the protein derived from the recombinant K15 ex6-8 construct, which lacks the putative caveolin-binding sites in exon 1, 3 and 6, did not localise to lipid rafts as well. Notably, the K15-M variant also contains a potential caveolin-binding site in exon 1 (Y^3KKYLWGTW). Analysis of the cellular localisation of the protein derived from the K15 transcript identified by RT-PCR in Jsc-1 cells encoding the alternative 6 aa in exon 1 followed by exons 2-8 (figure 29) might reveal whether the caveolin-binding motif in exon 1 plays a role in lipid raft targeting.

Caveolin-1 is a major component of caveolae, which appear as rounded plasma membrane invaginations of 50-80 nm in diameter. The lipid composition of caveolae corresponds to that of lipid rafts, i.e. caveolae are rich in cholesterol and sphingolipids (reviewed in Simons & Toomre 2000, Brown & London 1998). Caveolae seem to be used by cells to internalize membrane components that are enriched in rafts. In Ptk2 cells transiently expressing full length K15 and GFP-tagged Caveolin-1, we did not observe co-localisation of these two proteins by immunofluorescence microscopy (figure 17 I). This may have several reasons: (i) K15 expression in co-transfected cells was very low, and only very few cells were found positive for expression of both proteins. (ii) The GFP protein fused to Caveolin-1 may influence the intercation between the two proteins. To overcome these limitations, the subcellular localisation could be determined with an antibody to endogenous Caveolin-1. However, in order to further address the possible interaction of K15 with Caveolin-1, co-immunoprecipitation experiments will be performed.

The LMP1 transmembrane domains, as well as those of LMP2A, do not show a region reminiscent of a putative caveolin-binding site. Both, LMP1 and LMP2A, have been shown to be palmitoylated, but palmitoylation was not crucial for lipid raft localisation of LMP1 and LMP2A or signaling activity of LMP1 (Higuchi et al., 2001). It has been shown that the first two transmembrane domains of LMP1 are sufficient for lipid raft association, but they do support NF-κB signaling less potently compared to wildtype LMP1 (Coffin et al., 2003). Gurezka et al. (1999) have found that proteins with clusters within their membrane spanning domains similar to the sequence LLXXLLXLLXXLLXL can self assemble and identified LMP1 to have this "leucine" pattern. Substitutions of leucines in the LMP1 leucine-motif yields a derivative which forms multimeres as wildtype LMP1, but cannot activate the NF-κB transcription factor (Kaykas et al., 2002). This provides further evidence for the crucial role of transmembrane domains in signaling. However, K15 does not show such a leucine motif as LMP1 in its transmembrane domains.

However, our immunofluorescence microscopy studies with the LMP1-K15 chimera showed a distribution pattern different from wildtype LMP1 (compare figures 15 A and C).

Whereas LMP1 showed a punctate expression pattern distributed over the entire cell, similar to K15 ex1-8 (figure 14 A), the LMP1-K15 chimera partially formed distinct patches in the plasma membrane similar to Caveolin-1-GFP (figure 14 C), localised to the ER and a perinuclear region. The patches in the plasma membrane observed with LMP1-K15 and Caveolin-1 are reminiscent of clustered lipid rafts. Lipid rafts can be visualised with fluorescently labeled cholera toxin B subunit, that binds glycosphingolipids, which then is cross-linked into distinct patches with anti-cholera toxin B subunit antibody (Janes et al., 1999). With this method we will further address the subcellular localisation of LMP1, LMP1-K15 and K15 ex1-8 by immunofluorescence microscopy.

Coffin et al. (2003) further showed that LMP1 chimeric proteins composed of either the first and second or the fifth and sixth transmembrane domain fused to the cytoplasmic domain were not able to bind to TRAFs. TRAFs are crucial effectors molecules for LMP1 signaling (see figure 35). We have shown binding of TRAFs -1, -2 and -3 to the C-terminal domain of K15 fused to the six transmembrane domains of LMP1 (Brinkmann et al., 2003), but have not proven yet whether K15 ex1-8 and K15 splice variants interacted with TRAFs. If the K15 splice variants were not able to interact with TRAFs, this may in part explain their impaired signaling capabilities. However, since the LMP1-K15 chimera was impaired in signaling compared to full length K15 (figures 21 and 22). TRAF binding seems not to be the only factor critical for efficient signaling. One interesting aspect for future experiments would be to identify further interaction partners of K15, with focus on its membrane domains or loop regions. Since K15 localises to lipid rafts, co-immunoprecipitations could be performed from lipid raft fractions containing the K15 ex1-8 protein. LMP1 expression for example results in the recruitment of TRAF-3 to lipid rafts, but not of TRAF-1 and -2 (Higuchi et al., 2001, Kaykas et al., 2001).

When fused to the cytoplasmic domain of the CD40 receptor, the N-terminus and six transmembrane domains of LMP1 could mediate constitutive signaling of this chimeric protein in the absence of CD40 ligand (Floettmann & Rowe 1997, Gires et al., 1997, Hatzivassiliou et al., 1998). Interestingly, constitutive signaling of the KSHV K1 protein is attributed to its extracellular domain, since this domain can mediate constitutive signaling when transferred to other cytoplasmic domains containing an ITAM motif (Lagunoff et al., 1999). It would be of interest whether the K15 transmembrane domains would also be able to mediate constitutive signaling when fused to cytoplasmic domains involved in signaling, as for example to that of the CD40 receptor which induces NF-κB and binds TRAFs (see 1.3.1.1).

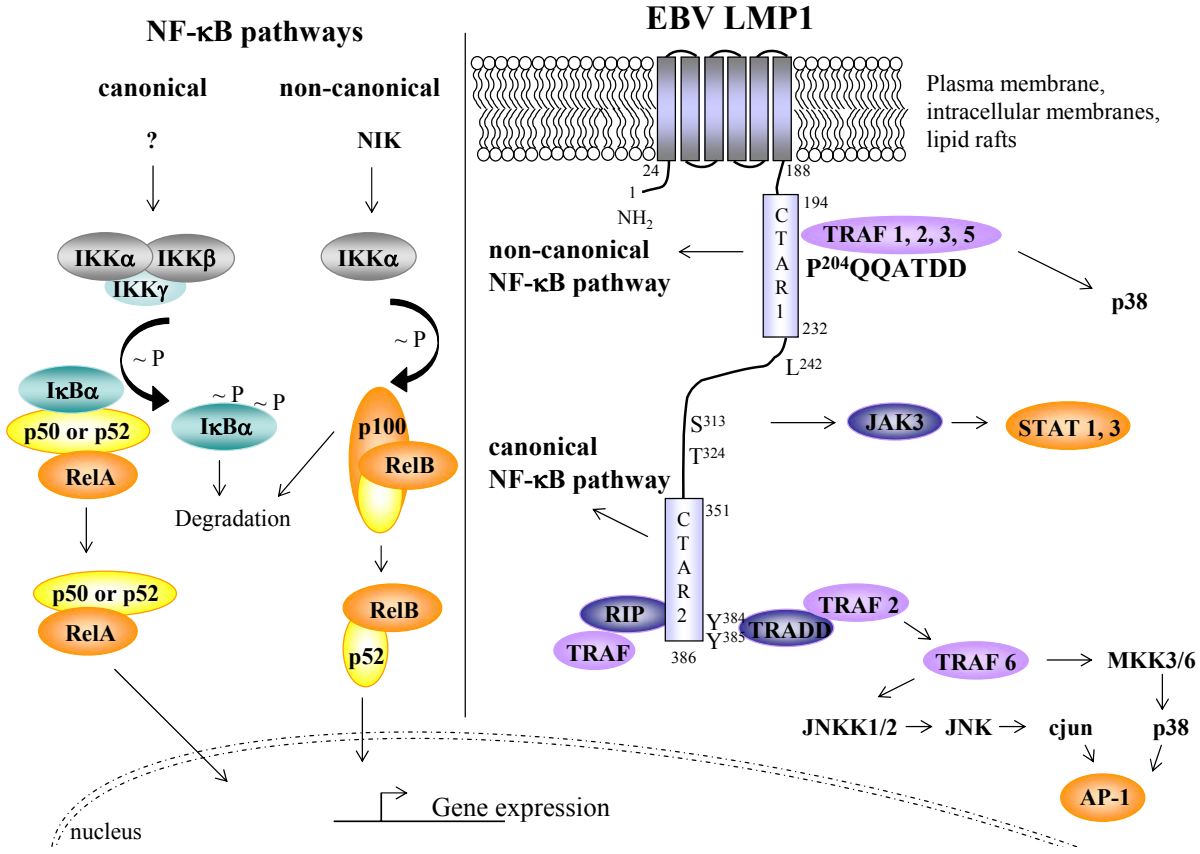

Figure 35: LMP1 signal transduction. The EBV LMP1 oncoprotein activates the NF-κB transcription factor via the canonical and non-canonical pathway. In addition, LMP1 activates the AP-1 transcription factor via MAPKs JNK1 and p38. TRADD and TRAFs are key effectors and mediators of LMP1 signaling. For details see 1.3.1.1.

Is there a functional role for the smaller K15 isoforms? The study by Choi et al. (2000a) suggests that a signaling-inactive K15 variant could inhibit intracellular signaling pathways. It is therefore conceivable that the smaller K15 isoforms may play a role in modulating the effect of the 8-exon isoform on the activation of the pathways reported here. This would represent a parallel to the presumed role of the LMP2 splice variant LMP2B, which is devoid of the amino-terminal intracellular domain of LMP2A, but could modify LMP2A-induced signaling by affecting the clustering of LMP2A molecules in the cell membrane (see 1.3.1.2). Another parallel comes from studies with lytic LMP1, which is expressed during the late lytic viral life cycle. Lytic LMP1 encodes the C-terminal 258 aa of LMP1 and thus is comprised of TMs 5 and 6 and the cytoplasmic domain (Hudson et al., 1985). This lytic form of LMP1, as well as an LMP1 mutant lacking the N-terminal 25 aa (Rothenberger et al., 2002, Brennan et al., 2001), have a dominant negative effect on full length LMP1 signaling. Lytic LMP1, which neither binds TRAFs nor shows signaling activity (Baichwal & Sugden 1989, Erickson & Martin 2000, Huen et al., 1995, Mitchell & Sugden 1995, Wang et al. 1988a, b), inhibits NF-κB and JNK1 signaling by full length LMP1 when the two isoforms are coexpressed (Erickson & Martin 1997, 2000).

Lytic LMP1 protein does not form patches as full length LMP1, but shows a diffuse staining pattern and localises to intracellular membranes in B-cells, and does not localise to lipid rafts (Wang et al., 1988a, b, Higuchi et al., 2001). This is reminiscent of splice variant K15 ex1 as/4-8 (figure 16 A), which showed an immunostaining very different from splice variant K15 ex1/6-8 (figure 16 E) or full length K15 ex1-8 (figure 14 A). We are currently collecting reagents to perform co-localisation studies to further elucidate the subcellular localisation of splice variant K15 ex1 as/4-8. Interestingly, lytic LMP1 was reported to localise to extracellular EBV virions (Erickson & Martin 1997), and also in intracellular enveloped virions (Vazirabadi et al., 2003) which would suggest a possible role in virus assembly. So far, we have not systematically analysed KSHV virions for the presence of K15 protein.

RT-PCR studies on PEL cell lines (Glenn et al., 1999, Choi et al., 2000a) suggest that the transcript encoding the longest K15 isoform is more strongly expressed than those for the smaller isoforms. This is confirmed by our RT-PCR experiments on the Jsc-1 cell line (figure 29), although we also found abundant incompletely spliced transcripts whose translation and functional importance (if any) remains to be studied. A recent report (Sharp et al., 2002) attributed the presence of an approximately 23 kDa K15-derived protein in PEL cell lines to internal proteolytic processing of the ~45 kDa (exon 1-8) K15 precursor protein (see 1.3.6). We have seen proteins of a similar size in PEL cells which were not associated with cellular membranes in contrast to the 21 kDa proteins translated from splice variants K15 ex1 as/4-8 and K15 ex1 as/6-8, that have been shown to associate with lipid rafts (figure 13 B and C). Whether the balance in virus-infected cells is therefore in favour of the 45 kDa ‘activating’ K15 protein, or in favour of the smaller ‘non-activating’ forms, is currently unclear and may be difficult to predict from the relative abundance of individual transcripts.

We have shown in this study that the full length K15 isoform, K15 ex1-8, activates the AP-1 transcription factor via the classical Ras-Raf-MEK-Erk pathway, via the MAPK JNK1 but not via MAPK p38 (summarised in figure 36). In this respect, K15 resembles LMP2A which has recently been reported to activate Erk2 and JNK1, but not p38, when stably expressed in 293 cells (Chen et al., 2002), although others have not seen an activation of Ras/MAPK by LMP2A in epithelial cells (Scholle et al., 2000). We have clearly shown that K15 induces the activity of the MAPK Erk2 via Ras, Raf-1 and MEK1/2 by using dominant negative mutants and chemical inhibitors, and that TRAF-2 seems to play a role possibly by linking K15 signaling to the Ras-Raf-MEK1/2 cascade. It has not been shown yet which cellular effector molecules link LMP2A signaling to Erk2.

One effect of stably expressed LMP2A in 293 cells was increased stability of c-jun (Chen et al., 2002). We found a moderately increased JNK1 activity following transfection of K15 in in vitro kinase assays (figure 23), but have not investigated whether K15 expression resulted in increased c-jun stability in vivo. It remains a possibility that the activation of the JNK1 pathway by K15 occurs indirectly, perhaps as a consequence of the activation of other

pathways, such as Ras/MAPK. Our preliminary studies on cDNA arrays also indicate that the expression of c-jun might be increased at the transcriptional level following K15 transfection (not shown). There may therefore be multiple routes for LMP2A and K15 to increase the activity of the JNK/c-jun pathway, which would contribute to the increased activity of the AP-1 transcription factor following K15 expression, as reported here. Gene array studies of different LMP2A expressing cell systems indicate that LMP2A has multiple effects on global cellular gene expression (Portis et al., 2003, Portis & Longnecker 2003). K15 gene arrays are planned.

It is a contentious issue whether LMP1 activates the MAPK Erk1/2. One group found that LMP1 activated Erk1/2 by Ras in Rat-1 fibroblasts, and a dominant negative Ras mutant was able to impair the ability of LMP1 to induce transformation (Roberts & Cooper 1998). However, Erk2 activation by LMP1 in 293 epithelial cells was not observed by us (not shown) and others (Kieser et al., 1997). The Herpesvirus saimiri oncoprotein StpC directly interacts with cellular Ras and activates the Ras signaling pathway, which seems to be an important factor for the oncogenecity of the StpC protein (Jung & Desrosiers 1994, 1995, Guo et al., 1998). Furthermore, the K1 protein was shown to activate the AP-1 transcription factor via Ras (Lagunoff et al., 2001).

Since the two KSHV terminal membrane proteins K1 and K15 are both expressed during the lytic viral life cycle at the transcript level, we wondered whether these two viral proteins would co-localise. Initial experiments with Ptk2 cells transiently expressing K1 and K15 showed significant co-localisation (figure 17 C). This is reminiscent of the EBV LMP1 and LMP2A (but not LMP2B) proteins that co-localise in latently EBV infected B lymphocytes (Longnecker et al., 1991, Longnecker & Kieff 1990). Interestingly, LMP2A (but not LMP2B) seems to augment signaling of LMP1 by prolonging its half-life (Dawson et al., 2001). However, the co-localisation studies with K1 and K15 need to be extended to cell types more relevant for KSHV, as for example human epithelial cells, B-cells or endothelial cells.

K15 shares several features with the LMP1 protein regarding its signaling activity (see figures 35 and 36). The NF-κB transcription factor plays a key role in the oncogenic potential of LMP1, and is activated by LMP1 via the canonical and, as recently described, the non-canonical pathway (see 1.3.1.1 and figure 35). We have shown that K15 was an inducer of the NF-κB pathway, less potent than LMP1, but have not yet analysed the pathway K15 uses to activate NF-κB. Viral TMPs K1 (KSHV), Tip (HVS), and StpC (HVS) have also been shown to activate NF-κB in some cell systems (see table 1 and figure 6). As mentioned in 1.3.1.1, the activation of the NF-κB transcription factor does not seem to be the only factor crucial for the transforming activities of the LMP1 oncoprotein. TRAF-2, which plays a major role in LMP1 signaling to NF-κB, was also shown to be the key mediator of LMP1 signaling to the MAPKs

p38 and JNK1 together with TRAF-1 and TRAF-6 (Kaye et al., 1996, Eliopoulos & Young 1998, Kieser et al., 1999).

Our results suggest an involvement of TRAF-2 in the K15-induced activation of the Ras/MAPK pathway, since a dominant negative TRAF-2 mutant inhibited the activity of Erk2 and AP-1 in K15-transfected cells (figures 24 and 25). We observed weak binding of TRAF-2 to the cytoplasmic domain of K15, which was abolished by deleting the last 17 aa including the Y^{481}EEV motif, as well as the sequence ATQPTDD which appears distantly related to the TRAF binding consensus site PxQxS/T (residues identical with the CTAR1 of LMP1 are underlined) (Brinkmann et al., 2003, see figure 36). Interaction of K15 with TRAF-1 and -3 seems to occur through a more membrane-proximal region of K15 (Brinkmann et al., 2003, see figure 36). LMP1 binds TRAF-2 indirectly via its CTAR-2 region, most probably via the TRADD protein (figure 35), and it is possible that the interaction of the K15 cytoplasmic domain with TRAF-2 occurs in an indirect manner. Experiments with a dominant negative TRAF-2 mutant have shown that TRAF-2 is involved in NF-κB signaling of the StpC protein in Rat-1 fibroblasts (Lee et al., 1999). Interestingly, despite being capable of binding to TRAFs, the StpA and StpB proteins of HVS strain A and B are not activating NF-κB (Lee et al., 1999, Choi et al., 2000b), which may explain their reduced oncogenic potential compared to StpC.

As depicted in figure 35, the effect on the MAPKs p38 and JNK1 by LMP1 also involves TRAF-6 downstream of TRAF-2 (Schultheiss et al., 1999), and TRAF-6 has recently been shown to be involved in the IL-1 induced activation of p38/MAPK via Ras (McDermott & O´Neill 2002) and in the CD40-induced activation of Erk via a Ras-independent pathway (Kashiwada et al., 1998). However, K15-induced AP-1 activity was not affected by co-expressing a dominant-negative TRAF-6 mutant (figure 25), suggesting that other cellular factors may link the cytoplasmic domain of K15, phosphorylated on Y^{481}, to the activation of the Ras/MAPK pathway. This issue, and the identity of cellular and viral genes affected by K15-induced Ras/MAPK activation, is currently under investigation.

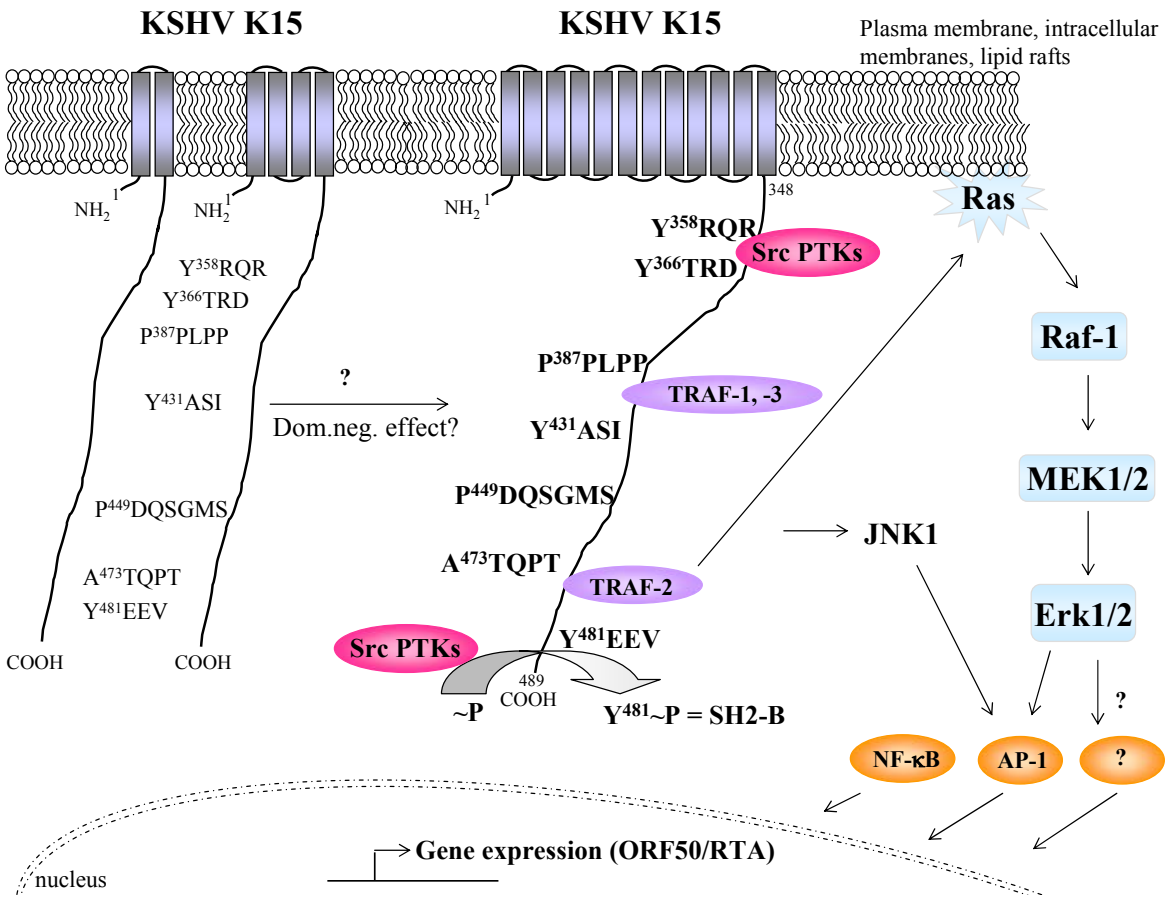

Figure 36: K15 signal transduction. The full length K15 protein, composed of up to 12 transmembrane domains, localised to the plasma membrane and intracellular membranes, as well as to lipid rafts. K15 splice variants were shown not to be able to activate the NF-κB and AP-1 pathway as full length K15 did via MAPKs Erk2 and JNK1. K15 was shown to interact with and to be phosphorylated at Y^{481} by members of the Src kinase family of non-receptor tyrosine kinases (PTKs).

Transient expression in cos7, 293-T or Vero cells of the K15 ex1-8 expression construct gave rise to a major protein of ~45 kDa, and two minor protein species of 34 and 23 kDa (figure 10 A). Sharp et al. (2002) described strongly expressed proteins of 35 and 23 kDa and a weakly expressed 50 kDa protein derived from a K15 ex1-8 construct and suggested that the smaller proteins were derived by cleavage from the 50 kDa precursor protein. However, we believe that the smaller proteins were derived from internal initiation at in frame ATG codons in exon 4 or exon 6 (figure 10 C). In 293 cells transiently transfected with K15, Sharp et al. (2002) observed a cytoplasmic and strong perinuclear immunolabelling pattern, which differs from the immunolabelling we observed with our K15 ex1-8 expression construct (figure 14 A). Since the 23 kDa protein derived from K15 ex6-8, which initiates at the in frame ATG codon in exon 6, did not localise to lipid rafts (figure 12 B) and showed an immunolabelling that differed from the full length K15 ex1-8 protein (figure 16 C and D), we postulate that the subcellular localisation of K15 observed by Sharp et al. (2002) by microscopy does not correspond to the 45/50 kDa protein, but rather to the 34 and 23 kDa proteins. This is further supported by the observation by Sharp et al. (2002) who described ER localisation of K15 in

Hela cells treated with the ER dye $DiOC_6$. In our hands, the K15 ex1-8 protein did clearly not colocalise with the ER marker protein Calnexin (figure 17 D-F).

The role of the two smaller proteins derived from K15 ex1-8 (34 and 23 kDa) is not yet clear. Both proteins were membrane associated, but did not localise to lipid rafts (data not shown). Whether they could act as dominant negative K15 forms, as already discussed for the K15 splice isoforms, was not investigated.

In summary, we have shown that the K15 ORF of KSHV encoded a protein of 45 kDa that associated with the cellular plasma membrane, intracellular membranes and lipid rafts, and showed signaling activities reminiscent of its positional equivalent in the EBV genome LMP2A, as well as of terminal membrane proteins K1 of KSHV, LMP1 of EBV, StpA, B and C and Tip of HVS, R1 of RRV and Tio of HVA. Remarkably, although LMP2A, the two K15 variants K15-P and K15-M, and the putative R15 protein share only little amino acid identity, they show striking structural similarities. Comparative studies between these "right end side" terminal membrane proteins may help to further understand their role in viral infection.

4.2 K15 in vivo expression and the viral lytic life cycle

In vivo expression of K15

RT-PCR studies indicate that K15 may be expressed during the latent viral life cycle, but K15 transcripts are clearly upregulated upon TPA induction, which is a characteristic for lytic genes (Glenn et al., 1999, Choi et al., 2000a). In addition, gene array studies indicate that K15 is predominantly expressed during the lytic cycle in PEL cell lines upon TPA induction (Paulose-Murphy et al., 2001) or ectopic expression of the viral lytic switch protein RTA (Nakamura et al., 2003).

We detected a protein of 23 kDa in latently infected PEL cell lines with a polyclonal K15 antibody raised against the cytoplasmic domain of K15 (figure 27), and its expression was found to be slightly upregulated after lytic cycle induction with TPA, which would correspond to the RT-PCR data. However, when we characterised the 23 kDa protein by cellular fractionation, it was found to localise to the cytosolic fraction (figure 28). In contrast to our data, expression of the 23 kDa protein observed by Sharp et al. (2002) in the latently infected PEL cell line Jsc-1 decreased upon TPA treatment. According to Sharp et al. (2002), immunolabelling of Jsc-1 cells with a monoclonal antibody raised against the K15 C-terminus showed a cytoplasmic staining pattern, which supports our observation that the 23 kDa protein in Jsc-1 cells probably is a soluble protein. The LMP1 protein can be cleaved near the beginning of the C-terminal cytoplasmic domain at leucine residue L^{242}, which results in a soluble C-terminal domain of 25 kDa (Moorthy & Thorley-Lawson 1990, 1993b). However, when we analysed an expression construct encompassing the cytoplasmic domain of K15 by Western blotting, this protein clearly migrated faster than the 23 kDa Jsc-1 protein (figure 28).

In some latently infected Burkitt´s lymphoma cells, LMP1 expression can be induced during the lytic phase (Laux et al., 1988, Boos et al., 1987). The promoter for full length LMP1 expression in lytic infection has not been characterized, but in late lytic infection, a promoter in the third exon drives transcription of an alternative LMP1 transcript encoding the last two transmembrane domains and the C-terminal cytoplasmic domain (Hudson et al., 1985). This smaller protein (lytic LMP1) localises to cytoplasmic membranes but does not patch and is not transforming (Mann et al., 1985, Liebowitz et al., 1987, 1992). In theory, the 23 kDa K15 protein in Jsc-1 cells may be derived from alternative splice events that have not been characterised so far. Regarding the multiple splicing events described so far for ORF K15 (Glenn et al., 1999, Choi et al., 2000a, figures 5 and 29), further alternative splicing events could potentially result in a protein with low hydrophobicity, although we could not identify such a transcript (figure 29).

The most prominent transcript identified in this work and by Glenn et al. (1999), Choi et al. (2000a) and Poole et al. (1999) in PEL cell lines Jsc-1, BCP-1 and BCBL-1 was completely spliced and contained all exons, which gave rise to a major protein of 45 kDa when transiently expressed in cos7, 293-T or Vero cells (figure 10 A). We did not detect a protein of this size in PEL cell lines (figure 27) or endothelial cell lines T24 rKSHV.152, DU145 rKSHV.152 or Vero rKSHV.219 (figure 30) with our polyclonal or monoclonal K15 antibodies. This may be due to low in vivo expression or a short half life of the 45 kDa K15 protein. The EBV LMP2A protein interacts with members of the Nedd4-like ubiquitin protein ligase family via the two PPPPY motifs of its cytoplasmic domain (see 1.3.1.2). This interaction results in ubiquitination and degradation of LMP2A and LMP2A-associated proteins such as Lyn and Syk (Longnecker et al., 2000, Ikeda et al., 2000, 2001, 2002, Winberg et al., 2000). Although K15 contains a proline rich motif in its cytoplasmic domain ($PP^{387}PLPP$, table 3, figure 18) similar to those of LMP2A, these do not correspond to the PPY consensus of Nedd4 binding proteins, and a function of this K15 motif has not been adressed yet.

The regulation of K15 gene expression is not well understood, but we have evidence that the K15 promoter is located within the terminal repeat (TR) region based on primer extension analysis (L. Rainbow, personal communication). When one subunit of the terminal repeat region (803 bp) was cloned upstream of a luciferase gene in a vector lacking promoter elements, this element showed strong promoter activity (A. Tittel, diploma thesis). The latency-associated antigen 1 (LANA-1) of KSHV is expressed during latency and tethers viral episomes to host chromatin by binding to two motifs of 16 nucleotides within the terminal repeat subunits (LANA binding sites 1 and 2) via its C-terminus, and to heterochromatin via its N-terminus (reviewed in Viejo-Borbolla & Schulz 2003). Lana-1 has been shown to function as a transcriptional repressor as well as transactivator (see 1.2, latent replication). When Lana-1 was co-expressed with the TR reporter plasmid, the promoter activity of the TR

was significantly downregulated (A. Tittel, diploma thesis). Hence, during the latent viral life cycle, LANA-1 might repress K15 gene expression, but this needs further investigation.

KSHV infection of primary human B-cells in vitro has been reported by one group (Kliche et al., 1998), but another group reported that de novo infection of human B-cells such as Raji (EBV positive, KSHV negative) with KSHV obtained from induced PEL cell lines failed (Bechtel et al., 2003). Our attempts to de novo infect the human B-cell lines BJAB and Raji and the PEL cell line BCBL-1 with recombinant rKSHV.219 did not succeed. In contrast, we could de novo infect human epithelial cell lines 293 and 293-T as well as the African green monkey epithelial cell line Vero with rKSHV.219 (figure 31 B).

When we analysed the expression of K15 after de novo infection of 293-T cells with rKSHV.219, we detected K15 transcripts by RT-PCR at timepoints 24, 48 and 72 h post infection (figure 32 B). However, K15 protein was not detected in 293-T lysates collected at 24, 48 and 72 h post infection with our polyclonal K15 antibody by Western blotting (figure 32 C), suggesting that K15 protein is expressed at levels too low to be detected with our antibody.

The present study is the first documenting K15 gene expression after de novo infection with recombinant KSHV.219 of human epithelial cells. A very recent study investigated the expression kinetics of KSHV genes immediately after primary KSHV infection of primary human dermal microvascular endothelial (HMVEC-d) and human foreskin fibroblast (HFF) cells by real time RT-PCR and whole genome array (Krishnan et al., 2004).

Upon entry into the in vitro target cells, members of α-, β-, and γ-herpesviruses have been shown to enter the lytic replicative cycle, which is characterised by a cascade of gene expression (reviewed in Kieff & Rickinson 2002, Mocarski & Courcelle 2002, Roizman & Knipe 2002 and Roizman & Pellett 2002). Unlike many members of α-, β-, and γ-herpesviruseses, lytic γ_1-herpesvirus EBV replication has not been demonstrated during in vitro infection of susceptible primary human B-cells. Instead, EBV establishes a latent infection in these cells, resulting in the transformation and establishment of LCLs (see 1.3.1). Like EBV, KSHV has so far not been shown to initiate a lytic gene expression cascade and formation of progeny virus from the input KSHV in vitro, but KSHV establishes a latent infection in many in vitro systems and lytic replication can be supported by activation with TPA or the lytic switch protein ORF50/RTA.

KSHV gene expression analyses by whole genome arrays published so far were conducted with latently infected B-cells and lytic gene expression was induced with RTA or TPA (Paulose-Murphy et al., 2001, Nakamura et al., 2003). The study by Krishnan et al. (2004) is the first that adresses KSHV gene expression following a primary infection of target cells. They have shown that early during infection (2 h p.i.), KSHV expresses the lytic ORF50/RTA gene and the latent ORF73/LANA-1 gene concurrently, with ORF50 expression rapidly

declining 24 h p.i. and ORF73 expression being maintained up to 120 h p.i.. In addition, they found a limited number of lytic genes being expressed immediately after infection, most of which decline sharply or were undetectable during the course of infection (8 h p.i. in HMVEC-d, 24 h p.i. in HFF). The study by Krishnan et al. (2004) suggests that lytic gene expression of KSHV is initiated soon after the infection, but this initial lytic activation is not enough to proceed to a complete lytic replication and progeny virus development.

According to their gene array data, K15 did not belong to the lytic genes expressed after de novo infection. Notably, K15 expression was analysed by whole genome array and not by RT-PCR as in our study, and they analysed K15 expression at timepoints 2 h and 8 h post infection for HMVEC-d and 8 and 24 h p.i. for HFF cells, whereas we analysed K15 expression at timepoints 24, 48 and 72 h post infection. Hence, Krishnan et al. (2004) looked for K15 transcripts at earlier timepoints. Furthermore, they used KSHV prepared from TPA-induced BCBL-1 cells, whereas we used recombinant KSHV.219 obtained from the Vero rKSHV.219 cell line induced with n-butyrate and Baculovirus ORF50/RTA for our infection studies. Notably, early during infection, lytic KSHV genes were found to be expressed that have a role in immune modulation and have an anti-apoptotic function (Krishnan et al., 2004). This observation together with our results that K15 was expressed during de novo infection might point at a hypothetical immunmodulatory or anti-apoptotic function for K15.

K15 and the lytic viral life cycle

What might be the role of K15 signaling during KSHV infection? K15 does not seem to have oncogenic properties (unpublished results) as viral TMPs LMP1, K1, R1, Stp and Tip. Studies on EBV gene regulation have defined several AP-1 binding elements in various EBV lytic gene promoters. These AP-1 elements respond to both AP-1 and the EBV transactivator ZTA and therefore play important roles in the regulation of these promoters (Lieberman et al., 1990). We have shown in this study that K15 activated the AP-1 transcription factor via the Ras-Raf-MEK1/2-Erk2 signaling cascade involving TRAF-2, and have also shown that K15 can activate the MAPK JNK1. Further, we showed that K15 activated the promoter of the lytic switch protein ORF50/RTA, which contains several putative AP-1 binding sites (figure 33 A). Luciferase reporter assays with dominant negative mutants of Ras, TRAF-2 and Erk2 revealed that Ras and Erk2 and, to a lesser extent, TRAF-2 play a role in the activation of the ORF50 promoter by K15 (figure 33 B). TPA is thought to induce lytic gene expression in B-cells by the induction of AP-1 activity via the Ras-Raf-MEK-Erk pathway and via JNK. We therefore asked whether K15 was also able to induce the viral lytic life cycle in vivo.

In cells latently infected with KSHV, overexpression of RTA can activate the KSHV immediate early/early (K8, K5, K2, K12, Nut1, ORF6, K3) and late (K1, K8.1, ORF21) lytic cycle genes, either alone or in synergy with other viral regulatory genes such as K8 and ORF57 (Dourmishev et al., 2003, reviewed in Moore & Chang 2001, Sun et al., 1999, West & Wood 2003). Activation of the lytic cycle by RTA results in the production of virus progeny

(Bechtel et al., 2003, Dourmishev et al., 2003, West & Wood 2003, Sun et al., 1999). We could show that in an epithelial cell line infected with recombinant rKSHV.219, Vero rKSHV.219, the lytic viral life cycle could be induced by ectopic expression of RTA (figure 31 A, 34 C) and infectious virus progeny was obtained as monitored by the appearance of GFP expressing 293, 293-T or Vero cells 48 hours after de novo infection with rKSHV.219 (figure 31 B). Addition of n-butyrate further enhanced the induction of the lytic cycle in Vero rKSHV.219 cells as monitored by expression of RFP and the late lytic K8.1 protein (figure 34 D).

The major mechanism by which n-butyrate as well as trichostatin A are thought to activate viral lytic gene expression is by blocking histone deacetylases. Acetylation of the N-terminal domain of histones (at lysine residues) tends to destabilise chromatin structure, which allows transcription to take place, whereas histone deacetylation decreases the accessibility of DNA in the affected chromatin. Hence, in the presence of n-butyrate, RTA and other transcription factors involved in lytic gene expression may better access viral DNA to initiate transcription. This would be reminiscent of the immediate early protein IE86 of human cytomegalovirus that activates viral early gene expression by directly interacting with histone acetyltransferases (Bryant et al., 2000).

When we transiently expressed the K15 ex1-8 expression construct in Vero rKSHV.219 cells, RFP expression was not observed (figure 34 B). Hence, although K15 was shown to activate the ORF50 promoter in luciferase reporter assays, it seemed not to enhance expression of ORF50/RTA of recombinant KSHV.219, which would subsequently drive lytic gene expression resulting in virus progeny production. Notably, Krishnan et al. (2004) observed high levels of ORF50/RTA expression soon after infection, but only a subset of ORF50/RTA target genes were activated during the early stage of infection, and these were not sustained at later times of infection. This implies that expression of ORF50/RTA alone is not sufficient to completely activate the lytic cycle during the early time of infection.

Assuming that transiently expressed K15 does activate RTA expression in Vero rKSHV.219 cells, posttranslational modifications of ORF50/RTA synthesized from the genome may potentially differ from the ORF50/RTA provided in *trans*. Furthermore, host cell factors and other viral factors may influence the activation of the lytic life cycle such that K15 expression alone does not result in lytic cycle induction. The transcriptional transactivator protein ICP-4 of herpes simplex virus type I undergoes multiple modifications including phosphorylation, poly-ADP ribosylation and nucleotidylation. Whether ORF50 undergoes such modifications has not been investigated so far.

Furthermore, the KSHV genome, that is associated with host chromatin during latency, may be modified. Methylation is common among γ-herpesvirus genomes such as EBV and HVS (Karlin et al., 1994). Interestingly, the KSHV genome is not significantly methylated with the

exception of the ORF50 promoter region during latency (Chen et al., 2001). Hence, if K15 was expressed and activated the AP-1 transcription factor, AP-1 could possibly not activate ORF50/RTA gene expression due to methylation of the promoter region in Vero rKSHV.219 cells. The ORF50 promoter reporter plasmid may not be methylated due to non-methylation of plasmid DNA prepared in *E. coli*. The hypermethylated region of the ORF50 promoter region was found to be situated between base -315 and -255 (see figure 33) and demethylation was shown to be essential for ORF50 expression in vitro (Chen et al., 2001). Treatment of the PEL cell line BCBL-1 with 5´azacytidine, a DNA methyltransferase inhibitor that reduces the level of DNA methylation, induces the lytic viral life cycle and treatment of BCBL-1 cells with TPA resulted in demethylation of the ORF50 promoter (Chen et al., 2001).

In order to show that methylation of the ORF50 promoter prevents K15 from activating ORF50 expression, Vero rKSHV.219 cells could be treated with 5´azacytidine and subsequently transfected with K15 ex1-8. Another approach would be a methylation cassette assay as described in Chen et al. (2001) and Robertson & Ambinder (1997), in which the ORF50 promoter can be in vitro methylated by a methylation enzyme. If K15 could not activate the in vitro methylated ORF50 promoter region in luciferase reporter assays (see figure 33 B), this could explain why we did not observe RFP expression in Vero rKSHV.219 cells.

Little is known about how RTA expression is triggered initially at the earliest stages after TPA induction. Treatment with TPA proved to significantly induce AP-1 DNA binding activity in EBV immortalised B-cells (Lieberman et al., 1990, Ruf & Rawlins 1995) and in KSHV positive PEL cells (Lee et al., 2002). Wang et al. (2004) recently found that co-transfected c-jun plus c-Fos, both members of the AP-1 family, transactivated the KSHV RTA promoter in an AP-1 binding site-dependent manner. When they mutated the AP-1 site located at position -86 (see figure 33), they lost RTA promoter transactivation by the c-jun-c-Fos heterodimer. Exogenously introduced c-jun plus c-Fos was shown to trigger endogenous RTA protein expression in PEL cells (Wang et al., 2004). We have shown that K15 ex1-8 induced the MAP kinase JNK1. JNK1 is known to regulate c-jun activity through phosporylation, and we saw a slight upregulation of c-jun in 293-T cells expressing K15 in preliminary gene array experiments (not shown). We have not analysed yet whether K15 may induce RTA expression in PEL cells, but this will be an aspect to be analysed in the near future.

5 References

Internet sites used in this study:

http://www.cbs.dtu.dk (transmembrane prediction programme TMHMM)

http://scansite.mit.edu (phosphorylation site prediction programme)

http://cbs.dtu.dk (phosphorylation site prediction programme)

http://transfac.gbf.de (Mat Inspector programme)

Akula SM, Pramod NP, Wang FZ, and Chandran B. 2001a. Human herpesvirus 8 envelope-associated glycoprotein B interacts with heparan sulfate-like moieties. Virology 284:235-249.

Akula SM, Wang FZ, Vieira J, and Chandran B. 2001b. Human herpesvirus 8 interaction with target cells involves heparan sulfate. Virology 282:245-255.

Akula SM, Pramod NP, Wang FZ, and Chandran B. 2002. Integrin alpha3beta1 (CD 49c/29) is a cellular receptor for Kaposi's sarcoma-associated herpesvirus (KSHV/HHV-8) entry into the target cells. Cell 108:407-419.

Akula SM, Naranatt PP, Walia NS, Wang FZ, Fegley B, and Chandran B. 2003. Kaposi's sarcoma-associated herpesvirus (human herpesvirus 8) infection of human fibroblast cells occurs through endocytosis. J Virol 77:7978-7990.

Albrecht JC, Nicholas J, Cameron KR, Newman C, Fleckenstein B, and Honess RW. 1992. Herpesvirus saimiri has a gene specifying a homologue of the cellular membrane glycoprotein CD59. Virology 190:527-530.

Albrecht JC, Friedrich U, Kardinal C, Koehn J, Fleckenstein B, Feller SM, and Biesinger B. 1999. Herpesvirus ateles gene product Tio interacts with nonreceptor protein tyrosine kinases. J Virol 73:4631-4639.

Albrecht JC. 2000. Primary structure of the Herpesvirus ateles genome. J Virol 74:1033-1037.

Alessi DR, Cuenda A, Cohen P, Dudley DT, and Saltiel AR. 1995. PD 098059 is a specific inhibitor of the activation of mitogen-activated protein kinase kinase in vitro and in vivo. J Biol Chem 270:27489-27494.

Alexander L, Denekamp L, Knapp A, Auerbach MR, Damania B, and Desrosiers RC. 2000. The primary sequence of rhesus monkey rhadinovirus isolate 26-95: sequence similarities to Kaposi's sarcoma-associated herpesvirus and rhesus monkey rhadinovirus isolate 17577. J Virol 74:3388-3398.

An J, Lichtenstein AK, Brent G, and Rettig MB. 2002. The Kaposi sarcoma-associated herpesvirus (KSHV) induces cellular interleukin 6 expression: role of the KSHV latency-associated nuclear antigen and the AP1 response element. Blood 99:649-654.

An J, Sun Y, Sun R, and Rettig MB. 2003. Kaposi's sarcoma-associated herpesvirus encoded vFLIP induces cellular IL-6 expression: the role of the NF-kappaB and JNK/AP1 pathways. Oncogene 22:3371-3385.

An J, Sun Y, and Rettig MB. 2004. Transcriptional coactivation of c-Jun by the KSHV-encoded LANA. Blood 103:222-228.

Andreoni M, El Sawaf G, Rezza G, Ensoli B, Nicastri E, Ventura L, Ercoli L, Sarmati L, and Rocchi G. 1999. High seroprevalence of antibodies to human herpesvirus-8 in Egyptian children: evidence of nonsexual transmission. J Natl Cancer Inst 91:465-469.

Andreoni M, Sarmati L, Nicastri E, El Sawaf G, El Zalabani M, Uccella I, Bugarini R, Parisi SG, and Rezza G. 2002. Primary human herpesvirus 8 infection in immunocompetent children. JAMA 287:1295-1300.

Aoki Y and Tosato G. 1999a. Role of vascular endothelial growth factor/vascular permeability factor in the pathogenesis of Kaposi's sarcoma-associated herpesvirus-infected primary effusion lymphomas. Blood 94:4247-4254.

Aoki Y, Jaffe ES, Chang Y, Jones K, Teruya-Feldstein J, Moore PS, and Tosato G. 1999b. Angiogenesis and hematopoiesis induced by Kaposi's sarcoma-associated herpesvirus-encoded interleukin-6. Blood 93:4034-4043.

Ardila-Osorio H, Clausse B, Mishal Z, Wiels J, Tursz T, and Busson P. 1999. Evidence of LMP1-TRAF3 interactions in glycosphingolipid-rich complexes of lymphoblastoid and nasopharyngeal carcinoma cells. Int J Cancer 81:645-649.

Arenzana-Seisdedos F, Fernandez B, Dominguez I, Jacque JM, Thomas D, Diaz-Meco MT, Moscat J, and Virelizier JL. 1993. Phosphatidylcholine hydrolysis activates NF-kappa B and increases human immunodeficiency virus replication in human monocytes and T lymphocytes. J Virol 67:6596-6604.

Arvanitakis L, Yaseen N, and Sharma S. 1995. Latent membrane protein-1 induces cyclin D2 expression, pRb hyperphosphorylation, and loss of TGF-beta 1-mediated growth inhibition in EBV-positive B-cells. J Immunol 155:1047-1056.

Arvanitakis L, Geras-Raaka E, Varma A, Gershengorn MC, and Cesarman E. 1997. Human herpesvirus KSHV encodes a constitutively active G-protein-coupled receptor linked to cell proliferation. Nature 385:347-350.

Asou H, Said JW, Yang R, Munker R, Park DJ, Kamada N, and Koeffler HP. 1998. Mechanisms of growth control of Kaposi's sarcoma-associated herpes virus-associated primary effusion lymphoma cells. Blood 91:2475-2481.

Atkinson PG, Coope HJ, Rowe M, and Ley SC. 2003. Latent membrane protein 1 of Epstein-Barr virus stimulates processing of NF-kappa B2 p100 to p52. J Biol Chem 278:51134-51142.

Aviel S, Winberg G, Massucci M, and Ciechanover A. 2000. Degradation of the epstein-barr virus latent membrane protein 1 (LMP1) by the ubiquitin-proteasome pathway. Targeting via ubiquitination of the N-terminal residue. J Biol Chem 275:23491-23499.

Baer R, Bankier AT, Biggin MD, Deininger PL, Farrell PJ, Gibson TJ, Hatfull G, Hudson GS, Satchwell SC, Seguin C, and . 1984. DNA sequence and expression of the B95-8 Epstein-Barr virus genome. Nature 310:207-211.

Baeuerle PA and Baltimore D. 1996. NF-kappa B: ten years after. Cell 87:13-20.

Baichwal VR and Sugden B. 1987. Posttranslational processing of an Epstein-Barr virus-encoded membrane protein expressed in cells transformed by Epstein-Barr virus. J Virol 61:866-875.

Baichwal VR and Sugden B. 1988. Transformation of Balb 3T3 cells by the BNLF-1 gene of Epstein-Barr virus. Oncogene 2:461-467.

Baichwal VR and Sugden B. 1989. The multiple membrane-spanning segments of the BNLF-1 oncogene from Epstein-Barr virus are required for transformation. Oncogene 4:67-74.

Bais C, Santomasso B, Coso O, Arvanitakis L, Raaka EG, Gutkind JS, Asch AS, Cesarman E, Gershengorn MC, Mesri EA, and Gerhengorn MC. 1998. G-protein-coupled receptor of Kaposi's sarcoma-associated herpesvirus is a viral oncogene and angiogenesis activator. Nature 391:86-89.

Baker SJ and Reddy EP. 1996. Transducers of life and death: TNF receptor superfamily and associated proteins. Oncogene 12:1-9.

Ballestas ME, Chatis PA, and Kaye KM. 1999. Efficient persistence of extrachromosomal KSHV DNA mediated by latency-associated nuclear antigen. Science 284:641-644.

Bechtel JT, Liang Y, Hvidding J, and Ganem D. 2003. Host range of Kaposi's sarcoma-associated herpesvirus in cultured cells. J Virol 77:6474-6481.

Belanger C, Gravel A, Tomoiu A, Janelle ME, Gosselin J, Tremblay MJ, and Flamand L. 2001. Human herpesvirus 8 viral FLICE-inhibitory protein inhibits Fas-mediated apoptosis through binding and prevention of procaspase-8 maturation. J Hum Virol 4:62-73.

Ben Bassat H, Goldblum N, Mitrani S, Goldblum T, Yoffey JM, Cohen MM, Bentwich Z, Ramot B, Klein E, and Klein G. 1977. Establishment in continuous culture of a new type of lymphocyte from a "Burkitt like" malignant lymphoma (line D.G.-75). Int J Cancer 19:27-33.

Benschop RJ and Cambier JC. 1999. B-cell development: signal transduction by antigen receptors and their surrogates. Curr Opin Immunol 11:143-151.

Bieleski L and Talbot SJ. 2001. Kaposi's sarcoma-associated herpesvirus vCyclin open reading frame contains an internal ribosome entry site. J Virol 75:1864-1869.

Biesinger B, Trimble JJ, Desrosiers RC, and Fleckenstein B. 1990. The divergence between two oncogenic Herpesvirus saimiri strains in a genomic region related to the transforming phenotype. Virology 176:505-514.

Biesinger B, Muller-Fleckenstein I, Simmer B, Lang G, Wittmann S, Platzer E, Desrosiers RC, and Fleckenstein B. 1992. Stable growth transformation of human T lymphocytes by herpesvirus saimiri. Proc Natl Acad Sci U S A 89:3116-3119.

Biesinger B, Tsygankov AY, Fickenscher H, Emmrich F, Fleckenstein B, Bolen JB, and Broker BM. 1995. The product of the Herpesvirus saimiri open reading frame 1 (tip) interacts with T cell-specific kinase p56lck in transformed cells. J Biol Chem 270:4729-4734.

Birkenbach M, Liebowitz D, Wang F, Sample J, and Kieff E. 1989. Epstein-Barr virus latent infection membrane protein increases vimentin expression in human B-cell lines. J Virol 63:4079-4084.

Birkmann A, Mahr K, Ensser A, Yaguboglu S, Titgemeyer F, Fleckenstein B, and Neipel F. 2001. Cell surface heparan sulfate is a receptor for human herpesvirus 8 and interacts with envelope glycoprotein K8.1. J Virol 75:11583-11593.

Bonifacino JS and Dell'Angelica EC. 1999. Molecular bases for the recognition of tyrosine-based sorting signals. J Cell Biol 145:923-926.

Boos H, Berger R, Kuklik-Roos C, Iftner T, and Mueller-Lantzsch N. 1987. Enhancement of Epstein-Barr virus membrane protein (LMP) expression by serum, TPA, or n-butyrate in latently infected Raji cells. Virology 159:161-165.

Boshoff C, Schulz TF, Kennedy MM, Graham AK, Fisher C, Thomas A, McGee JO, Weiss RA, and O'Leary JJ. 1995. Kaposi's sarcoma-associated herpesvirus infects endothelial and spindle cells. Nat Med 1:1274-1278.

Boshoff C, Endo Y, Collins PD, Takeuchi Y, Reeves JD, Schweickart VL, Siani MA, Sasaki T, Williams TJ, Gray PW, Moore PS, Chang Y, and Weiss RA. 1997. Angiogenic and HIV-inhibitory functions of KSHV-encoded chemokines. Science 278:290-294.

Boshoff C, Gao SJ, Healy LE, Matthews S, Thomas AJ, Coignet L, Warnke RA, Strauchen JA, Matutes E, Kamel OW, Moore PS, Weiss RA, and Chang Y. 1998. Establishing a KSHV+ cell line (BCP-1) from peripheral blood and characterizing its growth in Nod/SCID mice. Blood 91:1671-1679.

Bourboulia D, Whitby D, Boshoff C, Newton R, Beral V, Carrara H, Lane A, and Sitas F. 1998. Serologic evidence for mother-to-child transmission of Kaposi sarcoma-associated herpesvirus infection. JAMA 280:31-32.

Bowman T, Garcia R, Turkson J, and Jove R. 2000. STATs in oncogenesis. Oncogene 19:2474-2488.

Bowser BS, DeWire SM, and Damania B. 2002. Transcriptional regulation of the K1 gene product of Kaposi's sarcoma-associated herpesvirus. J Virol 76:12574-12583.

Bradford MM. 1976. A rapid and sensitive method for the quantitation of microgram quantities of protein utilizing the principle of protein-dye binding. Anal Biochem 72:248-254.

Brennan P, Floettmann JE, Mehl A, Jones M, and Rowe M. 2001. Mechanism of action of a novel latent membrane protein-1 dominant negative. J Biol Chem 276:1195-1203.

Brinkmann MM, Glenn M, Rainbow L, Kieser A, Henke-Gendo C, and Schulz TF. 2003. Activation of mitogen-activated protein kinase and NF-kappaB pathways by a Kaposi's sarcoma-associated herpesvirus K15 membrane protein. J Virol 77:9346-9358.

Brodeur SR, Cheng G, Baltimore D, and Thorley-Lawson DA. 1997. Localization of the major NF-kappaB-activating site and the sole TRAF3 binding site of LMP-1 defines two distinct signaling motifs. J Biol Chem 272:19777-19784.

Broker BM, Tsygankov AY, Muller-Fleckenstein I, Guse AH, Chitaev NA, Biesinger B, Fleckenstein B, and Emmrich F. 1993. Immortalization of human T cell clones by Herpesvirus saimiri. Signal transduction analysis reveals functional CD3, CD4, and IL-2 receptors. J Immunol 151:1184-1192.

Brown DA and London E. 1998. Functions of lipid rafts in biological membranes. Annu Rev Cell Dev Biol 14:111-136.

Brown DA and London E. 2000. Structure and function of sphingolipid- and cholesterol-rich membrane rafts. J Biol Chem 275:17221-17224.

Brown KD, Hostager BS, and Bishop GA. 2001. Differential signaling and tumor necrosis factor receptor-associated factor (TRAF) degradation mediated by CD40 and the Epstein-Barr virus oncoprotein latent membrane protein 1 (LMP1). J Exp Med 193:943-954.

Bruder JT, Heidecker G, and Rapp UR. 1992. Serum-, TPA-, and Ras-induced expression from Ap-1/Ets-driven promoters requires Raf-1 kinase. Genes Dev 6:545-556.

Bryant LA, Mixon P, Davidson M, Bannister AJ, Kouzarides T, and Sinclair JH. 2000. The human cytomegalovirus 86-kilodalton major immediate-early protein interacts physically and functionally with histone acetyltransferase P/CAF. J Virol 74:7230-7237.

Buhl AM, Pleiman CM, Rickert RC, and Cambier JC. 1997. Qualitative regulation of B-cell antigen receptor signaling by CD19: selective requirement for PI3-kinase activation, inositol-1,4,5-trisphosphate production and Ca2+ mobilization. J Exp Med 186:1897-1910.

Burger M, Burger JA, Hoch RC, Oades Z, Takamori H, and Schraufstatter IU. 1999. Point mutation causing constitutive signaling of CXCR2 leads to transforming activity similar to Kaposi's sarcoma herpesvirus-G protein-coupled receptor. J Immunol 163:2017-2022.

Burkhardt AL, Bolen JB, Kieff E, and Longnecker R. 1992. An Epstein-Barr virus transformation-associated membrane protein interacts with Src family tyrosine kinases. J Virol 66:5161-5167.

Burysek L, Yeow WS, Lubyova B, Kellum M, Schafer SL, Huang YQ, and Pitha PM. 1999. Functional analysis of human herpesvirus 8-encoded viral interferon regulatory factor 1 and its association with cellular interferon regulatory factors and p300. J Virol 73:7334-7342.

Byun H, Gwack Y, Hwang S, and Choe J. 2002. Kaposi's sarcoma-associated herpesvirus open reading frame (ORF) 50 transactivates K8 and ORF57 promoters via heterogeneous response elements. Mol Cells 14:185-191.

Cahir McFarland ED, Izumi KM, and Mosialos G. 1999. Epstein-barr virus transformation: involvement of latent membrane protein 1-mediated activation of NF-kappaB. Oncogene 18:6959-6964.

Calabro ML, Sheldon J, Favero A, Simpson GR, Fiore JR, Gomes E, Angarano G, Chieco-Bianchi L, and Schulz TF. 1998. Seroprevalence of Kaposi's sarcoma-associated herpesvirus/human herpesvirus 8 in several regions of Italy. J Hum Virol 1:207-213.

Caldwell RG, Wilson JB, Anderson SJ, and Longnecker R. 1998. Epstein-Barr virus LMP2A drives B-cell development and survival in the absence of normal B-cell receptor signals. Immunity 9:405-411.

Caldwell RG, Brown RC, and Longnecker R. 2000. Epstein-Barr virus LMP2A-induced B-cell survival in two unique classes of EmuLMP2A transgenic mice. J Virol 74:1101-1113.

Cambier JC, Pleiman CM, and Clark MR. 1994. Signal transduction by the B-cell antigen receptor and its coreceptors. Annu Rev Immunol 12:457-486.

Cannon JS, Ciufo D, Hawkins AL, Griffin CA, Borowitz MJ, Hayward GS, and Ambinder RF. 2000. A new primary effusion lymphoma-derived cell line yields a highly infectious Kaposi's sarcoma herpesvirus-containing supernatant. J Virol 74:10187-10193.

Cannon M, Philpott NJ, and Cesarman E. 2003. The Kaposi's sarcoma-associated herpesvirus G protein-coupled receptor has broad signaling effects in primary effusion lymphoma cells. J Virol 77:57-67.

Cannon ML and Cesarman E. 2004. The KSHV G protein-coupled receptor signals via multiple pathways to induce transcription factor activation in primary effusion lymphoma cells. Oncogene 23:514-523.

Carbone A, Cilia AM, Gloghini A, Capello D, Todesco M, Quattrone S, Volpe R, and Gaidano G. 1998. Establishment and characterization of EBV-positive and EBV-negative primary effusion lymphoma cell lines harbouring human herpesvirus type-8. Br J Haematol 102:1081-1089.

Carbone A, Cilia AM, Gloghini A, Capello D, Fassone L, Perin T, Rossi D, Canzonieri V, De Paoli P, Vaccher E, Tirelli U, Volpe R, and Gaidano G. 2000. Characterization of a novel HHV-8-positive cell line reveals implications for the pathogenesis and cell cycle control of primary effusion lymphoma. Leukemia 14:1301-1309.

Cerimele F, Curreli F, Ely S, Friedman-Kien AE, Cesarman E, and Flore O. 2001. Kaposi's sarcoma-associated herpesvirus can productively infect primary human keratinocytes and alter their growth properties. J Virol 75:2435-2443.

Cesarman E, Chang Y, Moore PS, Said JW, and Knowles DM. 1995. Kaposi's sarcoma-associated herpesvirus-like DNA sequences in AIDS-related body-cavity-based lymphomas. N Engl J Med 332:1186-1191.

Cesarman E, Nador RG, Bai F, Bohenzky RA, Russo JJ, Moore PS, Chang Y, and Knowles DM. 1996. Kaposi's sarcoma-associated herpesvirus contains G protein-coupled receptor and cyclin D homologs which are expressed in Kaposi's sarcoma and malignant lymphoma. J Virol 70:8218-8223.

Chang L and Karin M. 2001. Mammalian MAP kinase signaling cascades. Nature 410:37-40.

Chang PJ, Shedd D, Gradoville L, Cho MS, Chen LW, Chang J, and Miller G. 2002. Open reading frame 50 protein of Kaposi's sarcoma-associated herpesvirus directly activates the viral PAN and K12 genes by binding to related response elements. J Virol 76:3168-3178.

Chang Y, Cesarman E, Pessin MS, Lee F, Culpepper J, Knowles DM, and Moore PS. 1994. Identification of herpesvirus-like DNA sequences in AIDS-associated Kaposi's sarcoma. Science 266:1865-1869.

Chaudhary PM, Jasmin A, Eby MT, and Hood L. 1999. Modulation of the NF-kappa B pathway by virally encoded death effector domains-containing proteins. Oncogene 18:5738-5746.

Chen H, Lee JM, Wang Y, Huang DP, Ambinder RF, and Hayward SD. 1999. The Epstein-Barr virus latency BamHI-Q promoter is positively regulated by STATs and Zta interference with JAK/STAT activation leads to loss of BamHI-Q promoter activity. Proc Natl Acad Sci U S A 96:9339-9344.

Chen H, Lee JM, Zong Y, Borowitz M, Ng MH, Ambinder RF, and Hayward SD. 2001a. Linkage between STAT regulation and Epstein-Barr virus gene expression in tumors. J Virol 75:2929-2937.

Chen H, Hutt-Fletcher L, Cao L, and Hayward SD. 2003. A positive autoregulatory loop of LMP1 expression and STAT activation in epithelial cells latently infected with Epstein-Barr virus. J Virol 77:4139-4148.

Chen J, Ueda K, Sakakibara S, Okuno T, Parravicini C, Corbellino M, and Yamanishi K. 2001b. Activation of latent Kaposi's sarcoma-associated herpesvirus by demethylation of the promoter of the lytic transactivator. Proc Natl Acad Sci U S A 98:4119-4124.

Chen SY, Lu J, Shih YC, and Tsai CH. 2002. Epstein-Barr virus latent membrane protein 2A regulates c-Jun protein through extracellular signal-regulated kinase. J Virol 76:9556-9561.

Cheng EH, Nicholas J, Bellows DS, Hayward GS, Guo HG, Reitz MS, and Hardwick JM. 1997. A Bcl-2 homolog encoded by Kaposi sarcoma-associated virus, human herpesvirus 8, inhibits apoptosis but does not heterodimerize with Bax or Bak. Proc Natl Acad Sci U S A 94:690-694.

Cheng G, Cleary AM, Ye ZS, Hong DI, Lederman S, and Baltimore D. 1995. Involvement of CRAF1, a relative of TRAF, in CD40 signaling. Science 267:1494-1498.

Choi JK, Lee BS, Shim SN, Li M, and Jung JU. 2000a. Identification of the novel K15 gene at the rightmost end of the Kaposi's sarcoma-associated herpesvirus genome. J Virol 74:436-446.

Choi JK, Ishido S, and Jung JU. 2000b. The collagen repeat sequence is a determinant of the degree of herpesvirus saimiri STP transforming activity. J Virol 74:8102-8110.

Chou J and Roizman B. 1986. The terminal a sequence of the herpes simplex virus genome contains the promoter of a gene located in the repeat sequences of the L component. J Virol 57:629-637.

Ciufo DM, Cannon JS, Poole LJ, Wu FY, Murray P, Ambinder RF, and Hayward GS. 2001. Spindle cell conversion by Kaposi's sarcoma-associated herpesvirus: formation of colonies and plaques with mixed lytic and latent gene expression in infected primary dermal microvascular endothelial cell cultures. J Virol 75:5614-5626.

Clausse B, Fizazi K, Walczak V, Tetaud C, Wiels J, Tursz T, and Busson P. 1997. High concentration of the EBV latent membrane protein 1 in glycosphingolipid-rich complexes from both epithelial and lymphoid cells. Virology 228:285-293.

Clements GB, Klein G, and Povey S. 1975. Production by EBV infection of an EBNA-positive subline from an EBNA-negative human lymphoma cell line without detectable EBV DNA. Int J Cancer 16:125-133.

Coffin WF, III, Erickson KD, Hoedt-Miller M, and Martin JM. 2001. The cytoplasmic amino-terminus of the Latent Membrane Protein-1 of Epstein-Barr Virus: relationship between transmembrane orientation and effector functions of the carboxy-terminus and transmembrane domain. Oncogene 20:5313-5330.

Coffin WF, III, Geiger TR, and Martin JM. 2003. Transmembrane domains 1 and 2 of the latent membrane protein 1 of Epstein-Barr virus contain a lipid raft targeting signal and play a critical role in cytostasis. J Virol 77:3749-3758.

Cook PM, Whitby D, Calabro ML, Luppi M, Kakoola DN, Hjalgrim H, Ariyoshi K, Ensoli B, Davison AJ, and Schulz TF. 1999. Variability and evolution of Kaposi's sarcoma-associated herpesvirus in Europe and Africa. International Collaborative Group. AIDS 13:1165-1176.

Cook RD, Hodgson TA, Waugh AC, Molyneux EM, Borgstein E, Sherry A, Teo CG, and Porter SR. 2002. Mixed patterns of transmission of human herpesvirus-8 (Kaposi's sarcoma-associated herpesvirus) in Malawian families. J Gen Virol 83:1613-1619.

Coscoy L and Ganem D. 2000. Kaposi's sarcoma-associated herpesvirus encodes two proteins that block cell surface display of MHC class I chains by enhancing their endocytosis. Proc Natl Acad Sci U S A 97:8051-8056.

Coscoy L and Ganem D. 2001. A viral protein that selectively downregulates ICAM-1 and B7-2 and modulates T cell costimulation. J Clin Invest 107:1599-1606.

Couet J, Li S, Okamoto T, Ikezu T, and Lisanti MP. 1997. Identification of peptide and protein ligands for the caveolin-scaffolding domain. Implications for the interaction of caveolin with caveolae-associated proteins. J Biol Chem 272:6525-6533.

Couty JP, Geras-Raaka E, Weksler BB, and Gershengorn MC. 2001. Kaposi's sarcoma-associated herpesvirus G protein-coupled receptor signals through multiple pathways in endothelial cells. J Biol Chem 276:33805-33811.

Cuomo L, Ramquist T, Trivedi P, Wang F, Klein G, and Masucci MG. 1992. Expression of the Epstein-Barr virus (EBV)-encoded membrane protein LMP1 impairs the in vitro growth, clonability and tumorigenicity of an EBV-negative Burkitt lymphoma line. Int J Cancer 51:949-955.

D'Souza BN, Edelstein LC, Pegman PM, Smith SM, Loughran ST, Clarke A, Mehl A, Rowe M, Gelinas C, and Walls D. 2004. Nuclear factor kappa B-dependent activation of the antiapoptotic bfl-1 gene by the Epstein-Barr virus latent membrane protein 1 and activated CD40 receptor. J Virol 78:1800-1816.

Dairaghi DJ, Fan RA, McMaster BE, Hanley MR, and Schall TJ. 1999. HHV8-encoded vMIP-I selectively engages chemokine receptor CCR8. Agonist and antagonist profiles of viral chemokines. J Biol Chem 274:21569-21574.

Damania B, Li M, Choi JK, Alexander L, Jung JU, and Desrosiers RC. 1999. Identification of the R1 oncogene and its protein product from the rhadinovirus of rhesus monkeys. J Virol 73:5123-5131.

Damania B, DeMaria M, Jung JU, and Desrosiers RC. 2000a. Activation of lymphocyte signaling by the R1 protein of rhesus monkey rhadinovirus. J Virol 74:2721-2730.

Damania B, Choi JK, and Jung JU. 2000b. Signaling activities of gammaherpesvirus membrane proteins. J Virol 74:1593-1601.

Daniel MD, Melendez LV, Hunt RD, King NW, Anver M, Fraser CE, Barahona H, and Baggs RB. 1974. Herpesvirus saimiri: VII. Induction of malignant lymphoma in New Zealand white rabbits. J Natl Cancer Inst 53:1803-1807.

Dawson CW, Rickinson AB, and Young LS. 1990. Epstein-Barr virus latent membrane protein inhibits human epithelial cell differentiation. Nature 344:777-780.

Dawson CW, George JH, Blake SM, Longnecker R, and Young LS. 2001. The Epstein-Barr virus encoded latent membrane protein 2A augments signaling from latent membrane protein 1. Virology 289:192-207.

Dawson CW, Tramountanis G, Eliopoulos AG, and Young LS. 2003. Epstein-Barr virus latent membrane protein 1 (LMP1) activates the phosphatidylinositol 3-kinase/Akt pathway to promote cell survival and induce actin filament remodeling. J Biol Chem 278:3694-3704.

Dedicoat M and Newton R. 2003. Review of the distribution of Kaposi's sarcoma-associated herpesvirus (KSHV) in Africa in relation to the incidence of Kaposi's sarcoma. Br J Cancer 88:1-3.

Dedicoat M, Newton R, Alkharsah K, Sheldon J, Szabados I, Ndlovu B, Page T, Casabonne D, Gilks C, Cassol S, Whitby D, Schulz TF. 2004. Mother to child transmission of human herpesvirus 8 in South Africa. J. Inf. Dis. in press.

Deng H, Young A, and Sun R. 2000. Auto-activation of the rta gene of human herpesvirus-8/Kaposi's sarcoma-associated herpesvirus. J Gen Virol 81:3043-3048.

Derijard B, Hibi M, Wu IH, Barrett T, Su B, Deng T, Karin M, and Davis RJ. 1994. JNK1: a protein kinase stimulated by UV light and Ha-Ras that binds and phosphorylates the c-Jun activation domain. Cell 76:1025-1037.

Desrosiers RC and Falk LA. 1982. Herpesvirus saimiri strain variability. J Virol 43:352-356.

Desrosiers RC, Bakker A, Kamine J, Falk LA, Hunt RD, and King NW. 1985. A region of the Herpesvirus saimiri genome required for oncogenicity. Science 228:184-187.

Desrosiers RC, Silva DP, Waldron LM, and Letvin NL. 1986. Nononcogenic deletion mutants of herpesvirus saimiri are defective for in vitro immortalization. J Virol 57:701-705.

Desrosiers RC, Sasseville VG, Czajak SC, Zhang X, Mansfield KG, Kaur A, Johnson RP, Lackner AA, and Jung JU. 1997. A herpesvirus of rhesus monkeys related to the human Kaposi's sarcoma-associated herpesvirus. J Virol 71:9764-9769.

Devergne O, Hatzivassiliou E, Izumi KM, Kaye KM, Kleijnen MF, Kieff E, and Mosialos G. 1996. Association of TRAF1, TRAF2, and TRAF3 with an Epstein-Barr virus LMP1 domain important for B-lymphocyte transformation: role in NF-kappaB activation. Mol Cell Biol 16:7098-7108.

Devergne O, Cahir McFarland ED, Mosialos G, Izumi KM, Ware CF, and Kieff E. 1998. Role of the TRAF binding site and NF-kappaB activation in Epstein-Barr virus latent membrane protein 1-induced cell gene expression. J Virol 72:7900-7908.

Dirmeier U, Neuhierl B, Kilger E, Reisbach G, Sandberg ML, and Hammerschmidt W. 2003. Latent membrane protein 1 is critical for efficient growth transformation of human B-cells by epstein-barr virus. Cancer Res 63:2982-2989.

Djerbi M, Screpanti V, Catrina AI, Bogen B, Biberfeld P, and Grandien A. 1999. The inhibitor of death receptor signaling, FLICE-inhibitory protein defines a new class of tumor progression factors. J Exp Med 190:1025-1032.

Dorn P, DaSilva L, Martarano L, and Derse D. 1990. Equine infectious anemia virus tat: insights into the structure, function, and evolution of lentivirus trans-activator proteins. J Virol 64:1616-1624.

Dourmishev LA, Dourmishev AL, Palmeri D, Schwartz RA, and Lukac DM. 2003. Molecular genetics of Kaposi's sarcoma-associated herpesvirus (human herpesvirus-8) epidemiology and pathogenesis. Microbiol Mol Biol Rev 67:175-212, table.

Duboise SM, Guo J, Czajak S, Desrosiers RC, and Jung JU. 1998a. STP and Tip are essential for herpesvirus saimiri oncogenicity. J Virol 72:1308-1313.

Duboise SM, Lee H, Guo J, Choi JK, Czajak S, Simon M, Desrosiers RC, and Jung JU. 1998b. Mutation of the Lck-binding motif of Tip enhances lymphoid cell activation by herpesvirus saimiri. J Virol 72:2607-2614.

Dudley DT, Pang L, Decker SJ, Bridges AJ, and Saltiel AR. 1995. A synthetic inhibitor of the mitogen-activated protein kinase cascade. Proc Natl Acad Sci U S A 92:7686-7689.

Dumitru CD, Ceci JD, Tsatsanis C, Kontoyiannis D, Stamatakis K, Lin JH, Patriotis C, Jenkins NA, Copeland NG, Kollias G, and Tsichlis PN. 2000. TNF-alpha induction by LPS is regulated posttranscriptionally via a Tpl2/ERK-dependent pathway. Cell 103:1071-1083.

Duro D, Schulze A, Vogt B, Bartek J, Mittnacht S, and Jansen-Durr P. 1999. Activation of cyclin A gene expression by the cyclin encoded by human herpesvirus-8. J Gen Virol 80 (Pt 3):549-555.

Dykstra ML, Longnecker R, and Pierce SK. 2001. Epstein-Barr virus coopts lipid rafts to block the signaling and antigen transport functions of the BCR. Immunity 14:57-67.

Eliopoulos AG, Dawson CW, Mosialos G, Floettmann JE, Rowe M, Armitage RJ, Dawson J, Zapata JM, Kerr DJ, Wakelam MJ, Reed JC, Kieff E, and Young LS. 1996. CD40-induced growth inhibition in epithelial cells is mimicked by Epstein-Barr Virus-encoded LMP1: involvement of TRAF3 as a common mediator. Oncogene 13:2243-2254.

Eliopoulos AG, Stack M, Dawson CW, Kaye KM, Hodgkin L, Sihota S, Rowe M, and Young LS. 1997. Epstein-Barr virus-encoded LMP1 and CD40 mediate IL-6 production in epithelial cells via an NF-kappaB pathway involving TNF receptor-associated factors. Oncogene 14:2899-2916.

Eliopoulos AG and Young LS. 1998. Activation of the cJun N-terminal kinase (JNK) pathway by the Epstein-Barr virus-encoded latent membrane protein 1 (LMP1). Oncogene 16:1731-1742.

Eliopoulos AG, Gallagher NJ, Blake SM, Dawson CW, and Young LS. 1999a. Activation of the p38 mitogen-activated protein kinase pathway by Epstein-Barr virus-encoded latent membrane protein 1 coregulates interleukin-6 and interleukin-8 production. J Biol Chem 274:16085-16096.

Eliopoulos AG, Blake SM, Floettmann JE, Rowe M, and Young LS. 1999b. Epstein-Barr virus-encoded latent membrane protein 1 activates the JNK pathway through its extreme C terminus via a mechanism involving TRADD and TRAF2. J Virol 73:1023-1035.

Eliopoulos AG and Young LS. 2001. LMP1 structure and signal transduction. Semin Cancer Biol 11:435-444.

Eliopoulos AG, Davies C, Blake SS, Murray P, Najafipour S, Tsichlis PN, and Young LS. 2002. The oncogenic protein kinase Tpl-2/Cot contributes to Epstein-Barr virus-encoded latent infection membrane protein 1-induced NF-kappaB signaling downstream of TRAF2. J Virol 76:4567-4579.

Eliopoulos AG, Caamano JH, Flavell J, Reynolds GM, Murray PG, Poyet JL, and Young LS. 2003a. Epstein-Barr virus-encoded latent infection membrane protein 1 regulates the processing of p100 NF-kappaB2 to p52 via an IKKgamma/NEMO-independent signaling pathway. Oncogene 22:7557-7569.

Eliopoulos AG, Waites ER, Blake SM, Davies C, Murray P, and Young LS. 2003b. TRAF1 is a critical regulator of JNK signaling by the TRAF-binding domain of the Epstein-Barr virus-encoded latent infection membrane protein 1 but not CD40. J Virol 77:1316-1328.

Ellis M, Chew YP, Fallis L, Freddersdorf S, Boshoff C, Weiss RA, Lu X, and Mittnacht S. 1999. Degradation of p27(Kip) cdk inhibitor triggered by Kaposi's sarcoma virus cyclin-cdk6 complex. EMBO J 18:644-653.

Endres MJ, Garlisi CG, Xiao H, Shan L, and Hedrick JA. 1999. The Kaposi's sarcoma-related herpesvirus (KSHV)-encoded chemokine vMIP-I is a specific agonist for the CC chemokine receptor (CCR)8. J Exp Med 189:1993-1998.

Engels N, Merchant M, Pappu R, Chan AC, Longnecker R, and Wienands J. 2001. Epstein-Barr virus latent membrane protein 2A (LMP2A) employs the SLP-65 signaling module. J Exp Med 194:255-264.

Erickson KD and Martin JM. 1997. Early detection of the lytic LMP-1 protein in EBV-infected B-cells suggests its presence in the virion. Virology 234:1-13.

Erickson KD and Martin JM. 2000. The late lytic LMP-1 protein of Epstein-Barr virus can negatively regulate LMP-1 signaling. J Virol 74:1057-1060.

Fahraeus R, Rymo L, Rhim JS, and Klein G. 1990. Morphological transformation of human keratinocytes expressing the LMP gene of Epstein-Barr virus. Nature 345:447-449.

Fahraeus R, Chen W, Trivedi P, Klein G, and Obrink B. 1992. Decreased expression of E-cadherin and increased invasive capacity in EBV-LMP-transfected human epithelial and murine adenocarcinoma cells. Int J Cancer 52:834-838.

Fairbairn LJ, Stewart JP, Hampson IN, Arrand JR, and Dexter TM. 1993. Expression of Epstein-Barr virus latent membrane protein influences self-renewal and differentiation in a multipotential murine haemopoietic 'stem cell' line. J Gen Virol 74 (Pt 2):247-254.

Falk LA, Wolfe LG, and Deinhardt F. 1972. Isolation of Herpesvirus saimiri from blood of squirrel monkeys (Saimiri sciureus). J Natl Cancer Inst 48:1499-1505.

Farrell PJ. 1995. Epstein-Barr virus immortalizing genes. Trends Microbiol 3:105-109.

Favata MF, Horiuchi KY, Manos EJ, Daulerio AJ, Stradley DA, Feeser WS, Van Dyk DE, Pitts WJ, Earl RA, Hobbs F, Copeland RA, Magolda RL, Scherle PA, and Trzaskos JM. 1998. Identification of a novel inhibitor of mitogen-activated protein kinase kinase. J Biol Chem 273:18623-18632.

Fennewald S, van S, V, and Kieff E. 1984. Nucleotide sequence of an mRNA transcribed in latent growth-transforming virus infection indicates that it may encode a membrane protein. J Virol 51:411-419.

Fickenscher H, Bokel C, Knappe A, Biesinger B, Meinl E, Fleischer B, Fleckenstein B, and Broker BM. 1997. Functional phenotype of transformed human alphabeta and gammadelta T cells determined by different subgroup C strains of herpesvirus Saimiri. J Virol 71:2252-2263.

Fickenscher H and Fleckenstein B. 2001. Herpesvirus saimiri. Philos Trans R Soc Lond B Biol Sci 356:545-567.

Flanagan J, Middeldorp J, and Sculley T. 2003. Localization of the Epstein-Barr virus protein LMP 1 to exosomes. J Gen Virol 84:1871-1879.

Floettmann JE, Ward K, Rickinson AB, and Rowe M. 1996. Cytostatic effect of Epstein-Barr virus latent membrane protein-1 analyzed using tetracycline-regulated expression in B-cell lines. Virology 223:29-40.

Floettmann JE and Rowe M. 1997. Epstein-Barr virus latent membrane protein-1 (LMP1) C-terminus activation region 2 (CTAR2) maps to the far C-terminus and requires oligomerisation for NF-kappaB activation. Oncogene 15:1851-1858.

Floettmann JE, Eliopoulos AG, Jones M, Young LS, and Rowe M. 1998. Epstein-Barr virus latent membrane protein-1 (LMP1) signaling is distinct from CD40 and involves physical cooperation of its two C-terminus functional regions. Oncogene 17:2383-2392.

Flore O, Rafii S, Ely S, O'Leary JJ, Hyjek EM, and Cesarman E. 1998. Transformation of primary human endothelial cells by Kaposi's sarcoma-associated herpesvirus. Nature 394:588-592.

Flory E, Hoffmeyer A, Smola U, Rapp UR, and Bruder JT. 1996. Raf-1 kinase targets GA-binding protein in transcriptional regulation of the human immunodeficiency virus type 1 promoter. J Virol 70:2260-2268.

Foreman KE, Friborg J, Jr., Kong WP, Woffendin C, Polverini PJ, Nickoloff BJ, and Nabel GJ. 1997. Propagation of a human herpesvirus from AIDS-associated Kaposi's sarcoma. N Engl J Med 336:163-171.

Frank R. 2002. The SPOT-synthesis technique. Synthetic peptide arrays on membrane supports – principles and applications. J Immunological Methods 267 (1):13-26.

Franken M, Devergne O, Rosenzweig M, Annis B, Kieff E, and Wang F. 1996. Comparative analysis identifies conserved tumor necrosis factor receptor-associated factor 3 binding sites in the human and simian Epstein-Barr virus oncogene LMP1. J Virol 70:7819-7826.

Friborg J, Jr., Kong W, Hottiger MO, and Nabel GJ. 1999. p53 inhibition by the LANA protein of KSHV protects against cell death. Nature 402:889-894.

Fries KL, Miller WE, and Raab-Traub N. 1996. Epstein-Barr virus latent membrane protein 1 blocks p53-mediated apoptosis through the induction of the A20 gene. J Virol 70:8653-8659.

Fruehling S, Lee SK, Herrold R, Frech B, Laux G, Kremmer E, Grasser FA, and Longnecker R. 1996. Identification of latent membrane protein 2A (LMP2A) domains essential for the LMP2A dominant-negative effect on B-lymphocyte surface immunoglobulin signal transduction. J Virol 70:6216-6226.

Fruehling S and Longnecker R. 1997. The immunoreceptor tyrosine-based activation motif of Epstein-Barr virus LMP2A is essential for blocking BCR-mediated signal transduction. Virology 235:241-251.

Fruehling S, Swart R, Dolwick KM, Kremmer E, and Longnecker R. 1998. Tyrosine 112 of latent membrane protein 2A is essential for protein tyrosine kinase loading and regulation of Epstein-Barr virus latency. J Virol 72:7796-7806.

Fu C, Turck CW, Kurosaki T, and Chan AC. 1998. BLNK: a central linker protein in B-cell activation. Immunity 9:93-103.

Fujimuro M, Wu FY, ApRhys C, Kajumbula H, Young DB, Hayward GS, and Hayward SD. 2003. A novel viral mechanism for dysregulation of beta-catenin in Kaposi's sarcoma-associated herpesvirus latency. Nat Med 9:300-306.

Galbiati F, Razani B, and Lisanti MP. 2001. Emerging themes in lipid rafts and caveolae. Cell 106:403-411.

Gao SJ, Boshoff C, Jayachandra S, Weiss RA, Chang Y, and Moore PS. 1997. KSHV ORF K9 (vIRF) is an oncogene which inhibits the interferon signaling pathway. Oncogene 15:1979-1985.

Garber AC, Shu MA, Hu J, and Renne R. 2001. DNA binding and modulation of gene expression by the latency-associated nuclear antigen of Kaposi's sarcoma-associated herpesvirus. J Virol 75:7882-7892.

Garber AC, Hu J, and Renne R. 2002. Latency-associated nuclear antigen (LANA) cooperatively binds to two sites within the terminal repeat, and both sites contribute to the ability of LANA to suppress transcription and to facilitate DNA replication. J Biol Chem 277:27401-27411.

Gaubatz S, Lindeman GJ, Ishida S, Jakoi L, Nevins JR, Livingston DM, and Rempel RE. 2000. E2F4 and E2F5 play an essential role in pocket protein-mediated G1 control. Mol Cell 6:729-735.

Geck P, Whitaker SA, Medveczky MM, and Medveczky PG. 1990. Expression of collagenlike sequences by a tumor virus, herpesvirus saimiri. J Virol 64:3509-3515.

Gessain A, Mauclere P, van Beveren M, Plancoulaine S, Ayouba A, Essame-Oyono JL, Martin PM, and de The G. 1999. Human herpesvirus 8 primary infection occurs during childhood in Cameroon, Central Africa. Int J Cancer 81:189-192.

Ghosh S and Karin M. 2002. Missing pieces in the NF-kappaB puzzle. Cell 109 Suppl:S81-S96.

Gires O, Zimber-Strobl U, Gonnella R, Ueffing M, Marschall G, Zeidler R, Pich D, and Hammerschmidt W. 1997. Latent membrane protein 1 of Epstein-Barr virus mimics a constitutively active receptor molecule. EMBO J 16:6131-6140.

Gires O, Kohlhuber F, Kilger E, Baumann M, Kieser A, Kaiser C, Zeidler R, Scheffer B, Ueffing M, and Hammerschmidt W. 1999. Latent membrane protein 1 of Epstein-Barr virus interacts with JAK3 and activates STAT proteins. EMBO J 18:3064-3073.

Glenn M, Rainbow L, Aurade F, Davison A, and Schulz TF. 1999. Identification of a spliced gene from Kaposi's sarcoma-associated herpesvirus encoding a protein with similarities to latent membrane proteins 1 and 2A of Epstein-Barr virus. J Virol 73:6953-6963.

Greensill J and Schulz TF. 2000. Rhadinoviruses (gamma2-herpesviruses) of Old World primates: models for KSHV/HHV8-associated disease? AIDS 14 Suppl 3:S11-S19.

Gregory CD, Dive C, Henderson S, Smith CA, Williams GT, Gordon J, and Rickinson AB. 1991. Activation of Epstein-Barr virus latent genes protects human B-cells from death by apoptosis. Nature 349:612-614.

Groves AK, Cotter MA, Subramanian C, and Robertson ES. 2001. The latency-associated nuclear antigen encoded by Kaposi's sarcoma-associated herpesvirus activates two major essential Epstein-Barr virus latent promoters. J Virol 75:9446-9457.

Guo J, Duboise M, Lee H, Li M, Choi JK, Rosenzweig M, and Jung JU. 1997. Enhanced downregulation of Lck-mediated signal transduction by a Y114 mutation of herpesvirus Saimiri tip. J Virol 71:7092-7096.

Guo J, Williams K, Duboise SM, Alexander L, Veazey R, and Jung JU. 1998. Substitution of ras for the herpesvirus saimiri STP oncogene in lymphocyte transformation. J Virol 72:3698-3704.

Gurezka R, Laage R, Brosig B, and Langosch D. 1999. A heptad motif of leucine residues found in membrane proteins can drive self-assembly of artificial transmembrane segments. J Biol Chem 274:9265-9270.

Gwack Y, Hwang S, Lim C, Won YS, Lee CH, and Choe J. 2002. Kaposi's Sarcoma-associated herpesvirus open reading frame 50 stimulates the transcriptional activity of STAT3. J Biol Chem 277:6438-6442.

Gwack Y, Baek HJ, Nakamura H, Lee SH, Meisterernst M, Roeder RG, and Jung JU. 2003. Principal role of TRAP/mediator and SWI/SNF complexes in Kaposi's sarcoma-associated herpesvirus RTA-mediated lytic reactivation. Mol Cell Biol 23:2055-2067.

Hagemann D, Troppmair J, and Rapp UR. 1999. Cot protooncoprotein activates the dual specificity kinases MEK-1 and SEK-1 and induces differentiation of PC12 cells. Oncogene 18:1391-1400.

Hammarskjold ML and Simurda MC. 1992. Epstein-Barr virus latent membrane protein transactivates the human immunodeficiency virus type 1 long terminal repeat through induction of NF-kappa B activity. J Virol 66:6496-6501.

Hammerschmidt W, Sugden B, and Baichwal VR. 1989. The transforming domain alone of the latent membrane protein of Epstein-Barr virus is toxic to cells when expressed at high levels. J Virol 63:2469-2475.

Hammond C, Braakman I, and Helenius A. 1994. Role of N-linked oligosaccharide recognition, glucose trimming, and calnexin in glycoprotein folding and quality control. Proc Natl Acad Sci U S A 91:913-917.

Haque M, Chen J, Ueda K, Mori Y, Nakano K, Hirata Y, Kanamori S, Uchiyama Y, Inagi R, Okuno T, and Yamanishi K. 2000. Identification and analysis of the K5 gene of Kaposi's sarcoma-associated herpesvirus. J Virol 74:2867-2875.

Hartley DA, Hurley TR, Hardwick JS, Lund TC, Medveczky PG, and Sefton BM. 1999. Activation of the lck tyrosine-protein kinase by the binding of the tip protein of herpesvirus saimiri in the absence of regulatory tyrosine phosphorylation. J Biol Chem 274:20056-20059.

Hartley DA, Amdjadi K, Hurley TR, Lund TC, Medveczky PG, and Sefton BM. 2000. Activation of the Lck tyrosine protein kinase by the Herpesvirus saimiri tip protein involves two binding interactions. Virology 276:339-348.

Hartley DA and Cooper GM. 2000. Direct binding and activation of STAT transcription factors by the herpesvirus saimiri protein tip. J Biol Chem 275:16925-16932.

Hatzivassiliou E, Miller WE, Raab-Traub N, Kieff E, and Mosialos G. 1998. A fusion of the EBV latent membrane protein-1 (LMP1) transmembrane domains to the CD40 cytoplasmic domain is similar to LMP1 in constitutive activation of epidermal growth factor receptor expression, nuclear factor-kappa B, and stress-activated protein kinase. J Immunol 160:1116-1121.

Hayward GS. 1999. KSHV strains: the origins and global spread of the virus. Semin Cancer Biol 9:187-199.

Hayward GS. 2003. Initiation of angiogenic Kaposi's sarcoma lesions. Cancer Cell 3:1-3.

He Z, Xin B, Yang X, Chan C, and Cao L. 2000. Nuclear factor-kappaB activation is involved in LMP1-mediated transformation and tumorigenesis of rat-1 fibroblasts. Cancer Res 60:1845-1848.

Henderson S, Rowe M, Gregory C, Croom-Carter D, Wang F, Longnecker R, Kieff E, and Rickinson A. 1991. Induction of bcl-2 expression by Epstein-Barr virus latent membrane protein 1 protects infected B-cells from programmed cell death. Cell 65:1107-1115.

Hennessy K, Fennewald S, Hummel M, Cole T, and Kieff E. 1984. A membrane protein encoded by Epstein-Barr virus in latent growth-transforming infection. Proc Natl Acad Sci U S A 81:7207-7211.

Higuchi M, Izumi KM, and Kieff E. 2001. Epstein-Barr virus latent-infection membrane proteins are palmitoylated and raft-associated: protein 1 binds to the cytoskeleton through TNF receptor cytoplasmic factors. Proc Natl Acad Sci U S A 98:4675-4680.

Higuchi M, Kieff E, and Izumi KM. 2002. The Epstein-Barr virus latent membrane protein 1 putative Janus kinase 3 (JAK3) binding domain does not mediate JAK3 association or activation in B-lymphoma or lymphoblastoid cell lines. J Virol 76:455-459.

Hor S, Ensser A, Reiss C, Ballmer-Hofer K, and Biesinger B. 2001. Herpesvirus saimiri protein StpB associates with cellular Src. J Gen Virol 82:339-344.

Hsu H, Shu HB, Pan MG, and Goeddel DV. 1996. TRADD-TRAF2 and TRADD-FADD interactions define two distinct TNF receptor 1 signal transduction pathways. Cell 84:299-308.

Hu HM, O'Rourke K, Boguski MS, and Dixit VM. 1994. A novel RING finger protein interacts with the cytoplasmic domain of CD40. J Biol Chem 269:30069-30072.

Hu LF, Zabarovsky ER, Chen F, Cao SL, Ernberg I, Klein G, and Winberg G. 1991. Isolation and sequencing of the Epstein-Barr virus BNLF-1 gene (LMP1) from a Chinese nasopharyngeal carcinoma. J Gen Virol 72 (Pt 10):2399-2409.

Hu LF, Chen F, Zheng X, Ernberg I, Cao SL, Christensson B, Klein G, and Winberg G. 1993. Clonability and tumorigenicity of human epithelial cells expressing the EBV encoded membrane protein LMP1. Oncogene 8:1575-1583.

Hudson GS, Farrell PJ, and Barrell BG. 1985. Two related but differentially expressed potential membrane proteins encoded by the EcoRI Dhet region of Epstein-Barr virus B95-8. J Virol 53:528-535.

Huen DS, Henderson SA, Croom-Carter D, and Rowe M. 1995. The Epstein-Barr virus latent membrane protein-1 (LMP1) mediates activation of NF-kappa B and cell surface phenotype via two effector regions in its carboxy-terminal cytoplasmic domain. Oncogene 10:549-560.

Hunt RD, Melendez LV, King NW, and Garcia FG. 1972. Herpesvirus saimiri malignant lymphoma in spider monkeys. A new susceptible host. J Med Primatol 1:114-128.

Hyun TS, Subramanian C, Cotter MA, Thomas RA, and Robertson ES. 2001. Latency-associated nuclear antigen encoded by Kaposi's sarcoma-associated herpesvirus interacts with Tat and activates the long terminal repeat of human immunodeficiency virus type 1 in human cells. J Virol 75:8761-8771.

Ikeda A, Caldwell RG, Longnecker R, and Ikeda M. 2003. Itchy, a Nedd4 ubiquitin ligase, downregulates latent membrane protein 2A activity in B-cell signaling. J Virol 77:5529-5534.

Ikeda M, Ikeda A, Longan LC, and Longnecker R. 2000. The Epstein-Barr virus latent membrane protein 2A PY motif recruits WW domain-containing ubiquitin-protein ligases. Virology 268:178-191.

Ikeda M, Ikeda A, and Longnecker R. 2001. PY motifs of Epstein-Barr virus LMP2A regulate protein stability and phosphorylation of LMP2A-associated proteins. J Virol 75:5711-5718.

Ikeda M, Ikeda A, and Longnecker R. 2002. Lysine-independent ubiquitination of Epstein-Barr virus LMP2A. Virology 300:153-159.

Inman GJ and Allday MJ. 2000. Resistance to TGF-beta1 correlates with a reduction of TGF-beta type II receptor expression in Burkitt's lymphoma and Epstein-Barr virus-transformed B lymphoblastoid cell lines. J Gen Virol 81:1567-1578.

Inoue N, Winter J, Lal RB, Offermann MK, and Koyano S. 2003. Characterization of entry mechanisms of human herpesvirus 8 by using an Rta-dependent reporter cell line. J Virol 77:8147-8152.

Irmler M, Thome M, Hahne M, Schneider P, Hofmann K, Steiner V, Bodmer JL, Schroter M, Burns K, Mattmann C, Rimoldi D, French LE, and Tschopp J. 1997. Inhibition of death receptor signals by cellular FLIP. Nature 388:190-195.

Isakov N and Biesinger B. 2000. Lck protein tyrosine kinase is a key regulator of T-cell activation and a target for signal intervention by Herpesvirus saimiri and other viral gene products. Eur J Biochem 267:3413-3421.

Ishiai M, Kurosaki M, Pappu R, Okawa K, Ronko I, Fu C, Shibata M, Iwamatsu A, Chan AC, and Kurosaki T. 1999. BLNK required for coupling Syk to PLC gamma 2 and Rac1-JNK in B-cells. Immunity 10:117-125.

Ishido S, Choi JK, Lee BS, Wang C, DeMaria M, Johnson RP, Cohen GB, and Jung JU. 2000b. Inhibition of natural killer cell-mediated cytotoxicity by Kaposi's sarcoma-associated herpesvirus K5 protein. Immunity 13:365-374.

Ishido S, Wang C, Lee BS, Cohen GB, and Jung JU. 2000a. Downregulation of major histocompatibility complex class I molecules by Kaposi's sarcoma-associated herpesvirus K3 and K5 proteins. J Virol 74:5300-5309.

Izumi KM, Kaye KM, and Kieff ED. 1994. Epstein-Barr virus recombinant molecular genetic analysis of the LMP1 amino-terminal cytoplasmic domain reveals a probable structural role, with no component essential for primary B-lymphocyte growth transformation. J Virol 68:4369-4376.

Izumi KM and Kieff ED. 1997. The Epstein-Barr virus oncogene product latent membrane protein 1 engages the tumor necrosis factor receptor-associated death domain protein to mediate B lymphocyte growth transformation and activate NF-kappaB. Proc Natl Acad Sci U S A 94:12592-12597.

Izumi KM, Kaye KM, and Kieff ED. 1997. The Epstein-Barr virus LMP1 amino acid sequence that engages tumor necrosis factor receptor associated factors is critical for primary B lymphocyte growth transformation. Proc Natl Acad Sci U S A 94:1447-1452.

Izumi KM, Cahir McFarland ED, Ting AT, Riley EA, Seed B, and Kieff ED. 1999a. The Epstein-Barr virus oncoprotein latent membrane protein 1 engages the tumor necrosis factor receptor-associated proteins TRADD and receptor-interacting protein (RIP) but does not induce apoptosis or require RIP for NF-kappaB activation. Mol Cell Biol 19:5759-5767.

Izumi KM, Cahir McFarland ED, Riley EA, Rizzo D, Chen Y, and Kieff E. 1999b. The residues between the two transformation effector sites of Epstein-Barr virus latent membrane protein 1 are not critical for B-lymphocyte growth transformation. J Virol 73:9908-9916.

Izumi KM. 2001. Identification of EBV transforming genes by recombinant EBV technology. Semin Cancer Biol 11:407-414.

Izumiya Y, Lin SF, Ellison T, Chen LY, Izumiya C, Luciw P, and Kung HJ. 2003. Kaposi's sarcoma-associated herpesvirus K-bZIP is a coregulator of K-Rta: physical association and promoter-dependent transcriptional repression. J Virol 77:1441-1451.

Jacobson LP, Jenkins FJ, Springer G, Munoz A, Shah KV, Phair J, Zhang Z, and Armenian H. 2000. Interaction of human immunodeficiency virus type 1 and human herpesvirus type 8 infections on the incidence of Kaposi's sarcoma. J Infect Dis 181:1940-1949.

Janes PW, Ley SC, and Magee AI. 1999. Aggregation of lipid rafts accompanies signaling via the T cell antigen receptor. J Cell Biol 147:447-461.

Jenner RG, Alba MM, Boshoff C, and Kellam P. 2001. Kaposi's sarcoma-associated herpesvirus latent and lytic gene expression as revealed by DNA arrays. J Virol 75:891-902.

Jeong J, Papin J, and Dittmer D. 2001. Differential regulation of the overlapping Kaposi's sarcoma-associated herpesvirus vGCR (orf74) and LANA (orf73) promoters. J Virol 75:1798-1807.

Jones KD, Aoki Y, Chang Y, Moore PS, Yarchoan R, and Tosato G. 1999. Involvement of interleukin-10 (IL-10) and viral IL-6 in the spontaneous growth of Kaposi's sarcoma herpesvirus-associated infected primary effusion lymphoma cells. Blood 94:2871-2879.

Judde JG, Lacoste V, Briere J, Kassa-Kelembho E, Clyti E, Couppie P, Buchrieser C, Tulliez M, Morvan J, and Gessain A. 2000. Monoclonality or oligoclonality of human herpesvirus 8 terminal repeat sequences in Kaposi's sarcoma and other diseases. J Natl Cancer Inst 92:729-736.

Jung JU, Trimble JJ, King NW, Biesinger B, Fleckenstein BW, and Desrosiers RC. 1991. Identification of transforming genes of subgroup A and C strains of Herpesvirus saimiri. Proc Natl Acad Sci U S A 88:7051-7055.

Jung JU and Desrosiers RC. 1991. Identification and characterization of the herpesvirus saimiri oncoprotein STP-C488. J Virol 65:6953-6960.

Jung JU and Desrosiers RC. 1992. Herpesvirus saimiri oncogene STP-C488 encodes a phosphoprotein. J Virol 66:1777-1780.

Jung JU and Desrosiers RC. 1994. Distinct functional domains of STP-C488 of herpesvirus saimiri. Virology 204:751-758.

Jung JU and Desrosiers RC. 1995. Association of the viral oncoprotein STP-C488 with cellular ras. Mol Cell Biol 15:6506-6512.

Jung JU, Lang SM, Jun T, Roberts TM, Veillette A, and Desrosiers RC. 1995a. Downregulation of Lck-mediated signal transduction by tip of herpesvirus saimiri. J Virol 69:7814-7822.

Jung JU, Lang SM, Friedrich U, Jun T, Roberts TM, Desrosiers RC, and Biesinger B. 1995b. Identification of Lck-binding elements in tip of herpesvirus saimiri. J Biol Chem 270:20660-20667.

Karin M, Liu Z, and Zandi E. 1997. AP-1 function and regulation. Curr Opin Cell Biol 9:240-246.

Karlin S, Mocarski ES, and Schachtel GA. 1994. Molecular evolution of herpesviruses: genomic and protein sequence comparisons. J Virol 68:1886-1902.

Kashiwada M, Shirakata Y, Inoue JI, Nakano H, Okazaki K, Okumura K, Yamamoto T, Nagaoka H, and Takemori T. 1998. Tumor necrosis factor receptor-associated factor 6 (TRAF6) stimulates extracellular signal-regulated kinase (ERK) activity in CD40 signaling along a ras-independent pathway. J Exp Med 187:237-244.

Kasolo FC, Monze M, Obel N, Anderson RA, French C, and Gompels UA. 1998. Sequence analyses of human herpesvirus-8 strains from both African human immunodeficiency virus-negative and -positive childhood endemic Kaposi's sarcoma show a close relationship with strains identified in febrile children and high variation in the K1 glycoprotein. J Gen Virol 79 (Pt 12):3055-3065.

Katano H, Sato Y, Kurata T, Mori S, and Sata T. 2000. Expression and localization of human herpesvirus 8-encoded proteins in primary effusion lymphoma, Kaposi's sarcoma, and multicentric Castleman's disease. Virology 269:335-344.

Kaye KM, Izumi KM, and Kieff E. 1993. Epstein-Barr virus latent membrane protein 1 is essential for B-lymphocyte growth transformation. Proc Natl Acad Sci U S A 90:9150-9154.

Kaye KM, Izumi KM, Mosialos G, and Kieff E. 1995. The Epstein-Barr virus LMP1 cytoplasmic carboxy terminus is essential for B-lymphocyte transformation; fibroblast cocultivation complements a critical function within the terminal 155 residues. J Virol 69:675-683.

Kaye KM, Devergne O, Harada JN, Izumi KM, Yalamanchili R, Kieff E, and Mosialos G. 1996. Tumor necrosis factor receptor associated factor 2 is a mediator of NF-kappa B activation by latent infection membrane protein 1, the Epstein-Barr virus transforming protein. Proc Natl Acad Sci U S A 93:11085-11090.

Kaye KM, Izumi KM, Li H, Johannsen E, Davidson D, Longnecker R, and Kieff E. 1999. An Epstein-Barr virus that expresses only the first 231 LMP1 amino acids efficiently initiates primary B-lymphocyte growth transformation. J Virol 73:10525-10530.

Kaykas A and Sugden B. 2000. The amino-terminus and membrane-spanning domains of LMP-1 inhibit cell proliferation. Oncogene 19:1400-1410.

Kaykas A, Worringer K, and Sugden B. 2001. CD40 and LMP-1 both signal from lipid rafts but LMP-1 assembles a distinct, more efficient signaling complex. EMBO J 20:2641-2654.

Kaykas A, Worringer K, and Sugden B. 2002. LMP-1's transmembrane domains encode multiple functions required for LMP-1's efficient signaling. J Virol 76:11551-11560.

Keller SA, Schattner EJ, and Cesarman E. 2000. Inhibition of NF-kappaB induces apoptosis of KSHV-infected primary effusion lymphoma cells. Blood 96:2537-2542.

Kieff E, and Rickinson AB. 2002. Epstein-Barr virus and its replication. In: Knipe DM, Howley PM, Griffin DE, Lamb RA, Martin MA, Roizman B, and Straus SE (ed.), Virology, 4th ed. Lippincott, Williams, and Wilkins, Philadelphia, PA: 2511-2573.

Kieser A, Seitz T, Adler HS, Coffer P, Kremmer E, Crespo P, Gutkind JS, Henderson DW, Mushinski JF, Kolch W, and Mischak H. 1996. Protein kinase C-zeta reverts v-raf transformation of NIH-3T3 cells. Genes Dev 10:1455-1466.

Kieser A, Kilger E, Gires O, Ueffing M, Kolch W, and Hammerschmidt W. 1997. Epstein-Barr virus latent membrane protein-1 triggers AP-1 activity via the c-Jun N-terminal kinase cascade. EMBO J 16:6478-6485.

Kieser A, Kaiser C, and Hammerschmidt W. 1999. LMP1 signal transduction differs substantially from TNF receptor 1 signaling in the molecular functions of TRADD and TRAF2. EMBO J 18:2511-2521.

Kilger E, Kieser A, Baumann M, and Hammerschmidt W. 1998. Epstein-Barr virus-mediated B-cell proliferation is dependent upon latent membrane protein 1, which simulates an activated CD40 receptor. EMBO J 17:1700-1709.

Kim KR, Yoshizaki T, Miyamori H, Hasegawa K, Horikawa T, Furukawa M, Harada S, Seiki M, and Sato H. 2000. Transformation of Madin-Darby canine kidney (MDCK) epithelial cells by Epstein-Barr virus latent membrane protein 1 (LMP1) induces expression of Ets1 and invasive growth. Oncogene 19:1764-1771.

Kim OJ and Yates JL. 1993. Mutants of Epstein-Barr virus with a selective marker disrupting the TP gene transform B-cells and replicate normally in culture. J Virol 67:7634-7640.

Kirchhoff S, Sebens T, Baumann S, Krueger A, Zawatzky R, Li-Weber M, Meinl E, Neipel F, Fleckenstein B, and Krammer PH. 2002. Viral IFN-regulatory factors inhibit activation-induced cell death via two positive regulatory IFN-regulatory factor 1-dependent domains in the CD95 ligand promoter. J Immunol 168:1226-1234.

Kjellen P, Amdjadi K, Lund TC, Medveczky PG, and Sefton BM. 2002. The herpesvirus saimiri tip484 and tip488 proteins both stimulate lck tyrosine protein kinase activity in vivo and in vitro. Virology 297:281-288.

Kledal TN, Rosenkilde MM, Coulin F, Simmons G, Johnsen AH, Alouani S, Power CA, Luttichau HR, Gerstoft J, Clapham PR, Clark-Lewis I, Wells TN, and Schwartz TW. 1997. A broad-spectrum chemokine antagonist encoded by Kaposi's sarcoma-associated herpesvirus. Science 277:1656-1659.

Kliche S, Kremmer E, Hammerschmidt W, Koszinowski U, and Haas J. 1998. Persistent infection of Epstein-Barr virus-positive B lymphocytes by human herpesvirus 8. J Virol 72:8143-8149.

Kliche S, Nagel W, Kremmer E, Atzler C, Ege A, Knorr T, Koszinowski U, Kolanus W, and Haas J. 2001. Signaling by human herpesvirus 8 kaposin A through direct membrane recruitment of cytohesin-1. Mol Cell 7:833-843.

Kretschmer C, Murphy C, Biesinger B, Beckers J, Fickenscher H, Kirchner T, Fleckenstein B, and Ruther U. 1996. A Herpes saimiri oncogene causing peripheral T-cell lymphoma in transgenic mice. Oncogene 12:1609-1616.

Krishnan HH, Naranatt PP, Smith MS, Zeng L, Bloomer C, and Chandran B. 2004. Concurrent expression of latent and a limited number of lytic genes with immune modulation and antiapoptotic function by Kaposi's sarcoma-associated herpesvirus early during infection of primary endothelial and fibroblast cells and subsequent decline of lytic gene expression. J Virol 78:3601-3620.

Krithivas A, Young DB, Liao G, Greene D, and Hayward SD. 2000. Human herpesvirus 8 LANA interacts with proteins of the mSin3 corepressor complex and negatively regulates Epstein-Barr virus gene expression in dually infected PEL cells. J Virol 74:9637-9645.

Kube D, Holtick U, Vockerodt M, Ahmadi T, Haier B, Behrmann I, Heinrich PC, Diehl V, and Tesch H. 2001. STAT3 is constitutively activated in Hodgkin cell lines. Blood 98:762-770.

Kulwichit W, Edwards RH, Davenport EM, Baskar JF, Godfrey V, and Raab-Traub N. 1998. Expression of the Epstein-Barr virus latent membrane protein 1 induces B-cell lymphoma in transgenic mice. Proc Natl Acad Sci U S A 95:11963-11968.

Lacoste V, Judde JG, Briere J, Tulliez M, Garin B, Kassa-Kelembho E, Morvan J, Couppie P, Clyti E, Forteza VJ, Rio B, Delmer A, Mauclere P, and Gessain A. 2000. Molecular epidemiology of human herpesvirus 8 in africa: both B and A5 K1 genotypes, as well as the M and P genotypes of K14.1/K15 loci, are frequent and widespread. Virology 278:60-74.

Lagunoff M and Roizman B. 1994. Expression of a herpes simplex virus 1 open reading frame antisense to the gamma(1)34.5 gene and transcribed by an RNA 3' coterminal with the unspliced latency-associated transcript. J Virol 68:6021-6028.

Lagunoff M and Ganem D. 1997. The structure and coding organization of the genomic termini of Kaposi's sarcoma-associated herpesvirus. Virology 236:147-154.

Lagunoff M, Majeti R, Weiss A, and Ganem D. 1999. Deregulated signal transduction by the K1 gene product of Kaposi's sarcoma-associated herpesvirus. Proc Natl Acad Sci U S A 96:5704-5709.

Lagunoff M, Lukac DM, and Ganem D. 2001. Immunoreceptor tyrosine-based activation motif-dependent signaling by Kaposi's sarcoma-associated herpesvirus K1 protein: effects on lytic viral replication. J Virol 75:5891-5898.

Lagunoff M, Bechtel J, Venetsanakos E, Roy AM, Abbey N, Herndier B, McMahon M, and Ganem D. 2002. De novo infection and serial transmission of Kaposi's sarcoma-associated herpesvirus in cultured endothelial cells. J Virol 76:2440-2448.

Laherty CD, Hu HM, Opipari AW, Wang F, and Dixit VM. 1992. The Epstein-Barr virus LMP1 gene product induces A20 zinc finger protein expression by activating nuclear factor kappa B. J Biol Chem 267:24157-24160.

Lam N and Sugden B. 2003. LMP1, a viral relative of the TNF receptor family, signals principally from intracellular compartments. EMBO J 22:3027-3038.

Laufs R and Melendez LV. 1973. Oncogenicity of Herpesvirus ateles in monkeys. J Natl Cancer Inst 51:599-608.

Laux G, Perricaudet M, and Farrell PJ. 1988. A spliced Epstein-Barr virus gene expressed in immortalized lymphocytes is created by circularization of the linear viral genome. EMBO J 7:769-774.

Laux G, Economou A, and Farrell PJ. 1989. The terminal protein gene 2 of Epstein-Barr virus is transcribed from a bidirectional latent promoter region. J Gen Virol 70 (Pt 11):3079-3084.

Lee BS, Alvarez X, Ishido S, Lackner AA, and Jung JU. 2000. Inhibition of intracellular transport of B-cell antigen receptor complexes by Kaposi's sarcoma-associated herpesvirus K1. J Exp Med 192:11-21.

Lee BS, Paulose-Murphy M, Chung YH, Connlole M, Zeichner S, and Jung JU. 2002. Suppression of tetradecanoyl phorbol acetate-induced lytic reactivation of Kaposi's sarcoma-associated herpesvirus by K1 signal transduction. J Virol 76:12185-12199.

Lee BS, Connole M, Tang Z, Harris NL, and Jung JU. 2003. Structural analysis of the Kaposi's sarcoma-associated herpesvirus K1 protein. J Virol 77:8072-8086.

Lee H, Trimble JJ, Yoon DW, Regier D, Desrosiers RC, and Jung JU. 1997. Genetic variation of herpesvirus saimiri subgroup A transforming protein and its association with cellular src. J Virol 71:3817-3825.

Lee H, Veazey R, Williams K, Li M, Guo J, Neipel F, Fleckenstein B, Lackner A, Desrosiers RC, and Jung JU. 1998a. Deregulation of cell growth by the K1 gene of Kaposi's sarcoma-associated herpesvirus. Nat Med 4:435-440.

Lee H, Guo J, Li M, Choi JK, DeMaria M, Rosenzweig M, and Jung JU. 1998b. Identification of an immunoreceptor tyrosine-based activation motif of K1 transforming protein of Kaposi's sarcoma-associated herpesvirus. Mol Cell Biol 18:5219-5228.

Lee H, Choi JK, Li M, Kaye K, Kieff E, and Jung JU. 1999. Role of cellular tumor necrosis factor receptor-associated factors in NF-kappaB activation and lymphocyte transformation by herpesvirus Saimiri STP. J Virol 73:3913-3919.

Li M, Damania B, Alvarez X, Ogryzko V, Ozato K, and Jung JU. 2000. Inhibition of p300 histone acetyltransferase by viral interferon regulatory factor. Mol Cell Biol 20:8254-8263.

Li SN, Chang YS, and Liu ST. 1996. Effect of a 10-amino acid deletion on the oncogenic activity of latent membrane protein 1 of Epstein-Barr virus. Oncogene 12:2129-2135.

Liang Y, Chang J, Lynch SJ, Lukac DM, and Ganem D. 2002. The lytic switch protein of KSHV activates gene expression via functional interaction with RBP-Jkappa (CSL), the target of the Notch signaling pathway. Genes Dev 16:1977-1989.

Lieberman PM, Hardwick JM, Sample J, Hayward GS, and Hayward SD. 1990. The zta transactivator involved in induction of lytic cycle gene expression in Epstein-Barr virus-infected lymphocytes binds to both AP-1 and ZRE sites in target promoter and enhancer regions. J Virol 64:1143-1155.

Liebowitz D, Wang D, and Kieff E. 1986. Orientation and patching of the latent infection membrane protein encoded by Epstein-Barr virus. J Virol 58:233-237.

Liebowitz D, Kopan R, Fuchs E, Sample J, and Kieff E. 1987. An Epstein-Barr virus transforming protein associates with vimentin in lymphocytes. Mol Cell Biol 7:2299-2308.

Liebowitz D, Mannick J, Takada K, and Kieff E. 1992. Phenotypes of Epstein-Barr virus LMP1 deletion mutants indicate transmembrane and amino-terminal cytoplasmic domains necessary for effects in B-lymphoma cells. J Virol 66:4612-4616.

Lin R, Genin P, Mamane Y, Sgarbanti M, Battistini A, Harrington WJ, Jr., Barber GN, and Hiscott J. 2001. HHV-8 encoded vIRF-1 represses the interferon antiviral response by blocking IRF-3 recruitment of the CBP/p300 coactivators. Oncogene 20:800-811.

Lin X, Cunningham ET, Jr., Mu Y, Geleziunas R, and Greene WC. 1999. The proto-oncogene Cot kinase participates in CD3/CD28 induction of NF-kappaB acting through the NF-kappaB-inducing kinase and IkappaB kinases. Immunity 10:271-280.

Liu C, Okruzhnov Y, Li H, and Nicholas J. 2001. Human herpesvirus 8 (HHV-8)-encoded cytokines induce expression of and autocrine signaling by vascular endothelial growth factor (VEGF) in HHV-8-infected primary-effusion lymphoma cell lines and mediate VEGF-independent antiapoptotic effects. J Virol 75:10933-10940.

Liu L, Eby MT, Rathore N, Sinha SK, Kumar A, and Chaudhary PM. 2002. The human herpes virus 8-encoded viral FLICE inhibitory protein physically associates with and persistently activates the Ikappa B kinase complex. J Biol Chem 277:13745-13751.

Liu LT, Peng JP, Chang HC, and Hung WC. 2003. RECK is a target of Epstein-Barr virus latent membrane protein 1. Oncogene 22:8263-8270.

Longan L and Longnecker R. 2000. Epstein-Barr virus latent membrane protein 2A has no growth-altering effects when expressed in differentiating epithelia. J Gen Virol 81:2245-2252.

Longnecker R and Kieff E. 1990. A second Epstein-Barr virus membrane protein (LMP2) is expressed in latent infection and colocalizes with LMP1. J Virol 64:2319-2326.

Longnecker R, Druker B, Roberts TM, and Kieff E. 1991. An Epstein-Barr virus protein associated with cell growth transformation interacts with a tyrosine kinase. J Virol 65:3681-3692.

Longnecker R, Miller CL, Miao XQ, Marchini A, and Kieff E. 1992. The only domain which distinguishes Epstein-Barr virus latent membrane protein 2A (LMP2A) from LMP2B is dispensable for lymphocyte infection and growth transformation in vitro; LMP2A is therefore nonessential. J Virol 66:6461-6469.

Longnecker R, Miller CL, Tomkinson B, Miao XQ, and Kieff E. 1993a. Deletion of DNA encoding the first five transmembrane domains of Epstein-Barr virus latent membrane proteins 2A and 2B. J Virol 67:5068-5074.

Longnecker R, Miller CL, Miao XQ, Tomkinson B, and Kieff E. 1993b. The last seven transmembrane and carboxy-terminal cytoplasmic domains of Epstein-Barr virus latent membrane protein 2 (LMP2) are dispensable for lymphocyte infection and growth transformation in vitro. J Virol 67:2006-2013.

Longnecker R. 1994. Biochemical and genetic studies of Epstein-Barr virus latent membrane protein 2. Leukemia 8 Suppl 1:S46-S50.

Longnecker R. 2000. Epstein-Barr virus latency: LMP2, a regulator or means for Epstein-Barr virus persistence? Adv Cancer Res 79:175-200.

Longnecker R, Merchant M, Brown ME, Fruehling S, Bickford JO, Ikeda M, and Harty RN. 2000. WW- and SH3-domain interactions with Epstein-Barr virus LMP2A. Exp Cell Res 257:332-340.

Lorenzo ME, Jung JU, and Ploegh HL. 2002. Kaposi's sarcoma-associated herpesvirus K3 utilizes the ubiquitin-proteasome system in routing class major histocompatibility complexes to late endocytic compartments. J Virol 76:5522-5531.

Low W, Harries M, Ye H, Du MQ, Boshoff C, and Collins M. 2001. Internal ribosome entry site regulates translation of Kaposi's sarcoma-associated herpesvirus FLICE inhibitory protein. J Virol 75:2938-2945.

Ludwig S, Engel K, Hoffmeyer A, Sithanandam G, Neufeld B, Palm D, Gaestel M, and Rapp UR. 1996. 3pK, a novel mitogen-activated protein (MAP) kinase-activated protein kinase, is targeted by three MAP kinase pathways. Mol Cell Biol 16:6687-6697.

Ludwig S, Hoffmeyer A, Goebeler M, Kilian K, Hafner H, Neufeld B, Han J, and Rapp UR. 1998. The stress inducer arsenite activates mitogen-activated protein kinases extracellular signal-regulated kinases 1 and 2 via a MAPK kinase 6/p38-dependent pathway. J Biol Chem 273:1917-1922.

Luftig MA, Cahir-McFarland E, Mosialos G, and Kieff E. 2001. Effects of the NIK aly mutation on NF-kappaB activation by the Epstein-Barr virus latent infection membrane protein, lymphotoxin beta receptor, and CD40. J Biol Chem 276:14602-14606.

Lukac DM, Renne R, Kirshner JR, and Ganem D. 1998. Reactivation of Kaposi's sarcoma-associated herpesvirus infection from latency by expression of the ORF 50 transactivator, a homolog of the EBV R protein. Virology 252:304-312.

Lukac DM, Kirshner JR, and Ganem D. 1999. Transcriptional activation by the product of open reading frame 50 of Kaposi's sarcoma-associated herpesvirus is required for lytic viral reactivation in B-cells. J Virol 73:9348-9361.

Lund T, Medveczky MM, Geck P, and Medveczky PG. 1995. A herpesvirus saimiri protein required for interleukin-2 independence is associated with membranes of transformed T cells. J Virol 69:4495-4499.

Lund T, Medveczky MM, Neame PJ, and Medveczky PG. 1996. A herpesvirus saimiri membrane protein required for interleukin-2 independence forms a stable complex with p56lck. J Virol 70:600-606.

Lund T, Medveczky MM, and Medveczky PG. 1997a. Herpesvirus saimiri Tip-484 membrane protein markedly increases p56lck activity in T cells. J Virol 71:378-382.

Lund TC, Garcia R, Medveczky MM, Jove R, and Medveczky PG. 1997b. Activation of STAT transcription factors by herpesvirus Saimiri Tip-484 requires p56lck. J Virol 71:6677-6682.

Lund TC, Prator PC, Medveczky MM, and Medveczky PG. 1999. The Lck binding domain of herpesvirus saimiri tip-484 constitutively activates Lck and STAT3 in T cells. J Virol 73:1689-1694.

Lundquist A, Barre B, Bienvenu F, Hermann J, Avril S, and Coqueret O. 2003. Kaposi sarcoma-associated viral cyclin K overrides cell growth inhibition mediated by oncostatin M through STAT3 inhibition. Blood 101:4070-4077.

Luppi M, Barozzi P, Santagostino G, Trovato R, Schulz TF, Marasca R, Bottalico D, Bignardi L, and Torelli G. 2000. Molecular evidence of organ-related transmission of Kaposi sarcoma-associated herpesvirus or human herpesvirus-8 in transplant patients. Blood 96:3279-3281.

Luppi M, Barozzi P, Rasini V, and Torelli G. 2002. HHV-8 infection in the transplantation setting: a concern only for solid organ transplant patients? Leuk Lymphoma 43:517-522.

Lynch DT, Zimmerman JS, and Rowe DT. 2002. Epstein-Barr virus latent membrane protein 2B (LMP2B) co-localizes with LMP2A in perinuclear regions in transiently transfected cells. J Gen Virol 83:1025-1035.

Mann KP, Staunton D, and Thorley-Lawson DA. 1985. Epstein-Barr virus-encoded protein found in plasma membranes of transformed cells. J Virol 55:710-720.

Mann KP and Thorley-Lawson D. 1987. Posttranslational processing of the Epstein-Barr virus-encoded p63/LMP protein. J Virol 61:2100-2108.

Mansfield KG, Westmoreland SV, DeBakker CD, Czajak S, Lackner AA, and Desrosiers RC. 1999. Experimental infection of rhesus and pig-tailed macaques with macaque rhadinoviruses. J Virol 73:10320-10328.

Markovitz NS, Filatov F, and Roizman B. 1999. The U(L)3 protein of herpes simplex virus 1 is translated predominantly from the second in-frame methionine codon and is subject to at least two posttranslational modifications. J Virol 73:8010-8018.

Martin J and Sugden B. 1991. Transformation by the oncogenic latent membrane protein correlates with its rapid turnover, membrane localization, and cytoskeletal association. J Virol 65:3246-3258.

Martin JM, Veis D, Korsmeyer SJ, and Sugden B. 1993. Latent membrane protein of Epstein-Barr virus induces cellular phenotypes independently of expression of Bcl-2. J Virol 67:5269-5278.

Massague J and Wotton D. 2000. Transcriptional control by the TGF-beta/Smad signaling system. EMBO J 19:1745-1754.

Matskova L, Ernberg I, Pawson T, and Winberg G. 2001. C-terminal domain of the Epstein-Barr virus LMP2A membrane protein contains a clustering signal. J Virol 75:10941-10949.

Mayama S, Cuevas LE, Sheldon J, Omar OH, Smith DH, Okong P, Silvel B, Hart CA, and Schulz TF. 1998. Prevalence and transmission of Kaposi's sarcoma-associated herpesvirus (human herpesvirus 8) in Ugandan children and adolescents. Int J Cancer 77:817-820.

McDermott EP and O'Neill LA. 2002. Ras participates in the activation of p38 MAPK by interleukin-1 by associating with IRAK, IRAK2, TRAF6, and TAK-1. J Biol Chem 277:7808-7815.

Means RE, Ishido S, Alvarez X, and Jung JU. 2002. Multiple endocytic trafficking pathways of MHC class I molecules induced by a Herpesvirus protein. EMBO J 21:1638-1649.

Medveczky MM, Szomolanyi E, Hesselton R, DeGrand D, Geck P, and Medveczky PG. 1989. Herpesvirus saimiri strains from three DNA subgroups have different oncogenic potentials in New Zealand white rabbits. J Virol 63:3601-3611.

Medveczky MM, Geck P, Vassallo R, and Medveczky PG. 1993a. Expression of the collagen-like putative oncoprotein of Herpesvirus saimiri in transformed T cells. Virus Genes 7:349-365.

Medveczky MM, Geck P, Sullivan JL, Serbousek D, Djeu JY, and Medveczky PG. 1993b. IL-2 independent growth and cytotoxicity of herpesvirus saimiri-infected human CD8 cells and involvement of two open reading frame sequences of the virus. Virology 196:402-412.

Medveczky P, Szomolanyi E, Desrosiers RC, and Mulder C. 1984. Classification of herpesvirus saimiri into three groups based on extreme variation in a DNA region required for oncogenicity. J Virol 52:938-944.

Mehl AM, Fischer N, Rowe M, Hartmann F, Daus H, Trumper L, Pfreundschuh M, Muller-Lantzsch N, and Grasser FA. 1998. Isolation and analysis of two strongly transforming isoforms of the Epstein-Barr-Virus(EBV)-encoded latent membrane protein-1 (LMP1) from a single Hodgkin's lymphoma. Int J Cancer 76:194-200.

Mehl AM, Floettmann JE, Jones M, Brennan P, and Rowe M. 2001. Characterization of intercellular adhesion molecule-1 regulation by Epstein-Barr virus-encoded latent membrane protein-1 identifies pathways that cooperate with nuclear factor kappa B to activate transcription. J Biol Chem 276:984-992.

Melen K, Krogh A, and von Heijne G. 2003. Reliability measures for membrane protein topology prediction algorithms. J Mol Biol 327:735-744.

Melendez LV, Daniel MD, Hunt RD, and Garcia FG. 1968. An apparently new herpesvirus from primary kidney cultures of the squirrel monkey (Saimiri sciureus). Lab Anim Care 18:374-381.

Melendez LV, Hunt RD, Daniel MD, Garcia FG, and Fraser CE. 1969a. Herpesvirus saimiri. II. Experimentally induced malignant lymphoma in primates. Lab Anim Care 19:378-386.

Melendez LV, Daniel MD, Garcia FG, Fraser CE, Hunt RD, and King NW. 1969b. Herpesvirus saimiri. I. Further characterization studies of a new virus from the squirrel monkey. Lab Anim Care 19:372-377.

Melendez LV, Castellanos H, Barahona HH, Daniel MD, Hunt RD, Fraser CE, Garcia FG, and King NW. 1972. Two new herpesviruses from spider monkeys (Ateles geoffroyi). J Natl Cancer Inst 49:233-238.

Melendez LV, Hunt RD, Garcia FG, Daniel MD, Fraser CE, Barahona HH, and King NW. 1973. Herpesvirus ateles, the second lymphoma virus of monkeys. Bibl Haematol 39:410-415.

Merchant M, Caldwell RG, and Longnecker R. 2000. The LMP2A ITAM is essential for providing B-cells with development and survival signals in vivo. J Virol 74:9115-9124.

Miller CL, Longnecker R, and Kieff E. 1993. Epstein-Barr virus latent membrane protein 2A blocks calcium mobilization in B lymphocytes. J Virol 67:3087-3094.

Miller CL, Lee JH, Kieff E, and Longnecker R. 1994a. An integral membrane protein (LMP2) blocks reactivation of Epstein-Barr virus from latency following surface immunoglobulin crosslinking. Proc Natl Acad Sci U S A 91:772-776.

Miller CL, Lee JH, Kieff E, Burkhardt AL, Bolen JB, and Longnecker R. 1994b. Epstein-Barr virus protein LMP2A regulates reactivation from latency by negatively regulating tyrosine kinases involved in sIg-mediated signal transduction. Infect Agents Dis 3:128-136.

Miller CL, Burkhardt AL, Lee JH, Stealey B, Longnecker R, Bolen JB, and Kieff E. 1995b. Integral membrane protein 2 of Epstein-Barr virus regulates reactivation from latency through dominant negative effects on protein-tyrosine kinases. Immunity 2:155-166.

Miller G, Heston L, Grogan E, Gradoville L, Rigsby M, Sun R, Shedd D, Kushnaryov VM, Grossberg S, and Chang Y. 1997a. Selective switch between latency and lytic replication of Kaposi's sarcoma herpesvirus and Epstein-Barr virus in dually infected body cavity lymphoma cells. J Virol 71:314-324.

Miller WE, Earp HS, and Raab-Traub N. 1995a. The Epstein-Barr virus latent membrane protein 1 induces expression of the epidermal growth factor receptor. J Virol 69:4390-4398.

Miller WE, Mosialos G, Kieff E, and Raab-Traub N. 1997b. Epstein-Barr virus LMP1 induction of the epidermal growth factor receptor is mediated through a TRAF signaling pathway distinct from NF-kappaB activation. J Virol 71:586-594.

Miller WE, Cheshire JL, and Raab-Traub N. 1998. Interaction of tumor necrosis factor receptor-associated factor signaling proteins with the latent membrane protein 1 PXQXT motif is essential for induction of epidermal growth factor receptor expression. Mol Cell Biol 18:2835-2844.

Milner AE, Johnson GD, and Gregory CD. 1992. Prevention of programmed cell death in Burkitt lymphoma cell lines by bcl-2-dependent and -independent mechanisms. Int J Cancer 52:636-644.

Minden A, Lin A, Smeal T, Derijard B, Cobb M, Davis R, and Karin M. 1994. c-Jun N-terminal phosphorylation correlates with activation of the JNK subgroup but not the ERK subgroup of mitogen-activated protein kinases. Mol Cell Biol 14:6683-6688.

Mitchell T and Sugden B. 1995. Stimulation of NF-kappa B-mediated transcription by mutant derivatives of the latent membrane protein of Epstein-Barr virus. J Virol 69:2968-2976.

Mizushima S and Nagata S. 1990. pEF-BOS, a powerful mammalian expression vector. Nucleic Acids Res 18:5322.

Mocarski ES, and Courcelle CT. 2002. Cytomegaloviruses and their replication. In: Knipe DM, Howley PM, Griffin DE, Lamb RA, Martin MA, Roizman B, and Straus SE (ed.), Virology, 4th ed. Lippincott, Williams, and Wilkins, Philadelphia, PA: 2629-2673.

Molden J, Chang Y, You Y, Moore PS, and Goldsmith MA. 1997. A Kaposi's sarcoma-associated herpesvirus-encoded cytokine homolog (vIL-6) activates signaling through the shared gp130 receptor subunit. J Biol Chem 272:19625-19631.

Montaner S, Sodhi A, Pece S, Mesri EA, and Gutkind JS. 2001. The Kaposi's sarcoma-associated herpesvirus G protein-coupled receptor promotes endothelial cell survival through the activation of Akt/protein kinase B. Cancer Res 61:2641-2648.

Moore PS and Chang Y. 1995. Detection of herpesvirus-like DNA sequences in Kaposi's sarcoma in patients with and without HIV infection. N Engl J Med 332:1181-1185.

Moore PS, Boshoff C, Weiss RA, and Chang Y. 1996. Molecular mimicry of human cytokine and cytokine response pathway genes by KSHV. Science 274:1739-1744.

Moore PS and Chang Y. 2001. Molecular virology of Kaposi's sarcoma-associated herpesvirus. Philos Trans R Soc Lond B Biol Sci 356:499-516.

Moorthy R and Thorley-Lawson DA. 1990. Processing of the Epstein-Barr virus-encoded latent membrane protein p63/LMP. J Virol 64:829-837.

Moorthy RK and Thorley-Lawson DA. 1993b. Biochemical, genetic, and functional analyses of the phosphorylation sites on the Epstein-Barr virus-encoded oncogenic latent membrane protein LMP-1. J Virol 67:2637-2645.

Moorthy RK and Thorley-Lawson DA. 1993a. All three domains of the Epstein-Barr virus-encoded latent membrane protein LMP-1 are required for transformation of rat-1 fibroblasts. J Virol 67:1638-1646.

Morand P, Buisson M, Collandre H, Chanzy B, Genoulaz O, Bourgeat MJ, Pinel N, Leclercq P, Leroux D, Marechal V, Fritsch L, Ruigrok R, and Seigneurin JM. 1999. Human herpesvirus 8 and Epstein Barr-virus in a cutaneous B-cell lymphoma and a malignant cell line established from the blood of an AIDS patient. Leuk Lymphoma 35:379-387.

Morrison JA, Klingelhutz AJ, and Raab-Traub N. 2003. Epstein-Barr virus latent membrane protein 2A activates beta-catenin signaling in epithelial cells. J Virol 77:12276-12284.

Moses AV, Fish KN, Ruhl R, Smith PP, Strussenberg JG, Zhu L, Chandran B, and Nelson JA. 1999. Long-term infection and transformation of dermal microvascular endothelial cells by human herpesvirus 8. J Virol 73:6892-6902.

Mosialos G, Birkenbach M, Yalamanchili R, VanArsdale T, Ware C, and Kieff E. 1995. The Epstein-Barr virus transforming protein LMP1 engages signaling proteins for the tumor necrosis factor receptor family. Cell 80:389-399.

Muralidhar S, Pumfery AM, Hassani M, Sadaie MR, Kishishita M, Brady JN, Doniger J, Medveczky P, and Rosenthal LJ. 1998. Identification of kaposin (open reading frame K12) as a human herpesvirus 8 (Kaposi's sarcoma-associated herpesvirus) transforming gene. J Virol 72:4980-4988.

Muralidhar S, Veytsmann G, Chandran B, Ablashi D, Doniger J, and Rosenthal LJ. 2000. Characterization of the human herpesvirus 8 (Kaposi's sarcoma-associated herpesvirus) oncogene, kaposin (ORF K12). J Clin Virol 16:203-213.

Murphy C, Kretschmer C, Biesinger B, Beckers J, Jung J, Desrosiers RC, Muller-Hermelink HK, Fleckenstein BW, and Ruther U. 1994. Epithelial tumours induced by a herpesvirus oncogene in transgenic mice. Oncogene 9:221-226.

Murthy SC, Trimble JJ, and Desrosiers RC. 1989. Deletion mutants of herpesvirus saimiri define an open reading frame necessary for transformation. J Virol 63:3307-3314.

Nakamura H, Lu M, Gwack Y, Souvlis J, Zeichner SL, and Jung JU. 2003. Global changes in Kaposi's sarcoma-associated virus gene expression patterns following expression of a tetracycline-inducible Rta transactivator. J Virol 77:4205-4220.

Naranatt PP, Akula SM, Zien CA, Krishnan HH, and Chandran B. 2003. Kaposi's sarcoma-associated herpesvirus induces the phosphatidylinositol 3-kinase-PKC-zeta-MEK-ERK signaling pathway in target cells early during infection: implications for infectivity. J Virol 77:1524-1539.

Naranatt PP, Krishnan HH, Svojanovsky SR, Bloomer C, Mathur S, and Chandran B. 2004. Host gene induction and transcriptional reprogramming in Kaposi's sarcoma-associated herpesvirus (KSHV/HHV-8)-infected endothelial, fibroblast, and B-cells: insights into modulation events early during infection. Cancer Res 64:72-84.

Natoli G, Costanzo A, Ianni A, Templeton DJ, Woodgett JR, Balsano C, and Levrero M. 1997. Activation of SAPK/JNK by TNF receptor 1 through a noncytotoxic TRAF2-dependent pathway. Science 275:200-203.

Neipel F, Albrecht JC, and Fleckenstein B. 1997. Cell-homologous genes in the Kaposi's sarcoma-associated rhadinovirus human herpesvirus 8: determinants of its pathogenicity? J Virol 71:4187-4192.

Nicholas J, Ruvolo VR, Burns WH, Sandford G, Wan X, Ciufo D, Hendrickson SB, Guo HG, Hayward GS, and Reitz MS. 1997. Kaposi's sarcoma-associated human herpesvirus-8 encodes homologues of macrophage inflammatory protein-1 and interleukin-6. Nat Med 3:287-292.

Nicholas J, Zong JC, Alcendor DJ, Ciufo DM, Poole LJ, Sarisky RT, Chiou CJ, Zhang X, Wan X, Guo HG, Reitz MS, and Hayward GS. 1998. Novel organizational features, captured cellular genes, and strain variability within the genome of KSHV/HHV8. J Natl Cancer Inst Monogr79-88.

Nordeen SK. 1988. Luciferase reporter gene vectors for analysis of promoters and enhancers. Biotechniques 6:454-458.

Ohtani N, Zebedee Z, Huot TJ, Stinson JA, Sugimoto M, Ohashi Y, Sharrocks AD, Peters G, and Hara E. 2001. Opposing effects of Ets and Id proteins on p16INK4a expression during cellular senescence. Nature 409:1067-1070.

Ohtani N, Brennan P, Gaubatz S, Sanij E, Hertzog P, Wolvetang E, Ghysdael J, Rowe M, and Hara E. 2003. Epstein-Barr virus LMP1 blocks p16INK4a-RB pathway by promoting nuclear export of E2F4/5. J Cell Biol 162:173-183.

Oksenhendler E, Cazals-Hatem D, Schulz TF, Barateau V, Grollet L, Sheldon J, Clauvel JP, Sigaux F, and Agbalika F. 1998. Transient angiolymphoid hyperplasia and Kaposi's sarcoma after primary infection with human herpesvirus 8 in a patient with human immunodeficiency virus infection. N Engl J Med 338:1585-1590.

Osborne J, Moore PS, and Chang Y. 1999. KSHV-encoded viral IL-6 activates multiple human IL-6 signaling pathways. Hum Immunol 60:921-927.

Panousis CG and Rowe DT. 1997. Epstein-Barr virus latent membrane protein 2 associates with and is a substrate for mitogen-activated protein kinase. J Virol 71:4752-4760.

Park J, Seo T, Hwang S, Lee D, Gwack Y, and Choe J. 2000. The K-bZIP protein from Kaposi's sarcoma-associated herpesvirus interacts with p53 and represses its transcriptional activity. J Virol 74:11977-11982.

Park J, Lee BS, Choi JK, Means RE, Choe J, and Jung JU. 2002. Herpesviral protein targets a cellular WD repeat endosomal protein to downregulate T lymphocyte receptor expression. Immunity 17:221-233.

Park J, Cho NH, Choi JK, Feng P, Choe J, and Jung JU. 2003. Distinct roles of cellular Lck and p80 proteins in herpesvirus saimiri Tip function on lipid rafts. J Virol 77:9041-9051.

Parravicini C, Chandran B, Corbellino M, Berti E, Paulli M, Moore PS, and Chang Y. 2000. Differential viral protein expression in Kaposi's sarcoma-associated herpesvirus-infected diseases: Kaposi's sarcoma, primary effusion lymphoma, and multicentric Castleman's disease. Am J Pathol 156:743-749.

Pati S, Cavrois M, Guo HG, Foulke JS, Jr., Kim J, Feldman RA, and Reitz M. 2001. Activation of NF-kappaB by the human herpesvirus 8 chemokine receptor ORF74: evidence for a paracrine model of Kaposi's sarcoma pathogenesis. J Virol 75:8660-8673.

Patriotis C, Makris A, Chernoff J, and Tsichlis PN. 1994. Tpl-2 acts in concert with Ras and Raf-1 to activate mitogen-activated protein kinase. Proc Natl Acad Sci U S A 91:9755-9759.

Paulose-Murphy M, Ha NK, Xiang C, Chen Y, Gillim L, Yarchoan R, Meltzer P, Bittner M, Trent J, and Zeichner S. 2001. Transcription program of human herpesvirus 8 (kaposi's sarcoma-associated herpesvirus). J Virol 75:4843-4853.

Pawson T and Gish GD. 1992. SH2 and SH3 domains: from structure to function. Cell 71:359-362.

Pawson T and Scott JD. 1997. Signaling through scaffold, anchoring, and adaptor proteins. Science 278:2075-2080.

Pearson G, Robinson F, Beers GT, Xu BE, Karandikar M, Berman K, and Cobb MH. 2001. Mitogen-activated protein (MAP) kinase pathways: regulation and physiological functions. Endocr Rev 22:153-183.

Pelkmans L, Kartenbeck J, and Helenius A. 2001. Caveolar endocytosis of simian virus 40 reveals a new two-step vesicular-transport pathway to the ER. Nat Cell Biol 3:473-483.

Peng-Pilon M, Ruuth K, Lundgren E, and Brodin P. 1995. The cytoplasmic C-terminal domain but not the N-terminal domain of latent membrane protein 1 of Epstein-Barr virus is essential for B-cell activation. J Gen Virol 76 (Pt 4):767-777.

Peng M and Lundgren E. 1992. Transient expression of the Epstein-Barr virus LMP1 gene in human primary B cells induces cellular activation and DNA synthesis. Oncogene 7:1775-1782.

Peng M and Lundgren E. 1993. Transient expression of the Epstein-Barr virus LMP1 gene in B-cell chronic lymphocytic leukemia cells, T cells, and hematopoietic cell lines: cell-type-independent-induction of CD23, CD21, and ICAM-1. Leukemia 7:104-112.

Plancoulaine S, Abel L, van Beveren M, Tregouet DA, Joubert M, Tortevoye P, de The G, and Gessain A. 2000. Human herpesvirus 8 transmission from mother to child and between siblings in an endemic population. Lancet 356:1062-1065.

Platt GM, Simpson GR, Mittnacht S, and Schulz TF. 1999. Latent nuclear antigen of Kaposi's sarcoma-associated herpesvirus interacts with RING3, a homolog of the Drosophila female sterile homeotic (fsh) gene. J Virol 73:9789-9795.

Pomerantz JL and Baltimore D. 2002. Two pathways to NF-kappaB. Mol Cell 10:693-695.

Poole LJ, Zong JC, Ciufo DM, Alcendor DJ, Cannon JS, Ambinder R, Orenstein JM, Reitz MS, and Hayward GS. 1999. Comparison of genetic variability at multiple loci across the genomes of the major subtypes of Kaposi's sarcoma-associated herpesvirus reveals evidence for recombination and for two distinct types of open reading frame K15 alleles at the right-hand end. J Virol 73:6646-6660.

Portis T, Dyck P, and Longnecker R. 2003. Epstein-Barr Virus (EBV) LMP2A induces alterations in gene transcription similar to those observed in Reed-Sternberg cells of Hodgkin lymphoma. Blood 102:4166-4178.

Portis T and Longnecker R. 2003. Epstein-Barr virus LMP2A interferes with global transcription factor regulation when expressed during B-lymphocyte development. J Virol 77:105-114.

Portis T and Longnecker R. 2004. Epstein-Barr virus (EBV) LMP2A alters normal transcriptional regulation following B-cell receptor activation. Virology 318:524-533.

Prakash O, Tang ZY, Peng X, Coleman R, Gill J, Farr G, and Samaniego F. 2002. Tumorigenesis and aberrant signaling in transgenic mice expressing the human herpesvirus-8 K1 gene. J Natl Cancer Inst 94:926-935.

Prokova V, Mosialos G, and Kardassis D. 2002. Inhibition of transforming growth factor beta signaling and Smad-dependent activation of transcription by the Latent Membrane Protein 1 of Epstein-Barr virus. J Biol Chem 277:9342-9350.

Puls A, Eliopoulos AG, Nobes CD, Bridges T, Young LS, and Hall A. 1999. Activation of the small GTPase Cdc42 by the inflammatory cytokines TNF(alpha) and IL-1, and by the Epstein-Barr virus transforming protein LMP1. J Cell Sci 112 (Pt 17):2983-2992.

Radkov SA, Kellam P, and Boshoff C. 2000. The latent nuclear antigen of Kaposi sarcoma-associated herpesvirus targets the retinoblastoma-E2F pathway and with the oncogene Hras transforms primary rat cells. Nat Med 6:1121-1127.

Rainbow L, Platt GM, Simpson GR, Sarid R, Gao SJ, Stoiber H, Herrington CS, Moore PS, and Schulz TF. 1997. The 222- to 234-kilodalton latent nuclear protein (LNA) of Kaposi's sarcoma-associated herpesvirus (human herpesvirus 8) is encoded by orf73 and is a component of the latency-associated nuclear antigen. J Virol 71:5915-5921.

Regamey N, Tamm M, Wernli M, Witschi A, Thiel G, Cathomas G, and Erb P. 1998. Transmission of human herpesvirus 8 infection from renal-transplant donors to recipients. N Engl J Med 339:1358-1363.

Renne R, Zhong W, Herndier B, McGrath M, Abbey N, Kedes D, and Ganem D. 1996. Lytic growth of Kaposi's sarcoma-associated herpesvirus (human herpesvirus 8) in culture. Nat Med 2:342-346.

Renne R, Blackbourn D, Whitby D, Levy J, and Ganem D. 1998. Limited transmission of Kaposi's sarcoma-associated herpesvirus in cultured cells. J Virol 72:5182-5188.

Renne R, Barry C, Dittmer D, Compitello N, Brown PO, and Ganem D. 2001. Modulation of cellular and viral gene expression by the latency-associated nuclear antigen of Kaposi's sarcoma-associated herpesvirus. J Virol 75:458-468.

Renwick N, Halaby T, Weverling GJ, Dukers NH, Simpson GR, Coutinho RA, Lange JM, Schulz TF, and Goudsmit J. 1998. Seroconversion for human herpesvirus 8 during HIV infection is highly predictive of Kaposi's sarcoma. AIDS 12:2481-2488.

Rickinson AB, and Kieff E. 2001. Epstein-Barr virus. In: Knipe DM, Howley PM, Griffin DE, Lamb RA, Martin MA, Roizman B, and Straus SE (ed.), Virology, 4th ed. Lippincott, Williams, and Wilkins, Philadelphia, PA: 2575-2627.

Rimessi P, Bonaccorsi A, Sturzl M, Fabris M, Brocca-Cofano E, Caputo A, Melucci-Vigo G, Falchi M, Cafaro A, Cassai E, Ensoli B, and Monini P. 2001. Transcription pattern of human herpesvirus 8 open reading frame K3 in primary effusion lymphoma and Kaposi's sarcoma. J Virol 75:7161-7174.

Rivas C, Thlick AE, Parravicini C, Moore PS, and Chang Y. 2001. Kaposi's sarcoma-associated herpesvirus LANA2 is a B-cell-specific latent viral protein that inhibits p53. J Virol 75:429-438.

Robbins DJ, Zhen E, Owaki H, Vanderbilt CA, Ebert D, Geppert TD, and Cobb MH. 1993. Regulation and properties of extracellular signal-regulated protein kinases 1 and 2 in vitro. J Biol Chem 268:5097-5106.

Roberts ML and Cooper NR. 1998. Activation of a ras-MAPK-dependent pathway by Epstein-Barr virus latent membrane protein 1 is essential for cellular transformation. Virology 240:93-99.

Robertson KD and Ambinder RF. 1997. Mapping promoter regions that are hypersensitive to methylation-mediated inhibition of transcription: application of the methylation cassette assay to the Epstein-Barr virus major latency promoter. J Virol 71:6445-6454.

Rochford R, Miller CL, Cannon MJ, Izumi KM, Kieff E, and Longnecker R. 1997. In vivo growth of Epstein-Barr virus transformed B-cells with mutations in latent membrane protein 2 (LMP2). Arch Virol 142:707-720.

Roizman B, and Knipe DM. 2002. Herpes simplex viruses and their replication. In: Knipe DM, Howley PM, Griffin DE, Lamb RA, Martin MA, Roizman B, and Straus SE (ed.), Virology, 4th ed. Lippincott, Williams, and Wilkins, Philadelphia, PA: 2399-2459.

Roizman B, and Pellett PE. 2002. The Family *Herpesviridae*: A Brief Introduction. In: Knipe DM, Howley PM, Griffin DE, Lamb RA, Martin MA, Roizman B, and Straus SE (ed.), Virology, 4th ed. Lippincott, Williams, and Wilkins, Philadelphia, PA: 2381-2397.

Rothe M, Wong SC, Henzel WJ, and Goeddel DV. 1994. A novel family of putative signal transducers associated with the cytoplasmic domain of the 75 kDa tumor necrosis factor receptor. Cell 78:681-692.

Rothe M, Sarma V, Dixit VM, and Goeddel DV. 1995. TRAF2-mediated activation of NF-kappa B by TNF receptor 2 and CD40. Science 269:1424-1427.

Rothenberger S, Rousseaux M, Knecht H, Bender FC, Legler DF, and Bron C. 2002. Association of the Epstein-Barr virus latent membrane protein 1 with lipid rafts is mediated through its N-terminal region. Cell Mol Life Sci 59:171-180.

Rowe M, Peng-Pilon M, Huen DS, Hardy R, Croom-Carter D, Lundgren E, and Rickinson AB. 1994. Upregulation of bcl-2 by the Epstein-Barr virus latent membrane protein LMP1: a B-cell-specific response that is delayed relative to NF-kappa B activation and to induction of cell surface markers. J Virol 68:5602-5612.

Ruf IK and Rawlins DR. 1995. Identification and characterization of ZIIBC, a complex formed by cellular factors and the ZII site of the Epstein-Barr virus BZLF1 promoter. J Virol 69:7648-7657.

Russo JJ, Bohenzky RA, Chien MC, Chen J, Yan M, Maddalena D, Parry JP, Peruzzi D, Edelman IS, Chang Y, and Moore PS. 1996. Nucleotide sequence of the Kaposi sarcoma-associated herpesvirus (HHV8). Proc Natl Acad Sci U S A 93:14862-14867.

Ruzzene M, Brunati AM, Marin O, Donella-Deana A, and Pinna LA. 1996. SH2 domains mediate the sequential phosphorylation of HS1 protein by p72syk and Src-related protein tyrosine kinases. Biochemistry 35:5327-5332.

Sadler R, Wu L, Forghani B, Renne R, Zhong W, Herndier B, and Ganem D. 1999. A complex translational program generates multiple novel proteins from the latently expressed kaposin (K12) locus of Kaposi's sarcoma-associated herpesvirus. J Virol 73:5722-5730.

Saito N, Courtois G, Chiba A, Yamamoto N, Nitta T, Hironaka N, Rowe M, Yamamoto N, and Yamaoka S. 2003. Two carboxyl-terminal activation regions of Epstein-Barr virus latent membrane protein 1 activate NF-kappaB through distinct signaling pathways in fibroblast cell lines. J Biol Chem 278:46565-46575.

Salmeron A, Ahmad TB, Carlile GW, Pappin D, Narsimhan RP, and Ley SC. 1996. Activation of MEK-1 and SEK-1 by Tpl-2 proto-oncoprotein, a novel MAP kinase kinase kinase. EMBO J 15:817-826.

Samaniego F, Markham PD, Gallo RC, and Ensoli B. 1995. Inflammatory cytokines induce AIDS-Kaposi's sarcoma-derived spindle cells to produce and release basic fibroblast growth factor and enhance Kaposi's sarcoma-like lesion formation in nude mice. J Immunol 154:3582-3592.

Samaniego F, Pati S, Karp JE, Prakash O, and Bose D. 2001. Human herpesvirus 8 K1-associated nuclear factor-kappa B-dependent promoter activity: role in Kaposi's sarcoma inflammation? J Natl Cancer Inst Monogr15-23.

Sambrook J, Fritsch EF, and Maniatis T. 1989. Molecular Cloning. A Laboratory Manual. 2nd edition. Cold Spring Harbor Press, Cold Spring Harbor, NY.

Sample J, Liebowitz D, and Kieff E. 1989. Two related Epstein-Barr virus membrane proteins are encoded by separate genes. J Virol 63:933-937.

Sanchez DJ, Coscoy L, and Ganem D. 2002. Functional organization of MIR2, a novel viral regulator of selective endocytosis. J Biol Chem 277:6124-6130.

Sandberg M, Hammerschmidt W, and Sugden B. 1997. Characterization of LMP-1's association with TRAF1, TRAF2, and TRAF3. J Virol 71:4649-4656.

Sarid R, Sato T, Bohenzky RA, Russo JJ, and Chang Y. 1997. Kaposi's sarcoma-associated herpesvirus encodes a functional bcl-2 homologue. Nat Med 3:293-298.

Scholle F, Longnecker R, and Raab-Traub N. 1999. Epithelial cell adhesion to extracellular matrix proteins induces tyrosine phosphorylation of the Epstein-Barr virus latent membrane protein 2: a role for C-terminal Src kinase. J Virol 73:4767-4775.

Scholle F, Bendt KM, and Raab-Traub N. 2000. Epstein-Barr virus LMP2A transforms epithelial cells, inhibits cell differentiation, and activates Akt. J Virol 74:10681-10689.

Scholle F, Longnecker R, and Raab-Traub N. 2001. Analysis of the phosphorylation status of Epstein-Barr virus LMP2A in epithelial cells. Virology 291:208-214.

Schultheiss U, Puschner S, Kremmer E, Mak TW, Engelmann H, Hammerschmidt W, and Kieser A. 2001. TRAF6 is a critical mediator of signal transduction by the viral oncogene latent membrane protein 1. EMBO J 20:5678-5691.

Schulz TF. 2000. Kaposi's sarcoma-associated herpesvirus (human herpesvirus 8): epidemiology and pathogenesis. J Antimicrob Chemother 45 Suppl T3:15-27.

Schulz TF. 2001. KSHV/HHV8-associated lymphoproliferations in the AIDS setting. Eur J Cancer 37:1217-1226.

Schwam DR, Luciano RL, Mahajan SS, Wong L, and Wilson AC. 2000. Carboxy terminus of human herpesvirus 8 latency-associated nuclear antigen mediates dimerization, transcriptional repression, and targeting to nuclear bodies. J Virol 74:8532-8540.

Schwarz M and Murphy PM. 2001. Kaposi's sarcoma-associated herpesvirus G protein-coupled receptor constitutively activates NF-kappa B and induces proinflammatory cytokine and chemokine production via a C-terminal signaling determinant. J Immunol 167:505-513.

Schweimer K, Hoffmann S, Bauer F, Friedrich U, Kardinal C, Feller SM, Biesinger B, and Sticht H. 2002. Structural investigation of the binding of a herpesviral protein to the SH3 domain of tyrosine kinase Lck. Biochemistry 41:5120-5130.

Screpanti I, Musiani P, Bellavia D, Cappelletti M, Aiello FB, Maroder M, Frati L, Modesti A, Gulino A, and Poli V. 1996. Inactivation of the IL-6 gene prevents development of multicentric Castleman's disease in C/EBP beta-deficient mice. J Exp Med 184:1561-1566.

Searles RP, Bergquam EP, Axthelm MK, and Wong SW. 1999. Sequence and genomic analysis of a Rhesus macaque rhadinovirus with similarity to Kaposi's sarcoma-associated herpesvirus/human herpesvirus 8. J Virol 73:3040-3053.

Seo T, Lee D, Lee B, Chung JH, and Choe J. 2000. Viral interferon regulatory factor 1 of Kaposi's sarcoma-associated herpesvirus (human herpesvirus 8) binds to, and inhibits transactivation of, CREB-binding protein. Biochem Biophys Res Commun 270:23-27.

Seo T, Park J, Lee D, Hwang SG, and Choe J. 2001. Viral interferon regulatory factor 1 of Kaposi's sarcoma-associated herpesvirus binds to p53 and represses p53-dependent transcription and apoptosis. J Virol 75:6193-6198.

Sharp TV, Wang HW, Koumi A, Hollyman D, Endo Y, Ye H, Du MQ, and Boshoff C. 2002. K15 protein of Kaposi's sarcoma-associated herpesvirus is latently expressed and binds to HAX-1, a protein with antiapoptotic function. J Virol 76:802-816.

Shepard LW, Yang M, Xie P, Browning DD, Voyno-Yasenetskaya T, Kozasa T, and Ye RD. 2001. Constitutive activation of NF-kappa B and secretion of interleukin-8 induced by the G protein-coupled receptor of Kaposi's sarcoma-associated herpesvirus involve G alpha(13) and RhoA. J Biol Chem 276:45979-45987.

Simons K and Toomre D. 2000. Lipid rafts and signal transduction. Nat Rev Mol Cell Biol 1:31-39.

Smit MJ, Verzijl D, Casarosa P, Navis M, Timmerman H, and Leurs R. 2002. Kaposi's sarcoma-associated herpesvirus-encoded G protein-coupled receptor ORF74 constitutively activates p44/p42 MAPK and Akt via G(i) and phospholipase C-dependent signaling pathways. J Virol 76:1744-1752.

Sodhi A, Montaner S, Patel V, Zohar M, Bais C, Mesri EA, and Gutkind JS. 2000. The Kaposi's sarcoma-associated herpes virus G protein-coupled receptor up-regulates vascular endothelial growth factor expression and secretion through mitogen-activated protein kinase and p38 pathways acting on hypoxia-inducible factor 1alpha. Cancer Res 60:4873-4880.

Song MJ, Li X, Brown HJ, and Sun R. 2002. Characterization of interactions between RTA and the promoter of polyadenylated nuclear RNA in Kaposi's sarcoma-associated herpesvirus/human herpesvirus 8. J Virol 76:5000-5013.

Songyang Z, Shoelson SE, Chaudhuri M, Gish G, Pawson T, Haser WG, King F, Roberts T, Ratnofsky S, Lechleider RJ, and . 1993. SH2 domains recognize specific phosphopeptide sequences. Cell 72:767-778.

Songyang Z, Blechner S, Hoagland N, Hoekstra MF, Piwnica-Worms H, and Cantley LC. 1994. Use of an oriented peptide library to determine the optimal substrates of protein kinases. Curr Biol 4:973-982.

Songyang Z, Lu KP, Kwon YT, Tsai LH, Filhol O, Cochet C, Brickey DA, Soderling TR, Bartleson C, Graves DJ, DeMaggio AJ, Hoekstra MF, Blenis J, Hunter T, and Cantley LC. 1996. A structural basis for substrate specificities of protein Ser/Thr kinases: primary sequence preference of casein kinases I and II, NIMA, phosphorylase kinase, calmodulin-dependent kinase II, CDK5, and Erk1. Mol Cell Biol 16:6486-6493.

Sorokina EM, Merlo JJ, Jr., and Tsygankov AY. 2004. Molecular mechanisms of the effect of herpesvirus saimiri protein StpC on the signaling pathway leading to NF-kappaB activation. J Biol Chem 279:13469-13477.

Soulier J, Grollet L, Oksenhendler E, Cacoub P, Cazals-Hatem D, Babinet P, d'Agay MF, Clauvel JP, Raphael M, Degos L, and . 1995. Kaposi's sarcoma-associated herpesvirus-like DNA sequences in multicentric Castleman's disease. Blood 86:1276-1280.

Sozzani S, Luini W, Bianchi G, Allavena P, Wells TN, Napolitano M, Bernardini G, Vecchi A, D'Ambrosio D, Mazzeo D, Sinigaglia F, Santoni A, Maggi E, Romagnani S, and Mantovani A. 1998. The viral chemokine macrophage inflammatory protein-II is a selective Th2 chemoattractant. Blood 92:4036-4039.

Speck P, Kline KA, Cheresh P, and Longnecker R. 1999. Epstein-Barr virus lacking latent membrane protein 2 immortalizes B-cells with efficiency indistinguishable from that of wild-type virus. J Gen Virol 80 (Pt 8):2193-2203.

Spiller OB, Blackbourn DJ, Mark L, Proctor DG, and Blom AM. 2003. Functional activity of the complement regulator encoded by Kaposi's sarcoma-associated herpesvirus. J Biol Chem 278:9283-9289.

Stacey DW, Roudebush M, Day R, Mosser SD, Gibbs JB, and Feig LA. 1991. Dominant inhibitory Ras mutants demonstrate the requirement for Ras activity in the action of tyrosine kinase oncogenes. Oncogene 6:2297-2304.

Staskus KA, Zhong W, Gebhard K, Herndier B, Wang H, Renne R, Beneke J, Pudney J, Anderson DJ, Ganem D, and Haase AT. 1997. Kaposi's sarcoma-associated herpesvirus gene expression in endothelial (spindle) tumor cells. J Virol 71:715-719.

Sudol M. 1996. Structure and function of the WW domain. Prog Biophys Mol Biol 65:113-132.

Sugden B, Marsh K, and Yates J. 1985. A vector that replicates as a plasmid and can be efficiently selected in B-lymphoblasts transformed by Epstein-Barr virus. Mol Cell Biol 5:410-413.

Sun R, Lin SF, Gradoville L, Yuan Y, Zhu F, and Miller G. 1998. A viral gene that activates lytic cycle expression of Kaposi's sarcoma-associated herpesvirus. Proc Natl Acad Sci U S A 95:10866-10871.

Sun R, Lin SF, Staskus K, Gradoville L, Grogan E, Haase A, and Miller G. 1999. Kinetics of Kaposi's sarcoma-associated herpesvirus gene expression. J Virol 73:2232-2242.

Suzuki Y, Demoliere C, Kitamura D, Takeshita H, Deuschle U, and Watanabe T. 1997. HAX-1, a novel intracellular protein, localized on mitochondria, directly associates with HS1, a substrate of Src family tyrosine kinases. J Immunol 158:2736-2744.

Swanton C, Mann DJ, Fleckenstein B, Neipel F, Peters G, and Jones N. 1997. Herpes viral cyclin/Cdk6 complexes evade inhibition by CDK inhibitor proteins. Nature 390:184-187.

Swart R, Fruehling S, and Longnecker R. 1999. Tyrosines 60, 64, and 101 of Epstein-Barr virus LMP2A are not essential for blocking B-cell signal transduction. Virology 263:485-495.

Swart R, Ruf IK, Sample J, and Longnecker R. 2000. Latent membrane protein 2A-mediated effects on the phosphatidylinositol 3-Kinase/Akt pathway. J Virol 74:10838-10845.

Sylla BS, Hung SC, Davidson DM, Hatzivassiliou E, Malinin NL, Wallach D, Gilmore TD, Kieff E, and Mosialos G. 1998. Epstein-Barr virus-transforming protein latent infection membrane protein 1 activates transcription factor NF-kappaB through a pathway that includes the NF-kappaB-inducing kinase and the IkappaB kinases IKKalpha and IKKbeta. Proc Natl Acad Sci U S A 95:10106-10111.

Szomolanyi E, Medveczky P, and Mulder C. 1987. In vitro immortalization of marmoset cells with three subgroups of herpesvirus saimiri. J Virol 61:3485-3490.

Takebe Y, Seiki M, Fujisawa J, Hoy P, Yokota K, Arai K, Yoshida M, and Arai N. 1988. SRα Promoter: an Efficient and Versatile Mammalian cDNA Expression System of the Simian Virus 40 Early Promoter and the R-U5 Segment of Human T-Cell Leukemia Virus Type 1 Long Terminal Repeat. Mol Cell Biol 8 (1):466-472.

Takeuchi M, Rothe M, and Goeddel DV. 1996. Anatomy of TRAF2. Distinct domains for nuclear factor-kappaB activation and association with tumor necrosis factor signaling proteins. J Biol Chem 271:19935-19942.

Talbot SJ, Weiss RA, Kellam P, and Boshoff C. 1999. Transcriptional analysis of human herpesvirus-8 open reading frames 71, 72, 73, K14, and 74 in a primary effusion lymphoma cell line. Virology 257:84-94.

Tang W, Pavlish OA, Spiegelman VS, Parkhitko AA, and Fuchs SY. 2003. Interaction of Epstein-Barr virus latent membrane protein 1 with SCFHOS/beta-TrCP E3 ubiquitin ligase regulates extent of NF-kappaB activation. J Biol Chem 278:48942-48949.

Teodoro JG and Branton PE. 1997. Regulation of apoptosis by viral gene products. J Virol 71:1739-1746.

Thome M, Schneider P, Hofmann K, Fickenscher H, Meinl E, Neipel F, Mattmann C, Burns K, Bodmer JL, Schroter M, Scaffidi C, Krammer PH, Peter ME, and Tschopp J. 1997. Viral FLICE-inhibitory proteins (FLIPs) prevent apoptosis induced by death receptors. Nature 386:517-521.

Thorley-Lawson DA. 2001. Epstein-Barr virus: exploiting the immune system. Nat Rev Immunol 1:75-82.

Tomescu C, Law WK, and Kedes DH. 2003. Surface downregulation of major histocompatibility complex class I, PE-CAM, and ICAM-1 following de novo infection of endothelial cells with Kaposi's sarcoma-associated herpesvirus. J Virol 77:9669-9684.

Tomlinson CC and Damania B. 2004. The K1 protein of Kaposi's sarcoma-associated herpesvirus activates the Akt signaling pathway. J Virol 78:1918-1927.

Trowbridge IS, Collawn JF, and Hopkins CR. 1993. Signal-dependent membrane protein trafficking in the endocytic pathway. Annu Rev Cell Biol 9:129-161.

Tsai CN, Tsai CL, Tse KP, Chang HY, and Chang YS. 2002. The Epstein-Barr virus oncogene product, latent membrane protein 1, induces the downregulation of E-cadherin gene expression via activation of DNA methyltransferases. Proc Natl Acad Sci U S A 99:10084-10089.

Uchida J, Yasui T, Takaoka-Shichijo Y, Muraoka M, Kulwichit W, Raab-Traub N, and Kikutani H. 1999. Mimicry of CD40 signals by Epstein-Barr virus LMP1 in B lymphocyte responses. Science 286:300-303.

Vazirabadi G, Geiger TR, Coffin WF, III, and Martin JM. 2003. Epstein-Barr virus latent membrane protein-1 (LMP-1) and lytic LMP-1 localization in plasma membrane-derived extracellular vesicles and intracellular virions. J Gen Virol 84:1997-2008.

Vieira J, O'Hearn P, Kimball L, Chandran B, and Corey L. 2001. Activation of Kaposi's sarcoma-associated herpesvirus (human herpesvirus 8) lytic replication by human cytomegalovirus. J Virol 75:1378-1386.

Viejo-Borbolla A and Schulz TF. 2003. Kaposi's sarcoma-associated herpesvirus (KSHV/HHV8): key aspects of epidemiology and pathogenesis. AIDS Rev 5:222-229.

Viejo-Borbolla A, Kati E, Sheldon JA, Nathan K, Mattsson K, Szekely L, and Schulz TF. 2003. A Domain in the C-terminal region of latency-associated nuclear antigen 1 of Kaposi's sarcoma-associated Herpesvirus affects transcriptional activation and binding to nuclear heterochromatin. J Virol 77:7093-7100.

Vockerodt M, Haier B, Buttgereit P, Tesch H, and Kube D. 2001. The Epstein-Barr virus latent membrane protein 1 induces interleukin-10 in Burkitt's lymphoma cells but not in Hodgkin's cells involving the p38/SAPK2 pathway. Virology 280:183-198.

Wan J, Sun L, Mendoza JW, Chui YL, Huang DP, Chen ZJ, Suzuki N, Suzuki S, Yeh WC, Akira S, Matsumoto K, Liu ZG, and Wu Z. 2004. Elucidation of the c-Jun N-terminal kinase pathway mediated by Estein-Barr virus-encoded latent membrane protein 1. Mol Cell Biol 24:192-199.

Wang D, Liebowitz D, and Kieff E. 1985. An EBV membrane protein expressed in immortalized lymphocytes transforms established rodent cells. Cell 43:831-840.

Wang D, Liebowitz D, Wang F, Gregory C, Rickinson A, Larson R, Springer T, and Kieff E. 1988a. Epstein-Barr virus latent infection membrane protein alters the human B-lymphocyte phenotype: deletion of the amino terminus abolishes activity. J Virol 62:4173-4184.

Wang D, Liebowitz D, and Kieff E. 1988b. The truncated form of the Epstein-Barr virus latent-infection membrane protein expressed in virus replication does not transform rodent fibroblasts. J Virol 62:2337-2346.

Wang F, Gregory C, Sample C, Rowe M, Liebowitz D, Murray R, Rickinson A, and Kieff E. 1990. Epstein-Barr virus latent membrane protein (LMP1) and nuclear proteins 2 and 3C are effectors of phenotypic changes in B lymphocytes: EBNA-2 and LMP1 cooperatively induce CD23. J Virol 64:2309-2318.

Wang FZ, Akula SM, Pramod NP, Zeng L, and Chandran B. 2001. Human herpesvirus 8 envelope glycoprotein K8.1A interaction with the target cells involves heparan sulfate. J Virol 75:7517-7527.

Wang FZ, Akula SM, Sharma-Walia N, Zeng L, and Chandran B. 2003a. Human herpesvirus 8 envelope glycoprotein B mediates cell adhesion via its RGD sequence. J Virol 77:3131-3147.

Wang HW, Sharp TV, Koumi A, Koentges G, and Boshoff C. 2002. Characterization of an anti-apoptotic glycoprotein encoded by Kaposi's sarcoma-associated herpesvirus which resembles a spliced variant of human survivin. EMBO J 21:2602-2615.

Wang S, Rowe M, and Lundgren E. 1996. Expression of the Epstein Barr virus transforming protein LMP1 causes a rapid and transient stimulation of the Bcl-2 homologue Mcl-1 levels in B-cell lines. Cancer Res 56:4610-4613.

Wang SE, Wu FY, Fujimuro M, Zong J, Hayward SD, and Hayward GS. 2003b. Role of CCAAT/enhancer-binding protein alpha (C/EBPalpha) in activation of the Kaposi's sarcoma-associated herpesvirus (KSHV) lytic-cycle replication-associated protein (RAP) promoter in cooperation with the KSHV replication and transcription activator (RTA) and RAP. J Virol 77:600-623.

Wang SE, Wu FY, Yu Y, and Hayward GS. 2003c. CCAAT/enhancer-binding protein-alpha is induced during the early stages of Kaposi's sarcoma-associated herpesvirus (KSHV) lytic cycle reactivation and together with the KSHV replication and transcription activator (RTA) cooperatively stimulates the viral RTA, MTA, and PAN promoters. J Virol 77:9590-9612.

Wang SE, Wu FY, Chen H, Shamay M, Zheng Q, and Hayward GS. 2004. Early activation of the Kaposi's sarcoma-associated herpesvirus RTA, RAP, and MTA promoters by the tetradecanoyl phorbol acetate-induced AP1 pathway. J Virol 78:4248-4267.

Weber-Nordt RM, Egen C, Wehinger J, Ludwig W, Gouilleux-Gruart V, Mertelsmann R, and Finke J. 1996. Constitutive activation of STAT proteins in primary lymphoid and myeloid leukemia cells and in Epstein-Barr virus (EBV)-related lymphoma cell lines. Blood 88:809-816.

Weber KS, Grone HJ, Rocken M, Klier C, Gu S, Wank R, Proudfoot AE, Nelson PJ, and Weber C. 2001. Selective recruitment of Th2-type cells and evasion from a cytotoxic immune response mediated by viral macrophage inhibitory protein-II. Eur J Immunol 31:2458-2466.

Wehner LE, Schroder N, Kamino K, Friedrich U, Biesinger B, and Ruther U. 2001. Herpesvirus saimiri Tip gene causes T-cell lymphomas in transgenic mice. DNA Cell Biol 20:81-88.

Weiss A and Littman DR. 1994. Signal transduction by lymphocyte antigen receptors. Cell 76:263-274.

West JT and Wood C. 2003. The role of Kaposi's sarcoma-associated herpesvirus/human herpesvirus-8 regulator of transcription activation (RTA) in control of gene expression. Oncogene 22:5150-5163.

Wienands J, Schweikert J, Wollscheid B, Jumaa H, Nielsen PJ, and Reth M. 1998. SLP-65: a new signaling component in B lymphocytes which requires expression of the antigen receptor for phosphorylation. J Exp Med 188:791-795.

Wiese N, Tsygankov AY, Klauenberg U, Bolen JB, Fleischer B, and Broker BM. 1996. Selective activation of T cell kinase p56lck by Herpesvirus saimiri protein tip. J Biol Chem 271:847-852.

Wilson JB, Weinberg W, Johnson R, Yuspa S, and Levine AJ. 1990. Expression of the BNLF-1 oncogene of Epstein-Barr virus in the skin of transgenic mice induces hyperplasia and aberrant expression of keratin 6. Cell 61:1315-1327.

Winberg G, Matskova L, Chen F, Plant P, Rotin D, Gish G, Ingham R, Ernberg I, and Pawson T. 2000. Latent membrane protein 2A of Epstein-Barr virus binds WW domain E3 protein-ubiquitin ligases that ubiquitinate B-cell tyrosine kinases. Mol Cell Biol 20:8526-8535.

Wu FY, Wang SE, Tang QQ, Fujimuro M, Chiou CJ, Zheng Q, Chen H, Hayward SD, Lane MD, and Hayward GS. 2003. Cell cycle arrest by Kaposi's sarcoma-associated herpesvirus replication-associated protein is mediated at both the transcriptional and posttranslational levels by binding to CCAAT/enhancer-binding protein alpha and p21(CIP-1). J Virol 77:8893-8914.

Xin B, He Z, Yang X, Chan CP, Ng MH, and Cao L. 2001. TRADD domain of Epstein-Barr virus transforming protein LMP1 is essential for inducing immortalization and suppressing senescence of primary rodent fibroblasts. J Virol 75:3010-3015.

Xu W, Harrison SC, and Eck MJ. 1997. Three-dimensional structure of the tyrosine kinase c-Src. Nature 385:595-602.

Yamanashi Y, Fukuda T, Nishizumi H, Inazu T, Higashi K, Kitamura D, Ishida T, Yamamura H, Watanabe T, and Yamamoto T. 1997. Role of tyrosine phosphorylation of HS1 in B-cell antigen receptor-mediated apoptosis. J Exp Med 185:1387-1392.

Yang TY, Chen SC, Leach MW, Manfra D, Homey B, Wiekowski M, Sullivan L, Jenh CH, Narula SK, Chensue SW, and Lira SA. 2000a. Transgenic expression of the chemokine receptor encoded by human herpesvirus 8 induces an angioproliferative disease resembling Kaposi's sarcoma. J Exp Med 191:445-454.

Yang X, He Z, Xin B, and Cao L. 2000b. LMP1 of Epstein-Barr virus suppresses cellular senescence associated with the inhibition of p16INK4a expression. Oncogene 19:2002-2013.

Ye H, Park YC, Kreishman M, Kieff E, and Wu H. 1999. The structural basis for the recognition of diverse receptor sequences by TRAF2. Mol Cell 4:321-330.

Ye H and Wu H. 2000. Thermodynamic characterization of the interaction between TRAF2 and tumor necrosis factor receptor peptides by isothermal titration calorimetry. Proc Natl Acad Sci U S A 97:8961-8966.

Yoon DW, Lee H, Seol W, DeMaria M, Rosenzweig M, and Jung JU. 1997. Tap: a novel cellular protein that interacts with tip of herpesvirus saimiri and induces lymphocyte aggregation. Immunity 6:571-582.

Zhang L, Wu L, Hong K, and Pagano JS. 2001. Intracellular signaling molecules activated by Epstein-Barr virus for induction of interferon regulatory factor 7. J Virol 75:12393-12401.

Zhou FC, Zhang YJ, Deng JH, Wang XP, Pan HY, Hettler E, and Gao SJ. 2002. Efficient infection by a recombinant Kaposi's sarcoma-associated herpesvirus cloned in a bacterial artificial chromosome: application for genetic analysis. J Virol 76:6185-6196.

Zhu L, Puri V, and Chandran B. 1999. Characterization of human herpesvirus-8 K8.1A/B glycoproteins by monoclonal antibodies. Virology 262:237-249.

Zong JC, Ciufo DM, Alcendor DJ, Wan X, Nicholas J, Browning PJ, Rady PL, Tyring SK, Orenstein JM, Rabkin CS, Su IJ, Powell KF, Croxson M, Foreman KE, Nickoloff BJ, Alkan S, and Hayward GS. 1999. High-level variability in the ORF-K1 membrane protein gene at the left end of the Kaposi's sarcoma-associated herpesvirus genome defines four major virus subtypes and multiple variants or clades in different human populations. J Virol 73:4156-4170.

6 Appendix

Erklärung

Hiermit erkläre ich an Eides Statt, dass ich die hier vorgelegte Arbeit selbstständig verfasst und durchgeführt und die benutzten Hilfsmittel und Quellen sowie die zu Hilfeleistungen herangezogenen Institutionen vollständig angegeben habe. Desweiteren erkläre ich, dass die vorliegende Dissertation nicht schon als Diplomarbeit oder ähnliche Prüfungsarbeit verwendet worden ist.

Hannover, den 28. April 2004

Curriculum vitae

Name	Melanie Margarete Brinkmann
Date of birth	6th of January 1974
Place of birth	Neustadt am Rübenberge, Germany
Parents	Klaus Brinkmann and Carola Brinkmann, née Wilden
Address	Bürgermeister-Fink-Strasse 9
	30169 Hannover
Marital status	single

School qualifications:

June 1993	University entrance qualification („Abitur“)

University studies:

1993 - 1994	Studies of english language and literature, sociology and pedagogics at the University of Hannover
1994 - 1996	Studies of Biology at the Georg-August University Göttingen
October 1996	Pre-diploma exam in Biology at the Georg-August University Göttingen with the final grade „very good“
1996 - 1999	Studies of Biology at the Humboldt-University of Berlin
Jan. – Sept. 1999	Laboratory work for the diploma thesis submitted for a diploma with the title „Untersuchungen zur Kopplung von Transport und ATP-Hydrolyse im Maltose-ABC-Transporter bei *Salmonella typhimurium*“ in the group “Physiology of microorganisms” of Prof. Dr. Erwin Schneider, Institute of Biology, Humboldt-University of Berlin Final grade of the diploma thesis „very good“
September 1999	University degree “Diploma Biologist” with the final grade „very good“ (major subject Microbiology, minor subjects Biochemistry and Animal Physiology)

Employments:

May 1997 - Sept. 1997 June 1998 - Sept. 1999	„Studentische Hilfskraft“ in the Mathematical-scientifical Faculty I of the Humboldt-University of Berlin in the group “Physiology of microorganisms” of Prof. Dr. E. Schneider
Dec. 1999 - April 2000	Phd student in the group “Physiology of microorganisms” of Prof. Dr. E. Schneider
May - July 2000	Phd student in the group of Prof. Dr. Thomas F. Schulz in the Department of Medical Microbiology and GUM of the University of Liverpool
July 2000 – April 2004	Phd student in the group of Prof. Dr. T. F. Schulz at the Institute of Virology, Medical High School Hannover (MHH)
2002 -	“Radiation representative” at the Institute of Virology, MHH
April 2004	Postdoc position in the group of Prof. Dr. T. F. Schulz at the Institute of Virology, Medical High School Hannover (MHH)

Stays abroad:

Oct. 1997 - March 1998	Student at the Imperial College of Science, Technology and Medicine in London, UK, at the Institute of Biochemistry (Socrates programme)
May - July 2000	Department of Medical Microbiology and GUM of the University of Liverpool

Practical training

July 1993 - March 1995	Editorial work for the newspaper “Hannoversche Allgemeine Zeitung”
July - September 1995	Photo-department of the “STERN” magazine in Hamburg
August - September 1996	Editorial work for the “GEO” magazine in Hamburg

Hannover, 28th of April 2004

Scientific publications

I. Scientific publications:

1. „Large-scale purification, dissociation and functional reassembly of the maltose ATP-binding cassette transporter ($MalFGK_2$) of *Salmonella typhimurium*“
Authors:
Heidi Landmesser, Anke Stein, Bettina Blüschke, Melanie Brinkmann, Sabine Hunke, Erwin Schneider
Biochimica et Biophysica Acta 1565 (2002) pp. 64-72

2. Chapter for the scientific book „Ganten/Ruckpaul (Hrsg.): Molekularmedizinische Grundlagen von hämatologischen Neoplasien“ with the title „Viren und die Entstehung hämatologischer Neoplasien“
Authors:
Melanie M. Brinkmann, Nils von Neuhoff, Hans L. Tillmann, Thomas F. Schulz
Springer-Verlag ISBN 3-540-41640-4, pp. 215-246, 2003

3. “Activation of Mitogen-activated Protein Kinase and NF-κB Pathways by a Membrane Protein encoded in the K15 Gene of Kaposi´s Sarcoma-associated Herpesvirus (KSHV)”
Authors:
Melanie M. Brinkmann, Mark Glenn, Lucille Rainbow, Arnd Kieser, Cornelia Henke-Gendo, Thomas F. Schulz
Journal of Virology, Vol. 77 (17), pp. 9346-9358, 2003

II. Posters presented at scientific meetings:

1. German Society of Virology Annual Meeting, Dresden, Germany, 2001:
“Proteins expressed from the K15 gene of KSHV”
Brinkmann M., Rainbow L., Glenn M. and Schulz T.F.

III. Oral presentations:

1. KSHV Annual meeting, Santa Cruz, California, USA, 2001: “Proteins translated from the K15 gene and their role in NF-κB activation and binding to members of the Src kinase family”. M. M. Brinkmann, M. Glenn, L. Rainbow, T.F. Schulz

2. German Society of Virology Annual Meeting, Erlangen, Germany, 2002: „Subcellular localisation and interaction with signaling pathways of proteins encoded by ORF K15 of KSHV/HHV-8". M. M. Brinkmann, M. Glenn, L. Rainbow, C. Henke-Gendo and T.F. Schulz

3. KSHV Annual meeting, Kloster Irsee, Germany, July 2002: "Individual K15-derived proteins differ in their intracellular localisation and functional properties". M. M. Brinkmann, M. Glenn, L. Rainbow, H. Pommer and T. F. Schulz

4. Workshop Cell biology of the Society of German Virology, Schloss Zeilitzheim, Germany, September 2002: "Individual ORF K15-derived proteins of the Kaposi´s sarcoma associated herpesvirus differ in their intracellular localisation and functional properties". M. M. Brinkmann, M. Glenn, L. Rainbow, H. Pommer and T. F. Schulz

5. German Society of Virology Annual Meeting, Berlin, Germany, March 2003: „Activation of Mitogen-activated Protein Kinase and NF-κB Pathways by a Membrane Protein encoded in the K15 Gene of Kaposi´s Sarcoma-associated Herpesvirus (KSHV)". M. M. Brinkmann, M. Glenn, L. Rainbow, A. Kieser, C. Henke-Gendo and T. F. Schulz

6. KSHV Annual meeting, Long Island, New York, USA, July 2003: „Activation of Mitogen-activated Protein Kinase and NF-κB Pathways by a K15 protein of Kaposi´s Sarcoma-associated Herpesvirus (KSHV)". M. M. Brinkmann, M. Glenn, L. Rainbow, A. Kieser, A. Viejo-Borbolla, C. Henke-Gendo and T. F. Schulz

7. Workshop Cell biology of the Society of German Virology, Schloss Zeilitzheim, Germany, September 2003: „Activation of Mitogen-activated Protein Kinase and NF-κB Pathways by a K15 protein of Kaposi´s Sarcoma-associated Herpesvirus (KSHV)". M. M. Brinkmann, M. Glenn, L. Rainbow, A. Kieser, A. Viejo-Borbolla, A. Tittel and T. F. Schulz

8. Virological Seminar of the Hannover Veterinary School (Tierärztliche Hochschule Hannover), Oktober 2003 (Prof. G. Herrler): „Activation of Mitogen-activated Protein Kinase and NF-κB Pathways by a K15 protein of Kaposi´s Sarcoma-associated Herpesvirus (KSHV)". M. M. Brinkmann

9. Virological Seminar of the Institute of Medical Virology, section Experimental Virology, Tübingen, February 2003 (Prof. Iftner): „Activation of mitogen-activated protein kinase and NF-κB pathways by a membrane signaling protein of the Kaposi´s Sarcoma-associated Herpesvirus (KSHV)". M. M. Brinkmann

Acknowledgements

I would like to thank my supervisor Prof. Dr. Thomas F. Schulz for this exciting project, for his support in "growing up" in the scientific world, for giving me the opportunity to travel around the world to present my work, for his patience and his humor.
Prof. Dr. W. Müller for his straight offer to become referee for my thesis.
Lucille Rainbow for her support with this multiply spliced gene when I started working on the K15 project in Liverpool.
Conny for her support to solve a big mystery.
Arnd Kieser and Stephan Ludwig for a lot of advice, plasmids and encouragement.
Ronald Frank for the synthesis of a 12 transmembrane protein on a piece of paper.
Heidi Pommer for DNA sequencing and testing out hundreds, well rather thousands of hybridoma supernatants. Ildiko Szabados for protein purification and ELISAs. Doris Findeisen for the generation of monoclonal antibodies. Achim Steinkopf, Meinhard Scharr and Ana Figueiredo for their support with the scientists´ everyday life. All members of the diagnostic section for keeping up with the strange scientists. The secretaries Anne Meyer, Annegret Kloth and Angelika Böttcher for keeping us up to date with Prof. Schulz´s time planer and letting us sneak in his office to present really urgent results.
The Sodeik lab for helpful discussions and antibodies, especially Katinka Döhner and André Wolfstein for their help at the microscope. Prof. Dr. Achim Gossler and his group, especially Natascha, for enjoyable coffee breaks and for letting us work in their radioactivity lab.

The HHV-8 lab for the great working atmosphere, many many enjoyable dinners, parties and DVD nights. Eva for squeezing Robbie Williams into our lab life. Dr. Abel Viejo-Borbolla for the generation of the RTA reporter plasmid, his advice, his singing to the Dirty Dancing soundtrack.

My parents and my brother Thomas for their love and support.
And Matthias for the sunshine.